Understanding KSHV vIRF-2-Cell Interactions

by

MOHAMED MUTOCHELUH

A thesis submitted to
The University of Birmingham
for the degree of
DOCTOR OF PHILOSOPHY

The School of Cancer Sciences
College of Medical and Dental Sciences
The University of Birmingham
August 2011

Abstract

Kaposi's sarcoma-associated herpes virus (KSHV) encodes genes with immunomodulatory potential, one of which is *vIRF-2* that shares homology to cellular interferon regulatory factors. The innate antiviral mechanism mediating the type I interferons is an essential host cell defence mechanism limiting viral replication. The aim of this study was to determine the range and type of cellular gene sets and associated biological pathways whose expression is deregulated by vIRF-2. HEK 293-derived cell clones were engineered to express doxycycline-inducible vIRF-2. Interferon (IFN) responses were induced with recombinant (r) IFN-α and measured by an IFN stimulated response elements (ISRE) luciferase reporter gene assay. The effects of vIRF-2 on cell transcriptome profile in response to rIFN-α were determined by DNA microarray analysis and confirmed by immunoblot assay. vIRF-2 protein inhibited activation of ISRE-luc by over 50% and significantly ($p<0.05$) down-regulated the expression of 57/78 (73%) of rIFN-α regulated genes. The DAVID and GSEA software packages revealed vIRF-2 down-regulates the RIG-I-like receptor, JAK-STAT and Ubiquitin ligase pathways and many gene sets involved in antiviral response, transcriptional regulation and apoptosis. Immunoblot assays demonstrated reduced levels of RIG-I/DDX58, TBK-1, p-38, STAT1, pSTAT1, IRF-9 and OAS3. The biological significance of the vIRF-2 anti-IFN property was demonstrated by the rescue of encephalomyocarditis virus (EMCV) replication in vIRF-2 expressing cells treated with rIFN-α; EMCV was titred by plaque assay on L929 cells. These data confirm the role of KSHV vIRF-2 in negative regulation of the IFN-α/β innate immune response by a mechanism dependent on negative regulation of RIG-I/DDX58, STAT1, IRF-9 and OAS3.

Acknowlegements

I would first like to give special thanks to my supervisor, Professor David Blackbourn for his continual support, encouragement and guidance through out my PhD course. Secondly, I would like to thank Dr. Simon Chanas, Dr. Christina Aresté, Miss Rachel Wheat, Miss Laura Hindle and all past and present members of the Blackbourn group for their support and contribution to this work. Additionally, I would like to thank Dr. Carmel McConville, Dr. Wenbin Wei, and Dr. John Arrand for their advice on the DNA microarray work. I am indebted to Miss Kym Lowry and Professor David Evans of the University of Warwick for their contribution to the EMCV work. Thirdly, I would like to thank the Ghana government and my employer (KNUST) for the PhD studentship. Finally, I would like to thank my wife Dr. Alimatu Salam, my daughters Salma and Alisha and my parents for their support throughout my time here at The University of Birmingham.

Table of Contents

List of Figures

List of Tables

Acronyms, abbreviation and notations

aa	Amino acid
AIDS	Acquired immune deficiency syndrome
ANG2	Angiopoitin 2
APC	Antigen presenting cell
APOBEC	Apolipoprotein B mRNA editing enzyme
APS	Ammonium persulphate
ATRA	All-trans retinoic acid
BAC	Bacterial artificial chromosome
BCBL-1	Body cavity-based lymphoma
BEC	Blood vascular endothelial cell
BSA	Bovine serum albumin
BCR	B cell receptor
bp	Base pair
CDC	Centers for Disease Control
CDK	Cyclin-dependent kinase
CCR	CC chemokines receptors
CD	Cluster of differentiation
CD95L	CD95 ligand
CMV	Cytomegalovirus
CTL	Cytotoxic T lymphocyte
CPE	Cytopatic effects
CBP	CREB-binding protein
Da	Daltons
DBD	DNA binding domain
DC	Dendritic cells
DMEM	Dulbeccos modified eagles medium
DNA	Deoxyribonucleic acid
ds	Double stranded
dNTP	Deoxyribonucleotide triphosphate
EBV	Eptein-Barr virus
EBNA-1	EBV nuclear antigen type 1
E. Coli	*Escherichia coli*
ELISA	Enzyme linked immunosorbent assay
ECL	Enhanced chemiluminescence
eIF-2α	Eukaryotic translation initiation factor 2α
EMCV	Encephalomyocarditis virus
EMSA	Electrophoretic mobility shift assay
EC	Expression console
EHV2	Equine herpesvirus 2
FBS	Feotal bovine serum
FCS	Feotal calf serum
FITC	Fluorscein isothiocyanate
FLICE	Fas ligand interleukin converting enzyme
g	Gram
g	Gravitational force
gB	Glycoprotein B
GAF	Gamma interferon activated factor

GAS	Gamma interferon activation site
GO	Gene ontology
GM-CSF	Granulocyte-monocyte colony stimulating factor
GPCR	G-protein coupled receptor
GRIM19	Retinoic-IFN-induced mortality 19
HAT	Histone acetyl transferase
HBV	Heptitis B virus
HCV	Heptitis C virus
HCMV	Human cytomegalovirus
HHV	Human herpesvirus
HIV	Human immune deficiency virus
HLA	Human leukocyte antigen
HPV	Human papillomavirus
HSV-1/2	Hepers simplex virus type 1/2
HVS	Herpesvirus saimiri
HUVECS	Human vascular endothelial cells
HRS	Horseradish peroxidase
ICAM-1	Intercellular adhesion molecule 1
ICSBP	Interferon concensus binding protein
IFA	Indirect immunofluorescence assay
IFN	Interferon
IL	Interleukin
Ig	Immunoglobulin
IFN-α/β/γ/λ	Interferon alpha/beta/gamma/lamda
IKK	IκB kinase
IRF	Interferon regulatory factor
ISG	Interferon stimulated gene
ISGF3	Interferon stimulated gene factor 3
ISRE	Interferon stimulated response elements
IFIT	Interferon induced protein with tetratricopeptide repeats
IU	International units
ITAM	Immunoreceptor tyrosine-based activation motif
JAK	Janus activation kinase
KS	Kaposi's sarcoma
KSHV	Kaposi's sarcoma-associated herpesvirus
KCP	KSHV complement control protein
LAMPs	Latency-associated membrane proteins
LANA	Latency-associated nuclear protein
LAR II	Luciferase assay reagent II
LTR	Long terminal repeat
Luc	Luciferase
LUR	Long unique region
LEC	Lymphatic endothelial cell
LPS	Lipopolysaccharide
LCMV	Lymphocytic choriomeningitis virus
mAB	Monoclonal antibody
MAPK	Mitogen activated protein kinase
MAVS	IPS-1/VISA/Cardif
MCD	Multicentric Castleman's Disease
MDA5	Melanoma differention-associated protein 5

MDM2	Mouse double minute 2
MHC	Major histocompartibility complex
MHV 68	Murine gammaherpesvirus 68
M-MLV RT	Moloney Murine Leukemia Virus Reverse Transcriptase
mRNA	Messenger RNA
MV	Myxovirus
NDV	New Castle Disease virus
NLS	Nuclear localisation signal
NFκB	Nuclear factor-κB
NFAT	Nuclear factor activated T cells
NK	Natural killer cells
NP40	Nonidet 40
NS	None structural
OAS	Oligoadenylate synthetase
ORF	Open reading frame
PAGE	Polyacrylamide gel electrophoresis
PAMP	Pathogen-associated molecular pattern
PBMC	Peripheral blood mononuclear cell
PBS	Phosphate buffered saline
PCR	Polimerase chain reaction
PEL	Primary effusion lymphoma
PFU	Plaque forming unit
PI3K	Phosphatidlyinositol 3-kinase
Poly I:C	Polyinosinic:polycytidylic acid
PKB/C	Protein kinase B or C
PRR	Pathogen recognition receptor
PRD	Positive regulatory domain
PRIDDs	Positive regulatory IFN-regulatory factor-dependent domains
PVDF	Polivinylidene fluoride
RA	IFN/all-trans-retinoic acid
RIG-1	Retinoic acid inducible gene 1
RTA	Replication and transcription activator
RRV	Rhesus rhadinovirus
RNA	Ribonucleic acid
SDS	Sodium dodecyl sulphate
SeV	Sendai virus
STAT	Signal transducer and activator of transcription
siRNA	Short interfering RNA
SV-40	Simian virus 40
TANK	TRAF family member-associated NFκB activator
Th	T helper cell
TGF-β	Transforming growth factor-β
TLR	Toll-like receptor
TNF	Tumour necrosis factor
TRIM	T cell receptor-interacting molecule
TYK-2	Tyrosine kinase-2
VEGF	Vascular endothelial growth factor
vFLIP	Viral FLICE apoptosis complex
vCyclin	Viral derived CyclinD protein

vIL-6	Viral derived IL-6
VSV	Vesicular stomatitis virus
vIRFS	Viral interferon regulatory factors
VZV	Varicella-zoster virus
WNV	West Nile virus
WT	Wild type

CHAPTER 1 Introduction

Kaposi's sarcoma-associated herpesvirus, formally called human herpesvirus 8 (HHV8), is the most recently identified human herpesvirus (Chang, Cesarman et al. 1994). KSHV was initially discovered on the basis of its association with Kaposi's sarcoma (KS), an endothelial neoplasm and was later classified as a member of the lymphotropic (γ) herpesvirus subfamily. The discovery of KSHV has advanced our knowledge of AIDS-related malignancies because since its discovery, KSHV has been identified in virtually all AIDS and non-AIDS-related KS lesions (Su, Hsu et al. 1995), (see Bouvard, Baan et al. 2009). KSHV infection is now recognized as the aetiologic agents in two proliferative diseases: KS and body cavity-based or primary effusion lymphoma (BCBL or PEL) (see Bouvard, Baan et al. 2009). KSHV is associated with some plasmablastic forms of multicentric Castleman's disease (MCD) (Soulier, Grollet et al. 1995).

The overall aim of this research project was to determine the range and type of cellular genes whose expression is deregulated by vIRF-2. In the present chapter, I shall review our current understanding of KSHV infection by exploring KSHV discovery, replication, epidemiology and associated diseases. The KSHV lytic gene vIRF-2 and other KSHV immunomodulatory genes shall be discussed followed by an overview of innate and adaptive immune responses.

Chapter 2 explains in detail the experimental procedures including the creation of vIRF-2 stable expressing clones and the 'empty vector' counterparts lacking vIRF-2. vIRF-2 expression and functional studies, techniques and procedures employed to prepare samples for DNA microarray investigations are discussed in Chapter 3. Studies of vIRF-2-deregulated gene sets and related biological signaling pathways and the mechanism of

inhibition of the JAK-STAT pathway by vIRF-2 are described in Chapter 4. The biological significance of vIRF-2 anti-interferon property is discussed in Chapters 5. The general discussion and conclusions drawn are presented in Chapter 6. Publications emanating from the present study, together with the list of materials, antibodies, chemicals and solutions are shown in the appendices.

1.1 Herpesviruses

Herpesvirus taxonomy has been revised recently (Davison, Eberle et al. 2009). Herpesviruses contain a linear, double-stranded DNA genome of 125-290 kbp, encased in an icosaheral capsid (T=16), which is contained by a proteinaceous matrix known as the tegument. The tegument is incased in a lipid envelope containing membrane-associated proteins (see Pellet PE 2006). The new classification made it possible for the former family *Herpesviridae* that contained all herpesviruses to be divided in to three families in the new order *Herpesvirales*. Herpesviruses have been genetically classified in to three distinct groups, which are weakly linked to each other (see Davison 1992; Davison 2002). The revised *Herpesviridae* family retains the viruses of birds and reptiles, mammals, the new family *Alloherpessviridae* includes the fish and frog viruses, and another new family *Malacoherpesviridae* (a bivalve virus) (Davison, Eberle et al. 2009).

Davison et al further divided *Herpesviridae* in to three subfamilies, the *Alphherpesvirinae*, the *Betaherpesvirinae* and the *Gammaherpesvirinae* (Davison, Eberle et al. 2009). KSHV is retained as a *Gammaherpesvirus* along with its simian relatives and falls under the genus *Rhadinovirus* and now contains four genera, macaviruses, percaviruses, lymphocrptoviruses and rhadinoviruses (**Figure 1.1**) (Davison, Eberle et al. 2009).

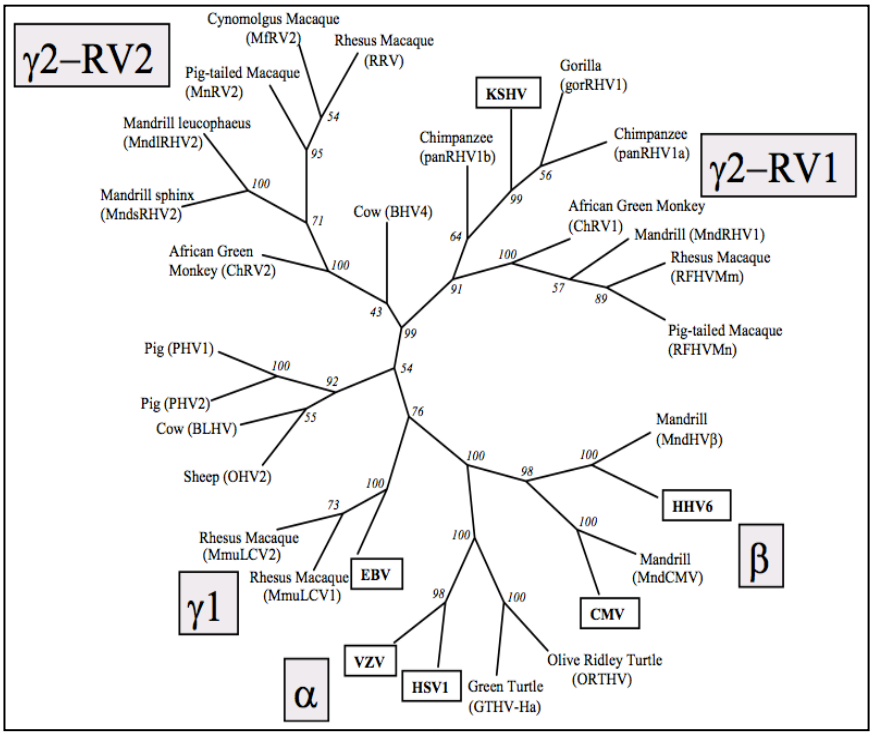

Figure 1.1 Phylogenetic tree of Herpesviridae family. The phylogenetic tree was generated using DNA polymerase sequences from 36 Herpesviruses and related to the sequences of the corresponding 6 representative human herpesviruses (boxed). The herpesvirus DNA polymerase sequence data were generated using PCR with concensus-degenerate hybrid oligonucleotide primers (CODEHOP), which were derived from amino acid sequence motifs highly conserved across Herpesviridae. This figure is reproduced from Rose (Rose 2005).

1.2 KS and KSHV Discovery

The Austro–Hungarian dermatologist Moritz Kaposi first described Kaposi's sarcoma in 1872 as an aggressive tumour affecting the older age group than is commonly seen today, suggesting a change in viral pathogenicity during more recent times. KS was considered classically an indolent disease of elderly men, but was later discovered to be more common in the Mediterranean basin, and in parts of Africa (see Antman and Chang 2000; Herndier and Ganem 2001). The advent of human immunodeficiency virus (HIV) infection pandemic in the 1980s revealed KS as the most common neoplasm complicating AIDS. Its development in the context of HIV infection is an AIDS-defining condition.

In 1994, using representational difference analysis to search for DNA sequences present in KS lesions but absent in normal tissue, Chang and colleagues (Chang, Cesarman et al. 1994) identified fragments of the KSHV genome. This seminal discovery led to the cloning of the entire viral genome (Neipel, Albrecht et al. 1997; Neipel, Albrecht et al. 1998) (Neipel F 1997; Neipel, Albrecht et al. 1998)and its complete DNA sequenced from a BC-1 PEL cell line (Russo, Bohenzky et al. 1996).

KSHV infection is characterized by a prolonged viral and clinical latency and an infection that is lifelong like all herpesviruses. It is now possible to grow recombinant KSHV (rKSHV) *in vitro* thus making virologic characterization posible through reverse genetics experiments with deletion viruses (Zhou, Zhang et al. 2002). The infectious rKSHV was generated from a recombinant bacterial artificial chromosome by homologous recombination in KSHV-infected BCBL-1 cells. Some cell lines including HEK293 clones were infected with the rKSHV to create cellular model system for the purpose of investigating KSHV infection and pathogenisis (Zhou, Zhang et al. 2002)

1.3 KSHV epidemiology

The individual clinicoepidemiologic forms of KS have been classified as classic or sporadic (in the Mediterranean region), epidemic (or AIDS related), endemic (in Subsaharan Africa), and iatrogenic (in organ or tissue transplant patients who have become immunocompromised). Seroconversion for KSHV occurs before progression of KS and is a strong predictor of clinical disease (Kedes, Operskalski et al. 1996; Moore, Kingsley et al. 1996). The risk of KS in most populations with or without AIDS is directly proportional to the prevalence of KSHV; while in non HIV infected populations, the prevalence varies widely in geographically distinct patterns (Gao, Kingsley et al. 1996; Lennette, Blackbourn et al. 1996; Whitby, Luppi et al. 1998).

Before the AIDS epidemic, "classic" KS was noted to have geographic clustering and occurred most frequently in elderly men of Mediterranean and Eastern European ecthnicity. Evidence for an environmental (i.e. infectious) component to this disease comes from geographic differences in KS rates. In the western world, AIDS-KS predominantly affects HIV-infected homosexual men. However, in Africa, since the spread of HIV, epidemic KS has become more common in both sexes, with a dramatic lowering of the male to female ratio, especially in east Africa (Wabinga, Parkin et al. 1993).

KSHV seroprevalence in northen Europe and North America is <5% in the general healthy population. In endemic regions of east and central Africa KSHV seroprevalence is >50% in adult populations (Boshoff and Weiss 2001). However, the highest KSHV seroprevalences have been reported in Native Americans from the Amazon region of Brazil (Cunha, Caterino-de-Araujo et al. 2005; Ishak Mde, Martins et al. 2007), French Guiana (Kazanji, Dussart et al. 2005), and Ecuador (Whitby, Marshall et al. 2004), where they exceed 80%.

1.4 Transmission of KSHV

KSHV was first thought to be transmitted only sexually but recent reports point to other sources, such as casual behaviours. Routes of transmission are discussed below.

1.4.1. Sexual Transmission

Transmission of KSHV through sexual activities has been documented (Martin, Ganem et al. 1998; Blackbourn, Osmond et al. 1999). In univariate analyses, KSHV seroprevalence was significantly associated with subjects reporting either ≥2 receptive anal intercourse partners (65% vs. 33%) or ≥2 receptive oral intercourse partners (57.4% vs 16.7%) (Blackbourn, Osmond et al. 1999). It was observed that KSHV prevalence increased with the presence of sexually transmitted diseases (STDs) and the number of male sexual partners (Martin, Ganem et al. 1998). HIV and KSHV coinfected individuals produced a 10-year probability of 50% for developing KS (Martin, Ganem et al. 1998). Some reports show that transmission from male genital secretions, specifically semen is unlikely due to the low prevalence of detectable KSHV in semen samples obtained from both HIV+ and HIV- individuals (Howard, Whitby et al. 1997; Pauk, Huang et al. 2000), also (see Blackbourn and Levy 1997).

1.4.2 Organ Transplant recipients

In a study of 356 post-transplant patients with KS, 40% had visceral involvement, a manifestation of KS with poor prognosis, and 17% of those with visceral KS died from the tumour (Penn 1997). KSHV seroconversion rate is reported to be higher in liver transplant patients compared to renal transplant patients. However, renal transplant patients tend to have higher risk of developing KS (Andreoni, Goletti et al. 2001). KS

tumours can regress after withdrawal of immunosuppressive therapy, but that can also cause graft rejection or organ impairment as a result of immunological recovery (Penn 1997). Some suggested that post-transplant KS is caused by emergence of latent KSHV after previous infection (Parravicini, Olsen et al. 1997). Immunosuppression of any cause and that of transplant recipients is known to facilitate reactivation of herpesviruses, (for example, disseminated herpes zoster) and is associated with an increased incidence of herpesvirus associated lymphoproliferative malignancies (Penn 1997).

1.4.3 Casual behaviour

In KSHV-endemic areas of Africa and the Amazon, the sharp and linear increases of KSHV seroprevalence in children before puberty, with modest increases later in life (He, Bhat et al. 1998; Cunha, Caterino-de-Araujo et al. 2005; de Souza, Sumita et al. 2007), and the association of KSHV seropositivity in children having at least 1 first-degree relative who is seropositive (Plancoulaine, Abel et al. 2000) suggest non sexual transmission of KSHV within families, possibly be through saliva (Dedicoat, Newton et al. 2004).

1.5 Diseases of KSHV

1.5.1 Primary Infection

In a 15-year longitudinal study of > 100 HIV negative men to determine the natural history of primary KSHV infection, five cases of KSHV seroconversion were identified (Akula, Pramod et al. 2001). The effects of KSHV primary infection were explored in the absence of HIV coinfection and no debilitating disease was observed in the five seroconverters. Four patients exhibited clinical symptoms, which ranged from

mild lymphadenopathy and diarrhoea to fatigue and localized rash. These symptoms were significantly associated with KSHV seroconverion when compared to the 102 seronegative subjects who remained well. Organ transplantation is another clinical setting for primary infection. In a patient receiving a renal transplant, bone morrow failure was associated with a syndrome of fever, marrow aplasia, and plasmacytosis (Browning, Sechler et al. 1994).

1.5.2 Kaposi's sarcoma

It is widely understood that KSHV infection is necessary for KS to develop and that cofactors play a key role. The most important cofactor is HIV infection. The incidence of KS in the general population is 1 in 100,000 but in HIV-infected individuals it is approximately 1 in 20 (Gallo 1998), climbing to almost 1 in 3 in HIV-infected homosexual men before the introduction of HAART (Beral, Peterman et al. 1990) although the debate is whether immunodeficiency itself is the main determinant of KS or HIV has a direct role.

The four epidemiological forms of KS as described below have different clinical parameters, such as anatomic involvement and aggressiveness of the clinical course they have KSHV infection in common with indistinguishable histopathology (Ablashi, Chatlynne et al. 2002).

1.5.3 Classic KS

The classical or sporadic form of KS (CKS) is an indolent tumour affecting the elderly, preferentially men, in Mediterranean countries such as Italy, Israel and Turkey (Iscovich, Boffetta et al. 2000). The lesions tend to be found in the lower extremities and

the diease, due to its non-aggressive course, usually does not kill those afflicted. HIV infection, is not typically associated with CKS (Hengge, Ruzicka et al. 2002).

1.5.4 AIDS-KS

In the context of AIDS, KS is the most common malignancy and it is a defining illness (Goedert 2000). AIDS-KS is a more aggressive tumour than CKS and can disseminate into the viscera with a greater likelihood of death (Schwartz 1996). Unlike CKS, it presents more often multifocally and more frequently on the upper body and head regions (Hengge, Ruzicka et al. 2002).

1.5.5 Endemic KS

KSHV was prevalent in Africa prior to the HIV epidemic, and therefore, was responsible for the large prevalence of KS seen on the continent before HIV changed the scope of KS presentation (Dourmishev, Dourmishev et al. 2003). KS accounted for about 4% of childhood cancers in Cameroon from 1986 to 1993 (Kasolo, Mpabalwani et al. 1997). Prior to HIV infections, endemic KS affected men with an average age of 35 years and very young children (Wabinga, Parkin et al. 1993). KS on this continent evolved to epidemic levels with the advent of the HIV pandemic. Clinically, KS in Africa is more frequent in children (Kasolo, Mpabalwani et al. 1997; Wawer, Eng et al. 2001) and females than anywhere in else in the world and occurs in three forms. One form is similar to CKS in its course but found in young adults. The other two forms are more aggressive and are similar to AIDS-KS in their progression: one of these remains cutaneous with local tissue invasion, while another occurs most often in young children with a mean age of 3 years, is aggressive with visceral progression, but often lacks the cutaneous

involvement (Wabinga, Parkin et al. 1993). In the pre-AIDS period in Uganda, KS was diagnosed in approximately 7% of male cancer patients with no female records. However, by 1991 KS prevalence in male cancer patients had risen to about 49% becoming the most frequently reported cancer in men while prevalence in females reached about 18%.

1.5.6 Iatrogenic KS

Iatrogenic KS represents another clinicoepidemiologic peculiarity of KSHV infection that presents either chronically or with rapid progression (Hengge, Ruzicka et al. 2002). Immunosuppression that occurs in transplant patients is known to facilitate reactivation of herpesviruses (Rady, Yen et al. 1995) including KSHV, transplant patients under immunosuppressive therapy can present with KS. Withdrawal of therapy can cause the KS to regress (Hengge, Ruzicka et al. 2002). Iatrogenic KS seems to vary in its geographic prevalence, most probably reflecting the varying KSHV seroprevalence in the general populations of different countries (Dourmishev, Dourmishev et al. 2003). KS appears most frequently in renal transplant patients (Iscovich, Boffetta et al. 2000).

1.5.7 Other forms of KSHV-associated diseases

PELs contain KSHV DNA sequences (Cesarman, Chang et al. 1995). They are characterized by several pathological features, some of which are: (1) they do not exhibit Burkitt lymphoma-like morphology and do not have c-myc rearrangements; (2) they occur frequently in men; (3) they present initially as a lymphomatous effusion and remain localized to the body cavity of origin; (4) patients with PELs, especially in the context of AIDS, invariably are infected with KSHV (Cesarman, Chang et al. 1995; Nador, Cesarman et al. 1996). PEL is rare even in AIDS patients, constituting only 0.13% of all AIDS-associated lymphomas in the United States, but previous KS diagnosis confers an

increased risk of PEL relative to all other AIDS-associated non-Hodgkins lymphomas (NHL) (Mbulaiteye, Biggar et al. 2002). In non-AIDS patients, the disease has been termed "classic" PEL by Ascoli and colleagues (Ascoli, Lo Coco et al. 2002) where it presents in HIV negative patients, but with similar risk factors as CKS.

KSHV has been found variably in association with MCD which is a rare polyclonal B cell angiolymphoproliferative disorder for which vascular proliferation has been found in germinal centers (Soulier, Grollet et al. 1995). More than 90% of patients with AIDS and MCD are infected with KSHV, while no more than 40% of HIV seronegative MCD patients are infected (Soulier, Grollet et al. 1995).

Taken together, these data suggest the four epidemiological forms of KS have KSHV infection in common with AID-KS being the most aggressive. The advent of the HIV epidemic drove endemic KS to epidemic levels in Africa. KSHV induced PEL and a variant of MCD causes lymphoproliferative disorder of B cells and can induce host lymphatic and blood vascular gene modulation (see below).

1.8 KSHV Evolution and Strain Variability

The origin of KSHV and whether or not it recently entered into the human population are scientific questions that are being explored actively. Comparisons between conserved herpesvirus genes suggest that KSHV separated from the herpesvirus saimiri (HVS) lineage about 35 million years ago, corresponding to separation between their respective Old and New World monkey hosts (Moore PS 1996; McGeoch DJ 1999). Phylogenetic examination of homologous genes allows a unique evolutionary analysis because both viral and host genes can be directly compared. For example, Moore and colleagues demonstrated the phylogenetic relationship of KSHV to other herpesviruses by a single-gene comparison of Open reading frame (ORF) 25 (Major Capsid Proteins)

homologue from a lamda phage clone (KS5) and 12 members of the family *Herpesviridae.* This resulted in the assignment of KSHV to the gamma-2 sublineage of the genus rhadinovirus (Moore, Gao et al. 1996). In another example, vIL-6 genes are present in KSHV and rhesus rhadinovirus (RRV) but not in HVS, and sequence analysis lends support to the notion that the ancestral KSHV-RRV virus captured this gene after the split between New World and Old World monkey (McGeoch DJ 1999).

At least two major variants of KSHV can be distinguished based on sequence differences at the right-hand end of the genome in the region between open reading frame 75 (*ORF 75*) and the terminal repeat region. The two well characterized variants are named P (for prototype) and M (for minority) alleles (Poole LJ 1999). Interestingly, both P and M alleles preserve a functional ORF K15 gene, encoding spliced, polytopic transmembrane signaling protiens that share only 33% amino acid identity. These allelic variants could have resulted from recombination events with an unkown progenitor herpesviral genome at some point in the past. Zong and colleagues used PCR DNA sequence analysis of the ORF-K1 gene among over 60 different tumour samples from across the globe; and reported four major subtypes (A, B, C, D) and 13 distinct variants or clades in different human populations (Zong, Ciufo et al. 1999). The A & C subgroups have been reported in Europe, USA, Middle East and Asia. While the group B subgroup has been reported in subsaharan Africa; type D subgroup are reported in Asia, Australia, and the Pacific islands (Hayward 1999). Zong and colleagues later discovered N and Q alleles at the right-hand end of the genome (Zong, Ciufo et al. 2002).

1.9 KSHV Structure

KSHV is a double-stranded linear DNA virus. The long unique region (LUR) of the KSHV genome is about 140.5 kb in length (**Figure 1.2**) and contains 86 genes of

which at least 22 are potentially immunomodulatory, (see Rezaee, Cunningham et al. 2006). The LUR is flanked at each end by variable numbers of a direct repeat (TR) resulting in genome size of approximately 170 kbp (Rezaee, Cunningham et al. 2006). This genome size is slightly larger than the 153-kb genome of herpes simplex virus type 1 (HSV-1), the prototypical herpesvirus and member of the *Alphaherpesvirinae* subfamily (Roizman 2001). It is however, smaller than the 230-kb genome (Chee, Bankier et al. 1990) of human cytomegalovirus (HCMV), a member of the *Betaherpesvirinae* subfamily. Varying numbers of TR units are present in each virus, and this variation may allow an assay of virus monoclonality within cells (Russo, Bohenzky et al. 1996; Judde JG 2000). The LUR sequence has 53.5% G+C content and includes all identified KSHV ORFs, while the TR regions consist of multiple 801-bp direct repeat units having 84.5% G+C content with potential packaging and cleavage sites (Russo, Bohenzky et al. 1996).

New genes, particularly spliced genes, continue to be described from transcription studies because the initial annotations of the genome were purposely conservative. KSHV genes that are not homologous to HVS genes are given a K prefix (e.g. ORF K1 to K15) and include many of the cellular homologue genes. Some KSHV genes can functionally substitute for HVS oncogenes (Lee, Veazey et al. 1998) or are homologues of cellular genes induced by EBV oncogenes (Moore PS 1998).

Virions of KSHV appear structurally similar to those of other herpesviruses. In the electron microscope (EM), they display an electron-dense nucleocapsid within a lipid bilayer envelope; in between these two structures is the tegument. KSHV envelope bears many glycoproteins some of which are conserved herpevirus glycoproteins. For example, KSHV glycoprotein B (KSHVgB) interacts with cell surface heparin sulphate molecules to gain entry in to cells (Akula, Pramod et al. 2001) and also plays a role in egress of the virus from infected cells (Krishnan, Sharma-Walia et al. 2005).

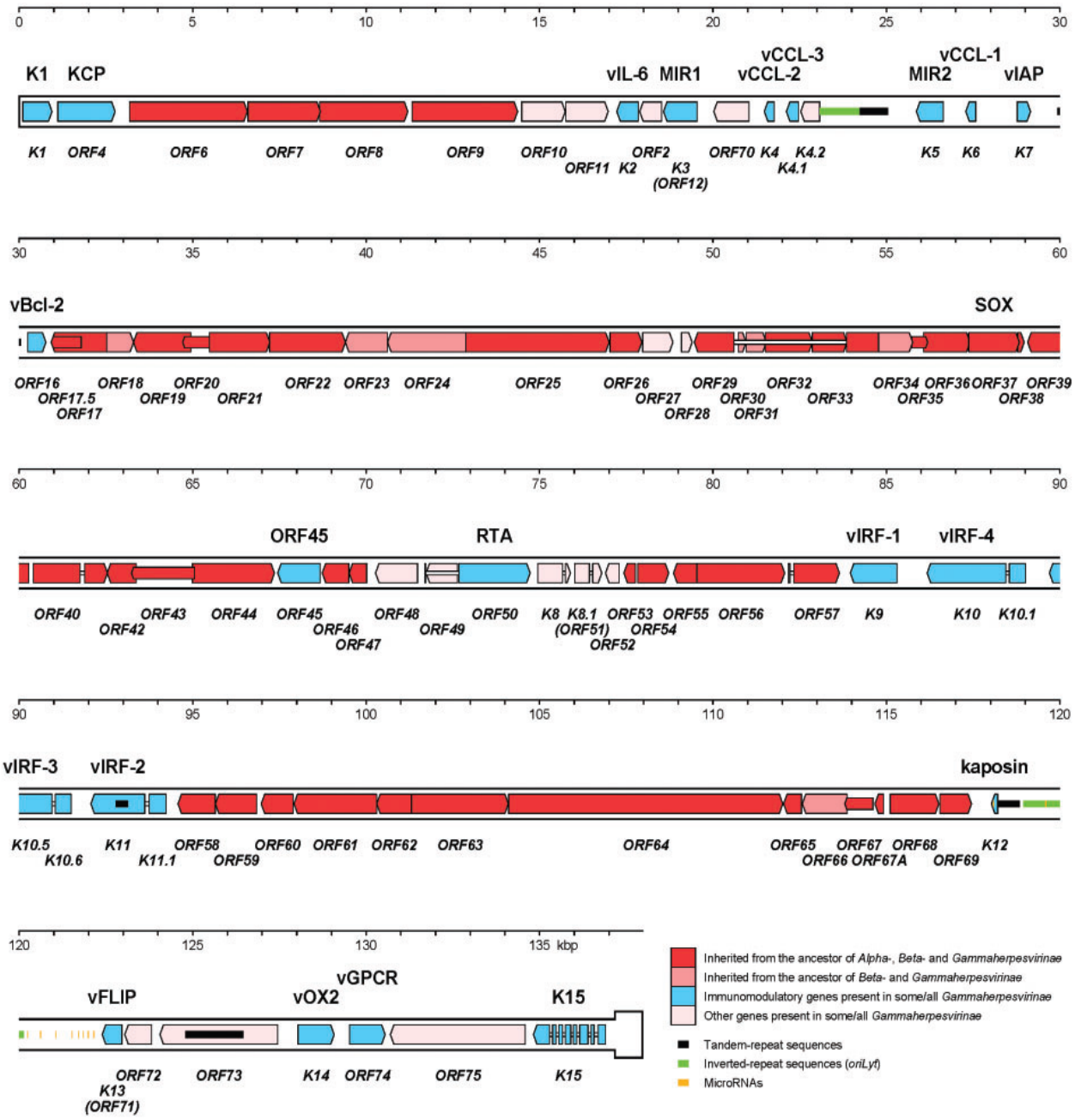

Figure 1.2. KSHV genome map. The genome consists of a unique region flanked at each end by variable numbers of a direct repeat totalling 35–45; the genome size is approximately 170 kbp. Each genome end terminates with a partial copy of TR, making it possible for circularization to create a complete copy. The coloured regions shown by arrows represent protein-coding sites (see the key). The names of the genes are shown below while the names of the encoded immunomodulatory proteins are shown above. Introns are shown as narrow white bars. This figure is reproduced from (Rezaee, Cunningham et al. 2006).

1.10 KSHV replication

Overview

Although precise knowledge of herpesvirus entry is limited, it is believed that herpesvirus enter cells by fusion of the viral envelope with the plasma membrane, resulting in the release of tegument proteins and the nucleocapsid into the cytoplasm, or alternatively by endocytosis followed by nucleocapsid release through the endosomal pore (Nicola, Hou et al. 2005). From there, capsids must be transferred to the nuclear envelope, following which the viral genome is delivered across the nuclear pore and into the nucleus. There, circularization of the genome occurs (Bruce J. Dezube 2002), which then becomes organized into chromatin via the assimilation of host histones, rendering it a suitable template for transcription by host RNA polymerase II.

As with all herpesviruses, KSHV is capable of two alternative genetic programs, latency and lytic replication. In the lytic phase, the virus produces infectious virions for dissemination and modulates cellular signalling pathways through unrestricted expression of viral genes (see Dourmishev, Dourmishev et al. 2003). During the latent phase, the virus is maintained as episomes and has restricted expression of genes which is essential for development of KSHV-induced malignancies. As a result, no virus is produced by latently infected cells; the nuclear viral genome is replicated as an episome at low copy number, and the replicated genomes are distributed to progeny cells during cell division. Although latently infected cells do not produce virus, they maintain the entire viral genome and, therefore, retain the potential for virion production (Ballestas and Kaye 2001). In fact, such cells can be induced to undergo lytic replication by a variety of exogenous signals. The identities of these signals in authentic *in vivo* infections are not

known, but in culture several agents such as sodium butyrate, phorbol ester tetradecanoyl phorbol acetate (TPA), ionomycin as well as interferon gamma and other cytokines (Miller, Heston et al. 1997; Blackbourn, Lennette et al. 2000; Chang, Renne et al. 2000).

Lytic infection involves the expression of virtually the entire viral genome, in temporally regulated cascades of transcription. The KSHV lytic switch protein whose activity is sufficient to reactivate KSHV is encoded by ORF50 locus and is known as replication and transcription activator (RTA) (Gradoville, Gerlach et al. 2000; Wang, Liu et al. 2001).

From this general overview, I take a closer look at each step.

1.10.1 KSHV Entry

Viruses have evolved to use host cell surface molecules to internalise cells through a complex multistep process and for most viruses, cell attachment and internalisation are distinct steps. When KSHV virions are applied to susceptible cell monolayers, cell binding is readily observed, even at 4^{o}C. As in HSV (Spear and Longnecker 2003), binding is initially mediated by interaction of the envelope with heparan sulphate (HS), an activity attributed to glycoprotein K8.1. Binding to heparan sulphate is thought to contribute to the efficiency of infection, because reduction in this binding by competition with soluble heparin impairs binding and reduces (but does not eliminate) infectivity (Spiller, Mark et al. 2006). The presence of residual infectivity in such studies suggest that, although helpful, HS may not be essential for infectivity, a finding compatible with the demonstration that mutant KSHV virions lacking the K8.1 glycoprotein retain infectivity in cultured cells (Luna, Zhou et al. 2004). KSHV encodes seven candidate envelope glycoproteins, but only three-gB, gH, and gL are required to mediate membrane fusion in transient expression assays that score for syncytium production (Pertel 2002). gB is reported to play critical roles in the infection process. The identification of an

argine-glycine-aspartate (RGD) integrin-binding motif in the gB sequence directed attention to integrins as possible receptor candidates. Akula and colleagues found that integrin α3β1 could be precipitated by anti-gB antibodies after initial binding of KSHV virions to cells (Akula, Pramod et al. 2002). Antibodies against the α3β1complex reduce infectivity, as do soluble versions of α3β1; RGD peptides derived from gB also inhibit infection (Akula, Pramod et al. 2002). Others have demonstrated another RGD-binding integrin, αvβ3, as a cellular receptor, which mediates KSHV entry to target cells by directly interacting with the gB (Garrigues, Rubinchikova et al. 2008). Krishnan et al also reported that besides a role in binding and entry into target cells, gB also plays a role in the maturation and egress of virus from the infected cells (Krishnan, Sharma-Walia et al. 2005).

Endothelial cells experimentally infected with KSHV express the KSHV lytic cycle protein KSHV complement protein (KCP). Because KCP is present on the virion, it is predicted to function as a ligand for virion binding to cells through heparan sulphate, and when KSHV was treated with an anti-KCP monoclonal antibody (MAb), infection of cells was inhibited by 35% (Spiller, Mark et al. 2006). These authors concluded that KCP confers on the virion its cell binding and complement evasion capability (Spiller, Mark et al. 2006).

Another study reported that the 12-transmembrane cystine transporter protein xCT as the fusion-entry receptor for KSHV in adherent cells (Kaleeba and Berger 2006). Recombinant xCT expression in non-permissive cell lines restored permissivity to authentic KSHV infection, and antibodies to xCT block infection (Kaleeba and Berger 2006). These data provide a strong case for xCT in KSHV entry. Interestingly, xCT exists as a heterodimer with the molecule CD98 and the complex is known to associate with cell

surface α3β1 (Kaleeba and Berger 2006). This gives credence to the earlier suggestion that integrins are part of the entry complex.

DC-SIGN (a type of lectin) expressed on dendritic cells (DC) is a receptor for KSHV entry to DC and macrophages. KSHV is reported to productively infect activated B cells expressing the DC-SIGN (Rappocciolo, Hensler et al. 2008). Rappocciolo and colleagues reported that this infection of B cells with KSHV was inhibited by pre-treatment of the cells with MAb against the DC-SIGN (Rappocciolo, Hensler et al. 2008). This publication was the first to confirm the role of DC-SIGN as entry receptor for KSHV (Rappocciolo, Hensler et al. 2008).

In addition to promoting virus entry, virus-cell binding triggers host cell signalling cascades, and these events alter the cellular microenvironment in a way that can favour the progression of infection. For example, virus binding to cultured fibroblasts triggers phosphorylation and activation of focal adhesion kinase (FAK); this in turn activates PI-3 kinase and PKC-zeta, events that upregulate the extracellular signal-regulated kinase (MEK-ERK) pathway (Akula SM 2004; Naranatt, Krishnan et al. 2004) known to ensure cell survival and proliferation. FAK-PI-3 kinase activation also activates Rho guanosine triphosphatase (GTPase), triggering cytoskeletal rearrangements as well (Sharma-Walia N 2004; Sharma-Walia N 2005) leading to the activation of adhesion molecules and promoting cell motility. Once capsids have been delivered to the cytosol, they must make their way to the nuclear envelope. However, how viral DNA actually enters the nucleus has yet to be examined directly in KSHV infection. Taken together, the KSHV entry in to the cell requires the concerted roles of the virus and cellular receptors stated in this subsection to ensure efficient viral entry, prevention of cell death and promotion of cell survival. Because the default replicative pathway of KSHV is latency it is discussed next.

1.10.2. Transition to latency

With the probable help of host enzymatic machinery, the linear viral DNA rapidly circularizes to form nuclear episomes upon entry to the nucleus (Bruce J. Dezube 2002). Prevailing cellular microenvironmental conditions will dictate which of the two known transcriptional programmes of the virus-latency or lytic cascade will ensue. In the first 12 hours after infection, many infected cells transiently display profiles of transcripts and antigens that indicate aberrant expression of a panoply of lytic-cycle genes, including selected members of immediate early (IE), delayed early (DE), and even late (L) classes (Krishnan 2004) whose expression ceases by 24 hours, giving way to latency. In some cases these transcripts may have been imported in to the cell by the virion (Bechtel, Grundhoff et al. 2005).

The appearance of some of these gene products can be explained by the discovery of 11 virally encoded, lytic mRNAs that are incorporated into the virion during particle assembly (Bechtel, Grundhoff et al. 2005); as with the tegument proteins, these are delivered into newly infected cells immediately on viral entry and, therefore, are available for translation. Some studies have detected small quantities of the lytic switch protein in virions (Bechtel, Winant et al. 2005; Lan, Kuppers et al. 2005), which might account for some of these observations, but why such a function would not trigger full lytic cascade is unexplained.

1.10.3 Latency

Much of the information gathered on KSHV latent gene expression comes from the study of cultured PEL cells. These cells stably maintain latent KSHV genomes and express latent viral transcripts in all cells in the culture (Ganem 2007). Although it is possible that latent gene expression in PEL is not representative of other forms of latency.

Besides, the latency programme may be variable since vIRF-3 (LANA2) is reported to be expressed in PEL cells but not in latent spindle cells (Rivas, Thlick et al. 2001). Spindle cells are elongated in shape, are of endothelial origin and are the particular cell types of the lesions infected by KSHV. Nevertheless, examination of PEL latency has revealed a number of latent functions that have been proposed to play roles in both viral persistence and disease induction. The main reservoir of latent KSHV is the B lymphocyte (Ambroziak, Blackbourn et al. 1995; Blackbourn, Lennette et al. 2000).

Below are some reported patterns of latent transcription and the functions of proteins encoded by these messages.

1.10.4 Latent Transcripts

The first transcripts to be discovered were derived from the LANA promoter located 5' to ORF73, the coding region for LANA (Dittmer, Lagunoff et al. 1998; Talbot, Weiss et al. 1999) as it is the most constitutively active in most cells that are infected with KSHV. The ORF73 gene is located in a cluster of four latency-associated genes and is expressed from a bi-cistronic singly spliced mRNA of 5.7 kb that also encodes ORF72, a viral cyclin D homologue, ORF71, a vFLIP protein and the kaposin gene (Zhong, Wang et al. 1996; Dittmer, Lagunoff et al. 1998). These kaposin transcripts are very likely responsible for a set of 12 microRNA (miRNA), which map to the 5' area of the kaposin repeats in the region. The KSHV latency gene products are discussed below.

Moreover, at least in KS, maintenance of latency is inefficient and is hypothesised to require at least low level lytic replication to infected endothelial cells (Rezaee, Cunningham et al. 2006). Lytic gene expression in this setting may therefore contribute to tumourigenesis (See below).

1.10.5 Latency-associated Nuclear Antigen

The product of ORF73 LANA (Kedes, Lagunoff et al. 1997; Rainbow, Platt et al. 1997), is a large, multifunctional protein that is localized to the nucleus of infected cells. LANA is highly immunogenic since anti-LANA antibodies were the first useful serologic markers of KSHV infection (Gao, Kingsley et al. 1996; Kedes, Operskalski et al. 1996; Lennette, Blackbourn et al. 1996). LANA has been detected in virtually every cell type in which latency has been described – endothelial, epithelial, or fibroblastic cells infected *in vitro*; PEL and KS tumour cells *in vivo*; and in many B cell in nodes from MCD (Dupin, Fisher et al. 1999).

The best-characterized function of LANA is that involved in the establishment and maintenance of the latent viral episome in the nucleus (Ballestas and Kaye 2001; Cotter, Subramanian et al. 2001). Once incoming viral genomes have been circularized in the nucleus, they must then be replicated. LANA plays many roles in this replicative process. It directly binds to DNA sequences within the terminal repeats (TR) (Cotter, Subramanian et al. 2001; Garber, Shu et al. 2001; Garber, Hu et al. 2002), an interaction that triggers semiconservative replication presumably by recruitment of host DNA replicative machinery to the genome (Grundhoff and Ganem 2003). LANA plays a critical role in a mechanism where dividing cells ensures proper partitioning of progeny KSHV episomes to daughter cells (Ballestas, Chatis et al. 1999). This finding by Bellestas and colleagues supports a model in which LANA binds to the mitotic chromosomes (via its N-terminus) and indirectly tethers the viral genome to which it is bound via its C-terminus to this structure. This tethering allows the host's chromosome segregation machinery to effectively deliver the piggy-backed viral genomes to both daughter cells following mitosis. Genetic evidence in support of this model has been provided by the observation that a KSHV mutant with a disrupted LANA gene cannot produce a stable latent episome

following infection (Ye, Zhou et al. 2004). Si and Robertson reported that stable expression of LANA in cell lines showed a dramatic increase in chromosomal instability, indicated by the presence of increased multinucleation, and aberrant centrosomes. In addition, these stable cell lines demonstrated increased proliferation as well as increased entry to S phase (Si and Robertson 2006). These authors also observed that p53 transcription and its transactivation activity were suppressed by LANA expression in a dose-dependent manner, and concluded that LANA may promote chromosomal instability by suppressing the functional activities of p53, thereby facilitating KSHV-mediated pathogenesis and cancer (Si and Robertson 2006).

LANA has also been shown to participate in the regulation of a number of cellular signaling activities by functioning as a transcriptional coactivator or corepressor (Blackbourn, Lennette et al. 2000; An, Sun et al. 2004). The evidence showing that LANA can induce B cell hyperplasia and lymphoma in transgenic mice as well as inhibit TGF-β signalling through epigenetic silencing (Di Bartolo, Cannon et al. 2008), suggest a potential role for LANA in dysregulation of B lymphocyte immune response beyond its functions related to viral genome maintenance. LANA is reported to play a role in lymphomagenesis. Fakhari and colleagues generated transgenic mice expressing LANA under the control of its own promoter, which is B cell specific (Fakhari, Jeong et al. 2006). The transgenic mice developed splenic follicular hyperplasia due to an expansion of immature B cells and increased germinal center formation (Fakhari, Jeong et al. 2006). These authors detected lymphomas in these mice indicating that LANA can activate B cells and provide the first step toward lymphomagenesis. Therefore, during LANA is not only responsible for the establishment of latency but also mediates tumourigensis.

1.10.6 v-cyclin

v-Cylin (ORF72) is a candidate KSHV oncogene with homology to the human cylin-D/Prad oncogene. Cyclin D proteins (D_1, D_2, D_3) normally associate with specific cyclin-dependent kinases (CDKs) and phophorylate Retinoblastoma (Rb) family members (Sherr 1996), which in turn librates E2F/DP-1 transactivation functions necessary to drive the cell cycle to S-phase. The primary function of cyclin D complexes is inactivation of retinoblastoma protein (pRb). In malignancies, cell cycle progression is often deregulated by mutations in these pRb G1 checkpoint pathway genes. The mRNA for this protein is derived by splicing out that for the LANA gene, yielding a bicistronic (ORF72 and 71) mRNA whose 5' gene encodes v-cylin (Talbot, Weiss et al. 1999). This protein can bind to and activate cdk6. It has several differences from host cyclin D, however: (a) it is much less active on cdk4 and (b), although both can trigger cdk6-mediated phosphorylation of Rb, the viral cyclin can also induce phosphorylation of p27, histone H1, Id-2, and cdc25a (Godden-Kent, Talbot et al. 1997; Li, Lee et al. 1997). Forced v-cyclin expression can induce S-phase entry in quiescent 3T3 cells, and also overcome an Rb-mediated growth arrest induced by cdk-inhibitors (Swanton, Mann et al. 1997). In fact, the v-cyclin-cdk6 complex is less sensitive to inhibition by cdk inhibitors such as p27, p21, and p16. Moreover, v-cyclin-cdk6 induces the degradation of p27 (Ellis, Chew et al. 1999; Mann, Child et al. 1999). v-cyclin over-expression induces transient proliferation as well as apoptosis (Ojala, Yamamoto et al. 2000). Interestingly v-cyclin may exert both growth–promoting and apoptotic functions in KS, depending on factors regulating CDK6 and v-bcl2 levels because of the observation that expression of v-cyclin in cells with elevated CDK6 accelerated entry into S phase but also led to their death by apoptosis, (Ojala, Tiainen et al. 1999). Moreover, when v-cyclin was targeted to the B-cell lineage in transgenic mice, lymphomas were observed only when the animals were also $p53^{-/-}$

(Verschuren, Klefstrom et al. 2002). Therefore, there is likelihood that the functional inactivation of p53 by LANA expression in KSHV latency might similarly potentiate the oncogenic potential of v-cyclin.

1.10.7 v-FLIP

The product of ORF71, v-FLIP is the KSHV homologue of the cellular FLICE inhibitory protein (FLIP). FLICE is the acronym for Fas-associated death domain (FADD)-like interleukin-1 beta-converting enzyme, now called caspase 8. Induction of apoptosis via death receptors (e.g. Tumour Necrosis Factor receptor 1 or Fas receptor) typically results in the formation of the death inducing signalling complex (DISC), which is made up of FADD, caspase 8 and caspase 10. Upon receptor clustering due to ligand binding, the adaptor molecules FADD & TRADD are recruited both have binding domains for the receptor and a conserved "Death effector domain" (DED) that binds and triggers the activation of caspase 8 (Hu, Vincenz et al. 1997). The death signal is then transduced through a number of cellular caspases resulting in the commencement of apoptosis. One possible mechanism of vFLIP action suggests competition with the adaptor molecule for binding to capase 8 via its DED. Others have found vFILIP to be involved in NFkB signalling. Thus, vFLIP uses its TRAF-binding domain to activte NF-kB signalling (Guasparri, Keller et al. 2004) which is antiapoptotic in most cell lines. In addition, vFLIP induced MHC-I expression through NF-kB in KSHV-infected lymphatic endothelial cells (Lagos, Trotter et al. 2007), which underscores the physiological importance of vFLIP-NF-kB interaction. Eliminating either vFLIP or NF-kB activity from PEL induces apoptosis (Godfrey, Anderson et al. 2005).

1.10.8 Kaposins

Kaposin is located immediately downstream of LANA, vCyclin and vFLIP on the KSHV latency locus. Aside from the common promoter that regulates LANA, vCyclin and vFLIP, kaposin is also regulated by a promoter located between LANA and cyclin (Li, Komatsu et al. 2002). Kaposin mRNA is the most abundant in latently infected PEL cells resulting in translated proteins some of which can transform NIH3T3 cell in culture (Muralidhar, Pumfery et al. 1998). Kaposin protein is found in every tumour cell (Staskus, Zhong et al. 1997). The expression of kaposin A ORF transforms cell in culture and induces tumour formation in athymic nude mice (Kliche, Nagel et al. 2001; Tomkowicz, Singh et al. 2005). This transforming ability is reported to be consistent with that attributed to latent genes of other gammaherpesviruses (see Damania 2004). McCormick and colleagues have reported that kaposin B induces cytokine production; for example, transfection of kaposin B into cells resulted in augmentation of both GM-CSF and IL-6 production, as determined by enzyme-linked immunosorbenassay (ELISA) of the culture medium 48 hours after transfection (McCormick and Ganem 2005).

1.11 Lytic replication

Although herpesvirus oncogenesis has been generally attributed to the activity of latent proteins, lytic proteins are increasingly believed to play an important role in KSHV tumorigenesis (see Nicholas, 2007). Grisotto and colleagues suggested that dysregulated expression of lytic genes during latent phase or during aborted lytic cycles triggers KSHV tumorigenesis (Montaner, Sodhi et al. 2003; Grisotto, Garin et al. 2006). One such KSHV lytic gene that has been frequently implicated in the pathogenesis of KSHV-associated PEL and MCD is viral IL-6, a structural and functional homologue of human IL-6 (hIL6) (Moore, Boshoff et al. 1996; Aoki, Jones et al. 2000). Lytic replication of KSHV induces

the expression of both viral interleukin-6 and hIL-6 (Jenner, Alba et al. 2001), both of which act as B-cell growth and differentiation factors and promote survival and proliferation of KSHV-infected cells (Jones, Aoki et al. 1999; Chatterjee, Osborne et al. 2002). How the lytic cycle contributes to KS development has been a matter of debate (Ganem 2007). One model suggests that growth and angiogenic factors released from lytically infected cells may influence tumour progression in a paracrine fashion. Many such factors are encoded by DE viral genes that have been identified, which include viral cytokines and chemokines (e.g. vGPCR, v-CCL1, v-CCL2, v-CCL3, v-IL-6) (Nicholas 2005).

Below, I consider these KSHV lytic proteins in more detail.

1.11.1 Cytokines

Many people have regarded cytokines as immune hormones. They are low molecular weight proteins that carry out their effects by binding to receptors on target cells. The cytokine network constitutes a communication circuit that links and orchestrates the early innate inflammatory responses and the subsequent developing adaptive immune responses to infection. The anti-cytokine strategies of viruses inhibit either cytokine production or cytokine activity (see Alcami 2003). The KSHV-related diseases, particularly KS, are associated with deregulation of the inflammatory-cytokine network (see Ensoli and Sturzl 1998; Nicholas 2005), suggesting the ability of the virus to block normal cytokine responses.

1.11.2 Viral Interleukin-6 (vIL-6)

The amino acid sequence of vIL-6 protein is 25% identical to hIL-6 (Molden, Chang et al. 1997). It displays biological properties typical for hIL-6 and IL-6 for other

species such as support of IL-6-dependent murine B9 cell growth and induction of acute-phase genes in hepatocytes (Moore, Boshoff et al. 1996; Neipel, Albrecht et al. 1997). vIL-6 also mediates signalling through the gp130 signal transducer to activate JAK/STAT and MAPK pathways (Molden, Chang et al. 1997; Osborne, Moore et al. 1999).

Chatterjee and colleagues (Chatterjee, Osborne et al. 2002) demonstrated that vIL-6 was specifically induced by treatment of PEL cells with IFN-α, and effectively blocked the cell cycle arrest and apoptotic activities of IFN-α. This report suggests that at least one role of vIL-6 is to protect latently infected cells against anti-viral host defenses mediated by IFN, and could presumably perform a similar role during *de novo* infection or lytic reactivation. The mitogenic signalling and vascular endothelial growth factor (VEGF)-inducing pro-angiogenic functions of vIL-6 (Burger, Neipel et al. 1998; Aoki, Jaffe et al. 1999; Klouche, Brockmeyer et al. 2002) suggest that it may be involved in establishing appropriate intracellular conditions for virus replication and extracellular conditions for dissemination of infected cells and virus from local sites of infection. Further, because VEGF has been reported to enhance KSHV entry into cells via post-binding events (Ford, Hamden et al. 2004), VEGF induced by vIL-6 may contribute to initial stages of KSHV infection via paracrine effects within cell populations consisting of infected and uninfected cells.

There is considerable evidence that vIL-6 does indeed contribute to disease development. As already mentioned, VEGF is induced by vIL-6 and consequently angiogenesis is promoted by the viral cytokine (Aoki, Jaffe et al. 1999). In murine models, cell lines stably expressing vIL-6, and secreting high levels of VEGF, are tumorigenic in nude mice and PEL cells introduced into nude mice develop lymphomatous effusions in a VEGF-dependent manner (Aoki, Jaffe et al. 1999; Aoki and Tosato 1999). Also, vIL-6 expression in mice led to increased haematopoiesis, plasmacytosis and organomegaly

features of MCD. vIL-6 is reported to upgrade angiopoeitin 2 (Ang2)-expression in lymphatic endothelial cells through the MAPK pathway (Vart, Nikitenko et al. 2007) and KSHV-induced Ang2 is angiogenic (Ye, Blackbourn et al. 2007). Taken together, these findings suggest that vIL-6 expression could mediate mitogenic and angiogenic activities of relevance to KSHV associated malignancies.

1.11.3 Viral Chemokines

There are three KSHV chemokines, named vCCL-1, vCCL-2 and vCCL-3, specified by ORFs K6, K4 and K4.1 respectively. The chemokines were previously called vMIP-1, vMIP-2, vMIP-3 (Moore, Boshoff et al. 1996; Nicholas, Ruvolo et al. 1997; Nicholas, Ruvolo et al. 1997). All of the KSHV v-chemokines are expressed during replication and chemoattract Th-2 cells, via their interactions either with the chemokine receptor CCR8 (vCCL-1, vCCL-2) or CCR4 (vCCL-3), and therefore have been postulated to mediate immune evasion via polarization away from anti-viral Th-1 responses (Dairaghi, Fan et al. 1999; Endres, Garlisi et al. 1999; Stine, Wood et al. 2000; Weber, Grone et al. 2001). One of the chemokines, vCCL-2, is also able to interact as a neutral (non-signalling) ligand with a range of chemokine receptors, including CCR2, CCR5, CCR10, CXCR4, and therefore to block agonist binding to these receptors, potentially mediating immune evasion via inhibition of immune cell infiltration into sites of lytic replication (Chen, Bacon et al. 1998; Luttichau, Lewis et al. 2001).

With regards to the potential roles of the v-chemokines as contributors to KSHV neoplasia, the most notable of their properties is their pro-angiogenic activity (Boshoff, Endo et al. 1997; Stine, Wood et al. 2000). Thus, as for vIL-6, the induction of angiogenic factors would be expected to have a positive influence on endothelial/KS cell activation and proliferation and also to play a role in the progression and dissemination of PEL. It

has been demonstrated that vCCL-1 can induce VEGF expression in PEL cells, suggesting that autocrine signalling by the v-chemokine can promote the release of this and possibly other angiogenic factors (Liu, Okruzhnov et al. 2001).

1.11.4 Viral G protein-Coupled Receptor (vGPCR)

G protein-coupled receptors form a diverse family of seven transmembrane spanning receptors that function in numerous cellular processes by activating signal transduction networks via heterotrimeric G proteins. Mammalian genomes encode ~ 1000 GPCRs that function to regulate physiological processes ranging from cardiac contractility to lymphocytes chemotaxis. Initiation of GPCR signaling typically occurs following the binding of agonist to the extracellular domains of the receptor. The agonist-bound GPCR, via a series of conformational changes with its transmembrane domain, enables the receptor to calalyze GDP to GTP exchange on a Gα subunit of the heterotrimeric G protein complex. The G protein complex then dissociates generating a free GTP-bound Gα subunit and a free Gβγ heterodimers, both of which can modulate the activity of various downstream effectors including phospholipase C (PLC) and adenylate cyclase to generate second messenger molecules (Janeway 2001).

Herpesviruses seem to have taken advantage of the utility of the GPCR signaling network as multiple family members encode proteins sharing sequence homology to cellular chemokine GPCRs. Just like any other oncogenic herpesvirus, the genes for these viral GPCRs homologues are postulated as having been acquired from the host genome and maintained with the viral genome throughout its co-evolution with the host. Many of the herpesvirus-encoded GPCR homologues including US28 from the human cytomegalovirus (HCMV), M33 from murine cytomegalovirus (MCMV), and ORF74 from KSHV can initiate traditional G protein signalling cascades as well as other

signalling networks involved in gene transcription, cytoskeletal rearrangement, and cell motility. Additionally, some of the viral GPCRs, including MCMV M33 for example, have been shown to affect viral pathogenesis *in vivo* (Davis-Poynter, Lynch et al. 1997; Beisser, Vink et al. 1998). KSHV GPCRs are constitutively active. Also, they contribute to KS and possibly PEL and MCD via angiogenic and cytokine-inducing activities. The strongest evidence for a pathogenic role of vGPCR comes from the finding that transgenic or vector-transduced mice expressing the receptor in endothelial or other cell types, develop endothelial lesions with remarkable resemblance to KS tumours (Yang, Chen et al. 2000; Guo, Sadowska et al. 2003; Montaner, Sodhi et al. 2003). It is noteworthy that transgenic mice expressing the engineered version of KSHV vGPCR that is unable to bind chemokines, but is unaltered with respect to constitutive activity, fails to induce high rates of KS-like lesions in transgenic mice, implicating agonist-activated Gαq/MAPK signalling and MAPK-effected VEGF induction as key to vGPCR pathogenicity (Sodhi, Montaner et al. 2000; Holst, Rosenkilde et al. 2001). However, KSHV vGPCR is known to activate a range of pro-inflammatory, growth and angiogenic factors, such as TNF-α, IL-1β, IL-2, IL-4, IL-6, IL-8, and bFGF, principally via NFkB activation, and these cytokines are also potential contributors to KS, and also PEL and MCD (Pati, Cavrois et al. 2001; Schwarz and Murphy 2001). Recent studies by Ma and colleagues showed that vGPCR upregulation of Angiopeitin-like 4 (ANGPTL4) played a prominent role in promoting angiogenesis and vessel permeability manifested by KS (Ma, Jham et al. 2010). The inhibition of ANGPTL4 effectively blocked vGPCR promotion of the angiogenic switch and vascular leakage in vitro and tumourigenesis in vivo (Ma, Jham et al. 2010). Taken together, these findings suggest these KSHV lytic genes promote tumourigenesis just like the latent gene counterparts.

1.12 Teminal membrane signaling proteins

Human γ herpesviruses contain genes located adjacent to the terminal repeat region of their genomes which encode membrane proteins that mediate signal transduction. These membrane proteins are called 'terminal membrane proteins' (TMP). TMP directly bind to a variety of signaling molecules to start signaling cascades including the PI3K, NF-κB and JAK/STAT pathways (Devergne, Hatzivassiliou et al. 1996; Gires, Kohlhuber et al. 1999; He, Xin et al. 2000).

TMP of KSHV are the highly variable K1/VIP and K15 located at left and right ends respenctively of the viral genome, see below. K1 and K15 are also lytic genes (Lagunoff 1997; Jenner, Alba et al. 2001; Nakamura, Lu et al. 2003) suspected to play roles in KSHV tumourigenesis.

1.12.1 Variable ITAM-containing protein (VIP)

An immunoreceptor tyrosine-based activation motif (ITAM) is a conserved sequence of four amino acids that is repeated twice in the cytoplasmic tails of certain cell surface proteins of the immune system. The motif contains a tyrosine separated from a leucine/isoleucine by any two other amino acids giving the signature YxxL/I (Benschop and Cambier 1999). ITAMs are important for signal transduction in immune cells; they are found in the tails of important cell signaling molecules such as the CD3 and ζ-chains of the T cell receptor complex, the CD79-alpha and -beta chains of the B cell receptor complex, and certain Fc receptors (Benschop and Cambier 1999). The tyrosine residues within these motifs become phosphorylated following interaction of the receptor molecules with their ligands and form docking sites for other proteins involved in the signaling pathways of the cell (Janeway 2001).

KSHV VIP is specifed by ORF K1, at the extreme left end of the genome. Transforming gammaherpesviruses HVS and EBV have genes at analoguos genomic positions that encode signaling membrane proteins STP (saimiri transformation-associated protein) and LMP-1 (latency membrane protein-1), and these function as transforming proteins. STP and LMP-1 are not detectably homologous and neither of these proteins is homologuos to KSHV VIP, but all three proteins are constitutively active signal transducers (Moorthy and Thorley-Lawson 1993; Jung and Desrosiers 1995; Lagunoff, Majeti et al. 1999). HVS STP is required for HVS-mediated T cell transformation *in vitro* and for tumourigenesis in infected primate models. STP can mediate transformation of Rat-1 cells, and transgenic mice expressing STP develop T cell lymphomas or epithelia tumours (depending on the STP subtype) (Duboise, Guo et al. 1998). LMP-1 is necessary for EBV-mediated immortalization of lymphocytes, can immortalize or fully transform primary cells and cell lines in culture, and gives rise to B cell lymphomas in transgenic mice (Kaye, Izumi et al. 1993; Kilger, Kieser et al. 1998). Like STP and LMP-1, KSHV K1/VIP can transform cells in culture, and can also induce plasmablastic lymphomas and sarcomatoid tumours in transgenic mice expressing K1/VIP in multiple tissues (Lee, Veazey et al. 1998; Prakash, Tang et al. 2002). Importantly, K1/VIP can substitute for STP in *in vitro* and *in vivo* transformation assays in the context of the HVS genome and virus infection. When introduced into the murine gamma-2 herpesvirus MHV-68 K1/VIP was found to induce salivary gland adenocarcinomas in 25% of infected animals (Lee, Veazey et al. 1998; Douglas, Dutia et al. 2004). Thus, there is evidence to suggest that K1/VIP may play a role in KSHV-induced malignancies.

Apart from the possible role of K1/VIP in KSHV malignancies via direct cellular transformation, the receptor may contribute to viral neoplasia, particularly KS, via the induction of agiogenic factors and inflammatory cytokines. K1/VIP is known to activate

SH2 domain-containing Src-family kinases, p85 subunit of PI3K, and PLCγ to initate a range of downstream signaling cascades (Lagunoff, Lukac et al. 2001; Tomlinson and Damania 2004; Lee, Lee et al. 2005). Of these, the PI3K/Akt pathway is of paramount importance in the regulation of cytokine expression via Akt-mediated NFkB activation (Samaniego, Pati et al. 2001). These cytokines include IL-6, IL-12 and GM-CSF. The angiogenic factors VEGF and matrix metalloproteinase 9 (MMP-9) are also induced by K1/VIP, by a mechanism involving the SH2 binding motifs that comprise the C-tail ITAM. K1/VIP internalization is recently found to be associated to its function and blocking of K1/VIP's activation of Syk and P13K prevented K1 from internalizing (Tomlinson and Damania 2008). Pro-inflammatory and angiogenic factors are likely to contribute to KS, PEL and MCD by establishing the conditions for endothelial and B cell growth and promoting infiltration of inflammatory cells into sites of infection (Aoki, Yarchoan et al. 2000).

What might the function of K1/VIP be in KSHV biology? It is possible that dual mitogenic and survival signaling via the above-mentioned effector proteins (PI3K/Akt and PLCγ) allows efficient virus replication (Lagunoff, Lukac et al. 2001; Tomlinson and Damania 2004). A unique feature of K1/VIP relative to other KSHV proteins is the fact that domains within the extracellular regions are hypervariable, apparently the result of immune pressure (Kasolo, Monze et al. 1998; Zong, Ciufo et al. 1999).

1.12.2. Latency associated membrane protein (LAMP)

K15 (LAMP) is predicted to comprise an integral membrane protein with twelve trasmembrane domains and cytoplasmic N- and C-termini (Choi, Lee et al. 2000). The C-tail of LAMP contains SH2 and SH3 signaling motifs and sequences resembling C-terminal activation region-1 (CTAR-1) of EBV LMP-1. CTAR-1 binds TRAFs 1, 2 and 3.

LAMP can activate NF-kB signalling (Glenn, Rainbow et al. 1999; Brinkmann, Glenn et al. 2003). Src-family protein tyrosine kinases Src, Lck, Hck, Yes and Fyn can associate with and phosphorylate the C-tail of LAMP, at least *in vitro* (Brinkmann, Glenn et al. 2003). The SH2-binding motif (YEEVL), rather than the expected CTAR-like motif, is said to be required for NF-kB activation. In addition to NF-kB activation, LAMP can mediate signal transduction via the Ras/Raf/MAPK pathway. Both NF-kB and MAPK signaling are dependent on the YEEVL motif and TRAF-2 binding motif also appear to require other regions of the protein that are found in the full-length LAMP but not in "truncated" products of alternatively spliced mRNAs (Brinkmann, Glenn et al. 2003). In addition to potential mitogenic and survival signaling via Src-family kinases and NFkB activation, LAMP may also promote cell survival via interaction with the Bcl-2-related anti-apoptotic protein HAX-1 (Sharp, Wang et al. 2002). While there is as yet no demonstration that this interaction promotes cell survival, LAMP and HAX-1 have been found to co-localize to mitochondria, consistent with the notion of their association *in vivo* and the possibility of such a function (Sharp, Wang et al. 2002). The pro-mitogenic signal transducing and potential anti-apoptotic activities of LAMP could be relevant to KSHV neoplasia.

Taken together, these KSHV TMPs are described as having transforming and tumourigenic properties, maintain constitutively active survival and anti-apoptotic pathways that can promote KSHV tumourigenesis.

1.13 Virological aspects of KSHV in KS lesions

KS initially present typically as a skin lesion and may be preceded by oral, nodular or visceral involvment; lesions in all variants of KS are positive for LANA-1 (Dupin, Fisher et al. 1999). In KSHV infection, KS tumour cells acquire a characteristic

enlongated shape known as spindle cells. Stained KS spindle cells (**Figure 1.3**) of the lesion indicates about 10% of KSHV infection at the initial stage which increases to about 100% in the late nodular stage (Boshoff, Schulz et al. 1995; Dupin, Fisher et al. 1999). The low level of initial infection may suggest a praracrine mechanism to dictate how the disease will progress and may be the virus induces selective growth and proliferative profile in infected cells (Boshoff, Schulz et al. 1995) indicative of hyperplasia rather that real malignancy. For example KSHV infected KS express VEGF-C (Colman and Blackbourn 2008) a growth and angiogenic factor. However, at late stages of KS lesions all spindle cells are infected with the predominantly latent virus and there is evidence of low level of lytic replication (Boshoff, Schulz et al. 1995). Established lesions are monoclonal expansion of KSHV-infected cells whereas advanced lesions are said to be oligoclonal (Duprez, Lacoste et al. 2007).

KSHV sequences are reported to be about 40-80 times more abundant in the BCBLs than in KS lesions (Cesarman, Chang et al. 1995). In BCBLs, B cell genotypes indicate clonal rearrangement of immunoglobulin genes and frequently contained EBV (Knowles, Inghirami et al. 1989). The majority of KSHV infected cells in KS and PEL are latently infected and expess IL-6 in PEL (Decker, Shankar et al. 1996).

KSHV disease progression is influenced by cofactors such as genetic, behavioural, host immune status etc. HIV coinfection and organ transplant with immunosuppressive therapy are essential cofactors in KS progression. KS regresses spontaneously with the withdrawal of the immunosuppressive therapy or with increased CD4+ cells. Moreover, it is widely known that highly active antiretroviral therapy (HAART) restores immune function and reduces KS incidence (Martro, Esteve et al. 2007).

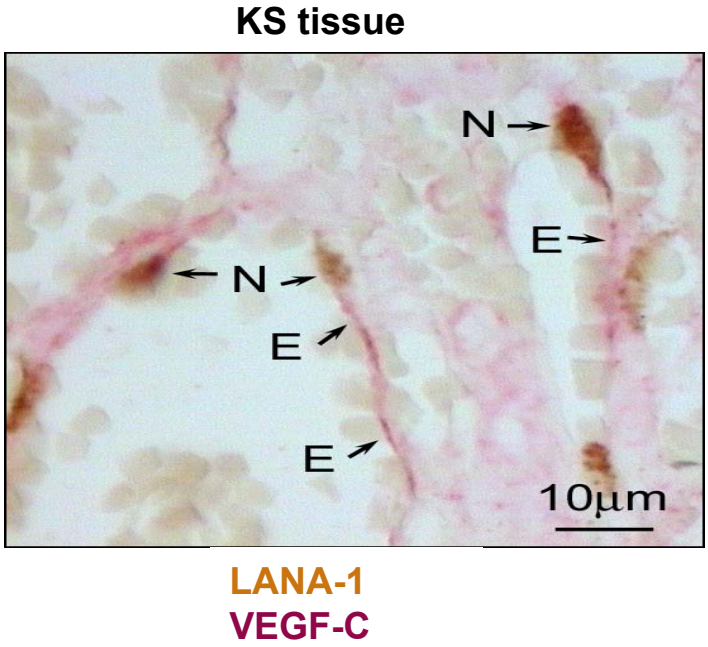

Figure 1.3 KSHV infects spindle-shaped endothelial cells in vascular tissues of KS lesions. The KS skin section was dually stained for vascular endothelial growth factor (VEGF-C) (red) and KSHV LANA-1 (brown). N=Nucleus of spindle-shaped LANA positive KS cells. E=endothelial cell cytoplasm staining for VEGF-C. This figure reproduced from (Colman and Blackbourn 2008).

1.14 Transcriptional Reprogramming

Global gene expression changes soon after KSHV infection of three susceptible cell types have been described (Naranatt, Krishnan et al. 2004) which revealed KSHV infection had a major impact on the expression pattern of cellular genes in a cell-type dependent manner. The differentially expressed genes belonged to a variety of cellular pathways. The striking cell type-specific behaviours suggested that at least in the intitial stages of infection, KSHV induced host cell gene modulation events in B cells may be different compared to observed in the adherent endothelial and fibroblast cells.

KSHV induced gene expression profile of KS is closer to lymphatic endothelial cells (LECs) than to that of blood vessle endothelial cells (BECs); KSHV infects both LECs and BECs *in vitro* (see Boshoff and Weiss 2002). This came to light when Wang and colleagues examined the impact of of KSHV infection of LECs and BECs which showed the genetic profile of KSHV-infected BECs was skewed towards that of LECs than that of uninfected BECs and vice versa. This transcriptome data demonstrate that KSHV mediates transcriptional reprogramming of both cell types resulting in their differentiation (Wang, Trotter et al. 2004). Wang et al suggested that PROX1 (a homeobox trancription factor) expression played a key role for KSHV-induced differentiation of LECs and BECs by upregulating LEC markers and downregulating BEC markers in KS tissue (Wang, Trotter et al. 2004). The role of KSHV in transcriptional reprogramming was given credence when it was reported that KSHV-encoded microRNAs (miRNAs) contribute to viral-induced reprogramming by silencing the cellular trascription factor musculoaponeurotic fibrosarcoma oncogene homogue (MAF) (Hansen, Henderson et al. 2010). MAF is expressed in LECs but not BECs. MAF drives tissue specification and terminal differentiation of a wide variety of cell types (Eychene, Rocques et al. 2008). MAF functions as a repressor of BEC-specific genes, thus maintaining the differentiation

status of LECs (Hansen, Henderson et al. 2010). However, MAF suppression in LECs was observed in KSHV-infected versus uninfected LECs, LECs transduced with KSHV miRNA versus empty lentiviral vector; the gene set enrichment analysis indicated a significant increase in expression of BEC-specific genes in the LECs infected with KSHV or transduced with KSHV miRNA (Hansen, Henderson et al. 2010). This down-regulation of MAF in LECs by KSHV miRNA suggest KSHV miRNA could contribute to the control of BEC markers through the suppression of MAF.

Another study demonstrated that KSHV upregulated Ang-2 mRNA (Ye, Blackbourn et al. 2007). Angiopoietins are necessary for blood vessel remodelling, sprouting, and maturation (Holash, Maisonpierre et al. 1999). It was further shown that KSHV infection activated a full-length Ang-2 promoter reporter construct which was in line with the induction of Ang-2 mRNA by KSHV.

Taken together, these studies show KSHV-infected cells result in the generation of a new lineage of cells adapted to provide the optimal condition for survival of the virus and concomitantly oncogenesis.

1.15 Interferons (IFNs)

Invasions by microorganisms are initially countered in all animals by the innate immune defense mechanisms that pre-exist in all individuals and begin to act within minutes of encounter of the host with an infectious agent. The innate response is described as being the first line of defence against a virus infection and involves the production of IFNs and other cytokines, activation of complement, and natural killer cells. These events in turn, stimulate the adaptive immune response, which enables recognition of antigens with a high degree of structural specificity. The effectiveness of the IFN response has led to many viruses developing specific mechanisms that antagonise the

production or actions of IFNs. Indeed, in order to replicate efficiently in vivo, it seems likely that all viruses must, at least to a degree, have some means of circumventing the IFN responses either by limiting IFN production or by blocking IFN actions (Randall and Goodbourn 2008).

IFNs are grouped into three classes called type I or IFN-α/β, type II or IFN-γ and type III or IFN-λ according to their amino acid sequence. Type I IFN was discovered in 1957 (Isaacs and Lindenmann 1957). A wide variety of interferon genes have been reported in mammals; for instance, 13 IFN-α genes, one IFN-β gene and others such as ω,ε,τ,δ, and κ (see Pestka, Krause et al. 2004) have been reported in humans. The role of ω,ε,τ,δ, and κ is not known. The biological significance of the multigenetic nature of IFNs is still contentious, as to whether IFNs are expressed differentially in different cell types, whether they are induced by different viruses and whether they have specialized funtions (Brideau-Andersen, Huang et al. 2007). T cells and natural killer cells activate the type II IFN. More recently, type III IFNs have been reported as λ1, λ2, λ3. They are referred to as IL-29, IL-28A, IL-28B respectively (Ank, West et al. 2006; Uze and Monneron 2007). Just like the type II IFNs, these cytokines are induced in direct response to virus infection and use the same signaling pathway (Onoguchi, Yoneyama et al. 2007).

The heterodimeric IFN-α receptor is composed of at least two polypeptides, IFN-αR1 and -αR2 which are used by both types I and II IFN (Pestka 2000). Two members of the Janus kinase (JAK) family, JAK1 and TYK2 (section 1.15) are recruited to this receptor upon ligand engagement and activate IFN signaling and concomittant responses (Stark, Kerr et al. 1998), that trigger the transcription of a diverse set of genes that together establish of an 'antiviral state' in target cells (**Figure 1.4**). These IFN stimulated genes are called IFN-induced or IFN-stimulated genes (ISGs). Some of these ISGs can be induced directly by viruses in IFN-independent manner but the antiviral effects are

reduced, (see Randall and Goodbourn 2008). Type I IFNs also modulate the immune system by activating effector-cell function and promoting the development of the acquired immune response.

When secreted, the type III IFN binds to receptors on cells (the IL-28 receptor, which comprises a heterodimers of IL-10R2 and IFNLR1) and elicit the same pattern of antiviral response as type I IFNs. The type III IFNs are also induced in many cells but show limited tissue distribution (Mennechet and Uze 2006; Zhou, Hamming et al. 2007). The role of type III IFNs remains elusive.

Types I and II IFNs share no obvious structural homology. However, functional similarities exist due to a broad overlap in the types of genes that they induce (Stark, Kerr et al. 1998). The importance of IFN-α/β in mediating response to virus infection is established by the fact that mice lacking IFN-α/β (Muller, Steinhoff et al. 1994; Fiette, Aubert et al. 1995) receptors are unable to mount efficient responses to a large number of viruses. Importantly, there are often differences in the requirements for types I and II IFNs in resolving specific virus infections. Both types of IFNs stimulate an 'antiviral state' in target cells, whereby the replication of virus is blocked or impaired due to the synthesis of a number of enzymes that interfere with cellular and virus processes. Both types of interferons can also slow the growth of target cells or make them more susceptible to apoptosis, thereby limiting the extent of virus spread. Finally, both types of IFNs have profound immunomodulatory effects and stimulate the adaptive response (**Figure 1.4**). However, whilst both IFN-α/β and IFN-γ influence the properties of immune effector cells, they show significant differences, and it is these extended cytokine functions that probably account for the different spectrum of antiviral activities of these types of IFNs (Randall and Goodbourn 2008).

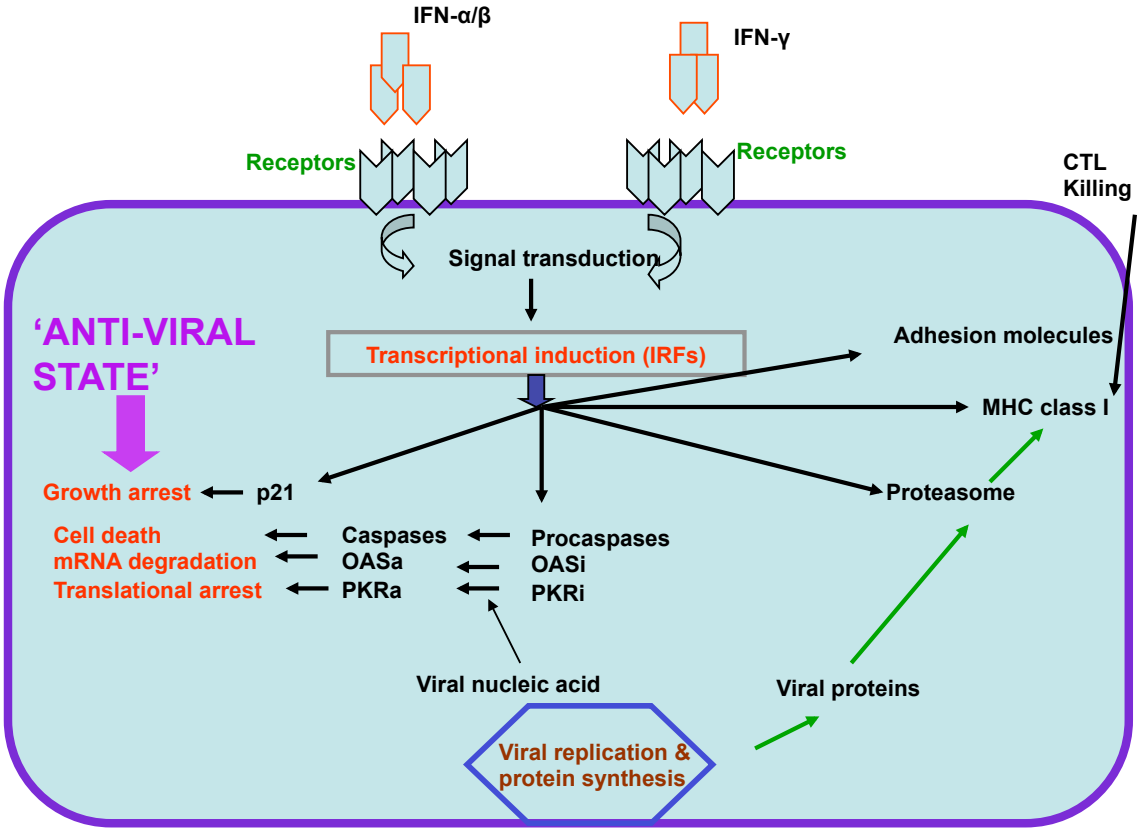

Figure 1.4. The biological effects of IFNα/β or IFNγ. IFNα/β or IFNγ molecules bind to and activate their receptors which then transmit the signals through other processes (see text) to activate interferon responsive proteins (e.g. PKR, OAS, Mx etc). Some of these enzymes are normally in an inactive state and require the presence of a viral cofactor to become activated. Their effects include mediating cell death (Caspases), translational arrest (PKR active), etc. This process eventually confers on the host cell an 'anti-viral state'. On the other hand, other interferon responsive proteins such as MHC class 1 process viral particles and present to the CTLs thereby connecting the innate immune response to adaptive immune response. IFNα/β molecules also have immunomodulatory functions such as promoting the maturation of DCs, upregulating the activities of natural killer cells and CD8+ T cells and inducing the synthesis of cytokines, such as IL-15 (promotes division of memory CD8+ T cells). This figure is redrawn from (Randall and Goodbourn 2008).

1.16 Virus induction of IFN genes

IFN induction studies have been performed using both virus and synthetic nucleic acids. Synthetic double stranded RNAs (dsRNAs) such as polyriboinosinic polyribocytidylic acid (poly I:C) has been used to efficiently induce IFNs (De Clercq 2006). Different ways by which a cell senses the presence of an invading pathogen or ways by which the host cell detects viruses and iniate IFN signal transduction through the pathogen-associated molecular patterns (PAMPs) that are detected by the pattern recognition receptors (PRRs) have been reported (Takeuchi and Akira 2010). For a long time toll-like receptors (TLRs) were the only known PRRs to sense viral nucleic acids. TLRs are membrane resident receptors found in the plasma membrane and endosomal compartments. The plasma membrane-bound TLRs generally detect molecules such as lipids and proteins, while the edosomal TLRs detect nucleic acids (Takeuchi and Akira 2010). Upon activation, TLR3, and TLR7/8 initiate a signaling cascade through adaptors TRIF and MyD88 leading to expression of IFN and proinflammatory cytokines. Recently other types of intracellular PRRs have been reported (Akira, Uematsu et al. 2006). These intracellular PRRs are the RIG-I-like receptors (RLRs) retinoic acid-inducible gene I (RIG-I) and the melanoma differentiation-associated gene 5 (MDA5) (Uematsu and Akira 2007). Both RIG-I and MDA5 are known to detect 5'triphosphate RNA and higher order RNA structures, respectively (Schlee, Roth et al. 2009; Schmidt, Schwerd et al. 2009). Ectopic expression of RIG-I enhances poly I:C responses, and small interfering RNA (siRNA) knockdowns of RIG-I limit IFN-β induction by poly I:C (Yoneyama, Kikuchi et al. 2004). MDA-5 has similar properties to RIG-I (Andrejeva, Childs et al. 2004; Yoneyama, Kikuchi et al. 2005), but binds with less avidity to poly I:C. RIG-1 and MDA5 contain a C-terminal DExD/H box RNA helicase domain as well as two N-terminal caspase recruitment domains (Yoneyama, Kikuchi et al. 2005). Binding of

5'triphosphate RNA to RIG-I mediates the activation of a signaling cascade that culminates in the expression of type I IFNs and other cytokines (see Schlee, Hartmann et al. 2009; Yoneyama and Fujita 2009).

Recently, intracellular DNA sensors capable of stimulatin IFN-α/β production and activation of NF-κB have been reported. Ablasser and colleagues showed a DNA-sensing mechanism involving RNA polymerase III and RIG-I (Ablasser, Bauernfeind et al. 2009). These authors revealed that RNA polymerase III was capable of transcribing AT-rich dsDNA into dsRNA containing the 5'triphosphate moiety, which is detectable by RIG-I (Ablasser, Bauernfeind et al. 2009). Both RIG-I and MDA5 initiate identical signaling cascades probably by acting in parallel after being triggered by their respective viral PAMPs (Yoneyama, Kikuchi et al. 2005), via the adaptor protein MAVS (known as VISA/CARDIF/IPS-1). MAVS is activated via CARD-CARD associated with RIG-I or MDA5 and transmits the signaling cascade culminating in the activation of downstream signaling events (see below), leading to the activation of IFN regulatory factor 3 (IRF-3) and NF-κB-dependant genes, including type I IFN (Yoneyama, Kikuchi et al. 2004; Kawai, Takahashi et al. 2005). Both RIG-I and MDA5 contain the N-terminal tandem CARD domains (C1 and C2) are required for interaction with MAVS CARD domain. The CARDs domains (C1 and C2) are required for down-stream signaling and constructs lacking either domain are dominant negative (Saito, Owen et al. 2008). DNA sensors are discussed more comprehensively in section 6.1

MAVS recruits and activates TRAF-6 (Xu, Wang et al. 2005) and TRAF-3 (Saha, Pietras et al. 2006). In intracellular signaling, the IKK component of NEMO acts as an essential adaptor both for NF-κB activation and TBK-1/IRF-3 activation, through its interaction with TANK (Zhao, Yang et al. 2007) (**Figure 1.5**). Once activated through phosphorylation, these transcription factor(s) relocate to the nucleus via their nuclear

localization signal (NLS) to start other processes leading to the induction and production of type I interferons.

It is commonly reported that the induction of IFN-β requires the activation of NF-κB and interferon regulatory factor 3 (IRF-3) (Paun and Pitha 2007). IRF-3 and NF-κB transcription factors reside in the cytoplasm prior to induction. Upon receipt of the appropriate signal, the C terminus of IRF-3 is phosphorylated resulting in dimerization and the unveiling of the NLS (Dragan, Hargreaves et al. 2007; Panne, Maniatis et al. 2007). The translocated IRF-3 is retained in the nucleus until it is dephosphorylated (Kumar, McBride et al. 2000). NF-κB is bound to the inhibitor of NF-κB (IκB) in the cytoplasm. When activated by upstream components of the signaling cascade in response to a viral infection, IκB becomes phosphorylated and subsequently ubiquitinated and degraded by the proteasome. The freed NF-κB translocates to the nucleus via its NLS (Wullaert, Heyninck et al. 2006). Optimal induction of the IFN-β gene also requires binding of a c-jun/ATF-2 heterodimer to the promoter (**Figure 1.5**). So that IRF-3, and NF-κB and c-jun/ATF-2 complexes assemble on the promoter in a co-operative manner to form what is known as the "enhanceasome", the formation of which is aided by the the high-mobility group (HMG) chromatin-associated protein HMGI(Y) (Merika and Thanos 2001). Once assembled the enhanceasome components aid the recruitment of CREB-binding protein (CBP)/p300 that in turn, promote the assembly of the basal transcriptional machinery and RNA polymerase II. Others (Berkowitz, Huang et al. 2002; Panne, Maniatis et al. 2004) have reported that the IRF-3, NF-κB and c-jun/ATF-2 complexes can each form a stable structure with the promoter without HMGI(Y). It is generally accepted that binding of IRF-3 and/or IRF-7 is indispensable for induction. However, the activation of both NF-κB and c-jun/ATF-2 may not be essential; for example IFN induction has been reported under conditions where NF-κB and c-jun/ATF-2 are not

activated or their binding site not required (Peters, Smith et al. 2002; Poole, He et al. 2002).

The production of IFN during viral infection leads to the induction of at least these transcription factors (IRF-1, IRF-3, IRF-7 and IRF-9) (section 1.15) that play important roles under some circumstances (Honda, Yanai et al. 2005). IRF-7 is also reported to bind to the IFN-β promoter (Panne, McWhirter et al. 2007) and can enhance transcription dramatically (Yang, Ma et al. 2004).

A recently identified adaptor protein STING (also known as MITA) (Ishikawa and Barber 2008) is required for IFN-β induction by intracellular DNA such as the synthetic oligonucleotides (poly (dA:dT)) and herpes simplex 1 virus (HSV-1). IFN-β responses to intracellular DNA involves the STING-TBK1-IRF-3 pathway (Ishikawa, Ma et al. 2009).

Taken together, these data show that viral nucleic acids or synthetic nucleic acids are detected by intracellular PRRs such as the RIG-I and MDA5, which initiate signaling cascades culminating in the induction of IFNs and ISGs of the innate antiviral pathway. Also, an intracellular DNA detector such as STING induces the IFN-β response pathway upon sensing viral infection.

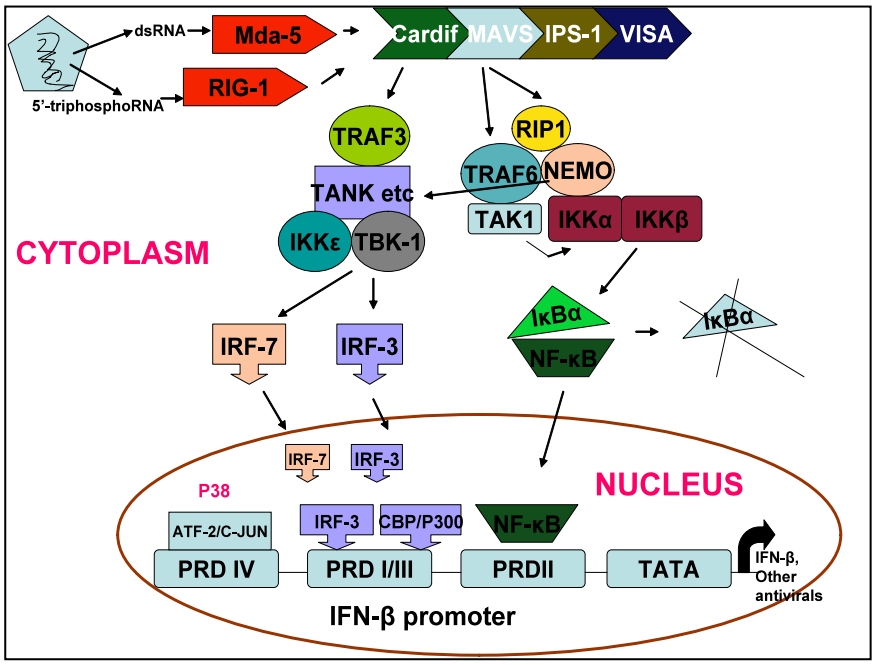

Figure 1.5. MDA-5- and RIG-I-dependent signaling. The presence of viral RNA in the cytoplasm activates the pattern-recognition receptors MDA-5 and RIG-I both of which are activated by dsRNA, whilst RIG-I can also be activated by RNA molecules with 5' triphosphates. These RNA helicases contain N-terminal CARD domains that recruit the adaptor protein Cardif/VISA/MAVS/IPS-1. This adaptor protein recruits signaling elements that feed into IRF-3 or the NF-κB routes of the IFN-β signaling pathways. NF-kB activation requires the recruitment of both TRAF6 and RIP1 to the adaptor protein Cardif/VISA/MAVS/IPS-1 and their co-operation in recruiting the IKK complex and TAK1. TAK1 phosphorylates the IKKβ subunit of the IKK complex, which leads to its activation and phosphorylation of IκB. Phosphorylated IκB is ubiquitinated and subsequently degraded by proteasomes, releasing NF-κB for migration to the nucleus and assembly on the IFN-β promoter. IRF-3 and IRF-7 activation requires that TRAF3 binds to TANK, which then binds to TBK-1 and/or IKKe, which are activated and can phosphorylate IRF-3/7 directly. The activated IRFs also migrate to the nucleus and assemble on the IFN-β promoter, either with or without NF-κB and ATF-2/c-jun, leading to the recruitment of co-factors such as CBP/p300 and RNA polymerase II and ultimately stimulation of transcription. This figure is reproduced from (Randall and Goodbourn 2008).

1.16.1 Regulatory element of the human interferon–β enhancer

The events leading to induction of transcription of the IFN-β gene provide one of the best examples of our understanding of how a set of transcription factors assemble on an enhancer to direct a specific gene expression programme (Thanos and Maniatis 1995). In humans, the IFN-β enhancer is located between nucleotides -110 and -45 relative to the transcription start site. It contains four overlapping positive regulatory domains (PRDs) that are recognised by sequence-specific trancription factors to form a transcriptionally competent enhanceosome (Merika and Thanos 2001). For example, on the IFN-β enhancer IRF-3 binds to PRDI and PRDIII elements. It interacts synergistically with NF-κB and ATF-2/c-Jun bound to adjacent PRDII and PRDIV elements respectively, and with HMGI (Y) protein (Kim and Maniatis 1997). In order to overcome histone-mediated transcriptional repression (**Figure 1.6A**), the enhanceosome recruits histone acetyl transferase (HATs) called, the general control-of amino-acid synthesis 5 (GCN5) and CREB binding protein. They acetylate lysine residues of histones H3 and H4 in the nucleosome (**Figure 1.6B**). These acetylated histones then recruit a nucleosome modification complex called, Brahma associated factor (BAF) complex, which forces the dislocation of the nucleosome from the transcription start site (**Figure 1.6C**). This nucleosomal dislocation facilitates the recruitment of the transcription complex TFIID to the promoter (**Figure 1.6D**), an essential event for the induction of IFN-β gene expression (Agalioti, Lomvardas et al. 2000).

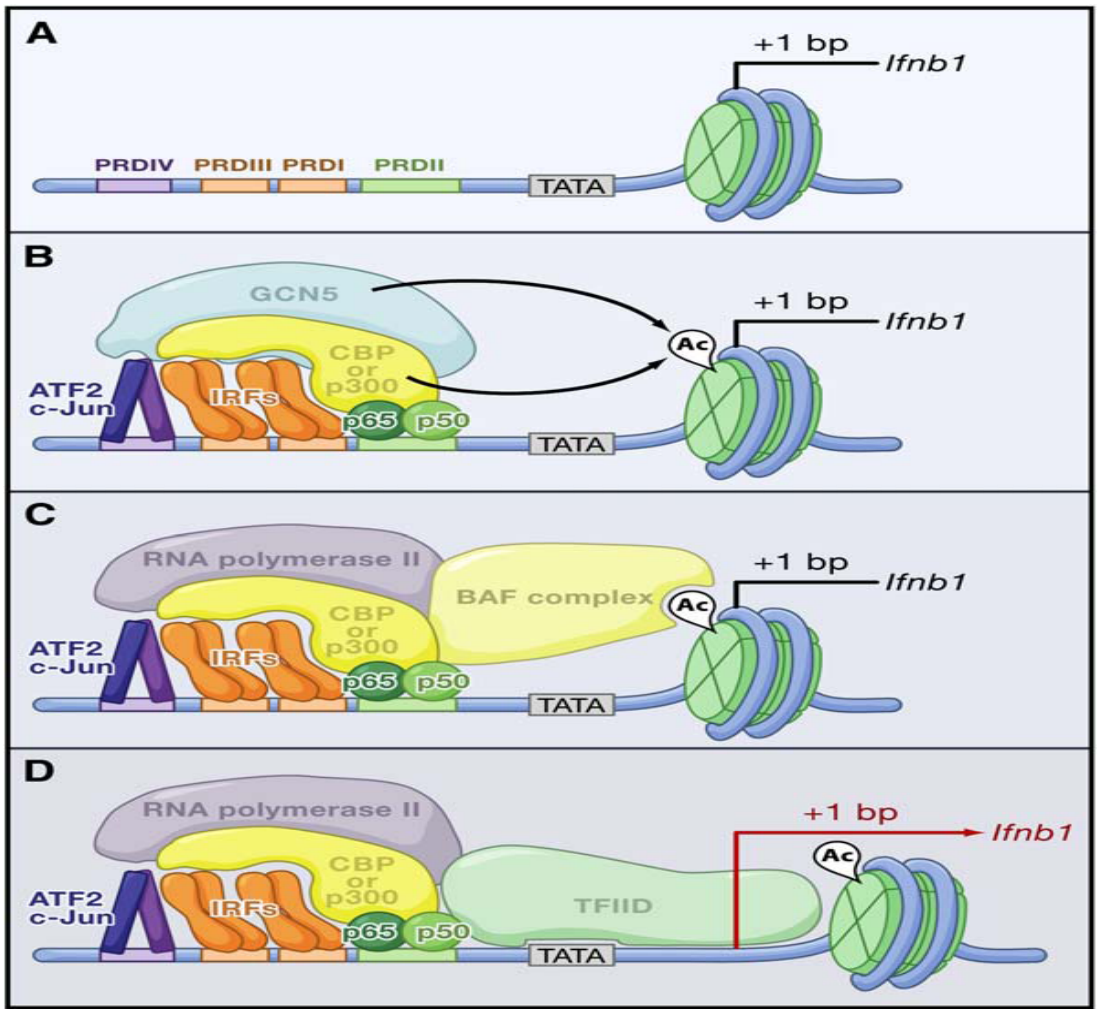

Figure 1.6. IFN-β gene transcription after viral infection. (A) The transcription start site (located at +1 base pairs, bp) of the IFN-β gene is covered by a positioned nucleosome when in the steady state. (B) During a viral infection, PRD I-IV direct the assembly of transcription factors such as ATF2, c-JUN, IRFs, NF-κB, and HMG-I(Y) on the enhanceosome. The enhanceosome then recruits HATs, such as GCN5 and CBP/p300, which acetylate (Ac) a subset of lysine residues of histones in the nucleosome. (C) Followed by the recruiment of the RNA polymerase II holoenzyme and the BAF complexes by contacting the acetylated histone. (D) The BAF complexes induce nucleosome displacement from the transcription start site, making it accessible to TFIID for the induction of IFN-β expression. This Figure is reproduced from (Honda, Takaoka et al. 2006).

1.17 Interferon regulatory factors (IRFs)

Recent studies have shown that IRFs are also involved in most PRR signaling events aside from NF-κB (section 1.14), thereby conferring a more diverse immune activation capability on the platform that links innate and adaptive immunities. The IRFs are transcription mediators of virus, bacteria and IFN-induced signalling pathways and as such play a critical role in antiviral defence, immune response, cell growth regulation and apoptosis. The IRF family of transcription factors comprises of nine members: IRF-1, IRF-2, IRF-3, IRF-4, IRF-5, IRF-6, IRF-7, IRF-8, and IRF-9 (IRF-9 is also known as ISGF3) (see Taniguchi and Takaoka 2001). These family members are reported to have a well-conserved amino (N)-terminal DNA binding domain (DBD) with tryptophan repeats resembling the DBD of myb transcription factors (see Taniguchi and Takaoka 2001). The helix-turn helix domain of the formed DBD recognises similar DNA sequences. The DBD of IRF-1 bound to the PRD1 of the IFN-β enhancer revealed that 5'-GAAA-3' is the recognition sequence of the helix turn helix motif of IRF-1 (Escalante, Yie et al. 1998). Subsequently 5'-AANNGAAA-3' was reported as the consensus IRF recognition sequence (Fujii, Shimizu et al. 1999). The 5'flanking AA sequence is essential for recognition. IRFs therefore do not bind to NF-κB sites since they contain a GAAA core sequence without a 5' flanking AA sequence. Subsequent data indicated that the interaction of an IRF DBD with the core motif GAAA result in DNA structure distortion allowing cooperative binding of another IRF DBD to the IRF binding site that usually contains dimeric repeats of the core sequence (Fujii, Shimizu et al. 1999). IRF-1, IRF-3, IRF-5, and IRF-7, have been reported as positive regulators of type I IFN gene transcription.

The rest of my discussion on the IRF family will focus on IRF-1, IRF-2, IRF-3, IRF-7 and IRF-9 because of their involvement in IFN signaling pathways. See below.

1.17.1 IRF-1 and IRF-2

Work on type I IFN led to the identification of IRF-1 as a protein that binds to the virus inducible elements of the human IFN-β gene (Miyamoto, Fujita et al. 1988). Overexpression of IRF-1 resulted in the induction of endogenous type I gene induction. However, the induction of both IFN-α and IFN-β genes occurred normally in IRF-1 defecient ($Irf^{-/-}$) mouse embryonic fibroblasts (MEFs) in response to virus infection (Matsuyama, Kimura et al. 1993). This observation means there is an IRF-1-independent mechanism of type 1 gene induction in some cells. IRF-1 expression was shown to be up-regulated during myeloid differention (Abdollahi, Lord et al. 1991). Moreso, others have confirmed IRF-1 as essential regulator of the differentiation and maturation of a subset of DCs, particularly the $CD8\alpha^{+}$ subset (Gabriele, Fragale et al. 2006). IRF-1 transcriptionally targets many genes, including those encoding nitric-oxide synthethase (iNOS) (Kamijo, Harada et al. 1994). The induction of iNOS and OAS (oligoadenylate synthetase) was impaired in IFN-γ-treated IRF-1 deficient MEFs (Kamijo, Harada et al. 1994; Kimura, Nakayama et al. 1994). However, IRF-2-/- MEFs showed about a three fold rise in type I IFN induction following Newcastle disease virus infection (Matsuyama, Kimura et al. 1993). Others reported that IRF-2 prevented virus-induced recruitment of transcriptional coactivator CBP in the IFN-β enhancesome (Senger, Merika et al. 2000). IRF-2 null mice exhibit NK cell deficiency and IRF-2 deficient NK cells show an immature phenotype and compromised receptor expression (Taki, Nakajima et al. 2005). IRF-2 was identified as a factor binding the same recognition site as IRF-1, which suppresses its transcriptional activity.

1.17.2 IRF-3 and IRF-7

The highly homologous IRF-3 and IRF-7 have been widely reported as the key regulators of the type I IFN gene expression induced by viruses (Wathelet, Lin et al. 1998) (see Servant, Tenoever et al. 2002). Overexpression of IRF-3 leads to a marked increase in virus-induced IFN-β mRNA expression (Sato, Tanaka et al. 1998). Homozygous deletion of IRF-3 in mice showed impairment in encephalomyocarditis virus (EMCV)-mediated induction of type I IFN. The expression levels of type I IFN in New Castle Disease virus (NDV) infected MEFs were also substantially decreased in this study, although IFN expression could be rescued by ectopic IRF-3 (Sato, Suemori et al. 2000). Others also showed that IRF-3 deficiency resulted in enhanced lethality in West Nile virus (WNV) infection of mice (Daffis, Samuel et al. 2007). IRF-3 plays a critical role in mediating the antiviral response because its ubiquitous expression makes it possible to stimulate the antiviral response and synthesis of IFN-β in infected cells (Lowther, Moore et al. 1999).

Conversely, the IRF-7 gene is expressed at a very low level in MEFs and is strongly induced by type I IFN through the activation of ISGF3; this induction is completely absent in ISGF3-deficient mice MEFs (Marie, Durbin et al. 1998; Sato, Hata et al. 1998). IRF-7 undergoes serine phosphorylation in its carboxyl-terminal upon viral activation resulting in nuclear translocation. Deletion of this region results in the inactivation of this transcription factor (Sato, Hata et al. 1998). Mice with a homozygous deletion of IRF-7 were unable to express type I IFN genes upon viral infection or activation of TLR9 by CpG-rich DNA, indicating that IRF-7 is also a regulator of type I IFN expression (Honda, Yanai et al. 2005). Moreover, IRF-7 is key to protective IFN-α response; as IRF-$7^{-/-}$ mice showed increased lethality to WNV compared to congenic wild type (Daffis, Samuel et al. 2008). In MEFs and splenocytes from mice doubly deficient

for IRF-3 and IRF-9 (DKO mice), in which IRF-7 mRNA induction is abolished, type I IFN mRNA induction was completely abolished (Sato, Suemori et al. 2000). These results demonstrate the distinct and essential roles of IRF-3 and IRF-7, which together ensure the transcriptional efficiency and diversity of type I IFN genes for antiviral response.

1.17.3 IRF-9

IRF-9, also called ISGF3γ/p48 is a DNA binding subunit of the hetero-trimeric transcriptional activator, termed IFN-stimulated gene factor 3 (ISGF3). ISGF-3 consists of IRF-9, STAT1, and STAT2. IRF-9 can also form a DNA binding complex with STAT1 homodimers and with STAT2 alone, with these complexes binding to DNA with the same specificity as ISGF3 (Kraus, Lau et al. 2003). The formation of ISGF3 is triggered by the type I IFN receptor-mediated signal resulting in the induction of many IFN-inducible genes (see Bluyssen, Durbin et al. 1996). Virus-induced expression of the IFN-α genes was dramatically reduced in IRF-$9^{-/-}$ and also type I receptor (IFNAR1)-deficient MEFs (Harada, Matsumoto et al. 1996), while virus-induced expression of IFN-β genes was slightly suppressed. There is evidence that ISGF3 binds to the IFN-β promoter (Kawakami, Matsumoto et al. 1995). A critical connection between type I IFNs and p53 was established when type IFNs transcriptionally activated the tumour suppressor p53 gene through ISGF3; IRF-$9^{-/-}$ MEFs failed to up-regulate p53 upon IFN-β stimulation (Takaoka, Hayakawa et al. 2003). These findings suggest that IRF-9 is a key regulator of type I pathway.

1.18 Signal transduction in response to IFNs

The biological activities of IFNs are initiated by the binding of IFN-α/β and IFN-γ to their cognate receptors on the surface of cells, which results in the activation of distinct

but related signaling pathways, known as the JAK/STAT pathways (Stark, Kerr et al. 1998). The ultimate outcome of this signaling is the activation of transcription of target genes that are normally expressed at low levels or are quiescent. The upstream regulatory sequences of most IFN-α/β-inducible genes contain a variation of the consensus sequences [GAAAN-(N)GAAA] called IFN-stimulated response elements (ISRE). The upstream regulatory regions of IFN-γ-inducible genes contain a unique element called the gamma activation sequence (GAS), which contains the consensus sequence TTNCNNNAA.

Upon IFN-α/β binding, both the IFNAR1 and IFNAR2 associate, facilitating the transphophorylation and activation of the tyrosine kinases TYK2 and JAK1 (Novick, Cohen et al. 1994). TYK2 then phosphorylates the tyrosine kinases at position 466 (Tyr466) on IFNAR1 (Colamonici, Yan et al. 1994), creating a new docking site for STAT2 through the latter's SH2 domain (Yan, Krishnan et al. 1996). STAT2 is then phosphorylated by TYK2 at Tyr690 and serves as a platform (Leung, Qureshi et al. 1995) for the recruitment of STAT1 (also through its SH2 domain), which is subsequently phosphorylated on Tyr701 by STAT2 (Shuai, Stark et al. 1993). The STAT1/STAT2 complex associates with a monomer of IRF-9 to form the ISGF3 heterotrimer that binds to the ISRE, present in the promoters of most IFN-responsive genes, and enhances their transcription (**Figure 1.7**). Initial reports indicated that the assembly of ISGF3 took place in the nucleus but Tang et al suggested that might be coordinated at the receptor (Tang, Gao et al. 2007). Thus, in response to IFN stimulation, the transcriptional co-factor CBP is recruited to the IFNAR2 chain of the receptor and catalyses IFNAR2 acetylation, which enables the receptor to create docking site for IRF-9 that in turn, also gets acetylated as do the receptor, bound STAT1 and STAT2. Acetylation of IRF-9 is required for DNA

binding, and acetylation of the STAT factors may aid ISGF3 complex assembly (Tang, Gao et al. 2007).

Type III IFN signaling (**Figure 1.7**) is reported to follow a similar pattern of response to type I IFN (Zhou, Hamming et al. 2007). IFN-γ receptors are composed of at least two major polypeptides, IFNGR1 and IFNGR2 (see Bach, Aguet et al. 1997). In unstimulated cells, IFNGR1 and IFNGR2 do not pre-associate strongly with one another (Bach, Tanner et al. 1996), but their intracellular domains specifically associate with the Janus kinases JAK1 and JAK2, respectively (Kotenko, Izotova et al. 1995; Sakatsume, Igarashi et al. 1995; Bach, Tanner et al. 1996). Binding of the dimeric IFN-γ to receptor triggers receptor dimerization (**Figure 1.7**), which brings JAK1 and JAK2 molecules on adjacent receptor molecules into close proximity (Greenlund, Farrar et al. 1994; Igarashi, Garotta et al. 1994); JAK2 is thus activated and in turn activates JAK1 by transphosphorylation (Briscoe, Rogers et al. 1996). The activated JAKs then phosphorylate a tyrosine-containing sequence near the C terminus of IFNGR1 (Tyr440-Tyr444) creating binding sites for STAT1 that interact through their SH2 domains (Greenlund, Farrar et al. 1994; Igarashi, Garotta et al. 1994) and are phosphorylated at Tyr701 culminating in their activation and receptor disassociation. The phosphorylated STAT1 proteins dissociate from the receptor and form a homodimer, which translocates to the nucleus through poorly characterized mechanism (Sekimoto, Nakajima et al. 1996). Activated STAT1 homodimers, also called gamma activated factor (GAF), bind to the specific IFN-γ activated site (GAS) that is present in the promoters of ISGs and stimulate their transcription. IFN-α/β can also induce the formation of STAT1 homodimers, albeit less efficiently than IFN-γ (Haque and Williams 1994), although the mechanism whereby STAT1 homodimers are activated by IFN-α/β remains obscure.

Some studies have revealed the important connection between STAT1 and the CRB/p300 transcription factors. The CBP/p300 family of transcription factors potentiate the activity of several groups of transcription factors (Janknecht and Hunter 1996). Both the C- and N- terminal domains of STAT1 have been shown to bind CBP/p300 (Zhang, Vinkemeier et al. 1996).

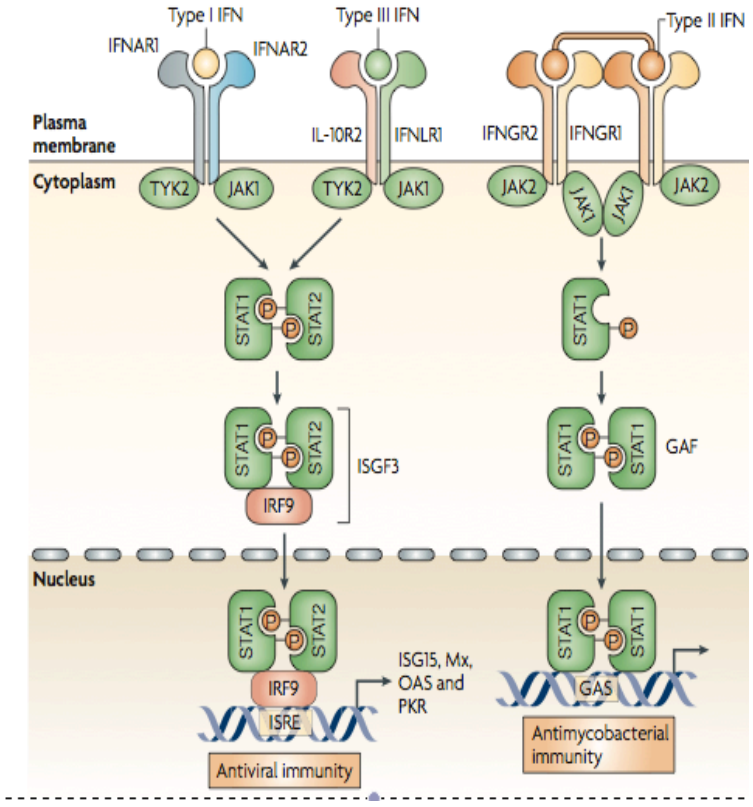

Figure 1.7. Inteferon receptor signaling. IFNs transmit signals via 3 receptor complexes: IFNAR1 & IFNAR2 bind type 1 IFNs; IL-10R2 associates with IFNLR1 to bind the three IFNλ subtypes; a tetramer consisting of two IFNGR2 chains and two IFNGR1 chains binds dimers of the type II IFNγ. When types 1 and III IFNs bind, signal transduction is initiated by the pre-associated JAK1 & TYK2, which phosphorylate IFNAR1 and lead to the recruitment and phosphorylation of the STATI and STAT2. The activated STAT1-STAT2 heterodimers associate with IRF-9 to form ISGF3. Similarly, when type II IFN binds, the activated JAKs pre-associated with IFNGRs recruit and activate STAT1 homodimers to form the GAF. These complexes translocate to the nucleus to induce IFN-stimulated genes from ISREs or GAS promoter elements, for types I and type III, or type II IFN responses, respectively. Divergence from this simplified signalling pathway can occur, for example, type I IFNs are reported to elicit STAT homodimers. This figure is reproduced from (Platanias 2005).

1.19 IFN Induced Responsive Elements

IFN induced genes and responsive elements eventually confer on the host and surrounding cells an 'antiviral state' through autocrine or paracrine activities. The number of ISGs is very large and therefore selected examples of genes and the functions of their proteins are discussed in this section to provide a representative overview of the nature of the type I IFN-induced antiviral reponse.

Therefore, I will discuss our current understanding of the role of protein kinase R, 2'5' Oligoadenylate synthetase (OAS) and Myxovirus resistance proteins in the antiviral host immune response. Other important antiviral proteins such as: the deaminases ADARI (adenosine deaminase, RNA specific) and APOBEC (apolipoprotein B mRNA-editing enzyme, catalytic polypeptide); members of the tripartite-motif-containing (TRIM) proteins; the highly IFN-induced translation regulators IFITs (IFN-induced protein with tetraricopeptide repeats) will however not be discussed in this chapter.

1.19.1 Protein Kinase R (PKR)

PKR induced by IFN is a serine/threonine kinase with multiple functions in control of transcription and translation (Clemens and Elia 1997). The two well characterized domains of PKR are the N-terminal regulatory domain containing the dsRNA binding site and a C-terminal catalytic domain that contains all of the conserved motifs for protein kinase activity (Meurs, Chong et al. 1990). Members of the PKR family of proteins phosphorylate the eukaryotic initiation factor 2α (EIF2α) resulting in the sequestration of guanine-nucleotide exchange factor EIF2β (Roberts, Hovanessian et al. 1976). The phosphorylation of EIF2α by PKR may be attributed to PKR's antiviral and antiproliferative activities. PKR is reported to be constitutively expressed in all tissues and is up-regulated in types I and II IFNs (Ank, West et al. 2006). PKR is always in an

inactive form until it becomes activated by a dsRNA or viral replication or other cofactors. It then dimerizes leading to the activation ElF2α to halt translation (Kimball 1999). Besides, elF2α phosphorylation can activate autophagy, by which the contents of a cell can be degraded (Espert, Codogno et al. 2007). Experiments in PKR-deficient mouse embryonic fibroblasts show that PKR is involved in protection against infection with several RNA viruses, including hepatitis C virus (HCV) (Noguchi, Satoh et al. 2001), hepatitis D virus (HDV) (Chen, Tsay et al. 2002), West Nile virus (WNV) (Samuel, Whitby et al. 2006) as well as some DNA viruses such as HSV-1 (Al-khatib, Williams et al. 2003).

1.19.2 2'5' Oligoadenylate synthetase (OAS)

First identified as IFN-induced proteins that generate low-molecular-weight inhibitors of cell-free protein synthesis, a distinct nature of OAS proteins is their ability to synthesize 2'5'-linked phosphodiester bonds to polymerize ATP oligomers of adenosine (Kerr, Brown et al. 1977; Kerr and Brown 1978). These unique 2'5'-oligomers specifically activate the latent form of ribonuclease L (RNaseL), which can then mediate RNA degradation (Clemens and Williams 1978). The four OAS identified in humans, termed OAS1, OAS2, OAS3 and OASL have been mapped to chromosome 12 (Hovanessian and Justesen 2007). The antiviral function of the OAS proteins has been investigated using RNaseL-deficient mice (Zhou, Paranjape et al. 1997). These mice showed increased susceptibility to RNA viruses from the Picornaviridae, Reoviridae, Togaviridae, Paramyxoviridae, Orthomyxoviridae, Flaviviridae and Retroviridae families (see Silverman 2007).

1.19.3 Myxovirus resistance (Mx) GTPase

The Mx family GTPases, which comprise MxA and MxB in humans and Mx1 and Mx2 in mice, were initially identified as antiviral proteins by the observation that the sensitivity of many inbred mouse strains to orthomyxovirus was solely due to mutation within the Mx locus on chromosome 16 (Lindenmann 1962; Haller, Arnheiter et al. 1979). This sensitivity could be rescued by restoration of Mx1 expression (Arnheiter, Skuntz et al. 1990). Interestingly, constitutive expression of the human equivalent of mouse Mx1, MxA, in IFNAR-deficent mice confers full resistance to otherwise fatal infection with Thogoto virus, LaCrosse virus or Semliki Forest virus (Arnheiter, Skuntz et al. 1990). The two human Mx proteins are encoded on chromosome 21 in a region syngeneic to the Mx region on mouse chromosome 16 (Horisberger, Wathelet et al. 1988). Members of some virus families such as: coxsackie virus (Picornaviridae) and hepatitis B virus (Hepardnaviridae) are susceptible to human MxA antiviral activity (Chieux, Chehadeh et al. 2001; Gordien, Rosmorduc et al. 2001). Besides, genetic studies of human populations have shown that a polymorphism in the MxA gene correlates with increased susceptibility to HCV (Hijikata, Ohta et al. 2000), HBV57 and measles virus, with the later associated with higher rates of subacute sclerosing panencephalitis (Torisu, Kusuhara et al. 2004). Both the central interacting domain and the C-terminal domain of Mx proteins are required to recognise target viral structures, the main viral target seems to be viral nucleocapsid-like structures (Kochs and Haller 1999).

1.20 Overview of immune modulation by KSHV vIRFs

KSHV encodes four *vIRFs* with homology to cellular *IRFs* (Russo, Bohenzky et al. 1996).These genes have probably evolved to subvert cellular *IRF* signalling, but other activities cannot be excluded and may therefore explain why the virus carries so many of

these genes. It is also possible that certain types of the *vIRFs* are expressed preferentially in different cell types or during different stages of the virus life cycle (Dittmer 2003). The *vIRFs* are not unique to KSHV, as rhesus rhadinovirus encodes nine, one of which appears to be spliced (Searles RP 1999; Alexander, Denekamp et al. 2000). KSHV vIRF-1, vIRF-2, and vIRF-3 have been cloned and characterized functionally, whilst vIRF-4 (K10/K10.1) has been detected by gene array (Jenner, Alba et al. 2001), Northern blot and RT-PCR analyses (Cunningham, Barnard et al. 2003).

KSHV vIRF-2 is the subject of the present thesis. In the following sections I will review the current understanding of the functions of each of the four KSHV vIRFs.

1.20.1 vIRF-1

The vIRF-1 protein is encoded by ORF K9. A 449 amino acid (aa) protein with homology to several IRFs. The amino terminal region contains a conserved tryptophan–rich DNA binding sequence and shows 13.4% homology to the IFN consensus sequence-binding protein (ICSBP) (Russo, Bohenzky et al. 1996). The mRNA has a size of 1.5 kb (Cunningham, Barnard et al. 2003). The expression of vIRF-1 can be induced by TPA treatment in BCBL-1 cells (Jenner, Alba et al. 2001; Cunningham, Barnard et al. 2003). Transcripts of vIRF 1 have been detected in KS biopsies by RT-PCR (Dittmer 2003) and also in MCD (Parravicini, Chandran et al. 2000). vIRF-1 (**Figure 1.8**) is a multifunctional protein; it inhibits IFN-β signal transduction as measured using an IFN-responsive ISG54 reporter construct co-transfected into HeLa and 293 cells. Some groups have shown that vIRF-1 can function as a repressor on promoters containing ISRE genes by suppressing the transcriptional activity of IRF-1 and IRF-3, interacting with them directly or competing for their binding to the transcriptional coactivator p300 (Burysek, Yeow et al. 1999; Lin, Genin et al. 2001) and that NIH 3T3 cells constitutively overexpressing vIRF-1

gained the ability to grow in soft agar and to form tumours in nude mice (Gao, Boshoff et al. 1997; Li, Lee et al. 1998). vIRF1 represses p53-dependent transcription and deregulates its apoptotic activity suggesting that vIRF1 could regulate cellular function by inhibiting p53 (Seo, Park et al. 2001). Roan and colleagues however, reported that vIRF-1 can act as a transcriptional activator in some settings (Roan, Zimring et al. 1999). Some studies showed that vIRF1 interacts with p300/CBP, inhibiting the transactivation of CBP, the histone acetyltransferase activity of p300 and the formation of transcriptionally active IRF-p300/CBP complexes (Burysek, Yeow et al. 1999; Lin, Genin et al. 2001). Another report showed that vIRF1 inhibits ataxia telangiectasia-mutated kinase (ATM) activity, leading to reduced p53 serine 15 phosphorylation and increased p53 ubiquination and degradation (Shin, Nakamura et al. 2006).

Clinical studies showed that a combination of retinoid acid (RA) and IFN inhibits cell growth *in vitro* and *in vivo* more potently than either agent alone (Lindner and Borden 1997). Retinoid-IFN-induced mortality-19 (GRIM19) is a gene associated with cell death caused by IFN/RA. In the presence of IFN/RA vIRF1 protein deregulates GRIM19-induced apoptosis (Seo, Lee et al. 2002).

Taken together, theses findings suggest vIRF-1 is multifunctional. Thus, vIRF-1 can inhibit IFN-β signal transduction, repress the functions of the promoters of some ISRE genes, causes tumour in nude mice and deregulate the apoptotic pathway by suppressing GRIM19.

1.20.2 vIRF-2

Burysek and colleagues 1999 cloned and characterised the first exon of vIRF-2 of 163 amino acid residues encoded by ORF-K11.1 (Burysek, Yeow et al. 1999), (**Figure 1.8**). These authors suggested ORF K11.1 is a DNA binding protein with specificity

distinct from the cellular IRFs because it formed homodimers, which specifically bound to the NF-κB binding site (Burysek, Yeow et al. 1999). Like vIRF-1, ORF-K11.1 bound various transcription factors including IRF-1, IRF-2, ICSBP, RelA/p65 and CBP/300 as demonstrated by pull-down assays (Burysek, Yeow et al. 1999). Subsequently, by studying KSHV-infected BCBL-1 cells, the same group revealed that the majority of ORF K11.1 was localized in the nuclear fraction while the cytoplasmic fraction showed low levels of the protein (Burysek and Pitha 2001). This finding suggested ORF-K11.1 was constitutively expressed in the nucleus.

More detailed studies by others (Jenner, Alba et al. 2001; Cunningham, Barnard et al. 2003), revealed that vIRF-2 encodes an inducible, 2.2 kbp, spliced transcript representing the two exons K11.1 and K11 from which full-length vIRF-2 protein is translated. In reporter gene assays in 293 cells, full-length vIRF-2 protein inhibited both type 1 and type III IFN-induced ISRE signaling (Fuld, Cunningham et al. 2006). Also, vIRF-2 blocked the transactivation of the full-length IFN-β reporter promoter by either IRF-3 or IRF-1 (Fuld, Cunningham et al. 2006). Recently, we reported that the inactivation of IRF-3 by vIRF-2 involved caspase 3 during poly I:C induced antiviral reponse in 293 cells (Areste, Mutocheluh et al. 2009).

These studies, suggest vIRF-2 have similar activities like vIRF-1, these activities include inhibition of IFN-β functions but unlike vIRF-1, vIRF-2 mediates signaling via IRF-3 and there are no yet reports of vIRF-2's oncogenic properties.

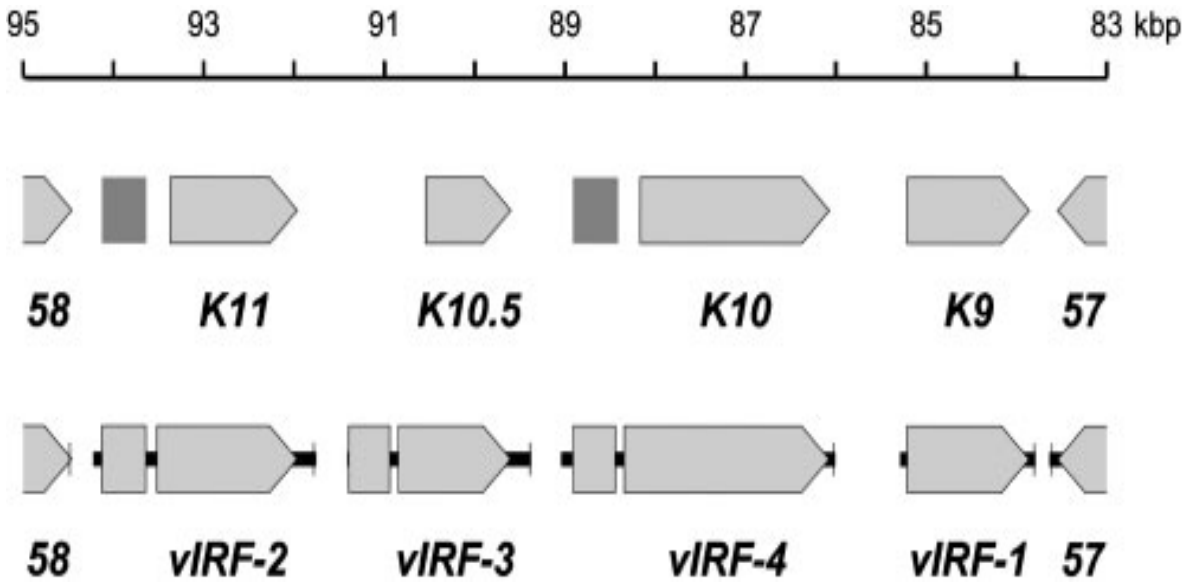

Figure 1.8. Gene arrangement in the vIRF region. The region between genes 57 and 58 (83–95 kbp) is shown in inverse orientation with respect to the HHV-8 DNA sequence (Russo et al., 1996). The shaded arrows representing the ORFs are labeled including two putative IRF regions in the shaded rectangles, which was proposed by Russo et al. (1996) Neipel et al (1997). The lower section (shaded arrows) are labeled as vIRFs and shows the expression pattern deduced from subsequent publications. RNAs and introns are shown as thick black lines. Polyadenylation signals are shown as vertical lines at the 3'-ends of mRNAs. This figure is reproduced from (Cunningham, Barnard et al. 2003)

1.20.3 vIRF-3.

vIRF-3 (also known as LANA-2), (**Figure 1.8**) has been shown to be expressed during latency in PEL cell lines, whereas the other vIRFs appear to be expressed exclusively or predominantly as lytic genes (Jenner, Alba et al. 2001; Rivas, Thlick et al. 2001; Fakhari and Dittmer 2002; Cunningham, Barnard et al. 2003). It is important to note that while vIRF-3 is a latent protein in PEL cell lines, it has also been detected in lymphocytes in MCD tissue, but is undetectable in KS cells (Rivas, Thlick et al. 2001) therefore might not be essential for KS-mediated cell survival. The size of vIRF-3 mRNA is 1.9 kb as assessed by northern blot hybridization (Cunningham, Barnard et al. 2003). The fundamental role of vIRF-3 in KSHV biology appears to be in blocking cellular IRF functions and IRF-stimulated pathways that lead to apoptosis. It has been reported that vIRF-3 can inhibit these activities of IRF-3 and IRF-7 and, as a consequence, suppress the interferon induction in response to virus infection (Lubyova and Pitha 2000). One way by which vIRF-3 inhibits IRF-7 activity is that vIRF-3 specifically interacts with either the DNA-binding domain or the central IRF association domain of IRF-7 leading to the inhibition of IRF-7 DNA binding activity and the inhibition of IFN-α production (Joo, Shin et al. 2007). Also, vIRF-3 interacts with cellular IRF-5 leading to the inhibition of IRF-5 binding to ISRE promoters (Wies, Hahn et al. 2009). vIRF-3 can also protect against apoptosis by inhibition of p53 activity, which may involve direct interactions with the tumour suppressor (Rivas, Thlick et al. 2001), and can interfere with immune response via inhibition of NF-kB-activating IkB kinase β (IKKβ) (Beissbarth, Hyde et al. 2004). The role of vIRF-3 would therefore be predicted to promote survival of latently infected cells and contribute to the KSHV malignancies involving B cells (PEL, MCD), in which it is expressed.

1.20.4 vIRF-4

vIRF-4 is encoded by the spliced genes ORF K10 and ORF K10.1 (**Figure 1.8**). It has been characterized incompletely and the extents of its functions are still unkown (Cunningham, Barnard et al. 2003; Kanno, Sato et al. 2006). Expression of K10 protein was induced by TPA in KSHV-infected PEL cell lines, suggesting K10 is a lytic proten (Katano, Sato et al. 2000). K10 protein is expressed in the nucleus by a few tumour cells in KS tissues, and also a few mantle zone B cells express K10 protein in their cytoplasm in MCD (Katano, Sato et al. 2000). Cunningham and others reported that the length of K10 gene is more than 2 kbp making it the longest of all the vIRFs (Cunningham, Barnard et al. 2003). DNA microarray analysis suggested the presence of 2 transcripts in addition to the K10/K10.1 spliced transcript (Jenner, Alba et al. 2001). Northern blot analysis showed that spliced transcript K10/K10.1 transcript (2.9 kb) was induced by TPA in TY-1 cells (Kanno, Sato et al. 2006), while western blotting analysis identifies showed a 110-kDa protein of K10/K10.1. Multiple sequence alignments revealed the K10.1 N-terminal region encoded DBD with homology to IRFs including a typtophan pentad repeat (Kanno, Sato et al. 2006). K10/K10.1 protein clustered with vIRF-1 in the same branch when a phylogenetic analysis was conducted leading to speculation that it might share similar functions to vIRF-1 (Kanno, Sato et al. 2006). Just like vIRF-1 and vIRF-3, vIRF-4 is reported to downregulate p53-mediated host immune surveillance against viral infections (Lee, Toth et al. 2009). However, vIRF-4 is reported not to inhibit early events in IFN pathway (Kanno, Sato et al. 2006).

Taken together, the immuno-modulatory potential of the three KSHV vIRFs (vIRFs 1-3) stems from their ability to down-regulate the IFN-regulatory pathway of the innate immune system. Also, the down-regulation of p53-mediated cell growth control is

a common characteristic of the four KSHV vIRFs suggesting these vIRFs deregulate the cell cycle.

1.21 Justification

In the present study, more detailed understanding of the biology of KSHV vIRF-2 has been sought. We hypothesise that KSHV has evolved to encode the vIRF-2 protein as an immune evasion strategy. The outcomes of understanding KSHV-host interactions in the context of vIRF-2 include:

1 Defining the molecular bases or details behind vIRF-2 function may further our understanding of cellular processes driving front-line defense against infecting pathogens, particularly viruses.
2 Discovering new immune system responses or components in the innate immune response to virus infection.
3 Discovering the role of vIRF-2 in KSHV biology could reveal mechanisms by which other DNA viruses evade the immune system and cause disease and therefore development of new therapies against such viruses.

1.22 Aims and objectives

We hypothesise that vIRF-2 is multifunctional and may target events up-stream and down-stream of the IFN-α receptor and other cellular genes involved in the IFN-α/β pathway. The aim of this study is therefore to determine the range and type of cellular genes whose expression is deregulated by vIRF-2. This approach will unravel cellular pathways sensitive for intervention in KSHV infected cells. These data should provide an understanding of the role of the vIRF-2 protein in the biology of KSHV.

The specific objectives are to:

1 Engineer cell clones stably transfected with an inducible vIRF-2 gene and in parallel empty vector cell clones.

2 Ensure the functionality of the vIRF-2 protein in the stable transfected cells by repeating the reporter gene experiments described (Fuld, Cunningham et al. 2006), which were originally perfomed in transiently transfected 293 cells.

3 Determine the impact of vIRF-2 on the cellular transcriptome by performing a DNA microarray investigation.

4 Confirm differential expression of vIRF-2 targeted biological pathways and their products by alternative approaches, including immunoblot assay.

CHAPTER 2 Materials and Methods

The experimental methodologies used throughout this research project will be outlined and described in this chapter, with reference to background literature where applicable. The appendices include comprehensive lists of commonly used chemicals and reagents (Appendix A), antibodies (Appendix B), plasmids (Appendix C), commonly used buffers and other solutions (Appendix D).

2.1. Mamalian cell culture techniques

The most commonly used cells in the present study are: Human embryonic kidney cells (HEK 293), African green monkey kidney cells (Vero cells) and mouse fibroblasts cells (L929 cells). The cells were cultured in culture media at 37^{o}C, in a humidified and 5% CO_2 condition. Depending on the type of experiment being conducted the cells were grown in T75 flasks, T25 flasks, 6-well plates, 24-well plates, 12-well plates and 96-well plates.

Cultured confluent cells were gently rinsed with phosphate buffered saline (PBS) and then covered in 0.5% Trypsin-EDTA for a few minutes to allow the cells to detach from each other. The flask was then given a vigorous shake by slapping it a few times to detach cells from the walls of the flask. The cells were then suspended in culture medium to quench the trypsin. Cells were plated on Dulbecco's modified Eagle's medium (DMEM) supplemented with 10% heat inactivated foetal bovine serum (FBS), 1% v/v penicillin/streptomycin, 1% non essential amino acids (this medium shall be referred to as culture medium). Aliquots of the culture cells were stored in liquid nitrogen (-196^{o}C) for long-term storage and -80^{o}C for short-term storage. Cells were counted prior to seeding the culture plates (section 2.2).

2.2. Culture cell count using trypan blue dye exclusion staining technique

Cell suspensions were diluted in 0.5% trypan blue solution (**Table 1**, **Appendix A)** the ratio ranging from 1:2 to 1:5 depending on cell concentration and incubated at room temperature for about 5 minutes after gently mixing. Dead cells normally take up this dye making it possible to distinguish between dead and live cells when counting under the light microscope. About 15 µl of Trypan blue–cell suspension mixture was transferred to both chambers of the heamocytometer (Nebauer Chamber), which was filled by capillary action. Starting with chamber 1 of the heamocytometer, all non-stained (viable) cells were counted. Each square of the heamocytometer with cover slip in place represents a total volume of 0.1 mm^3. 1 cm^3 is equivalent to 1 ml, so that cell concentration per ml was determined using the following calculations:

Cells per ml = the average count per square x dilution factor x 10^4 (a constant).

For example: if the average count per square is 50 cells x 5 x 10^4 = 2.5 x 10^6 cells/ml.

2.3 SDS-PAGE and Western blotting

2.3.1 Cell lysate preparation with lysis buffer E

Cells grown in each well of the 6-well plates were gently rinsed with ice cold PBS and suspended in 1 ml ice-cold PBS. Next, the cells were centrifuged (13,000 x *g,* 1 minute 4^o C), the pellets from each well of the 6-well plate were collected and suspended in 100 µl lysis buffer E (**Table 1, Appendix D**). The cell lysates were then incubated for ~ 20 minutes on ice and the insoluble material removed by centrifugation (13,000 x *g,* 5 minutes, 4^o C). The supernatant was transferred to fresh 1.5 ml eppendorf tubes and stored frozen at -80^{o}C.

2.3.2 Cell lysate preparation with non-ionic detergent lysis buffer

The cultured confluent cells (grown in 6-well plates) were first rinsed with ice cold PBS. 200µl of ice-cold non-ionic detergent lysis buffer solution (**Table 1, Appendix D**) was added to the cells and incubated (15 minutes, 4^{o} C) with shaking. Next, the cell suspension from each well of the 6-well plate were collected in to 1.5 ml Eppendorf tubes and sonicated for 15 seconds followed by another round of centrifugation (13,000 x *g,* 5 minutes, 4^{o} C). The supernatant was transferred to fresh 1.5 ml Eppendorf tubes and stored frozen at -80^{o}C

2.3.3 Sodium Dodecyl Sulfate PolyAcrylamide Gel Electrophoresis (SDS-PAGE)

SDS-PAGE was made to separate proteins under reducing and denaturing conditions. The resolving gel was prepared first according to **Table 2.1** and was adjusted to the desired percentage of acrylamide for different applications. The stacking gel was prepared according to **Table 2.2.**

Table 2.1 Resolving gel preparation chart

Stock solution	**Supplier**	**Acrylamide**		
		10% w/v	12% w/v	8% w/v
30% w/v Acryl/bis Acrylamide	SIGMA	5.0 ml	6.0 ml	4.0 ml
4X Tris-SDS-HCl, pH 8.8	Lab made solution	3.75 ml	3.75	3.75 ml
H_2O	Lab made solution	6.25 ml	5.25 ml	7.25 ml
10% APS	SIGMA	0.05 ml	0.05 ml	0.05 ml
TEMED	SIGMA	0.01	0.01	0.01

The resolving gel preparation chart was optimised for protein electrophoresis in the present study. The volumes shown are enough to prepare two gels of 0.75 mm, 1 mm, and 1.5 mm. The ammonium persulphate (APS) & TEMED were added last.

Table 2.2 Stacking gel preparation chart

Stock solution	Volume (ml)
30% Acryl/bis-Acrylamide	0.65
4X Tris-SDS-HCl, pH 6.8	1.25
H_2O	3.20
10% APS	0.025
TEMED	0.01

The stacking gel preparation chart was optimised for protein electrophoresis in the present study. The volumes shown are enough to prepare two gels of 0.75 mm, 1 mm, and 1.5 mm. The ammonium persulphate (APS) & TEMED were added last.

Briefly, the resolving gel mixtures were poured in to glass plate sandwiches and allowed to polymerize. The stacking gel mixtures were then poured on top of the resolving gel; combs were inserted and the gel allowed to polymerize. The desired volumes of the protein samples-2X loading buffer mixtures were then loaded on the wells of the gels. The protein markers were loaded on each gel in parallel with the samples. Gels were run at 40 mA or 150 V until the tracking dye had almost reached the bottom of the gasket. The proteins were electro blotted to polivinylidene difluoride (PVDF) membrane (**Table 1, Appendix A**) by applying 300 mA or 100 V for the desired time in a transfer chamber (**Table 1, Appendix B**).

2.3.4 Immunoblotting

The non-specific antibody binding sites on the blotted membranes were blocked with 5% w/v BSA, 1X TBS, 0.05% Tween-20 solution (**Table 1, Appendix D**) for approximately 1 hour at room temperature. Next, the membranes to which proteins had been blotted (blotted membranes) were probed with primary antibodies (**Table 1,**

Appendix B). The antibodies were diluted in the blocking buffer. The blotted membranes were incubated with the diluted primary antibody solution at 4°C with gently shaking overnight (approximately 16 hours). The blotted membranes were washed with 1X TBS, 0.05% Tween-20 solution for 2 times at 20 minutes intervals followed by another incubation step with the secondary antibodies (**Table 2, Appendix B**). The horseradish peroxidase (HRP) conjugated secondary antibodies were usually probed for 1 hour (incubation at 4°C, with gentle shaking). Following the manufacturer's instructions, the peroxidase activity of the secondary antibodies was detected with enhanced chemiluninescence (ECL) reagents (**Table 1, Appendix A**). The membranes were exposed to photographic films or X-ray films (**Table 1, Appendix A**) for a few seconds or up to 20 minutes. Protein images (bands) captured on the X-ray films were detected with Compact X4 automatic X-ray film processor.

2.3.5 Coomassie Blue staining

Where necessary, polyacrylamide gels were stained with Coomassie Blue solution (**Table 1, Appendix D**) with agitation for 30 minutes at room temperature and then destained in a destaining solution. Gels were then vacuum-dried on to Whatmann paper at 80°C for approximately 60 minutes.

2.4 Molecular techniques

2.4.1 RNA isolation

Total cellular RNA was isolated with RNAeasy mini kit (**Table 1, Appendix A**) according to the manufacturer's instruction. Briefly, cultured cell pellets from a 6-well plate were disrupted with the desired volume of the lysis buffer RLT. Using a blunt 20-

guage needle (0.9 mm diameter) fitted to an RNase-free syringe, the lysate was passed through at least 5 times. 70% ethanol was added to the homogenized lysates, which were then transferred to an Rneasy spin column and centrifuged (10,000 x *g*, 15 seconds, 4^{o}C) to allow the total RNA to bind to the membrane resins. This centrifugation was followed by 3 wash steps: (1) Buffer RW1 was added to the Rneasy spin columns and centrifuged (10,000 x *g*, 15 seconds, 4^{o}C) to wash the spin columns membranes, (2) buffer RPE was added to the Rneasy spin columns and centrifuged (10,000 x *g*, 15 seconds, 4^{o}C), this step was repeated. The Rneasy columns were then transferred to fresh Eppendorf collection tubes. Approximately 50 µl of Rnase-free water was added directly to each spin column membrane and centrifuged (10,000 x *g*, 15 seconds, 4^{o}C) to elute the ultra pure total RNA. Next, the concentration of the ultra pure total RNA was measured by spectroscopy (Nanodrop).

2.4.2 Complementary DNA (cDNA) synthesis

RNA for real time PCR assays was first reverse transcribed to cDNA using 1µg of the ultra pure total RNA in a 20-µl reaction volume. TaqMan mixture was used for the qPCR. Briefly, in a nuclease free microcentrifuge tube the following were added: 0.5 µl of random primers, 1 µg of RNA, 1 µl 10 mM of dNTP mix (10 mM each dATP, dGTP, dCTP and dTTP at neutral pH. Sterile distilled water was added to 11 µl and the mixture was incubated (65^{o}C, 5 minutes) and immediately placed on ice. Next, the following were added: 4 µl of 5X First–Strand Buffer, 2 µl 0.1 M DTT and 1 µl RNaseOUT (Recombinant Ribonuclease Inhibitor 40 units/µl (**Table 1, Appendix A**). The contents of the tube were gently mixed and incubated (37^{o}C, 2 minutes) followed by the addition of 1 µl (200 units) of M-MLV RT (**Table 1, Appendix A**), mixed again and incubated at room temperature for 10 minutes. The reaction was incubated (37^{o}C, 1 hour) and stopped by

further incubating (70^{o}C, 15 minutes). The cDNA was then ready to be used as template for amplification by PCR.

2.4.3 vIRF-2 primer and probe design

Real time PCR primer pairs were designed to amplify a 140 bp amplicon of the vIRF-2 gene. The primer sequences were: Forward 5'-TGGTTCCTGCGTCAAGTACA-CA-3' and reverse 5'-TATTAAGGACGGCCAATCGAGC-3'. The GC content of the primers was 50%. The vIRF-2 TaqMan probe was designed as: 5'-CACATCCCTTGTAT GGCCTAGGTG-3'. This 24 bp (50% GC) probe annealed 10 bp downstream of the 5'end of the forward primer. The probe was labelled with fluorescent reporter dyes; 6-FAM and quencher dye-TAMARA, at the 5' and 3' ends respectively. The primers and probe were designed to suit the following cycling conditions: a melting temperature (Tm) of 60^{o}C +/- 2^{o}C for each primer, a maximal Tm difference for both primers of $\leq$ 2^{o}C, a GC content of 50%, the primer lengths were 22 nucleotides. The GAPDH primers/probe mix (a predeveloped TaqMan Assay Reagent) (**Table 1, Appendix A**) was employed to amplify the GAPDH gene. The CT values were determined by the automated threshold analysis (ABI PRIZM software; Applied Biosystems).

2.4.4 Primers and probe efficiency measurements

Primers and probes efficiency values were measured using the C_T slope method. The 'slope' is a regression coefficient calculated from the regression line in the standard curve. This method involves generating a dilution series of the target template and determining the C_T value for each dilution. A plot of C_T versus log cDNA concentration was constructed. With this method, the expected slope for a 10-fold dilution of template DNA is approximately -3.32 indicating 100% amplification. In this study, % of

amplification efficiency was preferred over slope values. Calculations and data analyses were performed with the 7500 Software v2.0 Applied Biosystems.

2.4.5 Relative gene expression level was determined with Delta Delta C_T ($\Delta\Delta C_T$)

The relative level of gene expression was calculated using the $\Delta\Delta C_T$ method. The $\Delta\Delta C_T$ analysis of the data was performed automatically by the 7500 software package. Data are therefore presented as the fold change in gene expression normalized to an endogenous reference gene (*GAPDH* for this study) and relative to untreated control (calibrator sample). For the time course of gene expression experiments the calibrator sample represents the amount of transcript that is expressed at time zero.

Briefly, the relative expression (RE) of each target gene was calculated by normalising to the C_T value of endogenous control and relative to the calibrator sample (untreated control). This method assumes that amplification efficiency of both the target and endogenous control genes is very similar and close to 100% (± 10%).

2.5 Plasmid DNA propagation and purification with EndoFree plasmid Maxiprep Kit

Plasmid DNA was extracted from bacterial cultures with the Endo-free MaxiPrep kit (**Table 1, Appendix A**). Thus, the *E.coli* DH5α strain habouring pISRE-luc, or pRLSV-40-luc used in this study was retrieved from glycerol stocks and plated on Luria Bertani broth (LB) containing 100 µg/ml ampicillin and incubated (37^{o}C, 16 hours). Next, a single bacterial colony was picked and inoculated in a 3 ml LB medium containing 100 µg/ml ampicillin to generate a starter culture. Following incubation (37^{o}C, 16 hours) with

vigorous shaking, the starter culture was diluted 1:1000 in LB containing 100 µg/ml ampicillin and further incubated (37^{o}C, 16 hours) with vigorous shaking. At this stage the culture reached approximately 3-4 x 10^{9} cells/ml. The bacterial cells were harvested by centrifugation (4000 x *g*, 4^{o}C, 10 minutes). The pellets were recovered and the plasmid DNA was extracted using the EndoFree Maxi Prep Kit according to the manufacturer's instructions. Briefly, the bacterial cells were lysed with the 250 µl of the lysis buffer P2. Next, the released proteins were precipitated using buffer N3. Each sample was then centrifuged (13 000 x g, 4^{o}C, 10 minutes) and the supernatant applied to the QIAprep spin column. The QIAprep spin columns were washed by adding 0.5 ml of buffer PB before centrifuging (13 000 x g, 4^{o}C, 1 minute) and the flow through discarded. Another wash step involved the use of 0.75 ml of wash buffer PE. After the flow through was discarded another centrifugation step was carried out to remove residual wash buffer. The QIAprep column of each sample was placed in a fresh 1.5 ml tube and the DNA eluted by adding 50 µl of buffer EB to the QIAprep spin column and centrifuged (1300 x g, 4^{o} C, 1 minute). Plasmid yield was determined by spectroscopy (Nanodrop) and the quality was further confirmed by resolving on 1% agarose gel (**Figure 2.1**)

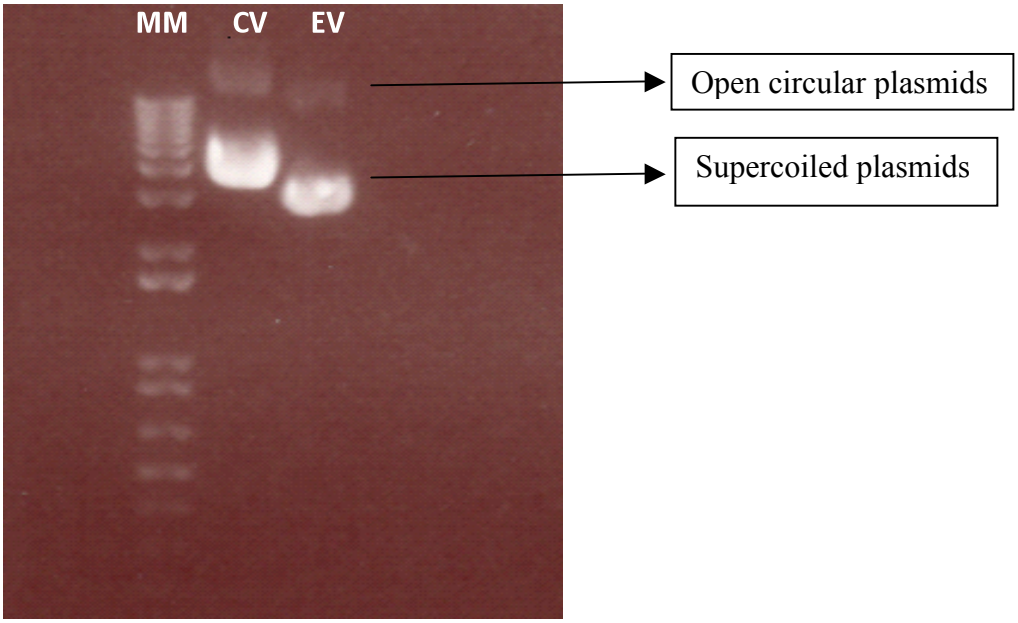

Figure 2.1 Agarose gel analysis of purified representative plasmid DNA. 1 µg of plasmid–1X loading buffer mixture of CV or EV was resolved on 1% agarose gel for analysis of purity after the Endotoxin Free Maxi Prep. 1 kb DNA ladder was loaded in parallel. The gel was run at 50 V for 1 hour. MM = DNA ladder, CV = Control vector, EV = empty vector: Lysates containing supercoiled (lower big bands) and open circular plasmid DNA (upper faint bands) are visible.

2.6 Reporter gene assays

2.6.1 Transient transfections

Cells were grown to confluence with initial seeding density of $5x10^5$ cells in 6-well plates and incubated overnight (~ 17 hours) in antibiotic free medium. The medium in each well of cells was replaced with fresh one (each well contained 2 ml culture medium). A transfection mixture containing the required amount of DNA (**Table 1, Appendix C**) and Lipofectamine (**Table 1, Appendix A**) in antibiotic free and serum free medium was made and incubated at room temperature for 20 minutes. Next, 250 µl of the transfection mixture was plated on each well of cells. The cells were then harvested 24 hours post transfection. Where reporter plasmids expressing the firefly luciferase gene were transfected, cells were cotransfected with a plasmid constitutively expressing the *Renilla* luciferase to which the firefly luciferase activity was normalized.

2.6.2 Dual Luciferase Reporter Assay

The reporter enzymes of two distinct luciferase reporter genes expressed in a single cell or within a single system can be simultaneously measured by the dual luciferase assay (DLA) with the luciferase assay kit (**Table 1, Appendix A**). In general, an "experimental" reporter gene is co-transfected with a "control" reporter gene, which serves as internal control and the baseline response to which the experimental reporter gene is normalized. This is necessary to minimise errors such as transfection inefficiency, differences in pippetting volumes, incomplete cell lysis or cell growth variability. In dual luciferase reaction (DLR) the activities of firefly (*Photinus pyralis*) and *Renilla* (*Renilla reniformis*) luciferases are measured sequentially from a single sample. The DLR systems are quantified using a luminometer. The firefly luciferase is first quantified by adding the Luciferase Assay Reagent II (LARII) to generate a stable luminescent signal, which is

quenched or stopped after the data is recorded. The *Renilla* luciferase activity is then simultaneously measured by adding the 'Stop & Glo' reagent to the same tube; it also generates a stable signal. This is possible because of the distinct structures of both the firefly (61 kDa monomeric protein) and *Renilla* (36 kDa monomeric protein) luciferases to selectively discriminate between their respective bioluminescent reactions. Photon emission is achieved through oxidation of beetle luciferin in a reaction that requires ATP, Mg^{2+} and O_2. The luminescence signal generated by *Renilla* luciferase utilizes O_2 and coelenterate-luciferin (coelentrazine). The luciferase assay reagents contain coenzyme A (CoA), which stabilises and significantly intensifies the luminescence signal. The firefly luciferase assay is very sensitive and extends over a linear range over seven orders of magnitude in enzyme concentration (sourced from Promega website, DLR Laboratory manual).

Therefore, luciferase activity was quantified by DLR assay, according to the manufacturer's instructions. Briefly, adequate volumes of the following solutions and reagents were prepared immediately before the start of the assay: 1 part of the 5X Passive lysis buffer was added to 4 parts of sterile distilled water to make up 1X passive lysis buffer. 20 µl of 50X Stop & Glo® substrate was added to 980 µl of the Stop & Glo® buffer contained in a polypropylene tube. The LAR II, Stop & Glo® Reagent and the samples were warmed to room temperature prior to performing the DLR assay. The two auto-injectors of the luminometer were purged by repeat priming/washing with 2 ml of sterile distilled water per each auto-injector. The system was then primed with 600 µl of LARII and 600 µl of the Stop & Glo Reagent solutions; both reagents used separate injectors. The luminometer was programmed to perform a 2-second premeasurement delay, followed by a 10-second measurement period for each reporter assay. The data

were automatically saved to Excel spread sheet (Microsoft). Normalised pISRE-luc activity was calculated as: Firefly luminescence / *Renilla* luminescence.

2.7 Creating a stable cell line engineered to individually express vIRF-2 clone 3-9

The clone 3-9 cell line, engineered to be stably transfected with an inducible vIRF-2 gene was constructed by Blackbourn et al prior to the start of the present study. The details of construction follows. The vIRF-2 gene was subcloned in to the pTRE2-pur-Myc Vector (Clontech) (**Table 1, Appendix C**). This plasmid is a Tet expression vector for tetracycline-regulated expression of a gene of interest bearing a Myc tag for use with the Tet-On and Tet-Off gene expression and the Tet-On and Tet-Off Cell lines (Gossen and Bujard 1992; Gossen, Freundlieb et al. 1995; Vectors: 2000). The vector also contains a gene for puromycin resistance regulated by an SV40 promoter. The Tet Expression Systems and Cell lines gives researchers ready access to tetracycline-regulated expression systems as described (Gossen, Freundlieb et al. 1995).

The HEK 293 Tet-On cells express the reverse tetracycline-controlled transactivator (rtTA) so that in the presence of tetracycline or doxycycline, rtTA binds TRE and activates transcription of the downstream gene. The 293 Tet-On cells were therefore transfected with the pTRE2-pur-Myc-*vIRF-2* or pTRE2-pur-Myc-*luc* or left untransfected using a lipid-based transfection reagent. Following antibiotic selection with G418 and puromycin, the cell clone carrying the *vIRF-2* expression cassette was obtained by limiting dilution and was called the 'vIRF-2 clone 3-9'. vIRF-2 expression was confirmed by both immunofluorescent assay and dual luciferase assay. The empty parental vector pTRE2-pur-Myc lacking *vIRF-2* was transfected in parallel to create an "empty vector" (EV) cell line lacking vIRF-2 expression.

Using similar techniques I constructed the vIRF-2 sister clones and their empty vector counterparts for the purpose of this study, see below (section 2.8).

2.8 Deriving vIRF-2 expressing and empty vector counterpart stable cell lines

First, HEK 293 Tet-On cells were transfected as described (section 2.6.1) with pTRE2pur-Myc (1000 ng/well) or pTRE2pur-myc-*vIRF-2* (1000 ng/well) or pTRE2-pur-Myc-*luc* (1000 ng/well) using a 6-well plate (**Table 1, Appendix C**). Approximately 24 hours post transfection; the medium in each well of cells was replaced with fresh medium supplemented with 400 µg/ml G418, 1 µg/ml puromycin and 3 µg/ml fungizone (**Table 1, Appendix A**). The medium was changed weekly until confluent growth of oligoclonal stable cell lines was achieved. Aliquots of each cell line were stored frozen in liquid nitrogen. The next task was to derive clones from each of the oligoclonal cell lines. Briefly, $1x10^6$ cells of each of these cell lines was plated in T25 flask containing DMEM supplemented with 400 µg/ml G418, 1 µg/ml puromycin and 3 µg/ml fungizone (**Table 1, Appendix A**). Upon reaching confluence the cells were trypsinised as described in section 2.1. Each cell line was suspended in the culture medium and diluted to 0.3 cells/100 µl medium and 100 µl was plated in to a 96-well flat bottom plate and incubated (37^oC, 5% CO_2) until confluent growth was achieved. Any outgrowing clones were expanded to one well of a 24-well plate containing 1 ml culture medium and incubated (37^oC, 5% CO_2). Upon reaching confluence, cell clones from each well of the 24-well plate were expanded by subculturing in a T25 flask, incubated (37^oC, 5% CO_2) until confluent and a sufficient quantity of cells was grown for further studies.

2.9 Cell culture and induction of vIRF-2 protein expression

Previously grown vIRF-2 clones or EV clones were split and quantified as described (sections 2.1 and 2.2). The cells were then plated 5 x 10^5 cells per well of the 6-well plate or 2 x 10^4 cells per well of the 96-well plate in the culture media supplemented with 400 μg/ml G418 and 1μg/ml puromycin and incubated for approximately 72 hours. The culture media were then replaced with a fresh culture media supplemented with or without 1μg/ml doxycycline and further incubated for the desired period of time. Where necessary cells were treated with the required concentration of recombinant IFN-αB2 (rIFN-α).

2.10 Indirect immunofluorescence assay (IFA)

IFA was employed to detect the subcellular localization of vIRF-2 in clone 3-9 vs EV cells. First, each of the glass coverslips (13 mm diameter) was placed in each well of the 24-well plate; 100 μl of fibronectin, 0.1% solution diluted (1:20 PBS) was dispensed in to each well of the 24-well plate to cover the glass coverslips and incubated (37^{o}C, 5% CO_2) overnight to allow for sufficient coating of the coverslips with fibronectin (**Table 1, Appendix A**). Next, the fibronectin was removed, replaced with fresh culture medium supplemented with 400 μg/ml G418 and 1 μg/ml puromycin, and plated with 1x10^3 cells in each well of 24-well plate. On confluence, the cells were treated with or without doxycycline (1μg/ml, 24 hours) and fixed in acetone:methanol (1:1) solution for 5 minutes at room temperature. They were then washed once in PBS/1% FBS, followed by incubation for 10 minutes in permeabilisation solution (**Table 1, Appendix D**). The cells were then washed twice and the non-specific binding sites were blocked with 10% heat inactivated sheep serum for 30 minutes at room temperature followed by a further wash. The cells were then incubated with the primary antibody (mouse anti-cmyc 1:100) for 1

hour at room temperature, washed three times at 5 minute intervals and incubated with the secondary antibody sheep anti-mouse IgG conjugated to fluorescein isothiocyanate (FITC) (1:100) (**Table 2, Appendix B**). Washing three times at 5 minute intervals at room temperature followed this incubation period. The nuclei were stained in 1 μg/ml DAPI (**Table 1, Appendix A**) in sterile distilled water for approximately 5 seconds and rinsed in sterile distilled water. Finally, the glass cover slips were mounted on Prolong Gold + antifade reagent (**Table 1, Appendix A)** for 24 hours and sealed with nail varnish (**Table 1, Appendix A**). In each experiment images were recorded under the same exposure conditions for comparative analysis using the fluorescent microscope.

2.11 Bioinformatics

The DNA microarray experiments used in the present study were performed on exon arrays (see section 4.1). Microarray technology is a widely used high-throughput tool for measuring gene expression (Schena, Shalon et al. 1996), (see Allison, Cui et al. 2006). The bioinformatics software packages employed for data analyses are stated below.

2.11.1 Data Preprocessing and QC

Gene level analysis of the Affymetrix exon arrays was performed using Affymetrix Expression Console (EC) with option Robust Multichip Average (RMA)-Sketch. The EC software package provides signal estimation and quality control (QC) functionality for GeneChip expression arrays (3' Expression and Exon arrays). Further, its workflow provides the more commonly used summarization probe set algorithms such as RMA.

2.11.2 Identification of differentially expressed genes

Differences in gene expression levels between cell treatments (-dox-ifn, +dox-ifn, -dox+ifn, +dox+ifn (phenotype features) were assessed with the Limma package (Smyth 2004). The Limma package provides a set of tools for background correction and scaling, as well as an option to average on-slide duplicate spots. The Limma p-value is a version of student *t*-test specifically adapted for microarray data analysis. Heatmaps were generated using dChip (http://www.dchip.org) with *default setting* option. This phase of the data pre-processing was performed by Dr. Wenbin Wei (School of Cancer Sciences, University of Birmingham).

2.11.3 Gene Ontology Analysis

One of two analytical software packages used in this work was DAVID (database for annotation, visualization and integrated discovery) (v6.7), bioinformatics and data mining resources which is capable of extracting biological meanings associated with large gene lists.

Probe set identifiers (gene identities or user gene list) were uploaded to the DAVID package (Huang da, Sherman et al. 2009). The classification stringency of the functional annotation clustering tool allowed users to choose higher stringency setting for tight, clean and smaller numbers of clusters. There were five predefined levels from the lowest to highest according to the user's choices. *Default setting* was medium and was chosen for our gene list because with the high setting, gene enrichment scores were very low. The *default settings* were used to cluster genes into functionally related groups to unravel their biological significance. The details of individual gene sets or related biological pathways were viewed with the functional annotation chart and/or table.

Gene Set Enrichment Analysis (GSEA) was the second analytical software package used to evaluate the array data (Subramanian, Tamayo et al. 2005). GSEA determines whether *a priori* defined set of genes shows statistically, concordant differences between two biological states such as phenotypes. It derives its power by focusing on gene sets, that is, groups of genes that share biological function, chromosomal location, or regulation. Enrichment analysis increases the likelihood for investigators to identify biological processes most pertinent to the biological phenomena being investigated. The Molecular Signature Database (MsigDB) package is a collection of gene sets for use with the GSEA package. For example, the canonical pathways (one of the 5 major collections of the GSEA), sorts gene sets from the pathway databases most of which are canonical representations of a biological process compiled by domain experts.

From the array raw data file, all spikes and positive and negative controls were deleted. Spikes are non-human DNAs (bacterial etc) added into the hybridization mix so that the technical aspects of the experiment can be assessed. The expression data set values above 50 units were considered to be above the baseline noise levels and were therefore recalculated and expressed as log (2). The expression data set were uploaded on to the GSEA software package (http//www.broadinstitute.org/gsea/). The *collapse dataset to gene symbols parameter* was set to TRUE when GSEA was run so that the expression dataset, which had 13798 native features, was reduced to 13542 after collapsing features to gene symbols. By collapsing the dataset, GSEA converts the probsets in the expression dataset in to a single entity or vector for the gene, which gets identified by its symbol. The data was then analysed with the standard guide procedure.

2.12 Chandipura virus and EMCV experimental procedures

The virus work experiments were employed to quantify viruses grown in the vIRF-2 induced cells vs EV counterpart pre-treated with IFN-α. Vero and L929 cells were maintained in DMEM supplemented with 1% penicillin-streptomycin, and 10% heat inactivated foetal bovine serum. Professor David Evans generously donated the Chandipura virus and EMCV. Clone 3-9 or EV clone 5 (5×10^5 cells/well) were grown in a 6-well plate for 72 hours. Next, the culture medium supplemented with 10% heat inactivated foetal bovine serum, 1% penicillin-streptomycin, 1% non essential amino acid, 1μg/ml puromycin and 400 μg/ml G418 was removed and the cells were incubated (37 ^oC, 5% CO_2, 24 hours) in fresh culture medium with or without 1μg/ml doxycycline and with or without increasing amounts of rIFN-α (3 U/ml, 30 U/ml, & 300 U /ml). The culture medium was taken off and the cells infected with either the Chandipura virus or EMCV at multiplicity of infection (MOI) of 0.1 in the culture medium; the required amount of viral stock was suspended in 500 μl of the culture medium and plated in each well of cells. After the 1 hour adsorption step (37 ^oC, 5% CO_2), the supernatant was removed and the cells rinsed twice with sterile PBS. The cells were again incubated (37 ^oC, 5% CO_2,) in a fresh culture medium with or without 1μg/ml doxycycline and with or without increasing amounts of IFN-α (3 U/ml, 30U/ml, & 300 U/ml). 24 hours later the supernatant was harvested in order to quantifiy virus by plaque assay.

2.13 Plaque assay

One of the most important procedures in virology is measuring the virus titer by plaque assay. This technique was developed to calculate the titers of bacteriophage stocks and was later updated by Renato Dulbecco in 1952 and has since been used for reliable

determination of the titers of many different viruses. The plaque assay was used to quantify virus titres in this section of the study.

Monolayers of vero or L929 cells were grown in DMEM GlutMAX (Invitrogen) supplemented with 10% heat inactivated FBS, 1% HEPES, 1% penicillin-streptomycin and incubated (37 ^{o}C, 5% CO_2) to confluence prior to the start of the plaque assay. To determine the virus titer, virus suspension stocks were titrated to 10^{-6} in the plaque assay medium (DMEM supplemented with 1% penicillin-streptomycin). The vero or L929 monolayer cells were infected with 250 µl of the diluted virus suspension per well of the 12-well plate and incubated (37^{o}C, 5% CO_2) for 30 minutes. The vero or L929 cells were then covered with an overlay medium consisting of 10% v/v Minimum Essential Medium (MEM) with Earl's salt (10X), 1% v/v L-glutamine, 3% v/v 7.5% sodium bicarbonate, 2% v/v foetal calf serum heat inactivated, 1% v/v penicillin/streptomycin, and 30 ml of 2% agar (0.6%). After the overlay medium had set (semisolid), the vero and L929 cells were incubated (37 ^{o}C, 5% CO_2) for 24 and 72 hours respectively. The plaques were stained by dispensing 2 ml crystal violet solution in to each well and incubated at room temperature with a gently shake. The overlay gel was removed by gently washing the plates with running tap water. The Plaques are readily seen at the bottom of the culture plate against a purple background. Number of plaques counted per well X 4 = plaques/ml X 10 = plaque forming units per ml (PFU/ml), 4 and 10 are dilution factors.

2.14 Quantifying proteins by densitometry

The relative densitometry was performed on the immunoblots for pSTAT1 and IRF-9/p48. Scanned Immunoblot images were uploaded on to Image J software package and blot band sizes and density were measured. See (http://lukemiller.org/index.php/2010/11/analyzing-gels-and-western-blots-with-image-j/).

2.15 Statistics

Microsoft spreadsheets excel and GraphPad Prism software packages carried out statistical analysis of the data. Because the p value measures the strength of evidence against the null hypothesis, statistical significance is presented as ($*p<0.05$), ($**p<0.01$) or ($***p<0.001$).

Chapter 3. KSHV vIRF-2 expression and functional studies

Research into KSHV *vIRF-2* expression in clone 3-9 cells will enable us to decipher its functions and protein partners, and provide a clearer picture of the complex regulatory networks that control fundamental biological processes that may be regulated by vIRF-2. The construction of the clone 3-9 cell line carrying doxycycline-inducible vIRF-2 and its empty vector counterpart lacking vIRF-2 are described in sections 2.7 and 2.8. vIRF-2 protein expression and function have been previously studied in HEK293 cells with transient transfection assays using *vIRF-2* expressing plasmid vectors (Fuld, Cunningham et al. 2006; Areste, Mutocheluh et al. 2009). However, a vIRF-2 expressing stable cell line in which every cell will express vIRF-2 was required (i) to validate vIRF-2 inhibition of pISRE-luc activity (Fuld, Cunningham et al. 2006) and (ii) for mechanistic studies of the impact of vIRF-2 on the second phase of the IFN-α/β pathway (JAK-STAT pathway). Additional vIRF-2 expressing cell lines were engineered and studied in parallel to clone 3-9 to ensure results were not clone specific. In the following chapter I will describe the characterization of vIRF-2 expression and function in clone 3-9 cells.

3.1 Evidence of vIRF-2 antiviral activities

Others have reported on vIRF-2 functional activities. Early studies indicated that part of vIRF-2 protein encoded by exon 1 inhibited IFN-α and IFN-β promoters in transient transfection assays (Burysek, Yeow et al. 1999). Burysek and Pitha further investigated the biological impact of the anti-IFN effect of vIRF-2 exon 1 and reported that HEK293 cells transfected with its expression vector rescued vesicular stomatitis virus (VSV) mRNA translation from IFN-induced block. VSV protein synthesis was not

significantly inhibited by up to 1000 IU/ml of IFN-α in the presence of vIRF-2 whereas in HEK293 cells transfected with empty vector, the synthesis of VSV matrix proteins was reduced significantly by IFN-α, at approximately 360 IU/ml.

Our group reported full-length vIRF-2 inhibits IFN-α-induced ISRE signalling by approximately 80%. In this study HEK293 cells were transiently cotransfected with a luciferase reporter regulated by the promoter of *ISG56* ISRE (pISRE-luc) and increasing amounts of vIRF-2 expressing vector. The cells were then treated with rIFN-α (200 IU/ml) (Fuld, Cunningham et al. 2006). One mechanism may have been the prevention of IRF-1 from binding to its cognate DNA in the ISRE; since ISRE sites overlaps with IRF1-E, to which IRF-1 binds within the IFN-β promoter (Taniguchi and Takaoka 2002). Alternatively, ISGF-3 may be targeted by vIRF-2.

Recently, our group reported another mechanism of vIRF-2 function: vIRF-2 suppressed IFN-β promoter transactivation by suppressing the activity of wild type IRF-3 protein levels by taking advantage of the phosphorylation of residues at the IRF-3 C-terminal site 2 (Areste, Mutocheluh et al. 2009). Phosphorylation at this site represses autoinhibition and permits interaction with CBP/p300, making it possible for site 1 to be phosphorylated as well resulting in homodimerization (Panne, McWhirter et al. 2007). When we mutated the IRF-3 C terminal sites 1 and 2 separately and together we showed that the transactivation capabilities of all the mutants were reduced by approximately 50 % compared to that of IRF-3 wild type (WT). Also, we showed the decay of phosphorylated IRF-3WT by vIRF-2 depends on caspase-3 activity, because studies with caspase-specific inhibitors demonstrated that IRF-3 decay was reduced when caspase-3 activity was inhibited (Areste, Mutocheluh et al. 2009). This study was performed in a system where the full-length IFN-β promoter driving luciferase reporter gene expression (p125-luc) was transiently cotransfected with a vIRF-2 expressing plasmid and also in

clone 3-9 cells (where vIRF-2 expression was induced); the IFN-α/β pathway was activated by synthetic double-stranded RNA (Areste, Mutocheluh et al. 2009).

Previous attempts at making vIRF-2 expressing stable cell lines by Fuld and Blackbourn proved unsuccessful as the cells died when vIRF-2 expression was constitutive (unpublished observations). Thus, the clone 3-9 cell line carrying the vIRF-2 expression cassette regulated by doxycycline was developed in the Blackbourn laboratory just before the present work began. Although clone 3-9 and its EV counterpart cells were used for some vIRF-2 functional studies (Areste, Mutocheluh et al. 2009), for the purpose of this study it was necessary to create more clones to ensure the data generated were not clone specific. The vIRF-2 functional studies described so far by the various research groups have all relied on the IFN-α/β pathway to represent the most immediate antiviral response in the host cells but none have reported on how vIRF-2 affects the JAK-STAT pathway. Much more information could be generated by investigating the impact of vIRF-2 on the cell transcriptome in response to IFN-α as determined by DNA microarray analyses.

Data presented in this chapter include those indicating that doxycycline induction of vIRF-2 expression in clone 3-9 peaked at 24–36 hours and that vIRF-2 was predominantly a nuclear resident protein as determined by IFA. Also, the luciferase reporter experiments in which IFN-α drove pISRE-luc activity demonstrated that vIRF-2 significantly ($p<0.001$, Student's *t* test) inhibited the pISRE-luc transactivation. The Agilent bioanalyser data showed the 12 RNA samples were of excellent condition to undergo DNA microarray investigations, which are subsequently discussed in chapter 4.

3.2 vIRF-2 expression studies in clone 3-9 cells

To establish the optimal amount of doxycycline required for the induction of the peak amount of vIRF-2 expression in the clone 3-9 cell line, confluent cells of this line were treated with increasing amounts of doxycycline up to 1 μg/ml for 24 hours. The cells were harvested and lysates prepared using a standard protocol. Equal amounts of cell lysates were then resolved by SDS-PAGE and immunoblotted with antibodies to the cmyc-epitope of vIRF-2. To ensure equal amounts of lysates were loaded, blots were also performed with anti-GAPDH antibodies. vIRF-2 expression accumulated in a dose dependent fashion and reached a plateau with 1 μg/ml of doxycycline compared with the non-doxycycline-treated cells. Residual amounts of vIRF-2 protein representing background levels were detected in non-doxycycline-treated cells (**Figure 3.1A**).

The next task was to determine the time point at which vIRF-2 protein expression peaked in clone 3-9 cells following induction. Confluent clone 3-9 cells were treated with 1 μg/ml doxycycline up to 144 hours. Equal amounts of cell lysates were then resolved on SDS-PAGE and immunoblotted with antibodies to cmyc-epitope of vIRF-2. Blots were also performed with anti-GAPDH antibodies to ensure equal amounts of lysates were loaded. vIRF-2 expression peaked at 36 hours post-doxycycline treatment. In untreated cells (0 hours) there was virtually no bands seen but a trace band representing weak accumulation of vIRF-2 could be seen in cells treated with doxycycline for 12 hours which then peaked at 36 hours and declined to background levels in cells treated for 72 hours onwards (**Figure 3.1B**). Another experiment performed as described for figure 3.1B was repeated up to 48 hours of doxycycline treatment (**Figure 3.1C**) and also demonstrates vIRF-2 expression peaked at 36 hours.

Taken together, vIRF-2 protein expression peaked at 24-36 hours in clone 3-9 cells following induction with 1 μg/ml of doxycycline.

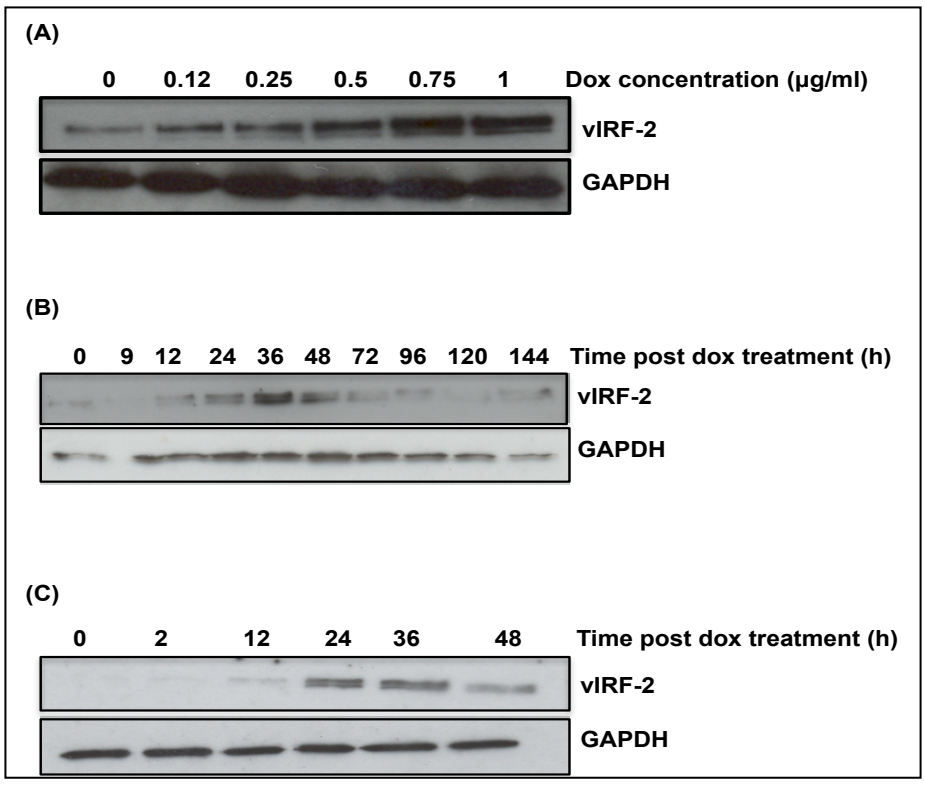

Figure 3.1. Establishing the concentration of doxycycline and the time of treatment providing maximal vIRF-2 expression in clone 3-9 cells. (A) Clone 3-9 cells were plated at a density of 5 x 10^5 cells/well in 35 mm wells and treated with the indicated concentrations of doxycycline for 24 hours. 20 µg of cell lysate were resolved on 10% SDS-PAGE and immunoblotted with antibody against the cmyc-epitope of vIRF-2 protein as primary antibody and horseradish peroxidase-conjugated anti-mouse antibody as secondary antibody. (B) and (C) Clone 3-9 cells were grown as described in (A), treated with doxycycline (1 µg/ml) and harvested at the indicated time points. Cell lysates were prepared as described in (A) and immunoblotted with antibody against the cmyc-epitope of vIRF-2 protein as primary antibody and horseradish peroxidase-conjugated anti-mouse antibody as secondary antibody. Probing for GAPDH ensured equal amounts of lysate were loaded in each lane. Blotted membranes were developed using enhanced chemiluminiscence and protein images (bands) were detected with the Compact X4 automatic X-ray film processor. These results are representative of three independent experiments showing the same pattern. Each image is representative of 3 experiments performed separately. h, hours.

3.3 Quantifying vIRF-2 mRNA by real time quantitative PCR (RT-qPCR)

The aim of this section of the study was to determine *vIRF-2* mRNA levels by RT-qPCR to verify the western blot data (**Figure 3.1**). In order to use the $\Delta\Delta C_T$ method for relative quantification of *vIRF-2* mRNA levels, the efficiency of the target amplification and the efficiency of the endogenous control amplification must be approximately equal (Livak and Schmittgen 2001; Liu and Saint 2002). Therefore, it was necessary to first determine the amplification efficiencies of *vIRF-2* and *GAPDH* primers/probes in singleplex and duplex reactions respectively (see section 2.4.4). The recommended amplification efficiency range is 90 %-110%.

The two most commonly used methods to analyse data from RT-qPCR experiments are absolute quantification and relative quantification. The absolute quantification determines the input copy number, usually by relating PCR signal to a standard curve whereas relative quantification relates the PCR signal of the target transcript in a treatment group to that of another sample such as an untreated control. Both techniques were used in this section of the study.

The clone 3-9 cells were treated with doxycycline 1μg/ml for 30 hours. Subsequently, total RNA was extracted from the cell lysate as described (see section 2.4.1) and the template cDNA synthesized (see section 2.4.2). The cDNA samples were 10-fold serially diluted with distilled water (range $1:10^{-1}$-$1:10^{-6}$). *vIRF-2* and *GAPDH* primers/probes binding efficiencies were measured by qPCR and TaqMan probe detection. Primers and probe efficiency values were measured using the C_T slope method and result expressed as % (see section 2.4.4). There was a linear correlation over all six data points plotted for each graph (**Figure 3.2**). Thus, *vIRF-2* amplification efficiency in singleplex reaction was 94.4% (**Figure 3.2A**) while in duplex reaction with *GAPDH* it was 90% (**Figure 3.2B**). The amplification efficiency of *GAPDH* in singleplex reaction was 91%

(**Figure 3.2C**) while in duplex reaction with *vIRF-2* was 90% (**Figure 3.2D**). These values are therefore within range to proceed with primers and probe together in multiplex assays.

Having validated *vIRF-2* and *GAPDH* real time quantification it was possible *vIRF-2* mRNA levels could be established to correlate with peak protein levels shown in **Figure 3.1**. Therefore, confluent clone 3-9 cells were treated with doxycycline (1μg/ml) for 2-48 hours or left untreated. The template cDNA was prepared as described (see 2.4.2) and mRNA levels determined with *vIRF-2* and *GAPDH* specific primers and probes. The relative expression of *vIRF-2* mRNA in cells treated with doxycycline increased with time peaking in cells treated with doxycycline for 36 hours at almost 10-fold above that of background levels. By 48 hours of doxycycline treatment, vIRF-2 levels had dropped (**Figure 3.3**).

Thus, vIRF-2 mRNA expression peaked at 36 hours post-doxycycline treatment consistent with the protein expression levels shown earlier.

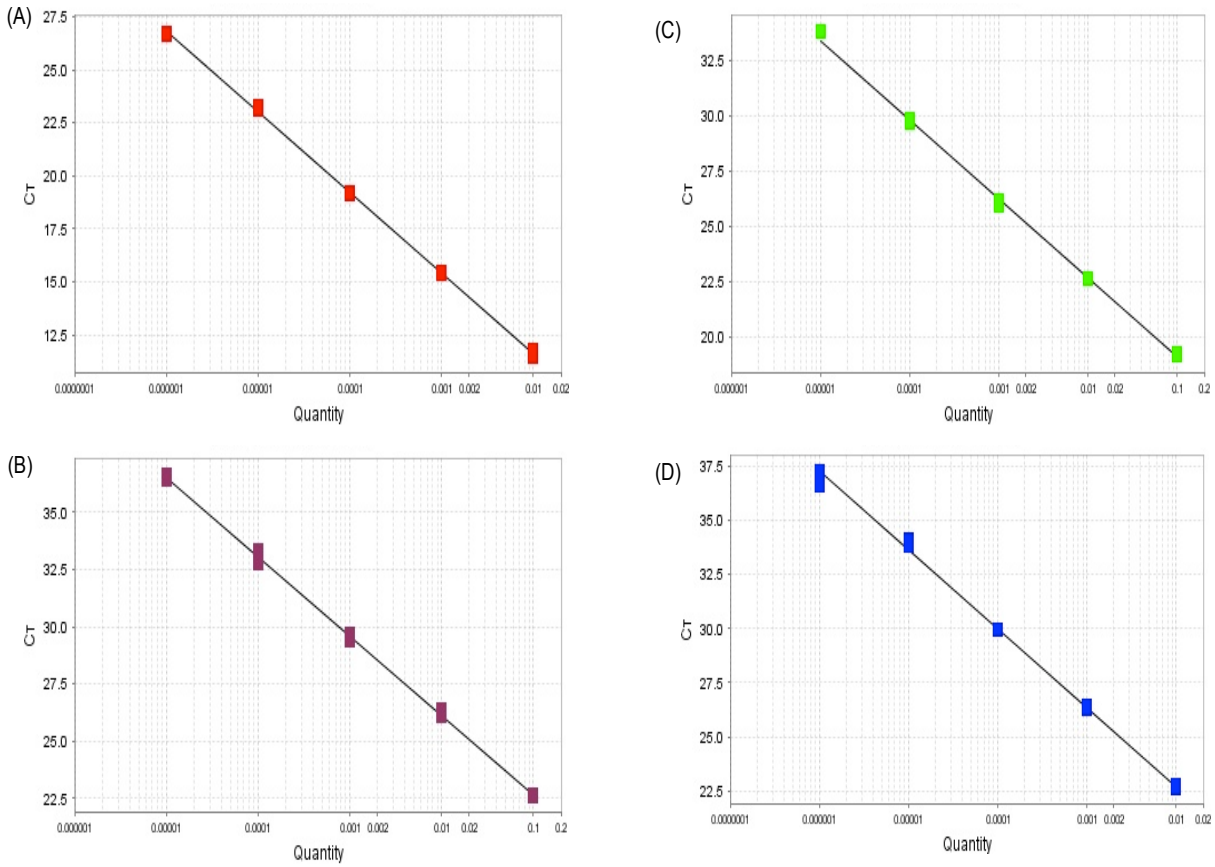

Figure 3.2 vIRF-2 and GAPDH primers and probe amplification efficiency validation study. The clone 3-9 cells were plated at a density of 5 x10^5 cells/well in 35 mm wells and were treated with doxycycline 1µg/ml for 30 hours. RNA was isolated and cDNA synthesized from 1µg RNA with random primers and serially diluted 10 fold for six data points (1:10^{-1}-1:10^{-6}). Using gene specific primers and probes, the amplification efficiency of the target *vIRF-2* and the endogenous control *GAPDH* were measured by qPCR. Primers and probes efficiency values (%) were measured using the C_T slope method. The amplification efficiency is calculated using the slope of the regression line in the standard curve (see 2.4.4). (A) *vIRF-2* amplification efficiency in singleplex reaction was 94% and (B) 90% in duplex reaction with *GAPDH*. (C) *GAPDH* amplification efficiency in singleplex reaction was 91% and (D) 90% in duplex reaction with *vIRF-2*. Data are representative of 3 independent replicates. Amplification efficiency reference values: 90% - 110%.

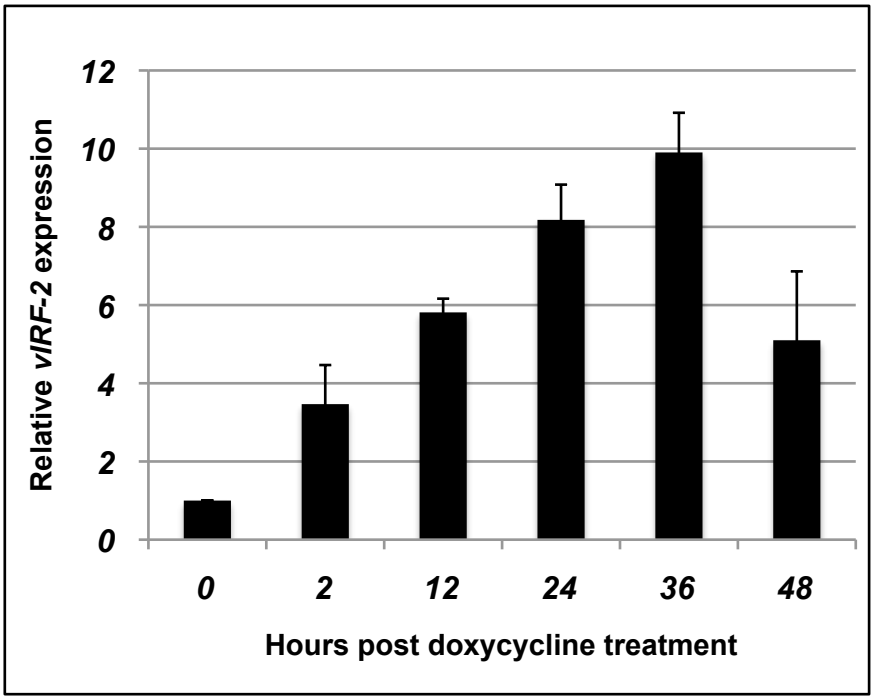

Figure 3.3 Quantifying vIRF-2 mRNA by RT-qPCR. The clone 3-9 cells were plated at a density of 5 x10^5 cells/well in 35 mm wells and were treated with or without doxycycline (1µg/ml) for the indicated time points. cDNA was synthesized and served as template for qPCR using *vIRF-2* and *GAPDH* specific primers and probes. *vIRF-2* mRNA levels were determined by the $\Delta\Delta C_T$ method. Data are presented as mean +/- SD of three individual experiments where each sample was run in triplicate.

3.4 Determining the maximal concentration and time of IFN-α activity

To ensure inducible vIRF-2 in clone 3-9 cells retains functional activity in terms of inhibition of IFN responsive reporter genes, these reporter assays were performed in clone 3-9 cells. Firstly, it was necessary to determine the concentration of IFN-α that would stimulate the maximal activity of the pISRE-luc IFN responsive reporter gene. These studies were performed in cells lacking vIRF-2, but that were stably transfected with empty vector and clonally selected. This cell line is called EV clone 5 or EV5. Confluent EV clone 5 cells were transiently co-transfected in 35 mm wells with pISRE-luc (250 ng) and pRLSV40-luc (1 ng) in a transfection mixture including lipofectamine. 24 hours later the cells were treated with rIFN-α at a range of concentrations from 0-400 IU/ml for 30 hours. As expected there was no normalised pISRE-luc activity in untreated cells (0 IU/ml). However, normalized pISRE-luc activity peaked approximately 25-fold above background levels in cells treated with 300 IU/ml rIFN-α and dropped sharply in cells treated with 400 IU/ml rIFN-α (**Figure 3.4A**). Thus, 300 IU/ml rIFN-α is required to induce maximal pISRE-luc activity in EV cells.

The next task was to determine the time point at which 300 IU/ml rIFN-α caused maximal pISRE-luc activity. Confluent EV clone 5 cells were transiently co-transfected with plasmids as described (**Figure 3.4A**). 24 hours later the cells were treated with 300 IU/ml rIFN-α from 0-48 hours. The normalised pISRE-luc activity peaked at approximately 25-fold at 12 hours (**Figure 3.4B**)

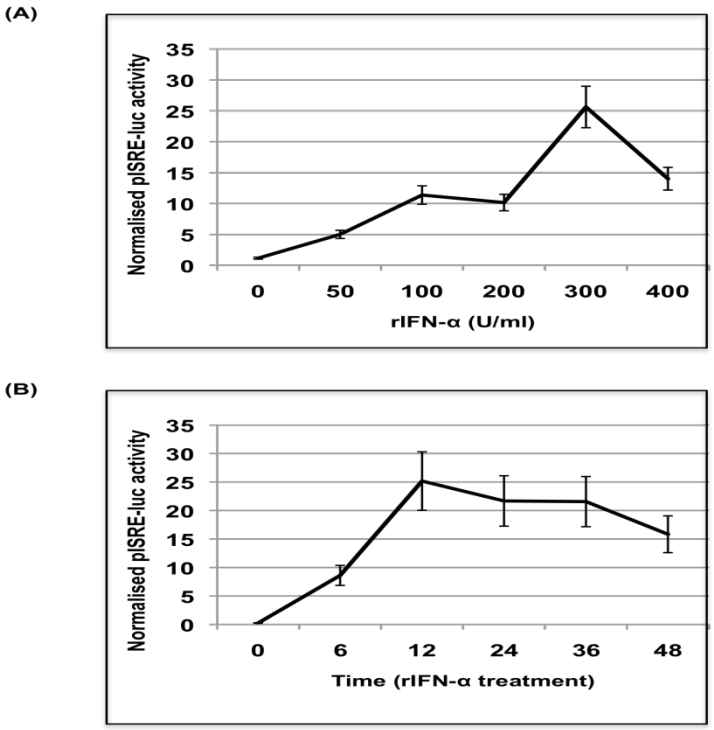

Figure 3.4 Determining the maximal concentration and time of IFN-α induction of ISRE-driven luciferase reporter gene activity in EV clone 5 cells. (A) The EV clone 5 cells were plated at a density of $5x10^5$ cells/well in 35 mm wells. Each well of confluent cells was transiently co-transfected using a transfection mixture consisting of pISRE-luc (250 ng) & pRLSV40-luc (1 ng) and lipofectamine in serum free medium. 24 hours post transfection the cells were treated with the indicated concentrations of rIFN-α for 30 hours. Cells were harvested and lysates prepared. The pRLSV40-luc plasmid vector constitutively expressing *Renilla* luciferase was added as an internal control to which pISRE-luc plasmid driving firefly luciferase activity was normalised. Both firefly luciferase and *Renilla* luciferase activities were determined by dual luciferase assay. Data are presented as mean normalised pISRE-luc activity (± standard deviation) of three independent experiments each performed in duplicate. (B) The cells were grown and transfected with plasmids as described in A. 24 hours later, the cells were treated with rIFN-α (300 IU/ml) for the indicated time points. Data are presented as mean normalised pISRE-luc activity (± standard deviation) of three independent experiments each performed in duplicate.

3.5 Functional studies of vIRF-2 in clone 3-9 cells

Having established that 300 IU/ml rIFN-α induced the optimum pISRE-luc activity in the EV clone 5 cells, the next task was to determine if vIRF-2 inhibits pISRE-luc activity in clone 3-9 cells following peak vIRF-2 expression. Clone 3-9 cells were transiently co-transfected with reporter plasmids as described (**Figure 3.4),** followed by treatment with doxycycline and rIFN-α as indicated (**Figure 3.5**).

This experiment was run in parallel with another set of clone 3-9 cells but those were not transfected with the reporter plasmids and were immunoblotted for vIRF-2. In cells transfected with the pISRE-luc promoter reporter plasmids (**Figure 3.5A**) both -dox-ifn (i.e. no doxycycline treatment and no rIFN-α treatment) and +dox-ifn (i.e. includes doxycycline treatment and no rIFN-α treatment) treated cells indicated background levels of the normalized pISRE-luc activity. Cells treated with -dox+ifn were described as having 100% pISRE-luc activity and showed approximately 250-fold increase from the background levels. This level was reduced by 52% in the +dox+ifn treated cells. The differences in the levels of normalized pISRE-luc activity between cells treated with -dox+ifn and +dox+ifn were statistically significant ($p<0.01$, Student's *t* test). Thus, vIRF-2 protein significantly inhibited rIFN-α driven pISRE-luc activity by 52% in clone 3-9 cells.

Consistent with **Figure 3.5A** the immunoblot data of cells that were treated in parallel showed substantial accumulation of vIRF-2 in cells treated with doxycycline (**Figure 3.5B**). Nonetheless, traces of vIRF-2 protein are seen in the non-doxycycline treated samples due to the leaky expression of the vIRF-2 expressing plasmid that became increasingly apparent.

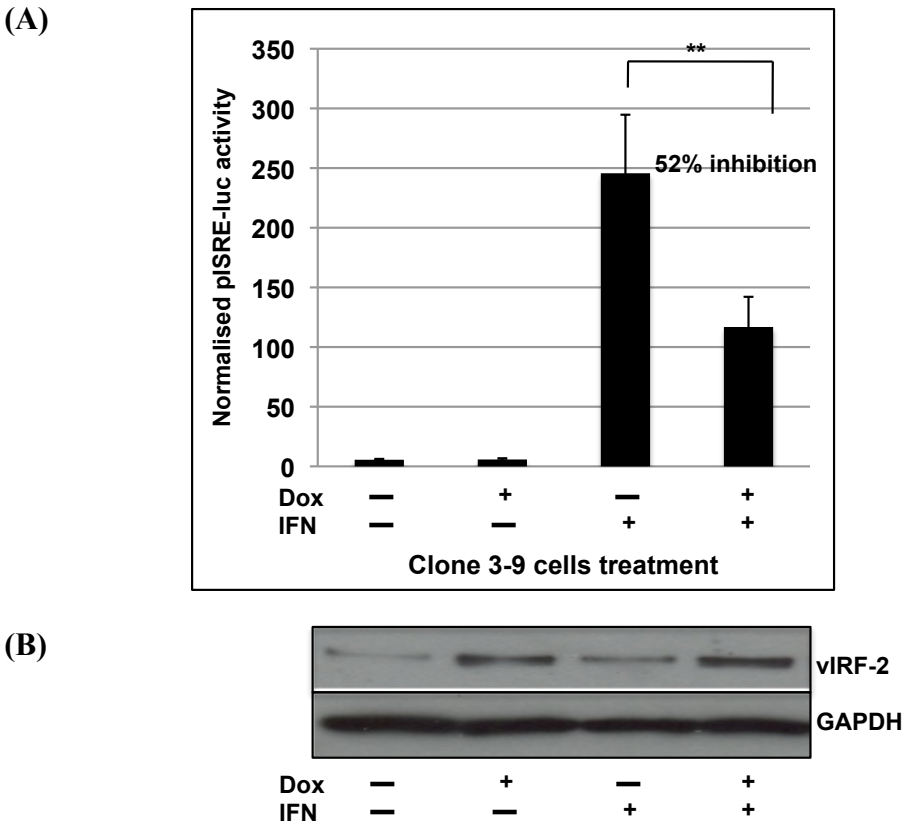

Figure 3.5 vIRF-2 inhibits the pISRE-luc promoter reporter activity. (A) The clone 3-9 cells were plated at a density of 5 x 10^5 cells / well in 35 mm wells. Each well of confluent cells was transiently co-transfected using a transfection mixture consisting of pISRE-luc (250 ng) & pRLSV40-luc (1 ng) and lipofectamine (2000 IU) in serum free medium. 24 hours after the transfection, the cells were treated with or without rIFN-α (300 IU/ml) and with or without doxcycycline (1μg/ml) for 30 hours. Cells treated as +ifn-dox were calculated to have 100% normalised pISRE-luc activity. Data are presented as mean normalised pISRE-luc activity (± standard deviation) of three independent experiments each performed in duplicate (**$p < 0.01$, Student's t test). (B) This experiment was performed in parallel to that described in A, except the cells were not transfected with reporter plasmids. Cell lysates were resolved on 10% SDS-PAGE and immunoblotted with antibodies against cmyc-epitope of vIRF-2 and GAPDH respectively. The size of vIRF-2 protein with the tagged cmyc-epitope was approximately 130 kDa. This experiment is representative of 3 independent experiments.

3.6 Engineering additional vIRF-2 expressing clones and their empty vector counterparts

To be certain that any mechanism of vIRF-2 inhibition of pISRE-luc activation identified in clone 3-9 cells in later studies was not clone-specific, additional independent clones stably transfected with the doxycycline-inducible vIRF-2 expression vector (showing inhibition of pISRE-luc activity) were established and selected for further study. Further, EV counterparts were also derived in parallel. The 293 Tet-On cell lines containing pTRE2pur-Myc-*vIRF-2* or pTRE2pur-Myc were constructed as described in section 2.8. The cells expressing vIRF-2 were screened for clones that behaved like the vIRF-2 clone 3-9 as described (**Figure 3.5A**). Over 300 clones were screened for their ability to suppress rIFN-α driven pISRE-luc activity. Representative clones are shown (**Figure 3.6**). As expected, the untreated cells (-dox-ifn) indicated background levels of the normalized pISRE-luc activity across all the clones. The majority of the vIRF-2-expressing clones did not exhibit the expected inhibitory effects of rIFN-α driven pISRE-luc activity. For example, there is no significant difference of the normalized pISRE-luc activity between cells treated with (-dox+ifn) and (+dox+ifn) although the levels of rIFN-α activated pISRE-luc activity peaked more than 60-fold above levels of untreated cells (**Figure 3.6A, B, C**). However, some vIRF-2-expressing clones did demonstrate the expected inhibitory effects of rIFN-α driven pISRE-luc activity and were therefore selected for further studies. These vIRF-2 expressing clones are: 293TetOn-vIRF-2, clone #20 and 293TetOn-vIRF-2, clone #24. Both showed rIFN-α driven pISRE-luc activity increased above 200-fold in cells treated with -dox+ifn compared to untreated cells and was significantly inhibited by vIRF-2 accumulation in cells treated with +dox+ifn, by 50% and 52%, respectively. In 293TetOn-vIRF-2, clone #20 and 293TetOn-vIRF-2, clone

#24 the differences in the levels of normalized pISRE-luc activity between cells treated with -dox+ifn and +dox+ifn were statistically significant ($p<0.01$, Student's *t* test) (**Figure 3.6D, E**).

The EV clones lacking vIRF-2 and engineered in parallel to 293TetOn-vIRF-2, clone #20 and 293TetOn-vIRF-2, clone #24 are: 293TetOn-EV, clone #1, and 293TetOn-EV, clone #4. A representative EV clone (293TetOn-EV, clone #5), analysed in parallel to the vIRF-2 expressing clones clearly demonstrates the absence of vIRF-2 since the levels of the rIFN-α driven pISRE-luc activity of cells treated with -dox+ifn and +dox+ifn remained the same after having increased more than 140-fold above levels of untreated cells (**Figure 3.6F**). Thus, vIRF-2 protein significantly inhibited rIFN-α driven ISRE-luc promoter reporter activity in vIRF-2 clone 20 and vIRF-2 clone 24. They were confirmed to express vIRF-2 by immunoblot assay and were selected for vIRF-2 mechanistic study in parallel with clone 3-9 (see chapter 4).

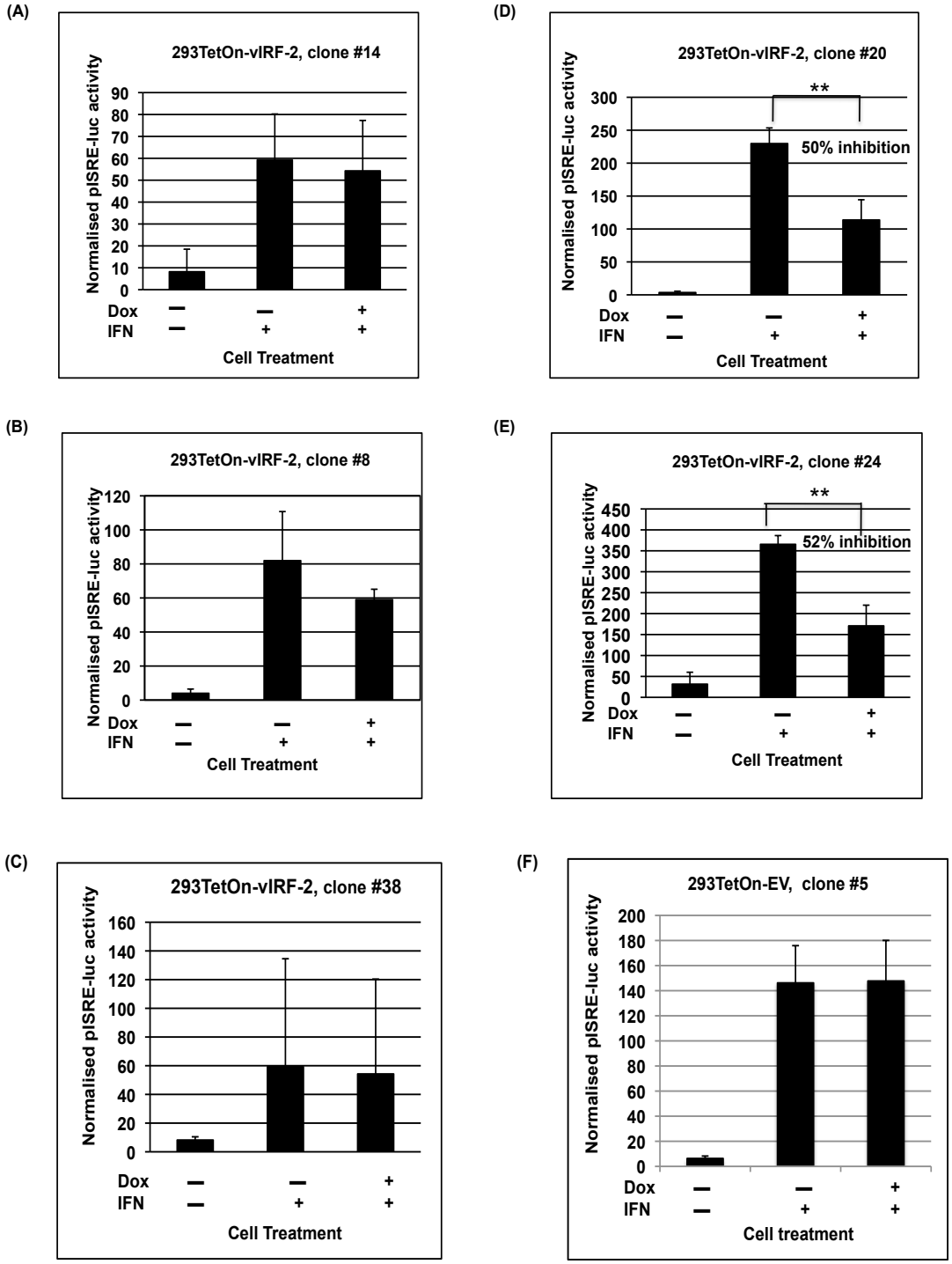

Figure 3.6 Representative vIRF-2-expressing and EV cell clones screened for their ability to inhibit rIFN-α driven pISRE-luc activity. (A-F) Transfection of plasmids was carried out in these experiments as described in Figure 3.5A. 24 hours later the cells were treated with or without rIFN-α (300 IU/ml) and with or without doxycycline (1μg/ml) for 30 hours. Cells treated with -dox+ifn were calculated to have 100% normalised pISRE-luc activity. Data are presented as

mean normalised pISRE-luc activity (± standard deviation) of three independent experiments each performed in duplicate (**p < 0.01, Student's *t* test).

3.7 Preparation of samples for DNA microarray studies

Having established that the clone 3-9 cell line stably transfected with inducible vIRF-2 expression vector could suppress rIFN-α induction of pISRE-luc activity analogous to our previous studies of transient transfections of vIRF-2 expression vector, the next task was to perform the clone 3-9 cells treatments for transcriptome profiling analysis in the presence and absence of vIRF-2 induction and rIFN-α treatment. Therefore, clone 3-9 cells treated with -dox-ifn, +dox-ifn, -dox+ifn and +dox+ifn for 30 hours were grown in triplicate (cell replicates are described as M11A, M11B and M10). The triplicate cultures were then analysed to (i) estimate the impact of vIRF-2 on IFN-α driven pISRE-luc activity, (ii) quantify the relative *vIRF-2* mRNA expression and (iii) perform transcriptome profiling analysis by DNA microarray.

In sample set M11A the induction of rIFN-α driven pISRE-luc activity peaked at approximately 300-fold in cells treated with -dox+ifn and was reduced by 50% by vIRF-2 in cells treated with +dox+ifn (**Figure 3.7A**) compared with the background levels of cells without rIFN-α treatment. The relative *vIRF-2* mRNA expression levels increased approximately 5-fold following doxycycline treatment compared with the background levels of non-doxycycline treated cells (**Figure 3.7B**). Consistent with **Figure 3.7B**, the immunoblot data showed vIRF-2 protein accumulated substantially in the doxycycline treated cells (**Figure 3.7C**). Probing for GAPDH ensured equal loading in each well and also provided evidence that GAPDH was not affected by the treatment. Samples set M11B (**Figure 3.7 D, E and F**) showed a similar pattern of results as in A, B and C although inhibition of rIFN-α driven pISRE-luc activity by vIRF-2 in cells treated with

+dox+ifn was 52% (**Figure 3.7D**). vIRF-2 mRNA levels increased between 3 and 4-fold in doxycycline treated cells relative to the background levels of non-doxycycline treated cells (**Figure 3.7E**). Sample set M10 (**Figure 3.7 G, H and I**) showed a similar pattern of result as in A, B and C and inhibition of rIFN-α driven pISRE-luc activity by vIRF-2 in cells treated as +dox+ifn was 47% (**Figure 3.7G**).

Having verified vIRF-2 inhibited pISRE-luc activity in sample sets M11A, M11B & M10, RNA was prepared from one of each sample set for microarray transcriptome profiling. Total RNA was extracted from the cell lysate and the RNA purity determined before further investigations were conducted. The data for these samples are summarized (**Table 3.1)**. Aliquots of the total RNA isolated from all 12 samples were then given to Dr. John Arrand (School of Cancer Sciences) to determine their integrity for microarray studies with the Agilent bioanalyser. The electrophoresis file indicated excellent RNA condition in all 12 samples as evidenced by both the 28S and 18S RNAs (**Figure 3.7J**). Moreover, the RNA integrity (RIN) ranged 9.40 – 10.0 on a scale of 1-10 (**Figure 3.7K**). These samples were therefore submitted for microarray profiling (see chapter 4).

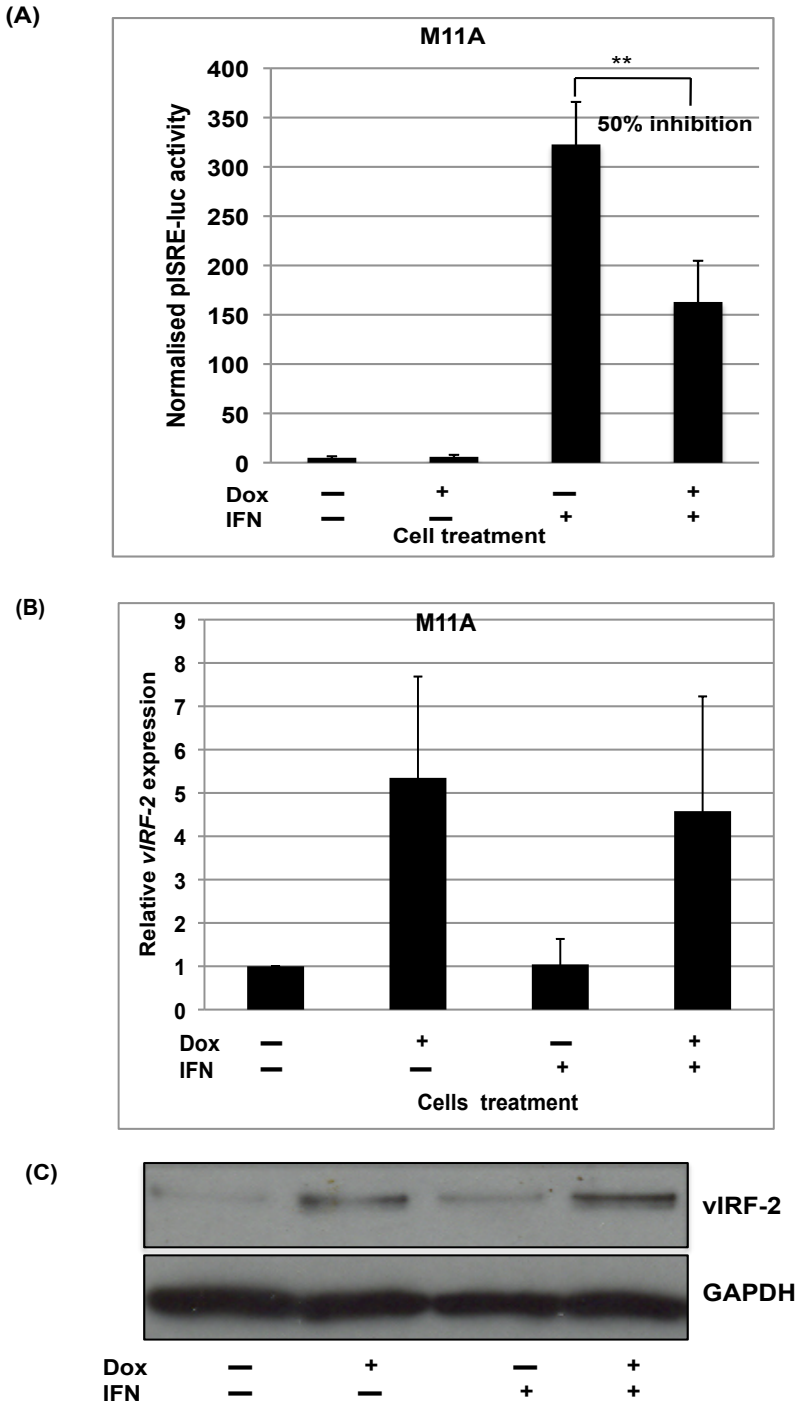

Figure 3.7 for legend see page 110.

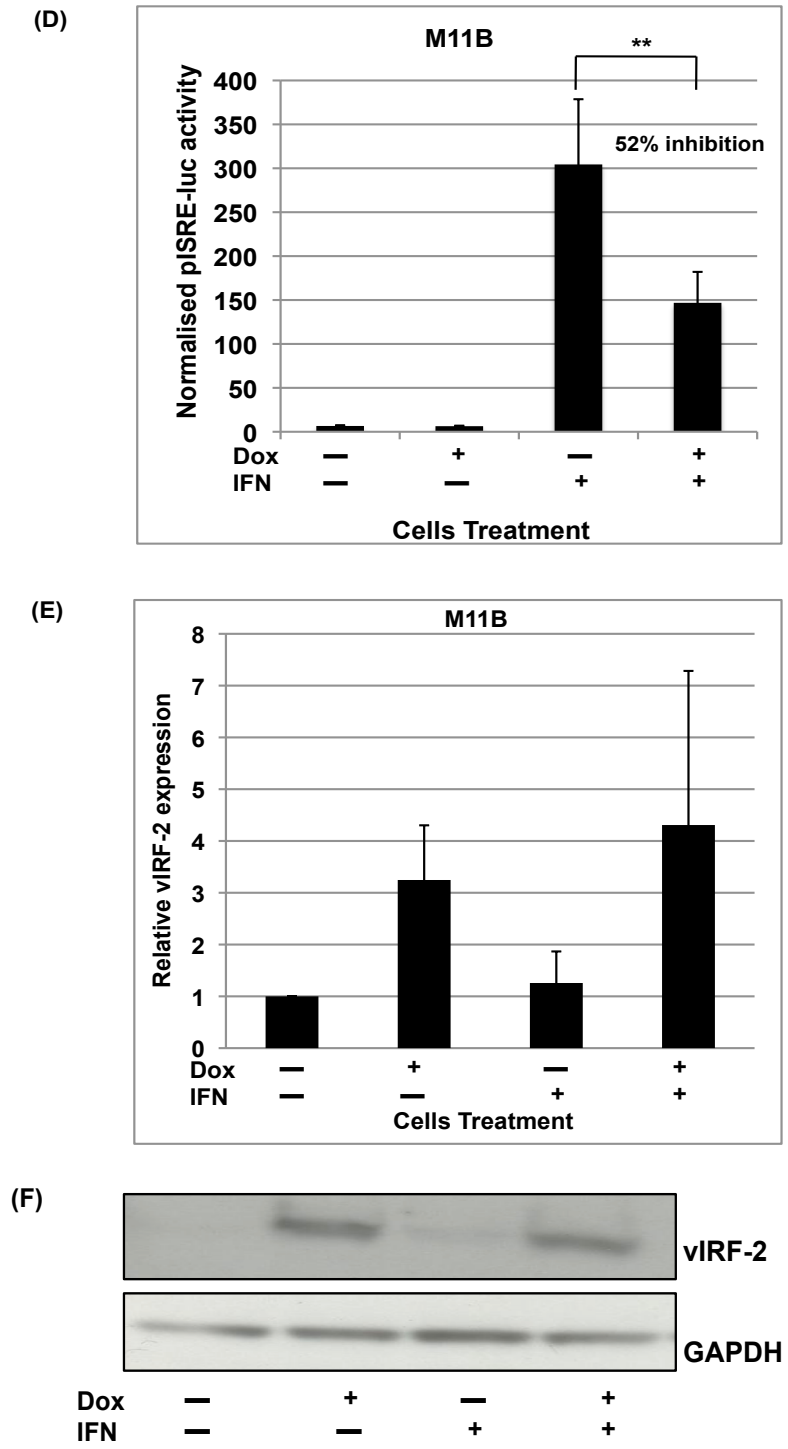

Figure 3.7 for legend see page 110.

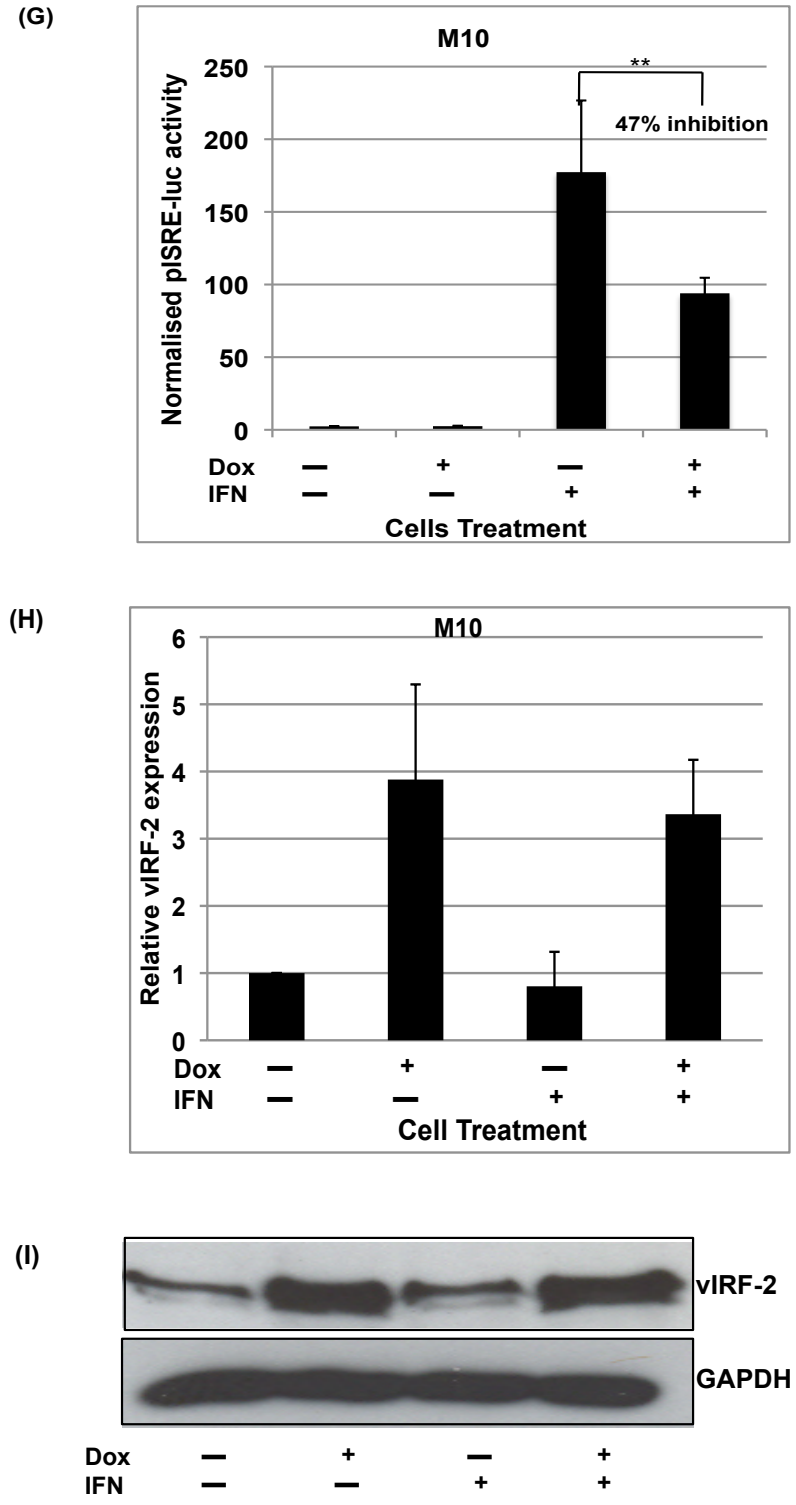

Figure 3.7 for legend see page 110.

J

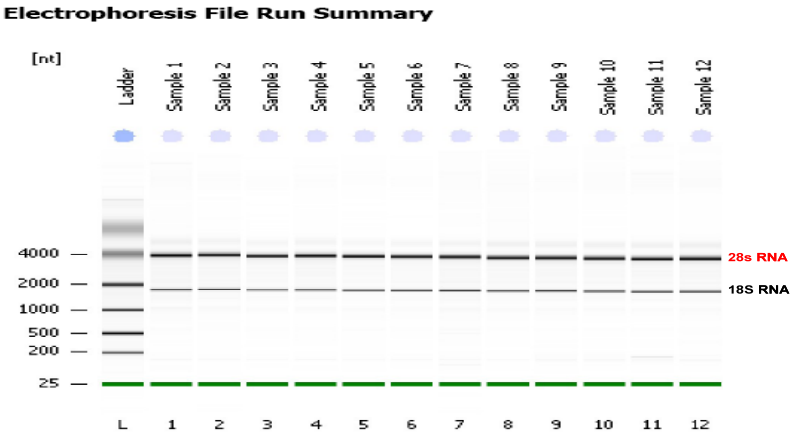

K

Assay Class: EukaryoteTotal RNA Nano
Data Path: C:\..._EukaryoteTotal RNA Nano_DE54700718_2009-07-13_15-10-16.xad
Created: 13/07/2009 15:10:16
Modified: 13/07/2009 15:36:21

Electrophoresis File Run Summary (Chip Summary)

Sample Name	Sample Comment	Status	Observation	Result Label	Result Color
(M11A) -Dox - IFN	Total RNA (for Mohamed Mutochelu)	✔		RIN: 9.40	
(M11A) +Dox - IFN	Total RNA (for Mohamed Mutochelu)	✔		RIN: 9.50	
(M11A) -Dox + IFN	Total RNA (for Mohamed Mutochelu)	✔		RIN: 9.40	
(M11A) +Dox + IFN	Total RNA (for Mohamed Mutochelu)	✔		RIN: 9.50	
(M11B) -Dox - IFN	Total RNA (for Mohamed Mutochelu)	✔		RIN: 9.40	
(M11B) +Dox - IFN	Total RNA (for Mohamed Mutochelu)	✔		RIN: 9.30	
(M11B) -Dox + IFN	Total RNA (for Mohamed Mutochelu)	✔		RIN:10	
(M11B)+Dox + IFN	Total RNA (for Mohamed Mutochelu)	✔		RIN: 9.40	
(M10) -Dox - IFN	Total RNA (for Mohamed Mutochelu)	✔		RIN: 9.50	
(M10) +Dox - IFN	Total RNA (for Mohamed Mutochelu)	✔		RIN: 8.50	
(M10) -Dox + IFN	Total RNA (for Mohamed Mutochelu)	✔		RIN: 9.60	
(M10) +Dox + IFN	Total RNA (for Mohamed Mutochelu)	✔		RIN: 9.60	

Chip Lot #
MB03BK05 Exp: 3.FEB.2010

Reagent Kit Lot #
0907 Exp: 9.FEB.2010

Chip Comments :

Figure 3.7 Representative data of studies performed on triplicate cultures prior to the Affymetrix exon array study (A), (D) and (G**)**. vIRF-2 inhibited the rIFN-α driven pISRE-luc activity by 50% (M11A), 52% (M11B) and 47% (M10), respectively. The experiments were performed as described in Figure 3.5A. Cells treated with -dox+ifn were described as having 100% normalised pISRE-luc activity. Data are presented as mean normalised pISRE-luc activity (± standard deviation) of three independent experiments each performed induplicate (**p < 0.01, Student's *t* test). Experimental data shown in (B), (E) and (H) were performed as described in

Figure 3.3. Data are presented as mean +/- SD of three individual experiments. Experimental data shown in (C), (F) and (I) were performed as described in figure 3.5B. (J) Electrophoresis file of 28S and 18S RNA of all the 12 samples. (K) Shows RNA integrity values of the samples.

Table 3.1 Data summary of additional investigations performed on the 12 biological samples prior to the bioanalyser and exon array investigations

Sample names	Treatment profile	Total RNA conc ng/µl	260/280nm ratio	Extent of inhibition
M11A	–dox–ifn	560	2	50%
M11A	+dox–ifn	526	2	50%
M11A	–dox+ifn	548	2	50%
M11A	+dox+ifn	616	2	50%
M11B	–dox–ifn	726	2	52%
M11B	+dox–ifn	746	2	52%
M11B	–dox+ifn	891	2	52%
M11B	+dox+ifn	968	2	52%
M10	–dox–ifn	872	2	47%
M10	+dox–ifn	650	2	47%
M10	–dox+ifn	1136	2	47%
M10	+dox+ifn	762	2	47%

3.8 Characterizing vIRF-2 subcellular localization by Immunofluorescence Assay

Additional experiments were performed to reveal the subcellular location of vIRF-2. In eukaryotic cells there is continuous exchange of macromolecules between the nucleoplasm and the cytoplasm. For example, nuclear localization is regulated for several proteins involved in gene expression and development, as well as for proteins involved in the cell cycle. To determine vIRF-2 subcellular localization, confluent vIRF-2 clone 3-9 or EV clone 5 cells were treated with doxycycline for 30 hours or left untreated. The fixed cells were probed with an antibody against the cmyc-epitope of vIRF-2 and visualised using FITC conjugated anti-mouse IgG. The nuclei were stained with DAPI. Images were captured for FITC and DAPI staining under the same exposure conditions (see section 2.10.).

As expected, the negative control EV clone 5 cells did not express vIRF-2 (**Figure 3.8 A and B**), panel A shows background staining that is predominantly confined to the cytoplasm (**Figure 3.8 A**), whereas panel B represents the nuclear staining. vIRF-2 was detected in clone 3-9 (**Figure 3.8 C and D**); panel C vIRF-2 is detected predominantly in the nucleus as evidenced by FITC staining of the nuclear compartment. This nuclear staining is confirmed by overlap with DAPI staining in panel D. Taken together, vIRF-2 is predominantly a nuclear resident protein in clone 3-9 cells.

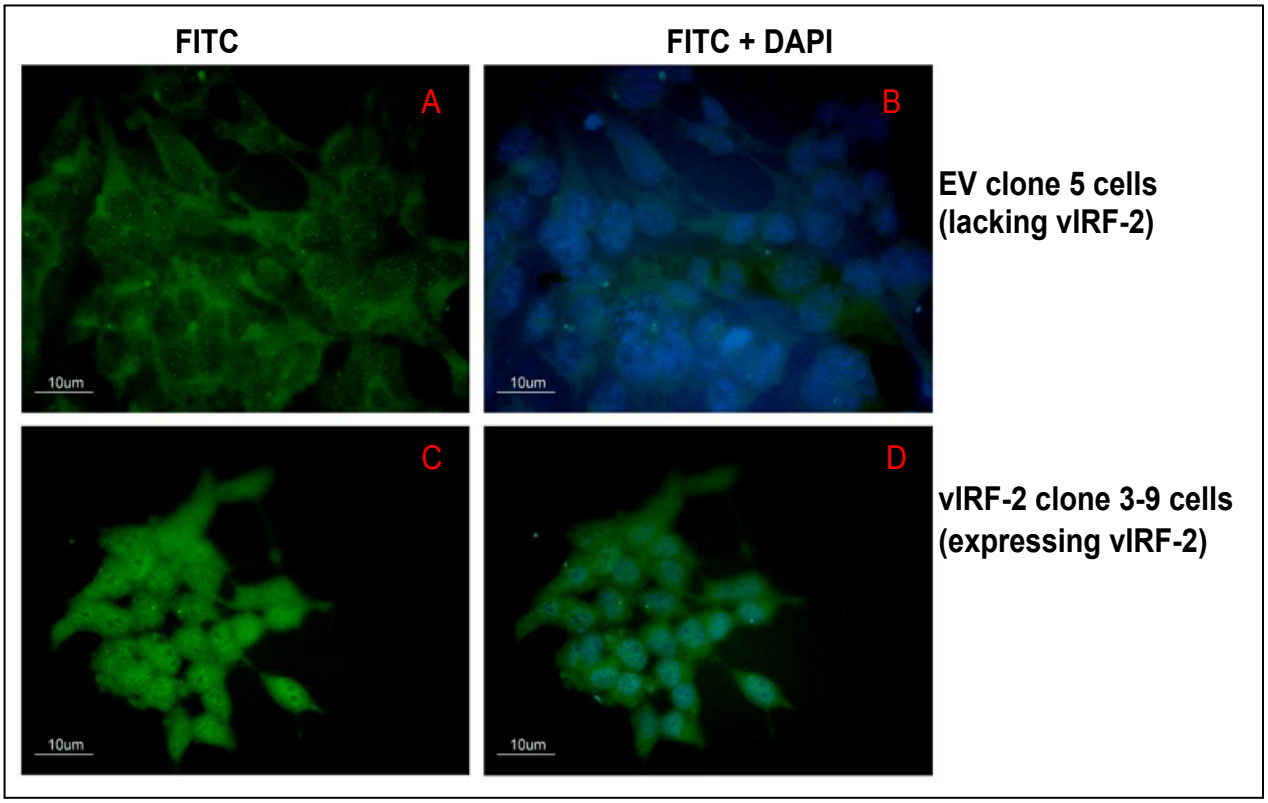

Figure 3.8 Determining vIRF-2 subcellular localization. Panel A & B, empty vector cells do not express vIRF-2 and panel C & D are vIRF-2-expressing clone 3-9 cells. The FITC staining of panel A shows background staining that are predominantly confined to the cells cytoplasm. Panel B shows DAPI staining of the cells nuclei. In panel C, the vIRF-2 protein is detected predominantly in the nucleus by FITC conjugated anti mouse IgG directed against cmyc epitope of vIRF-2. This nuclear staining is confirmed by overlap with DAPI staining in panel D. This image is representative of three independent experiments.

3.9 Discussion

Production of constitutively expressing vIRF-2 stable cell lines has been attempted (Fuld & Blackbourn, unpublished observation), but vIRF-2 expression in these cell lines was not sufficiently stable to enable mechanistic studies. The limitation of transient transfection studies using gene expression plasmid vectors is that the overexpressed gene(s) are not expressed in every cell. Stable cell lines in which every cell expresses vIRF-2 were therefore established for this study.

Investigations into vIRF-2 protein expression and functions in vIRF-2 expressing cells were performed. Cell lines stably transfected with the 'empty vector' pTRE2pur-Myc were analysed in parallel. vIRF-2 clone 3-9 cells are stably transfected with *vIRF-2*-expressing plasmid vector so that vIRF-2 expression is regulated by doxycycline. This was made possible because *vIRF-2* was subcloned into a site downstream of the tetracycline responsive elements of the pTRE2-pur-Myc plasmid vector (Clontech) and stably transfected in to 293Tet-On cells. Thus, in the presence of doxycycline *vIRF-2* will be responsive to the tetracycline transactivator (see 2.7 and 2.8). To maintain stable cell lines retaining the plasmid, clone 3-9 cells were maintained in media supplemented with both puromycin (1 μg/ml) and G418 (200 μg/ml). Furthermore, *vIRF-2* was tagged to a myc epitope since there are still no available antibodies to vIRF-2 proteins; vIRF-2 protein expression was therefore detected with anti c-myc antibodies.

The immunoblot data established that 1 μg/ml doxycycline induced maximum accumulation of vIRF-2 (**Figure 3.1A**). Cells treated with 2 μg/ml doxycycline did not survive, most probably due to toxicity of the drug (data not shown). Further immunoblot investigation revealed vIRF-2 expression peaked at 24-36 hours with the earliest time point of 12 hours (**Figure 3.1B, C**). RT-qPCR was employed to quantify vIRF-2 mRNA levels in experiments performed in parallel as described in **Figure 3.1C**. For the $\Delta\Delta C_T$

calculation to be valid, the amplification efficiencies of the target and reference must be approximately equal. The *vIRF-2* primer/probe amplification efficiency experiment (**Figure 3.2**) made it possible to choose *GAPDH* mRNA as the endogenous control since both *18S* mRNA and *β-actin* mRNA were not suitable, as evidenced by the poor binding or amplification of their primers/probes (data not shown). When *vIRF-2* and /or *GAPDH* were run as a singleplex or duplex assay, their amplification efficiencies remained within the recommended efficiency reference values (**Figure 3.2 A-D**). Consistent with protein expression data in **Figure 3.1C**, the RT-qPCR data showed *vIRF-2* mRNA expression peaked at 36 hours post doxycycline treatment (**Figure 3.3**).

The inhibition of antiviral effects of IFN-α by vIRF-2 has been used as a tool to functionally characterize either full-length vIRF-2 protein or that part encoded by exon 1 (Burysek, Yeow et al. 1999; Burysek and Pitha 2001; Fuld, Cunningham et al. 2006). However, Burysek and colleagues only studied exon 1 of vIRF-2, our group was the first to study the function of the complete (spliced) gene of vIRF-2 (Fuld, Cunningham et al. 2006).

In the present study, a luciferase reporter gene regulated by *ISG56* ISRE (pISRE-luc) was used as a measure of ISRE activity in response to rIFN-α in HEK293 cells expressing vIRF-2 or the EV clones counterparts. Among the most strongly induced virus stimulated or interferon stimulated genes is the ISG56 family of genes (Der, Zhou et al. 1998), comprising of four human members (ISG54/IFIT2, ISG56/IFIT1, ISG58/IFIT5 and ISG60/IFIT3) clustered on chromosome 10 (Wathelet, Moutschen et al. 1986; Bluyssen, Vlietstra et al. 1994; de Veer, Sim et al. 1998). These proteins are sometimes designated p54, p56, p58 and p60, contain arrays of multiple tetratricopeptide repeat helix-turn-helix motifs mediating a variety of protein-protein interactions which result in a number of effects on cellular and viral functions. Their activities include translation initiation, virus

replication, dsRNA signaling, cell migration and proliferation (D'Andrea and Regan 2003). A conspicuous characteristic of the ISG56 family of genes is that the promoters contain 2 IFN-stimulated response elements as the only identifiable *cis*-acting elements, located with 200 bp upstream of the TATA box promoter (Bluyssen, Vlietstra et al. 1994). These elements are recognised by the IRFs that are activated by various stimuli and induce transcription of the corresponding mRNAs (see Tamura, Yanai et al. 2008). Infection with a multitude of RNA- or DNA-viruses, such as Sendai virus (SeV), Respiratory syncytial virus (RSV), Lymphocytic choriomeningitis virus (LCMV), West Nile virus (WNV), Influenza virus, Reovirus, VSV, Herpes simplex virus (HSV), cytomegalovirus (CMV), and Adenovirus, efficiently induces these genes (Zhu, Cong et al. 1997; Nicholl, Robinson et al. 2000; Terenzi, Pal et al. 2005; Smith, Schmechel et al. 2006; Daffis, Samuel et al. 2007; Janssen, Pennings et al. 2007; Wacher, Muller et al. 2007). The use of cell lines with appropriate genetic deficiencies of the JAK-STAT pathway components was instrumental for demonstrating that viral and bacterial pathogen associated molecular patterns can directly (i.e., independently of IFN action) induce transcription of a subset of ISGs, including *ISG56* family genes (Bandyopadhyay, Leonard et al. 1995; Elco, Guenther et al. 2005). These genes are therefore termed viral stress-inducible genes (VSIG) (see Sarkar and Sen, 2004). The activation of IRFs plays a key role in the induction of these VSIGs by different stimuli, which recognise the ISREs in the VSIG promoters and initiate transcription. For example, ISGF3 composed of IRF-9 along with STATI and STAT2 and activated by the IFN-α/β receptor, mediates IFN responses; IRF-3, activated by dsRNA via TLR3 or via RIG-I/MDA5, and by lipopolysaccharides via TLR4, potentially induces the ISG56 family genes (Grandvaux, Servant et al. 2002; Sarkar, Peters et al. 2004; Ogawa, Lozach et al. 2005; Terenzi, Hui et

al. 2006). Therefore, consistent with this study, ISG56 is frequently used as the readout for the IFN-α/β pathway activity (Chattopadhyay, Marques et al. 2010).

Human and mouse p54 and p56 interact with different subunits of translation initiation factor 3 (eIF3), resulting in an inhibition of translation (Hinnebusch 2006). A reported complexity of murine p54 versus p56 protein expression *in vivo*, depending on the stimulus (IFN, dsRNA, or virus infection), tissue type and cell type revealed interesting findings; for example, whereas tail vein injection of dsRNA induced p54 and p56 in the liver and spleen, injection of VSV induced p54 in the spleen but not in the liver; this was observed at both protein and mRNA levels (Terenzi, White et al. 2007). These authors further showed that the relative induction of p54 versus p56 in organs such as the heart or lungs varies depending on the inducing stimulus. Therefore, we speculate that in evolutionary terms, vIRF-2 may have evolved to inhibit ISG56 expression in cells as a way of suppressing the innate antiviral pathway, due to the fact that ISG56 can be induced by both IFN and non-IFN (such as virus trigger) dependent factors whereas some interferon stimulated genes such as the MxA are known to be induced selectively by IFNs but not directly by virus infection (Holzinger, Jorns et al. 2007). In cell lines such as HEK293, IFN-induced levels of *ISG56* mRNAs are maintained at high levels even after 24 hours of treatment (Terenzi, Hui et al. 2006) indicating these cells respond to IFN. Moreover, HEK293 cells can be infected with KSHV.

ISGF3 from upstream stimuli such as activated IFN-α/β receptors or IRF-3/7 activated by double-stranded RNA via TLR3 or via RIG-I/MDA-5 potentially induces *ISG56* (Grandvaux, Servant et al. 2002; Ogawa, Lozach et al. 2005; Terenzi, Hui et al. 2006). In the present study, the optimum concentration of rIFN-α was determined to stimulate pISRE-luc activity in the EV clone 5 cells. The first phase of this experiment involved a titration of rIFN-α to stimulate pISRE-luc activity in EV clone 5 cells which

established that 300 IU/ml IFN-α stimulated the maximal pISRE-luc activity peaking about 25-fold (**Figure 3.4A**). It was observed that 200 IU/ml rIFN-α stimulation of HEK293 cells co-transfected with pISRE-luc induced the maximum luciferase activity in a rIFN-α2b titration assay (Fuld, Cunningham et al. 2006). It is worth noting that Fuld and colleagues harvested their cells 16 hours after addition of rIFN-α2b (Stratagene), about 14 hours earlier than in this study. Besides, their rIFN-α may differ subtly from our rIFN-α, since different manufacturers supplied them. The second experiment demonstrated that (300 IU/ml) rIFN-α stimulation of pISRE-luc activity peaked at 12 hours and was sustained around the same level until 36 hours (**Figure 3.4B**). These data are consistent with the observation by others (Terenzi, Hui et al. 2006) that the mRNA of some IFN-induced target genes, such as *ISG56*, are maintained beyond 24 hours of treatment. Because rIFN-α stimulation of the cells peaked around 30 hours and inducible vIRF-2 expression also peaked around 30 hours, cell treatment for this period was selected for further studies.

The inhibition of pISRE-luc activity by vIRF-2 (**Figure 3.5**), is consistent with previous reports that demonstrated vIRF-2 exon1 is a potent inhibitor of IFN-α promoters in transient transfection assays through binding to IRF-1, RelA and CBP/p300 culminating in the inhibition of their transactivating capabilities (Burysek, Yeow et al. 1999). Also, our group reported the repression of rIFN-α stimulated pISRE-luc activity by full-length vIRF-2 through IRF-3 inhibition in HEK293 cells (Fuld, Cunningham et al. 2006). More recently, our group reported that vIRF-2 repressed full-length IFN-β promoter transactivation via IRF-3 in a model system where the antiviral response and IRF-3 activation were triggered by poly I:C transfection of HEK293 cells (Areste, Mutocheluh et al. 2009). In conclusion, taken together the evidence indicates inducible

vIRF-2 protein is capable of inhibiting the type I IFN pathway. This may be its role in the context of KSHV infection.

Additional vIRF-2 expressing cells and their EV counterparts were engineered using techniques described (section 2.7 and 2.8). The confirmation of vIRF-2 expression and functional studies were performed as described (**Figure 3.5**). Representative data of over 300 clones screened indicated over 50% suppression of rIFN-α stimulated pISRE-luc activity in vIRF-2 clones 20 and 24 respectively (**Figure 3.6 D, E**). The most likely reason the vIRF-2 suppressing clones are in the minority is that vIRF-2 expression is so leaky that the established concentration of rIFN-α cannot induce ISRE activation. Therefore, the suppression of ISRE activation and lack of induction due to leaky vIRF-2 expression is what was experienced.

Having verified vIRF-2 expressed in sample sets M11A, M11B & M10 inhibited pISRE-luc activity (**Figure 3.7**) the RNA prepared from each sample set (data for these samples are summarised in **Table 3.1**) was submitted for DNA microarray profiling. The DNA profiling data are presented in chapter 4. Cell samples were prepared to investigate vIRF-2 regulation of the transcriptome by DNA microarray based on the data presented in this chapter. For reasons of cost only clone 3-9 cells were prepared for the DNA microarray investigations and follow up studies to validate the findings from this cell line were then performed on vIRF-2 clones 3-9, 20, 24, and the empty vector counterparts EV1, EV4 and EV5.

Further characterization of vIRF-2 by immunofluorescence assay indicated that it is a nuclear resident protein (**Figure 3.8**) consistent with Burysek et al., who reported a similar observation for vIRF-2 exon 1 in KSHV positive PEL cell lines (Burysek and Pitha 2001).

Chapter 4 vIRF-2-deregulated gene sets and signaling pathways

The aim of this chapter was to investigate (i) the impact of vIRF-2 on the cell transcriptome profile and (ii) reveal the mechanism by which vIRF-2 inhibits the type 1 IFN pathway. The data were generated from DNA microarray experiments performed with the sample sets M11A, M11B and M10 described in section 3.7. The GeneChip names for each sample for which the data were derived are presented in **Table 4.1**. We began by performing a comprehensive quality control assessment of the Affymetrix GeneChips to identify arrays with divergent probe signal intensity distributions relative to other arrays in the study; in other words to identify problematic GeneChips, but none was identified. Gene level analysis of the Affymetrix exon arrays was performed using the Affymetrix Expression Console. The bioinformatics analyses included the DAVID and GSEA packages to generate gene ontology and gene set enrichment data. Immunoblot assay was employed to validate some of the identified vIRF-2 deregulated gene sets and associated biological signaling pathways.

4.1 Introduction

Microarray technology is a widely used high-throughput tool for measuring gene expression (Schena, Shalon et al. 1996; Allison, Cui et al. 2006). The most popular platform is the Affymetrix GeneChip microarray. In this technique, gene level expression indices are computed based on hybridization of signal intensity measurements from multiple perfect match (PM) and mismatch (MM) probes targeting the 3' end of the mRNA sequence. Recently however, Affymetrix released another product called the Exon

array, which was used in this study. Exon arrays differ very much from 3' expression arrays in the number and placement of the probes [http://www.affymetrix.com/support /technical/datasheets/exon_arraydesign_datasheet.pdf]. In exon arrays, up to four probes are selected to target each putative exonic region thereby providing a more accurate measurement of gene expression than the traditional 3' arrays. The exon arrays also differ in that they do not use the PM/MM system, but instead have a limited number of control probes for assessing non-specific hybridization.

DNA microarray has been previously used to study vIRF-2; Jenner and colleagues used the PEL-derived cell line (BC-3) to study the expression of KSHV during latency and lytic replication. The authors revealed vIRF-2 and vIRF-3 were spliced transcripts (Jenner, Alba et al. 2001).

The ubiquitin proteasome pathway may be deregulated by vIRF-2 because of its active role in events upstream of the IFN-α/β receptor. It was discovered by Avram Hershko and colleagues in the late 1970's, and is required for the targeted degradation of most short-lived proteins in the eukaryotic cell. In all tissues, the majority of intracellular proteins are degraded by the ubiquitin proteasome pathway (Rock, Gramm et al. 1994). However, the ubiquitination of RIG-I is reported to promote the antiviral response (Gack, Shin et al. 2007). RIG-I activation by dsRNA promotes recruitment of unanchored lysine 63 (K63)-linked ubiquitin chains to the CARD domain of RIG-I and forms a potent viral RNA sensor that directly communicates with MAVS (also called IPS-1/VISA/Cardiff) to promote IRF-3 activation (Zeng, Sun et al. 2010), ultimately leading to an antiviral response.

Ubiquitin modification is an ATP-dependent process carried out by three classes of enzymes. A ubiquitin-activating enzyme (E1) which forms a thio-ester bond with ubiquitin. This allows subsequent binding of ubiquitin to the active site of one of the

approximately 40 ubiquitin conjugating enzymes (E2), followed by the formation of an isopeptide bond between the carboxyl-terminus of ubiquitin and a lysine residue on the substrate protein in a reaction requiring ubiquitin ligase 3 (E3). E3s can be single- or multi-subunit enzymes such that in some cases ubiquitin-binding and substrate-binding domains reside on separate polypeptides brought together by adaptor proteins (Pickart 2004). Many E3s provide specificity in that each can modify only a subset of substrate proteins. A single run of the reaction causes mono-ubiquitination of a target protein that could change its function. Multiple runs of the reaction lead to poly-ubiquitination of the substrate. Lysine-48-linked chains typically signals proteasomal degradation, whereas the conjugation of lysine-63-linked poly-ubiquitin chains is associated with DNA repair, kinase signaling pathways, and receptor regulation (see Konstantinova, Tsimokha et al. 2008). Because of this involvement of ubiquitination in the normal functioning of the antiviral response, consideration was given to its possible modulation by vIRF-2 in the present study, aside from IRF-3 and the JAK-STAT pathways.

4.2 Quality assessment of exon arrays

As stated earlier, the aim of this section of the study was to identify problematic GeneChips in **Table 4.1** but none was identified. The quality assessment procedures used in this study were computed from CEL files of the Human Exon 1.0 ST Array. The Affymetrix CEL file contains a single intensity value calculated for each probe on each GeneChip. CEL files are generated together with the expression data set and can be used to assess problems with data quality. The CEL files were first uploaded into Expression Console (EC) and a multi-chip analysis was performed according to suggestions stated in the exon array Whitepaper Collection (see Affymetrix). Once this analysis was complete, a number of quality assessment metrics were visualized graphically. These metrics can

identify outlier arrays within the expression data set. The metrics categories used in this study and their meaning are summarised in **Appendix II.**

Data shown (**Appendix II, Figure 1**) were performed in accordance with Affymetrix guidelines set out in the Exon Array Whitepapper Collection and sometimes referred to as Affymetrix criteria for quality assessment of exon arrays (see Affymetrix). The first set of quality assessment metrics are based on probe intensity level data such as pm_mean and bgrd_mean. Apart from dM11A_+Dox+IFN_RNA_220709.rma-gene-core, which was indicative of being slightly dim, all the other GeneChips were bright (**Appendix II, Figure 1A**). Affymetrix deal with this difference in intensity using a process called the quantile normalization, which puts all GeneChips on the same scale. The bgrd_mean was plotted together with the pm_mean to measure how the background signals varied from that of the pm_mean. As expected, the bgrd_mean data correlated with that of the pm_mean (**Appendix II, Figure 1B**). Generally, the mean of probe level intensity for all the perfect matched probes was consistently above that of the background levels, as expected.

The rle_mean is a probeset summarisation metric used for the quality assessment of the exon arrays. The box plots of the relative log expression for all the probesets analysed indicate there was no divergent probe intensity distributions relative to other arrays in the study as evidenced by the median rle (the middle bar in each box) (**Appendix II, Figure 1C**). This value is below 0.12 as shown on the y-axis of the graph and should be zero in most applications as suggested by Affymetrix although no specific median rle value was suggested as acceptable. Therefore, the 3 summarisation probesets metrics: rle_mean, pos_vs_neg_auc and mad_residual_mean are all within the parameters suggested by the Whitepaper Collection (**Appendix II, Figure 1D**).

The internal quality control metrics (mad_residual_mean of bac_spike, polya _ spike and pos_control) have all shown consistency in their probesets signal intensity distribution (**Appendix II, Figure 1E**) dM11A_+Dox+IFN _RNA_220709.ma.gene.core has a mean absolute deviation of residuals value of 0.44 and was not considered an outlier because Affymetrix considered 0.77 as outlier (see Affymetrix). It was therefore included in the study since the robust multichip and multiprobe analysis methods used (**Appendix II, Figure 1C**) indicated dM11A_+Dox+IFN_RNA_220709.ma. gene core was well within the range of signal intensities observed for all the GeneChips within the study.

Table 4.1 Affymetrix GeneChip names and profiles of the exon arrays

Sample names	Treatment profile	Total RNA conc ng/µl	260/280nm ratio	Extent of inhibition	GeneChip names
M11A	–dox–ifn	560	2	50%	aM11A_-Dox-IFN_RNA_22-709.rma-gene-core
M11A	+dox–ifn	526	2	50%	bM11A_+Dox-IFN_RNA_22-709.rma-gene-core
M11A	–dox+ifn	548	2	50%	cM11A_-Dox+IFN_RNA_22-709.rma-gene-core
M11A	+dox+ifn	616	2	50%	dM11A_+Dox+IFN_RNA_22-709.rma-gene-core
M11B	–dox–ifn	726	2	52%	aM11B_-Dox-IFN_RNA_22-709.rma-gene-core
M11B	+dox–ifn	746	2	52%	bM11B_+Dox-IFN_RNA_22-709.rma-gene-core
M11B	–dox+ifn	891	2	52%	cM11B_-Dox+IFN_RNA_22-709.rma-gene-core
M11B	+dox+ifn	968	2	52%	dM11B_+Dox+IFN_RNA_22-709.rma-gene-core
M10	–dox–ifn	872	2	47%	aM10_-Dox-IFN_RNA_22-709.rma-gene-core
M10	+dox–ifn	650	2	47%	bM10_+Dox-IFN_RNA_22-709.rma-gene-core
M10	–dox+ifn	1136	2	47%	cM10_-Dox+IFN_RNA_22-709.rma-gene-core
M10	+dox+ifn	762	2	47%	dM10_+Dox+IFN_RNA_22-709.rma-gene-core

During the DNA microarray studies Affymetrix GeneChip names were assigned to each of the sample sets M11A, M11B and M10 (section 3.7). These names are presented on the right column. The 'Extent of inhibition' column shows the percentage at which IFN-α induced pISRE-luc activity was inhibited by vIRF-2 expression (see section 3.7).

4.3 vIRF-2 modulated cell transcriptome in response to IFN-α treatment

Having shown that the Affymetrix GeneChips have passed the quality assessment criteria suggested by Affymetrix (section 4.2), the next task was to test the hypothesis that vIRF-2 deregulates cellular genes and related signaling pathways responsive to IFN-α. The expression data set was analysed using the EC. The exon array raw data revealed 13542 cellular genes were differentially expressed (expression data set not shown). The expression levels of these genes exhibited a range of values representing a range of fold change in response to IFN-α. The profiles of genes transcriptionally responsive to IFN-α are shown (**Figure 4.1 A, C**) and those modulated by vIRF-2 are shown in **Figure 4.1 B, D** & **E**.

Comparison of the differentially expressed genes from untreated cells (-dox-ifn) with those treated with -dox+ifn indicates 78 IFN-α genes were significantly up-regulated based on Limma p value < 0.001 (**Figure 4.1A**). The Limma p value is explained in section 2.11.2. The expression values of these 78 IFN-α up-regulated genes were then compared with those of vIRF-2 induced cells (+dox+ifn), which demonstrated that 57/78 (73%) were significantly down-regulated based on Limma p value < 0.05 (**Figure 4.1B**). Of the remaining 21 of 78 IFN-α up-regulated genes, 10 (13%) were less significantly down regulated by vIRF-2 expression based on Limma p values of between 0.05 and 0.1. The remaining 11/78 (14%) differentially expressed genes were not significantly changed by vIRF-2 expression with limma p-value >0.1. 17/26 (65%) of the 26 genes were up-regulated by vIRF-2 in the absence of IFN-α based on Limma p value < 0.05 and the remaining 9/26 (35%) of the genes down-regulated by vIRF-2 (Limma p<0.05) (**Figure 4.1E).** The heat maps show expression values arranged in descending order from the most down-regulated, i.e. *IFIT3* (**Figure 4.1 B, D**).

Comparison of the gene expression profile of cells treated with -dox-ifn and -dox +ifn identified 26 IFN-α down-regulated genes with Limma p value < 0.001 (**Figure 4.1C**). The expression values of these 26 IFN-α down-regulated genes were then compared between cells treated with -dox+ifn and +dox+ifn. Of these 26 genes, 13 (50%) were significantly up-regulated by vIRF-2 with Limma p value < 0.05 (**Figure 4.1D**). These data indicate that the effect of IFN-α treatment on the expression of these genes is modulated by vIRF-2 expression. Further, 3/26 (12%) of the IFN-α down-regulated genes were significantly up-regulated by vIRF-2 with Limma p value between 0.05 and 0.1. The remaining 10/26 (38%) genes were not significantly changed by vIRF-2 expression with Limma p value >0.1.

These data suggest vIRF-2 deregulates IFN-α regulated cellular genes because genes up-regulated by IFN-α were down-regulated by vIRF-2 and vice versa (**Figure 4.1**).

A

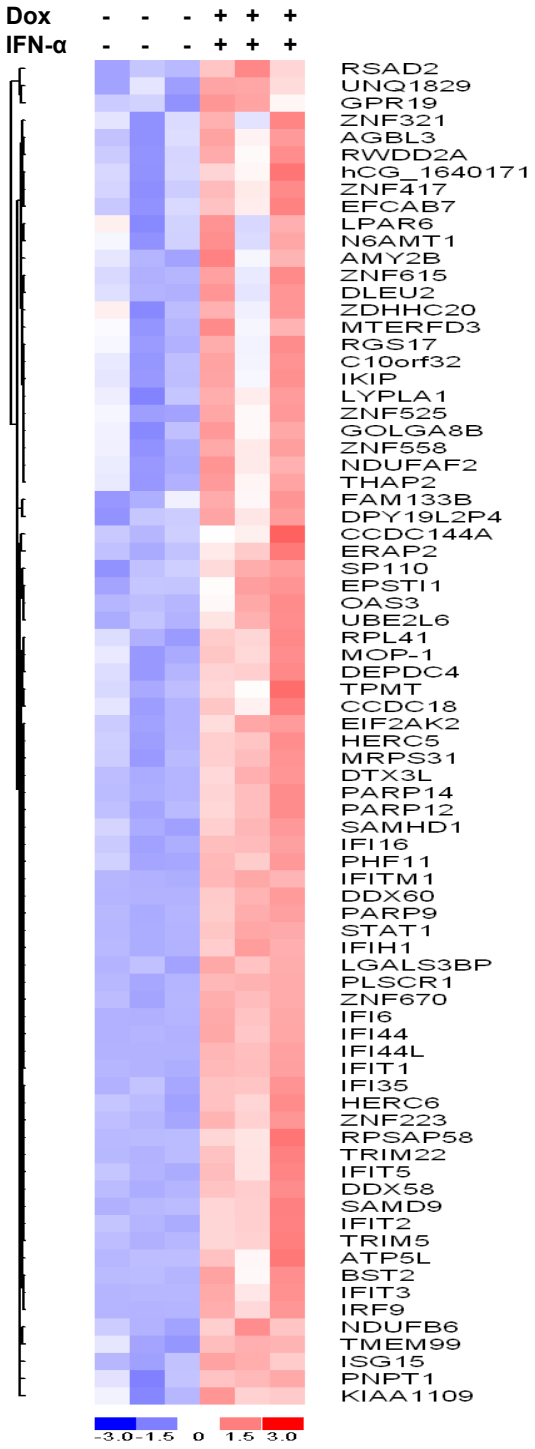

Figure 4.1. The 78 genes up-regulated by rIFN-α. (A) The expression values for a gene across all samples in the heatmap were standardized to have mean 0 and standard deviation 1. The colour scale at the bottom represents the expression pattern with white representing no change (=0), shades of red

representing up-regulation, and shades of blue representing the down-regulated genes. -Dox-IFN-α represents untreated cells, -Dox+IFN-α represent cells treated with rIFN-α. Each column represents a replicate experiment of three performed for each treatment condition. Comparison of the gene expression profiles of cells treated with -Dox-IFN-α with those of -Dox+IFN-α identified 78 IFN up-regulated genes based on Limma $p<0.001$.

B

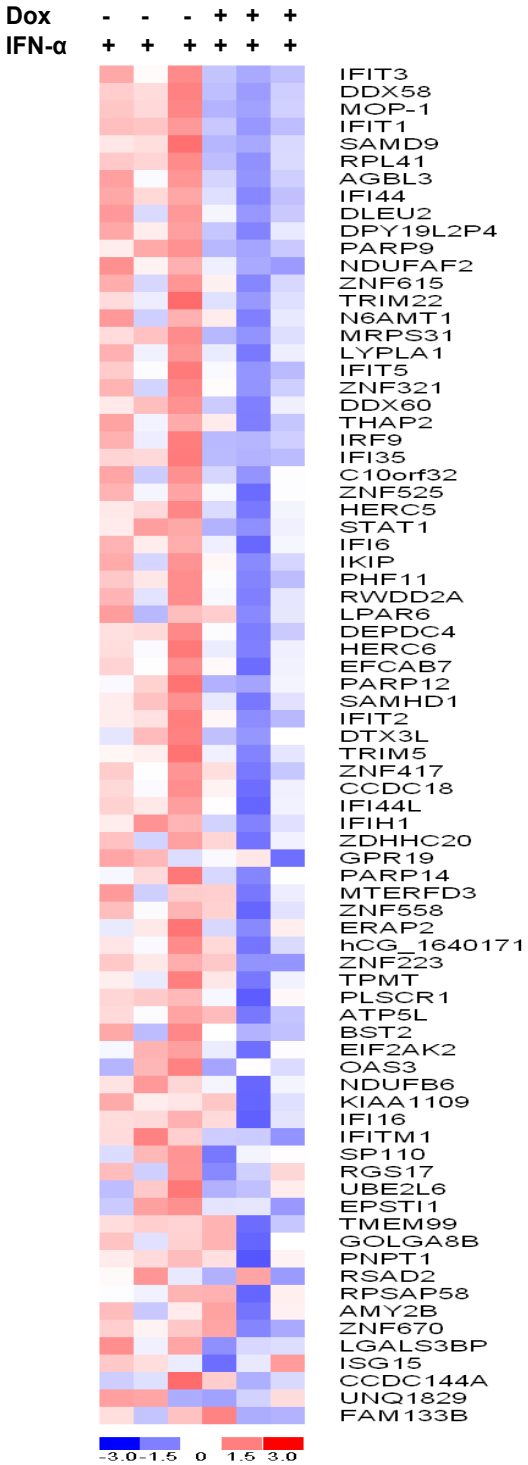

Figure 4.1. Effect of *vIRF-2* on the 78 genes up-regulated by rIFN-α. (B) The expression values for a gene across all samples in the heatmap were standardized to have mean 0 and standard deviation

1. The colour scale at the bottom represents the expression pattern with white representing no change (=0), shades of red representing up-regulation, and shades of blue representing the down-regulated genes. -Dox+IFN-α represents IFN-α treated cells, +Dox+IFN-α represents vIRF-2 induced cells treated with IFN-α. Each column represents a replicate experiment of three performed for each treatment condition. Comparison of the gene expression profiles of cells treated with -Dox+IFN-α with those of +Dox+IFN-α identified 57 genes as down-regulated by vIRF-2 based on Limma $p<0.05$.

C

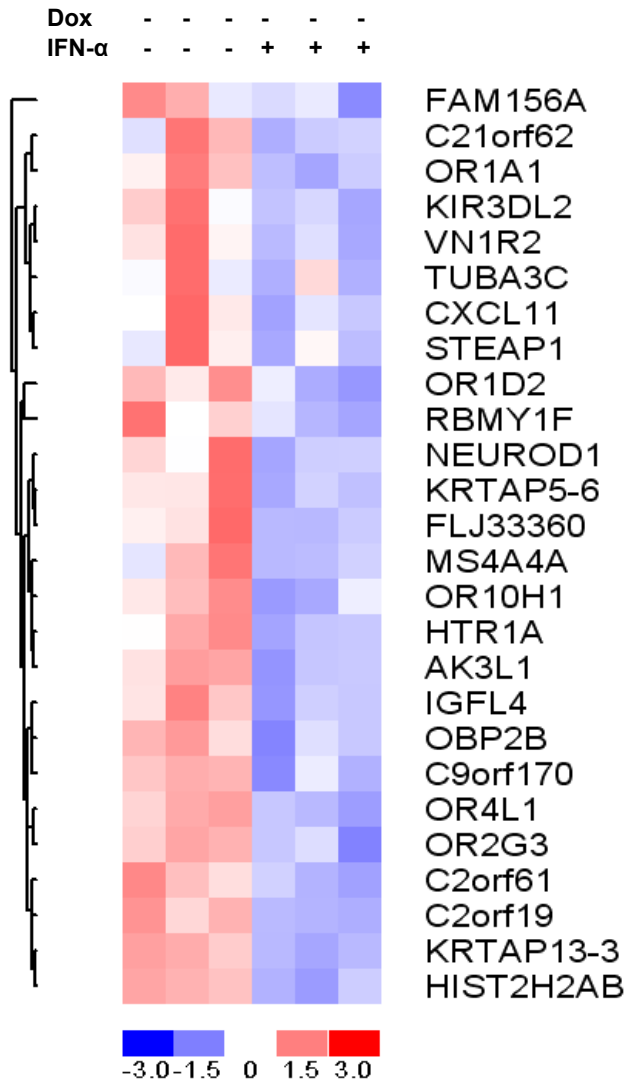

Figure 4.1. The 26 genes down-regulated by IFN-α. (C) The expression values for a gene across all samples in the heatmap were standardized to have mean 0 and standard deviation 1The colour scale at the bottom represents the expression pattern with white representing no change (=0), shades of red representing up-regulation, and shades of blue representing the down-regulated genes. -Dox-IFN-α represents untreated cells, -Dox+IFN-α represents cells treated with IFN-α. Each column represents a replicate experiment of three performed for each treatment condition. Comparison of the gene expression profiles of cells treated with -Dox-FN-α with those of -Dox+IFN-α identified 26 IFN-α down-regulated genes based on Limma $p<0.001$.

D

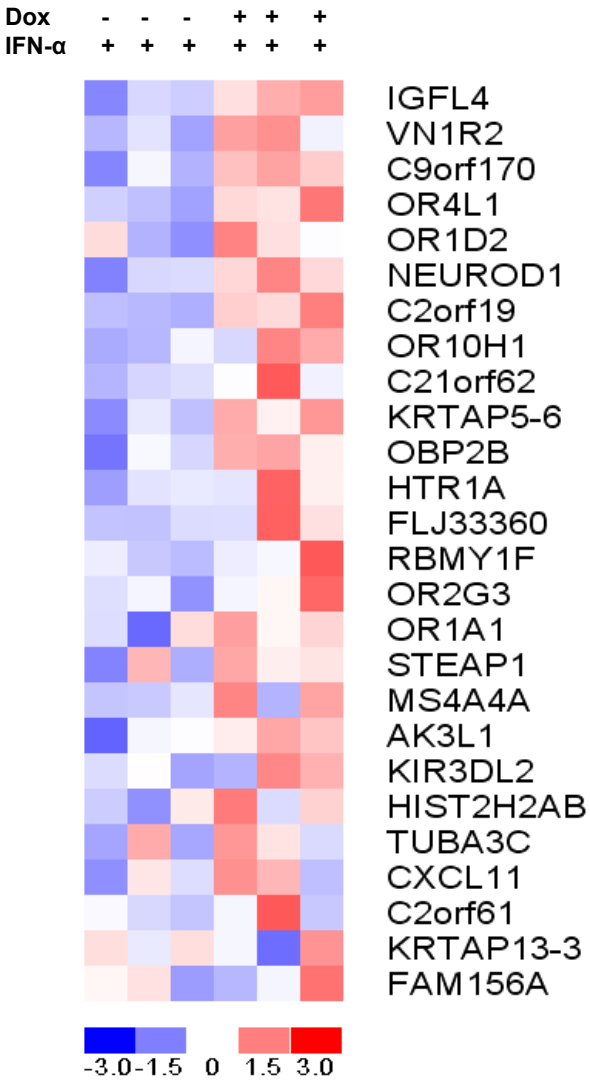

Figure 4.1. Effect of *vIRF-2* on the 26 genes down-regulated by rIFN-α. (D) The expression values for a gene across all samples in the heatmap were standardized to have mean 0 and standard deviation 1. The colour scale at the bottom represents the expression pattern with white representing no change (=0), shades of red representing up-regulation, and shades of blue representing the down-regulated genes. -Dox+IFN-α represents cells treated with rIFN-α, +Dox+IFN represents vIRF-2 induced cells treated with IFN-α. Each column represents a replicate experiment of three performed for each treatment condition. Comparison of the gene expression profiles of cells treated with -Dox+FN-α with those of +Dox+IFN-α identified 13 of the IFN-α down-regulated genes as up-regulated by vIRF-2 based on Limma $p<0.05$.

E

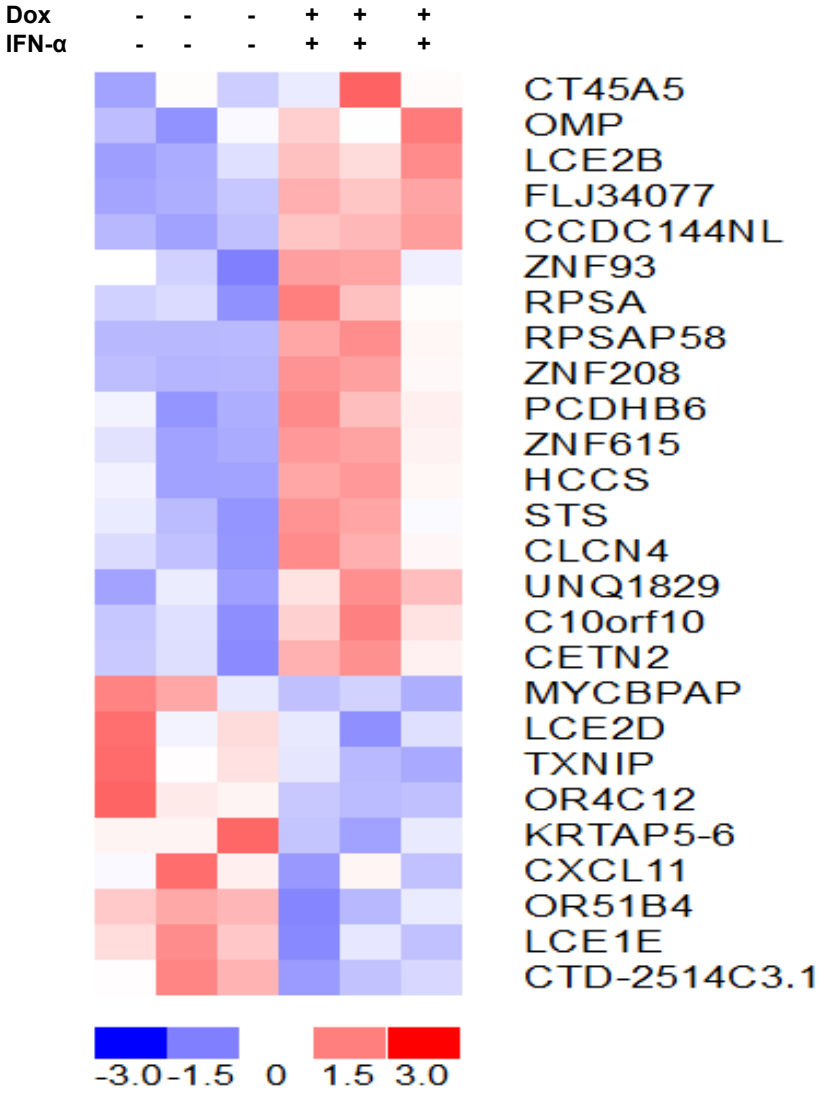

Figure 4.1. vIRF-2 regulated genes in the absence of IFN-α. (E) The expression values for a gene across all samples in the heatmap were standardized to have mean 0 and standard deviation 1. The colour scale at the bottom represents the expression pattern with white representing no change (=0), shades of red representing up-regulation, and shades of blue representing the down-regulated genes. -Dox-FN-α represents untreated cells, +Dox-IFN represents vIRF-2 induced cells. Each column represents a replicate experiment of three performed for each treatment condition. Comparison of the gene expression profiles of the untreated cells with those of +Dox-IFN-α identified 17 up-regulated and 9 down-regulated genes by vIRF-2 based on Limma $p<0.05$.

4.4 Bioinformatics analysis of the IFN-α up-regulated genes deregulated by vIRF-2

The bioinformatics analysis of the expression data set were performed by both DAVID and GSEA software packages to avoid over reliance on one package to generate the data because of the differences in the analytical capabilities of both packages (see section 2.11.3). For example, DAVID is not a gene set enrichment tool in the same way as GSEA (section 4.6), as DAVID focuses on the enrichment of GO terms, rather than gene sets. Genes identified by DAVID, belong to the same category, but their products do not necessarily interact with each other. This section will discuss the data generated by DAVID package.

The gene ontology analyses of the expression values of genes down-regulated by vIRF-2 in response to IFN-α treatment (**Figure 4.1B, C**) were subsequently performed with the DAVID package and are presented (**Table 4.2)**. Therefore, these IFN-α up-regulated genes that were down-regulated by vIRF-2 were identified and grouped in to GO terms having common biological functions or belonging to related pathways (**Table 4.2**). The DAVID analytical software package can perform gene ontology analysis to extract biological meanings, e.g. biological pathways (Huang da, Sherman et al. 2009). Probeset identifiers (IDs) of genes shown in **Figure 4.1 B**, **D** were uploaded on to the DAVID package and the details of biological information were viewed with the functional annotation clustering, table, chart and/or the pathways map viewer tools. The identified GO terms together with their associated gene sets were listed according to their enrichment score and DAVID $p < 0.01$ (**Table 4.2**). For example, Response to virus, Antiviral defence, Host-virus interactions and Innate immune response were the GO terms with the highest enrichment score of 8.86 (**Table 4.2**). Further search of DAVID via the KEGG_PATHWAYS tool for biological pathways deregulated by vIRF-2 identified 15 genes and their related biological pathways out of which only 6 (ISG15, RIG-I/DDX58, IFIH1, STAT1, IRF-9/p48 and UBE2L6) were associated

with **Table 4.2.** Genes presented in **Figure 4.1 D** and analysed by the DAVID package did not have GO terms significantly enriched (≥ 1.3) and $p < 0.01$ and were therefore not investigated further.

The next task was to analyse the biological pathways associated with the GO terms (**Table 4.2**). The protein expression of some biological pathways was confirmed by immunoblot (section 4.5).

Table 4.2 The functional annotation clusters of the IFN-α up-regulated genes down-regulated by vIRF-2. These data were derived from the expression data set shown (Figure 4.2 B) and generated by the DAVID package.

Antiviral Reponses			
Annotation cluster 1 (ES 8.86)[2]	**GO Term[1]**	**Genes**	**p-value**
GOTERM_BP_FAT[4]	Response to virus	(15) DDX58/RIG-I, ISG15, BST2, SAMHD1, EIF2AK2, IFIH1, IRF9, IFI16, IFI35, IFI44, PLSCR1, RSAD2, STAT1, TRIM22, TRIM5	<0.001
SP_PIR_KEYWORDS[4]	Antiviral defence	(11) DDX58/RIG-1, ISIG15, BST2, EIF2AK2, IFIH1, IRF9, PLSCR1, RSAD2, STAT1, TRIM22, TRIM5	<0.001
SP_PIR_KEYWORDS[4]	Host-virus interaction	(7) ISG15, SP110, EIF2AK2, IFIH1, STAT1, TRIM22, TRIM5	<0.001
SP_PIR_KEYWORDS[4]	Innate immune response	(4) DDX58/RIG-I, SAMDH1, ERAP2, IFIH1	<0.001
Annotation cluster 2 (ES 2.32)	**GO Term**	**Genes**	
INTERPRO[4] SP_PIR_KEYWORDS[4] SMART[4]	IFN induced proteins with tetratricopeptide repeats (TPR) TPR TPR	(4) IFIT1, IFIT2, IFIT3, IFIT5 (4) IFIT1, IFIT2, IFIT3, IFIT5 (4) IFIT1, IFIT2, IFIT3, IFIT5	<0.001
Transcription regulation			
Annotation cluster 3 (ES2.17)	**GO Term**	**Genes**	
INTERPRO[4] GOTERM_MF_FAT[4]	Poly (ADP-ribose) polymerase, catalytic region, transcription regulation NAD+ADP-ribosyltransferase activity	(3) PARP 9, PARP 12, PARP 14 (3) PARP 9, PARP 12, PARP 14	<0.001
Annotation cluster 4 (ES 2.17)	**GO Term**	**Genes**	
GOTERM_MF_FAT[4]	Regulation of transcription, DNA binding	(13) SP110, THAP2, IFIH1, IRF9, IFI16, STAT1, TRIM22, ZNF223, ZNF417, ZNF558, ZNF615, ZNF670, ZNF845	<0.001
Annotation cluster 5 (ES 1.11)	**GO Term**	**Genes**	
SP_PIR_KEYWORDS[4] SP_PIR_KEYWORDS[4]	Ligase Ubl conjugation pathway	(6) DTX3L, HERC5, HERC6, TRIM22, TRIM5, UBE2L6 (7) ISG15, DTX3L, HERC5, HERC6, TRIM22, TRIM5, UBE2L6	<0.01

1. GO Term: The associated biological annotation to which the gene list was mapped.
2. GO Term with enrichment scores ≥ 1.3 are recommended by the DAVID protocol for further analyses to be performed since they indicate significant difference. However the DAVID protocol (Huang et al, 2009) suggests gene groups with lower scores could be potentially interesting and should be explored as well, especially where they may be linked to groups of higher scores within the study.
3. Genes with enrichment scores below 1.3 were ignored.
4. GOTERM_MF_FAT, INTERPRO, SP_PIR_KEYWORDS, SMART: These are the original databases where the gene ontology (GO) terms originate. MF: molecular function; FAT: the GO Fat set attempts to filter the broadest terms so that they do not overshadow the more specific terms. PIR: protein

information resource (http://pir.georgetown.edu/) integrated protein informatics resource for genomic, proteomic and systems biology research; INTERPRO: is an integrated documentation resource for protein families, domains, regions and sites (http://www.ebi.ac.uk/interpro). Simple Modular Architecture Research (SMART) is a protein analysis database, which uses Uniprot/Ensembl to provide high quality and freely accessible resource of protein sequence and functional information (http://www.smart.embl.de).

4.5 IFN-α-responsive biological pathways identified as deregulated by vIRF-2 expression

We hypothesised that vIRF-2 deregulates events upstream or downstream of the IFN-α/β receptor. Therefore, five deregulated GO terms identified in **Table 4.2**, representing three signaling pathways were studied in further detail. The GO terms were: Response to virus, Antiviral defence, Host-virus interaction, Innate immune response and Ubiquitin ligase conjugation pathway.

The first phase of testing the hypothesis involved analysing the pathway details with the pathway map viewer tool of the DAVID package. The second phase involved investigating expression of proteins in these pathways by immunoblot assay. The pathways represented by GO terms "IFN induced proteins with tetratricopeptide repeats" and the "Poly (ADP-ribose) polymerase catalytic region" (**Table 4.2**) were not studied further due to time constrains.

The details of the RIG-like receptor, JAK-STAT and Ubiquitin ligase conjugation signaling pathways were analysed by DAVID pathway map viewer tool and confirmed by immunoblots assay are discussed below.

4.5.1 vIRF-2 modulates the JAK-STAT Signaling Pathway

The JAK-STAT signaling pathway downstream of the IFN-α/β receptor comprises the later phase of the IFN-α/β pathway and is discussed in section 1.15. Analysis of the JAK-STAT pathway with the DAVID package pathway map viewer tool revealed vIRF-2 inhibits signal transduction downstream of the activated IFN-α receptors by specifically targeting STAT-1 protein in the cell cytoplasm and IRF-9/p48 in the nuclear compartment (**Figure 4.2**). The next task was to confirm this bioinformatics result by immunoblot assay in the vIRF-2 induced clones compared with the EV clones (lacking vIRF-2). Therefore, for each pair of clones (vIRF-2 clone 3-9 vs EV clone 5, vIRF-2 clone 20 vs EV clone 1 and vIRF-2 clone 24 vs EV clone 4), a dual luciferase assay was performed to confirm vIRF-2 inhibited pISRE-luc activity as described (section 3.5), components of the IFN-α/β signaling pathway were investigated in parallel by immunoblot assay.

The luciferase assay result shows vIRF-2 clone 3-9 cells treated with -dox-ifn and +dox-ifn represent background levels of normalised pISRE-luc activity. The normalised pISRE-luc activity increased approximately 90-fold in response to IFN-α in cells treated with -dox+ifn and was reduced significantly ($p < 0.05$, Student's *t* test) by 52% in vIRF-2 induced cells treated with +dox+ifn (**Figure 4.3A**). Whereas with the EV clone 5 cells, the normalised pISRE-luc activity increased by approximately 250-fold in response to IFN-α in cells treated -dox+ifn and +dox+ifn. Comparatively, induced vIRF-2 expression significantly inhibited ($p < 0.01$, Student's *t* test) normalised pISRE-luc activity by 83% in vIRF-2 clone 3-9 cells treated with +dox+ifn compared with the same treatment profile in EV clone 5 cells (**Figure 4.3A**). To ensure this result (**Figure 4.3A**) was not clone specific, the experiment was performed on vIRF-2 clone 20 vs EV clone 1 and vIRF-2 clone 24 vs EV clone 4 cells.

The normalised pISRE-luc activity increased by approximately 250-fold above background levels of cells treated with -dox-ifn and +dox-ifn, in response to IFN-α in the

vIRF-2 clone 20 cells treated with -dox+ifn but was reduced significantly ($p < 0.05$, Student's *t* test) by 50% in the vIRF-2 induced cells treated with +dox+ifn (**Figure 4.3B**). Whereas in the EV clone 1 cells treated with -dox+ifn and +dox+ifn, the normalised pISRE-luc activity increased by approximately 500-fold in response to IFN-α from background levels and was significantly reduced ($p < 0.01$, Student's *t* test) by 74% when compared to the vIRF-2-induced cells of vIRF-2 clone 20 cells treated with +dox+ifn (**Figure 4.3B**).

As with vIRF-2 clones 3-9 and 20, the normalised pISRE-luc activity of vIRF-2 clone 24 increased by approximately 90-fold in response to IFN-α in cells treated with -dox +ifn compared to background levels of cells treated with -dox-ifn and +dox-ifn and was significantly reduced ($p < 0.05$, Student's *t* test) by 40% in vIRF-2 induced cells treated with +dox+ifn (**Figure 4.3C**). Whereas in the EV clone 4 cells, the normalised pISRE-luc activity in cells treated with -dox+ifn and +dox+ifn increased by approximately 170-fold in response to IFN-α from the background levels and was significantly reduced ($p < 0.01$, Student's *t* test) by 75% when compared to the vIRF-2-induced cells of vIRF-2 clone 24 cells treated with +dox+ifn.

Having confirmed by dual luciferase reporter assays that vIRF-2 inhibits ISRE promoter reporter activities, aliquots of lysates were analysed by immunoblot assay to study vIRF-2 deregulated proteins. The relative levels of proteins involved in the IFN-α-induced JAK-STAT pathway were measured by immunoblot assay. It must be emphasized that the dual luciferase and the corresponding immunoblot assays were performed more than 20 times as so much lysate were required for the large numbers of proteins being studied (data not shown).

The immunoblot assay was therefore performed with aliquots of lysates from each pair of cell clones described (**Figure 4.3**) and the results for each pair of clones are presented as two independent experiments (**Figure 4.4**). Across the three pairs of clones, vIRF-2

expression accumulated substantially in the vIRF-2 induced clones treated with doxycycline compared with the background levels of non-doxycycline treated cells and no vIRF-2 was seen in the EV clones (lacking vIRF-2) treated in parallel (**Figure 4.4, A-F, row 1).** Probing for GAPDH confirmed equal loading of lysates in each lane (**Figure 4.4, A-F, rows 6, 11, 14**).

In the ground state, IFNAR1 is associated with TYK2 while IFNAR2 with JAK1. IFN binding brings the heterodimeric IFN receptor subunits together which then facilitate phosphorylation across receptor associated tyrosine kinases (see Randall and Goodbourn 2008). IFN receptor mediated activation of the IFNα/β pathway was confirmed by the substantial accumulation of TYK2 phosphorylated at Tyr1054 and Tyr1055 (pTYK2 (Tyr1054/1055)) following treatment with IFN-α in all clones (**Figure 4.4, A-F, row 3).** In only one experiment was pTYK2 (Tyr1054/1055) of a vIRF-2-expressing clone reduced compared to its empty vector partner. This experiment was for vIRF-2 clone 24 compared to EV clone 4 counterpart (**Figure 4.4,** compare panels **E and F**). The levels of IFNAR1, TYK2 and JAK1 remained consistently unchanged across all clones regardless of vIRF-2 induction (**Figure 4.4, A-F, row 2, 4, 5)**. TYK2 phosphorylates STAT2 at tyrosine residue 689 (pSTAT2 (Tyr689)) (Yan, Krishnan et al. 1996), and the levels of pSTAT2 (Tyr689) increased in all clones following IFN-α treatment (**Figure 4.4, A-F, row 7)**. The levels of total STAT2 (**Figure 4.4, A-F, row 8)** were not changed between vIRF-2 induced clones and EV clones counterparts (lacking vIRF-2). Taken together, these data demonstrate that vIRF-2 does not modulate these IFN-α receptor-proximal events of the JAK-STAT pathway.

Interestingly, the levels of STAT1 phosphorylated at Tyr701 (pSTAT1 (Tyr701)) (**Figure 4.4, A-F, row 9)** and total STAT1 (**Figure 4.4, A-F, row 10)** were differentially regulated by vIRF-2 expression. The levels of total STAT1 increased substantially following IFN-α treatment across each pair of clones. However, both the background levels and the

IFN-α-induced levels of total STAT1 were lower in the vIRF-2 induced clones compared to their EV counterparts (lacking vIRF-2) (**Figure 4.4, A-E, row 10)**. As expected, the levels of pSTAT1 (Tyr701) were reduced concomitantly with the levels of total STAT1 (**Figure 4.4, A-E, row 9)**. In one replicate experiment, the vIRF-2 clone 24 total STAT1 (**Figure 4.4, F, row10)** did not respond to the IFN treatment for unknown reasons. The relative densitometry results indicate the levels of pSTAT1 (Tyr 701) were significantly reduced by about 2.7-fold ($p< 0.01$, Student's *t* test) in vIRF-2 clone 3-9 cells compared to EV clone 5, by 4.6-fold in vIRF-2 clone 20 compared to EV clone 1 ($p< 0.05$, Student's *t* test) and by 1.7-fold in vIRF-2 clone 24 compared to EV clone 4 ($p< 0.05$, Student's *t* test) (**Figure 4.5 A,C,E**).

Since the activated STAT1/2 heterodimer is known to associate with IRF-9/p48 to form the active heterotrimeric transcription factor ISGF-3, the levels of this protein were studied as well. As expected, the levels of IRF-9/p48 were substantially reduced by vIRF-2 in all vIRF-2 expressing clones compared to the EV clones counterparts (lacking vIRF-2) following IFN-α treatment (**Figure 4.4, A-F, row 12)**.

The relative densitometry results indicate the levels of IRF-9/p48 were significantly reduced by about 5.3-fold in vIRF-2 clone 3-9 cells compared to EV clone 5 ($p< 0.01$, Student's *t* test), by 3.8-fold in vIRF-2 clone 20 compared to EV clone 1 ($p< 0.05$, Student's *t* test) and by 6.1-fold in vIRF-2 clone 24 compared to EV clone 4 ($p< 0.05$, Student's *t* test) (**Figure 4.5 B, D, F**). Additionally, the levels of OAS3 (a representative IFN stimulated gene) were substantially reduced in all clones expressing vIRF-2 as compared to their EV clone counterparts (**Figure 4.4, A-F, row 13)**.

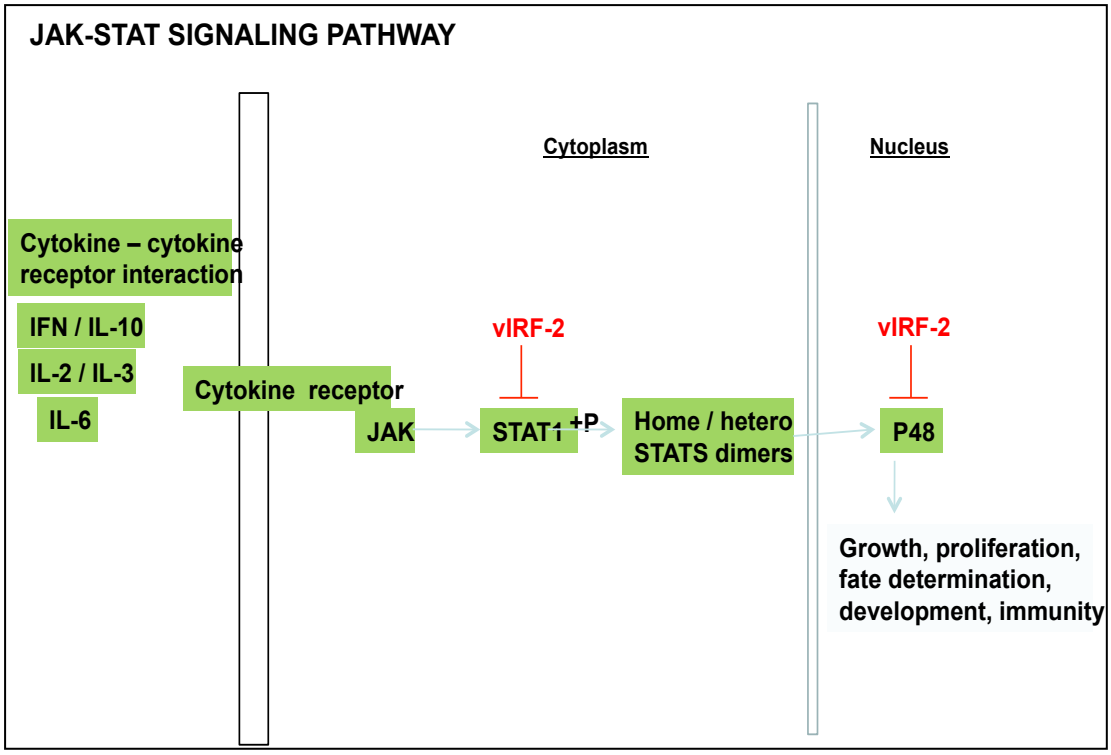

Figure 4.2 Mapping of vIRF-2 to the JAK-STAT pathway. The details of the JAK-STAT pathway down-regulated by vIRF-2 (Table 4.2) were viewed with the DAVID package pathways map viewer tool. Pathway information was generated by KEGG. vIRF-2 (red font) is shown to suppress or block signal transduction. +p = phosphorylated.

A

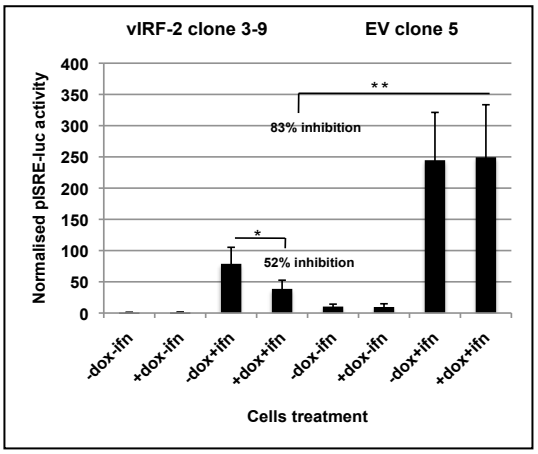

B

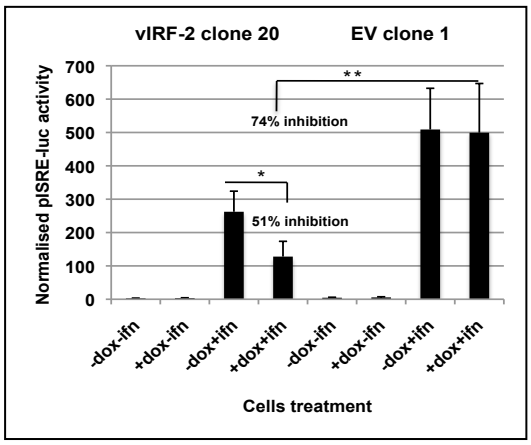

C

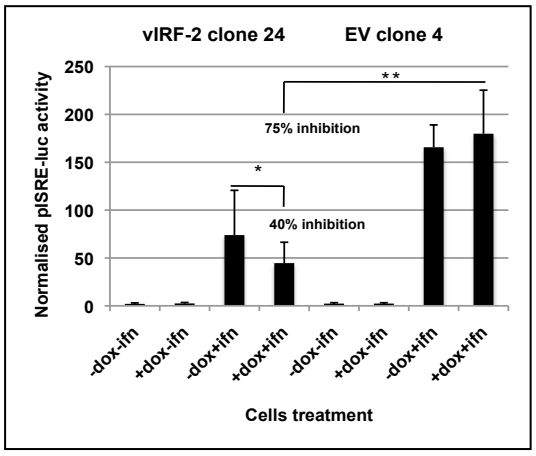

Figure 4.3 Investigating the impact of vIRF-2 on the IFN-α-induced JAK-STAT signaling pathway by dual luciferase assay. vIRF-2 expressing clones (3-9, 20 and 24) or clones lacking vIRF-2 (EV clones 1, 4 and 5) were plated at a density of 5 x 10^5 cells/well in 35 mm wells and transiently co-transfected with a transfection mixture consisting of pRLSV40-luc (1ng) constitutively

expressing *Renilla* luciferase to which pISRE-luc (250 ng) firefly luciferase was normalised and lipofectamine in serum free medium. 24 hours later, the cells were treated with or without rIFN-α (300 IU/ml) and with or without dox (1μg/ml) for 30 hours before analysis of luciferase activity by the dual luciferase assay. Data are presented as normalised pISRE-luc activity (± standard deviation) of three independent experiments each performed in duplicate. (A) vIRF-2 clone 3-9 vs EV clone 5 (lacking vIRF-2). (B) vIRF-2 clone 20 vs EV clone 1 (lacking vIRF-2). (C) vIRF-2 clone 24 vs EV clone 4 (lacking vIRF-2). *p <0.05, **p <0.01, Student's *t* test.

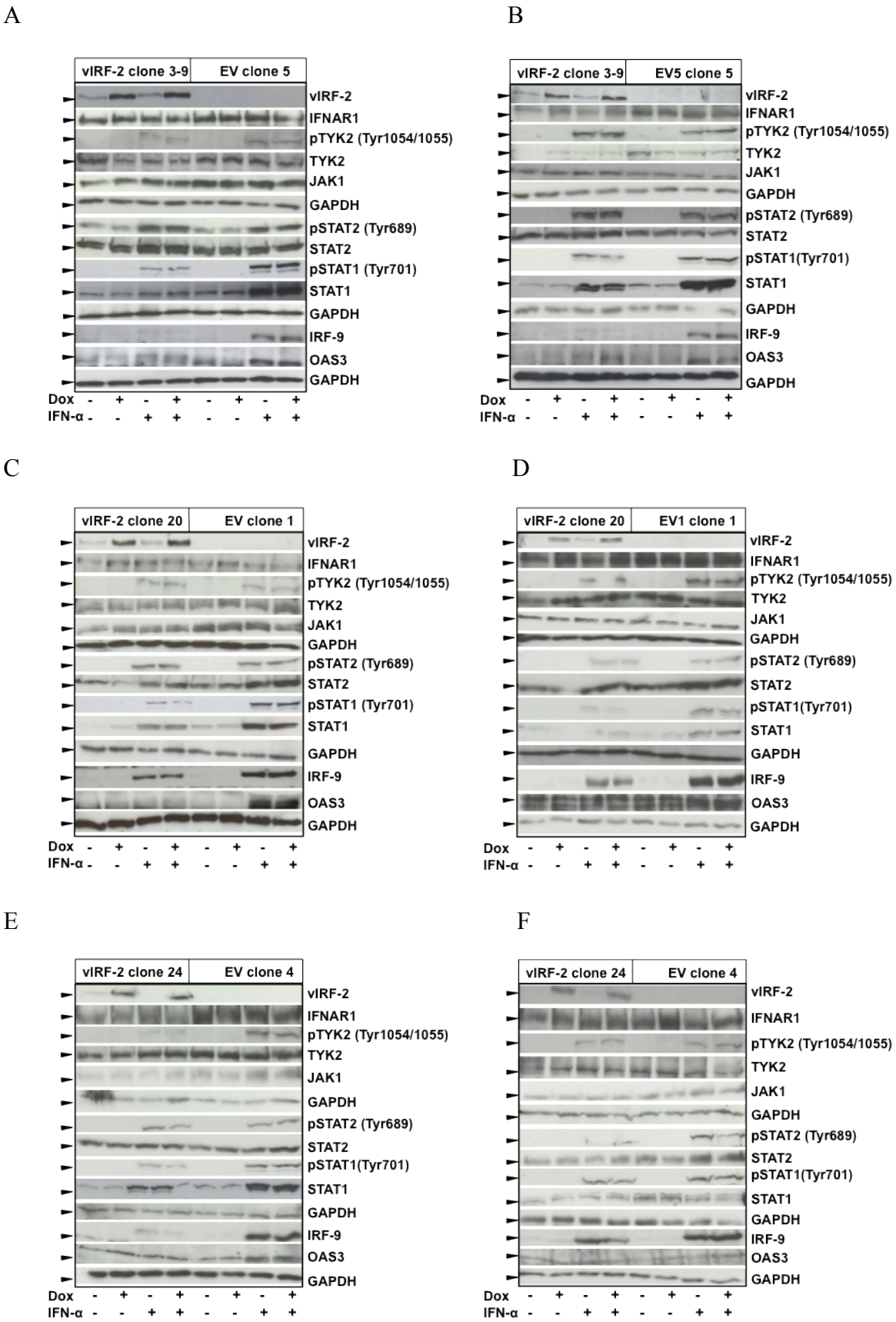

Figure legend page 147

Figure 4.4 Investigating the impact of vIRF-2 on key proteins of the IFN-α-induced JAK-STAT signaling pathway by immunoblot assay. (A-F) Aliquots of lysates for cells treated as described (Figure 4.3) were employed for relative quantification by immunoblot of components of the IFN-α-induced JAK-STAT signaling cascade. 20 or 40 μg of lysate was resolved on SDS-PAGE (8% or 10%) and immunoblotted with the following sets of primary antibodies: anti-cmyc epitope of vIRF-2, anti-IFNAR1, anti-pTYK2 (Tyr1054/1055), anti-TYK2, anti-JAK1, anti-pSTAT2 (Tyr689), anti-STAT2, anti-pSTAT1 (Tyr701), anti-STAT1, anti-IRF-9, anti-OAS3 and anti-GAPDH, The horseradish peroxidase-conjugated secondary antibodies employed were either polyclonal goat anti-rabbit or polyclonal goat anti-mouse. Probing GAPDH ensured equal amount of loading lysate in each well. Blotted membranes were developed using enhanced chemiluminiscence. Profiles of primary and secondary antibodies and conditions under which they were used are shown appendix B, tables 1 and 2 respectively.

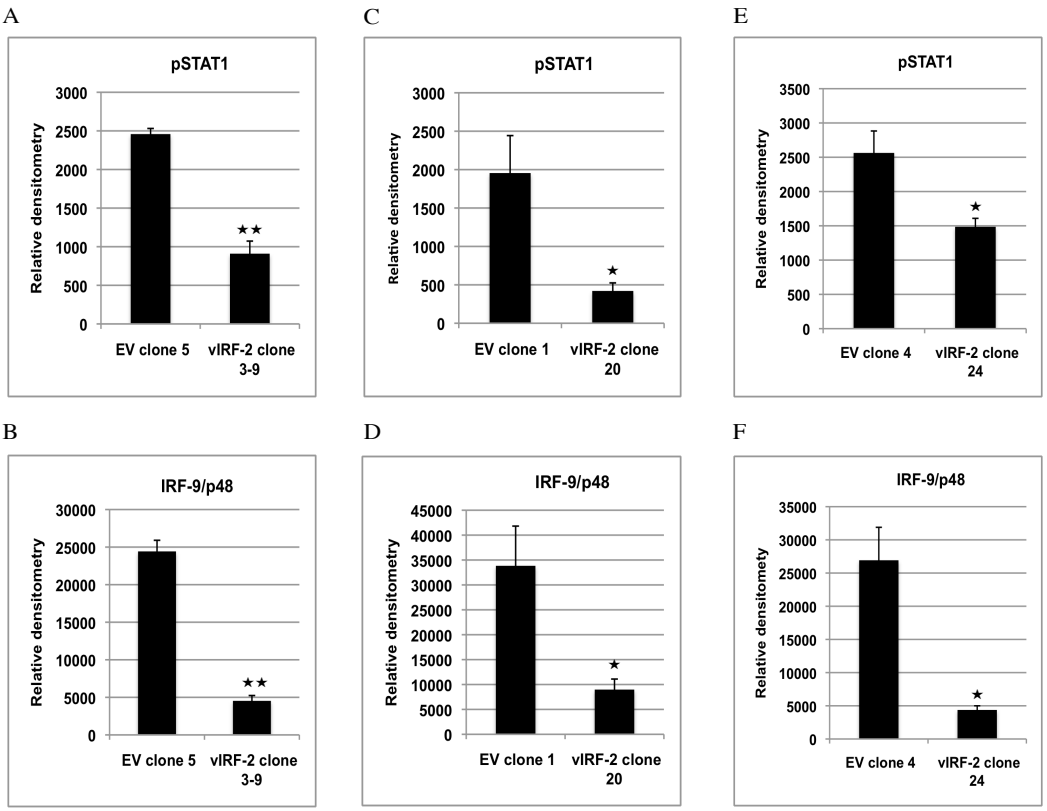

Figure 4.5 Quantifying STAT1 and IRF-9/p48 proteins in vIRF-2 clones vs EV clones with densitometry. The relative densitometry was performed on the immunoblots for pSTAT1 and IRF-9/p48 for each pair of clones. Scanned immunoblot images were uploaded on to Image J software package and blot band sizes and density were measured (see section 2.14). Error bars represent standard deviation of two independent readings of each blot (two blots in total) for Figure 4.4. Student's *t* test was performed for each pair of clones: ★$p< 0.05$ or ★★$p<0.01$ Student's *t* test.

4.5.2 The impact of vIRF-2 on RIG-I-Like Receptor Signaling Pathway

The RIG-I-like receptor-signaling pathway is one of the IFN-mediated events up-stream of IFN-α/β receptor pathways hypothesised to be suppressed by vIRF-2 and was identified to be down-regulated by vIRF-2 (**Table 4.2**). This section of the study will provide details of this pathway viewed with the DAVID package pathway map viewer tool and some key signaling proteins confirmed by immunoblot assay.

The RIG-I-like receptor signaling pathway is part of the IFN-α/β pathway and it is discussed in section 1.13. The down-regulation of *RIG-I/DDX58, IFIH1/MDA5* and *ISG15* by vIRF-2 is shown (**Figure 4.1B**), these are among a set of 15 genes associated with the GO terms such as: Response to virus, Antiviral defence, Host-virus interactions and Innate immune response and clustered with the highest enrichment score in **Table 4.2**.

Analysis with the DAVID package pathway map viewer tool has shown (**Figure 4.6A**) the down-regulation of *RIG-I/DDX58, IFIH1/MDA5* via IPS-1 that feeds in to CASP10, p38 MAPK and IRF-3 pathways to perform various biological activities such as activation of the antiviral, inflammatory, apoptotic and ubiquitin-mediated proteolysis pathways (**Figure 4.6A**). Therefore, the inhibition of *RIG-I/DDX58, p38 MAPK* and *TBK1* by vIRF-2 was investigated at the protein level in vIRF-2 clone 20 compared to EV clone 1 cells (**Figure 4.6B**).

vIRF-2 accumulated substantially in the vIRF-2 clone 20 cells treated with doxycycline, although basal amounts of vIRF-2 can be seen in the non-doxycycline treated clone 20 cells (**Figure 4.6B, row 1**). However, there was no vIRF-2 expression in EV clone 1 cells as expected. The levels of RIG-1/DDX58 accumulated in the pair of clones in response to IFN-α treatment were reduced in response to increased accumulation of vIRF-2 in the vIRF-2 clone 20 cells treated with +dox+ifn and was accumulated to a greater extent in the EV clone 1 cells treated with the same treatment profile (**Figure 4.6, row 2**). The level of

TBK1 also increased in response to IFN-α treatment in the pair of clones but was reduced by vIRF-2 in the vIRF-2 clone 20 cells; the non-IFN treated cells show basal TBKI levels (**Figure 4.6, row 3**). Additionally, the levels of p38 MAPK increased in response to IFN-α treatment in the pair of clones and were substantially reduced in vIRF-2-expressing clone 20 cells compared to the EV clone 1 counterpart. GAPDH ensured equal loading of lysates. Although this work could not be completed due to time constraints, the components of the pathway investigated (**Figure 4.6B**) are down-regulated by vIRF-2 consistent with that shown at the transcript level (**Figure 4.6A**).

Taken together, the data support our hypothesis that vIRF-2 interferes with the RIG-I-like receptor pathway which mediates events up-stream of the IFN-α/β receptor signaling pathway.

A

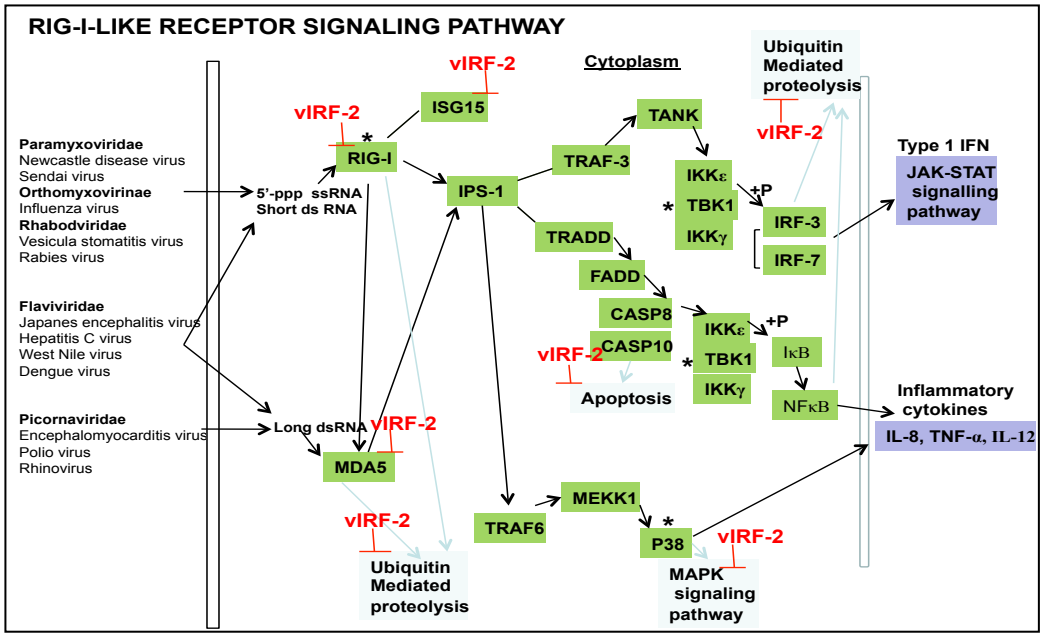

B

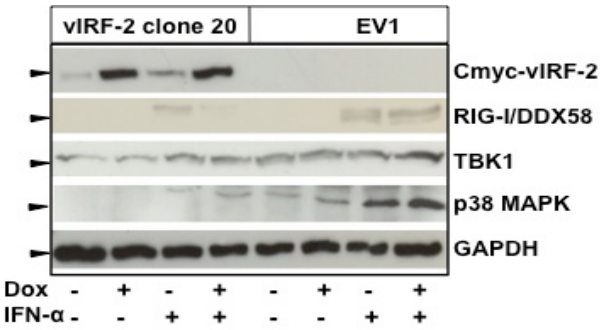

Figure 4.6 Mapping of vIRF-2 to the RIG-I-like receptor pathway. (A) The details of individual genes or biological pathways that were identified as downregulated by vIRF-2 at the transcript level (Table 4.2) were viewed with the DAVID pathway map viewer tool. The red vIRF-2 font is shown to suppress genes or block signal transduction. Pathway information was generated by KEGG. The proteins analysed in further details by immunoblot are identified with an asterix. (B) Confirmation of RIG-I/DDX58, TBK-1 & p38 MAPK by immunoblot. Both the vIRF-2 clone 20 & the EV1 cell lines were treated with or without dox (1µg/ml), and with or without IFN-α (300 IU/ml) for 30 hours. Cell lysates were resolved on SDS PAGE (8% or 10%) and immunoblotted with antibodies against RIG-I/DDX58, TBK-1 & p38 MAPK. Probing for GAPDH ensured equal loading in the wells.

4.5.3 *vIRF-2 suppresses the Ubiquitin-Proteasome Pathway*

The aim of this section was to test the hypothesis that the ubiquitin-ligase pathway (a key player in promoting signal transduction by activated RIG-I discussed in section 4.1) is down-regulated by vIRF-2. The ubiquitin ligase pathway is an integral part of the ubiquitin-proteasome pathway. The ubiquitination of RIG-I on its own is reported to promote the antiviral response (Gack, Shin et al. 2007). The ubiquitin ligase conjugation pathway shown to be down-regulated by vIRF-2 (**Table 4.2**) was identified by the DAVID package. Additional analysis of this pathway using the DAVID pathway map viewer tool indicated vIRF-2 inhibits *UBE2L6* one of the approximately 40 proteins of the ubiquitin-conjugating enzyme (E2) (**Figure 4.7**). The details of vIRF-2 down-regulated genes sets involved in the ubiquitin-ligase pathway are summarized (**Table 4.2**). The gene products could not be analysed further due to time constrains.

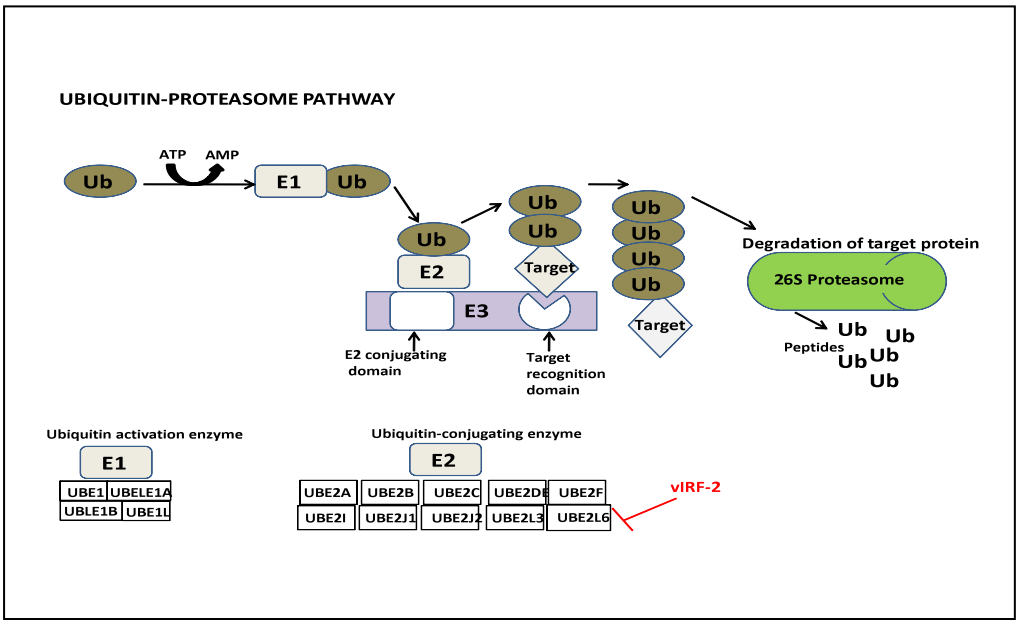

Figure 4.7. Mapping of *vIRF-2* to the Ubiquitin ligase conjugation pathway. *UBE2L6* is suppressed by vIRF-2. Pathway information was generated by KEGG.

4.6 Investigating the impact of vIRF-2 on membrane-resident proteins associated with IFN-α/β receptor

Membrane-resident proteins; IFNAR1, JAK and TYK2 shown in **Figure 4.4** were not detectable with the concentration of IFN-α (300 IU/ml) treatment used throughout this study. The IFN concentration was therefore increased to enable their detection. The optimal concentration was identified by dose response assay. The vIRF-2 clone 3-9 cells were transfected with pISRE-luc and the pRLSV40 and treated with doxycycline as described (**Figure 4.3**) and treated with increasing amounts of IFN-α up to 5000 IU/ml or left untreated (**Figure 4.8**). This experiment revealed no substantial differences in normalised pISRE-luc activity between cells treated with 300-4000 IU/ml (**Figure 4.8**).

Because the inhibitory effect of vIRF-2 was demonstrated in cells treated with 1000 IU/ml the membrane proteins could be detected following treatement at this concentration, these experiments were therefore performed with this concentration of IFN-α.

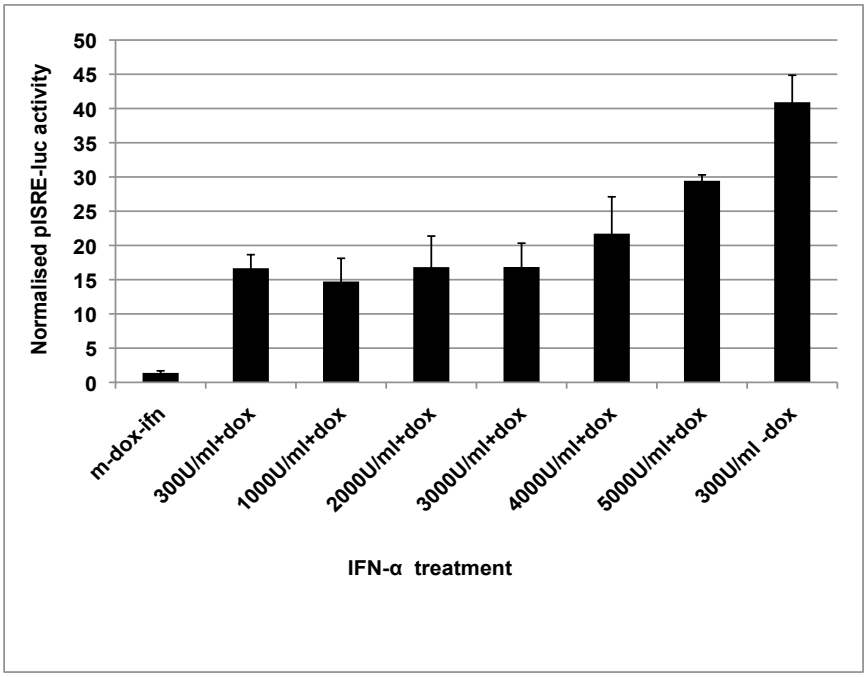

Figure 4.8. Investigating the impact of increasing amounts of IFN-α treatment on the inhibitory potential of vIRF-2 in vIRF-2 clone 3-9 cells. vIRF-2 clones 3-9 cells were plated at a density of $5x10^5$ cells/well in 35 mm wells and transiently co-transfected with a transfection mixture consisting of pRLSV40-luc (1ng) constitutively expressing *Renilla* luciferase to which pISRE-luc (250 ng) firefly luciferase was normalised and lipofectamine in serum free medium. 24 hours later, the cells were then treated with or without increasing amounts of rIFN-α (up to 5000 IU/ml) and with or without doxycycline (1μg/ml) for 30 hours before analysis of luciferase activity by dual luciferase assay. Data are presented as normalised pISRE-luc activity (± standard deviation) of three independent experiments each performed in duplicate. Wells treated with 300 IU/ml -dox are control samples for uninduced vIRF-2 cells.

4.7. Analysis of the expression data set by the GSEA package

The expression data set used to generate **Figure 4.1 A-D** was further analysed with the GSEA package. This analysis was expected to generate gene set enrichment data to augment the bioinformatics data generated by DAVID in section 4.5. Because GSEA derives its analytical power by focusing on gene sets, which consist of co-regulated genes and works in conjunction with the molecular signature database (MSigDB) (Subramanian, Tamayo et al. 2005) it was expected to (i) generate more gene set enrichment data than the DAVID package, (ii) reveal co-regulated genes and their biological pathways that might be enriched by vIRF-2.

The expression data set was uploaded on to the GSEA package and analysed according to the standard procedure (see section 2.11.3). The GSEA package generates an enrichment report when the expression data set has been analysed. The GSEA analysis report highlights enrichment gene sets with a false discovery rate (FDR) of less than 25% as those most likely to generate interesting hypotheses and drive further research, but does analyse results for all gene sets. GSEA also suggests that given the lack of coherence in most expression datasets and the relatively small number of gene sets being analysed, an FDR cutoff of 25% is appropriate. Therefore, our assessment of significance for enrichment scores was an FDR <25%. Gene sets enriched by IFN-α in the vIRF-2 clone 3-9 cells treated with -dox+ifn are presented in **Table 4.3**. Those gene sets enriched by vIRF-2 expression in vIRF-2 induced clone 3-9 cells treated with +dox+ifn are presented in **Table 4.4**. However, enrichment in -dox-ifn vs +dox-ifn showed no gene sets were significantly enriched (FDR<25%).

Table 4.3 Gene sets enriched by IFN-α in clone 3-9 cells.

Gene set	Brief description	GO biological process
Antiviral responses		
BROWNE_INTERFERON_RESPONSIVE_GENES	Up-regulated in fibroblasts at 6 hours following treatment with interferon-alpha.	Response to virus, activation of JAK-STAT pathway, microtubule bundle formation, positive regulation of transcription from RNA polymerase II promoter
DER_IFN_ALPHA_RESPONSE_DN	Genes up-regulated by interferon-alpha in HT1080 (fibrosarcoma).	Response to virus, antigen processing & presentation via MHC I, induction of apoptosis by extracellular signals.
DEBIASI_APOPTOSIS_BY_REOVIRUS_INFECTION_UP	Up-regulated at any time point up to 24 hours following infection of HEK293 cells with reovirus strain T3Abney	Antiviral response, inflammatory response, GPCR protein signal pathway
KRASNOSELSKAYA_ILF3_TARGETS_UP	Upregulated by ectopic expression of NF90 in GHOST(3) CXCR4 cells.	Response to virus, induction of IFN responsive proteins, response to exogenous dRNA, positive regulation of transcription from RNA polymerase II promoter
DER_IFN_BETA_RESPONSE_DN	Genes up-regulated by interferon-beta in HT1080 (fibrosarcoma).	Response to virus, production of antiviral proteins, positive regulation of transcription from RNA polymerase II promoter
DER_IFN_BETA_RESPONSE_UP	Upregulated 2-fold in HT1080 cells 6 hours following treatment with interferon beta.	Response to virus, positive regulation of transcription from RNA polymerase II promoter, positive regulation of JAK-STAT pathway
Cell cycle		
BIOCARTA_ATRBRCA_PATHWAY	BRCA1 and BRCA 2 block cell cycle progression in response to DNA damage and promote double-stranded break repair; mutations induce breast cancer susceptibility.	DNA damage repair, G1/S DNA damage checkpoint activity, regulation of cyclin-dependent protein kinase activity, cellular response to UV
WELCSH_BRCA1_TARGETS_1_UP	Upregulated by induction of exogenous BRCA1 in EcR-293 cells.	Positive regulation of cell cycle & cell growth, antiapoptosis
Transcription regulation		
DAZARD_UV_RESPONSE_CLUSTER_G6	Downregulated by UV-B light in normal human epidermal keratinocytes, cluster 6.	Positive regulation of transmission from RNA polymerase II promoter, angiogenesis, DNA repair
DAZARD_RESPONSE_TO_UV_NHEK_DN	Downregulated by UV-B light in normal human epidermal keratinocytes.	GPCR signaling pathway, positive regulation of cell proliferation, positive regulation of transmission from RNA polymerase II promoter

Apoptosis		
RADAEVA_IFN_ALPHA_RESPONSE_DN	Genes up-regulated by interferon-alpha in primary hepatocyte	Induction of apoptosis by extracellar signals, response to virus, tyrosine phosphorylation of STAT proteins
SANA_RESPONSE_TO_IFNG_UP	Genes up-regulated by interferon-gamma in colon,derm,iliac,aortic,lung endothelial cells.	Activation of pro-apoptotic gene products, antigen processing and presentation of peptide antigen via MHC class I

Table 4.4 Gene sets enriched by vIRF-2 in clone 3-9 cells

Gene set	**Brief description**	**GO biological process**
Cell growth, proliferation & adhesion pathway		
VERRECCHIA_RESPONSE_TO_TGBF1_C2	Upregulated by TGF-beta treatment of skin fibroblasts, cluster 2.	Cell adhesion, angiogenesis, skin morphogenesis
SA_MMP_CYTOKINE_CONNECTION	Cytokines can induce activation of matrix metalloproteinases, which degrade extracellular matrix	Positive regulation of cell matrix adhesion, TGFR signaling pathway, IL-6 mediated signaling pathway
Inflammatory pathway		
BIOCARTA_INFLAM_PATHWAY	Interleukins and TNF serve as signals to coordinate the inflammatory response, in which macrophages recruit and activate neutrophils, fibroblasts, and T cells.	Inflammatory response, regulation of immune response, angiogenesis, positive regulation of cell proliferation, TNF-mediated signaling pathway.

The expression data set used to generate (Figure 4.1) were also used to generate Tables 4.3 and 4.4 respectively with the GSEA package. GSEA enrichment score reflects the degree to which a gene set is overrepresented at the top or bottom of a ranked list of genes. By default, the ranking metric is the signal-to-noise ratio. Enrichment score of FDR <25% was considered significant.

4.8 Discussion

The quality assessment of the exon arrays expression dataset with the Affymetrix EC had established that the three probeset summarisation metrics: relative log expression, positive_ vs_negative_auc and mad-residual mean, including the probe level metrics and the probeset signal metrics evaluated (section 4.2) were all highly correlated and consistent with the suggested guidelines for quality assessment of exon arrays by Affymetrix.

Next, we proceeded to analyse the expression data set focusing on vIRF-2 deregulated IFN-α responsive genes. The gene expression data set analysis revealed vIRF-2 significantly down-regulated (Limma $p < 0.05$) 73% of the 78 IFN-α up-regulated genes including RIG-1/DDX58, STAT1, IRF-9/p48 & OAS3 (**Figure 4.1B**) and that vIRF-2 up-regulated 50% of the 26 IFN-α down-regulated genes (**Figure 4.1D**). Since our interest was not to study individual genes, rather gene sets and related biological pathways, the DAVID and the GSEA software packages were employed to independently analyse the expression data set and to extract GO terms and/or enriched gene sets with related biological pathways whose functions have been deregulated by vIRF-2 (see **Tables 4.2, 4.3, 4.4**).

vIRF-2 down-regulated GO terms: Response to virus, Antiviral defence, Host-virus interactions and Innate immune response were the most highly clustered GO terms by DAVID followed by those involved in transcription regulation and ubiquitin ligase pathways (**Table 4.2**). Both DAVID and GSEA showed gene sets participating in antiviral response, cell cycle, transcription regulation and apoptosis were deregulated by vIRF-2. Unlike DAVID, GSEA identified vIRF-2 enriched gene sets involved in positive regulation of cell adhesion, angiogenesis and inflammatory response (**Table 4.4**). These bioinformatics analyses therefore provided us with the opportunity to test the hypothesis that vIRF-2 down-regulates IFN mediated events up-stream and down-stream of the IFN-α/β receptor,

including pathways such as the RIG-I-like receptors (RLRS) and JAK-STAT. As mentioned earlier the Ubiquitin ligase pathway was not analysed further due to time constrains.

Analysis of the expression dataset with the DAVID package of vIRF-2-deregulated pathways identified 15 genes and related biological pathways, six (ISG15, RIG-I/DDX58 IFIH1, STAT1, IRF-9/p48 and UBE2L6) of them overlapped with the data presented in **Table 4.2**, the other 9 genes and related pathways could not be studied further as they were not significantly ($p > 0.01$) enriched by DAVID. Subsequent studies of the data generated by the DAVID package was therefore based on **Table 4.2**. The impact of vIRF-2 on these 6 genes and related biological pathways is discussed below beginning with the JAK-STAT pathway:

Key IFN-induced signaling components of the JAK-STAT pathway such as STAT1, IRF-9/p48 and OAS3 were among the individual genes shown to be down-regulated at the mRNA levels by vIRF-2 (**Figure 4.1B**). Further analysis with the DAVID package pathway map viewer confirmed the down-regulation of STAT1 and IRF-9/p48 (**Figure 4.2**). At the protein level, key components of the JAK-STAT signaling pathway were confirmed in the three pairs of clones by immunoblot assay (**Figure 4.4**). These results confirmed vIRF-2 consistently reduced to a greater extent the levels of pSTAT1, STAT1, IRF-9/p48 and OAS3 in the vIRF-2 induced clones compared to their EV clone counterparts (lacking vIRF-2) (**Figure 4.4)**.

Although pTYK2 was reduced in one of the two experiments of vIRF-2 clone 24 vs EV clone 4 (**Figure, 4.4, E, row 3**) the trend was not consistent in the other four experiments with the other two pairs of clones. Moreover, in the other four experiments with the other two pairs of clones it was pSTAT1, IRF-9/p48 and OAS3 proteins that were consistently down-regulated in all the six experiments (**Figure 4.4**). STAT1 was not reduced in one of the two experiments of vIRF-2 clone 24 vs EV clone 4 for unkown reasons (**Figure, 4.4, F, row 10**).

Although the antiviral activity of vIRF-2 has been reported (Burysek and Pitha 2001; Fuld, Cunningham et al. 2006; Areste, Mutocheluh et al. 2009) this is the first time vIRF-2 has been shown to inhibit the JAK-STAT pathway. The mechanism of the antiviral activity is through specific inhibition of pSTAT1, STAT1, IRF-9/p48 and OAS3. The upstream signaling components of the pathway (IFAR1, pTYK2, TYK2 and JAK1) remained unaffected by vIRF-2. This specificity is evident as pSTAT2/STAT2 are unaffected by vIRF-2 since together with pSTAT1/STAT1 and IRF-9/p48 they form the heterotrimeric transcription factor ISGF-3 which regulates antiviral gene transcription. Targeting specific components of the JAK-STAT pathway by viruses has been reported. For example, measles virus V protein disrupts the JAK-STAT pathway by specifically binding to STAT2 (Ramachandran, Parisien et al. 2008). West Nile virus protein NS5 disrupted the JAK-STAT pathway by inhibiting the phosphorylation and activation of JAK1 and TYK2 with the concomitant inhibition of STAT1 and STAT2 (Guo, Hayashi et al. 2005; Laurent-Rolle, Boer et al. 2010).

To counteract the important role-played by the IFN-α/β in antiviral host defence, many viruses have evolved to develop a variety of mechanisms to overcome the antiviral state elicited by IFN-α/β (Diamond 2009; Gale and Sen 2009). These viruses are able to express proteins that interfere with the type I IFN induction pathway. Examples include influenza A virus NS1 protein and the human papillomavirus E6 oncoprotein that inhibit expression of type 1 IFN by blocking the activation or activity of IRF-3 (Ronco, Karpova et al. 1998; Talon, Horvath et al. 2000). Additionally, the IFN-α/β pathway may also be targeted by viruses via the expression of IFN antagonist proteins acting at the level of STAT proteins, inducing STAT inhibition or degradation. For example, Johnson et al have shown the inhibition of STAT1 nuclear accumulation in cells that express ICP27 (Johnson and Knipe 2010). ICP27 is a multifunctional immediate early protein with homologues in all

herpesviruses (Roizman 2007) that is essential for transcription of some early and late viral proteins (Jean, LeVan et al. 2001). These authors reported that ICP27 also induces the secretion of a small, heat-stable type I IFN antagonizing protein that inhibits STAT1 nuclear accumulation (Johnson and Knipe 2010). It therefore makes biological sense for vIRF-2 to specifically inhibit STAT1 because of its role as the central mediator of both types 1 and 2 IFN signaling pathways that play key roles in cell growth regulation, antitumour activity, antiviral and immune defence.

The importance of STAT1 in the antiviral response is demonstrated by the variety of viruses that target it and also by *in vivo* evidence. Thus, Dupius et al studied two unrelated infants with severe mycobacterial and viral diseases not consistent with any reported primary immunodeficiency (Dupuis, Jouanguy et al. 2003). These infants were homozygous with respect to mutated *STAT1* alleles. After developing disseminated Bacillus Calmette-Guerin (BCG) vaccine infection, the first infant died of recurrent encephalitis caused by HSV-1 and the second infant died of a viral-like illness. STAT1 was considered as a likely candidate because of its involvement in both IFN-α/β and IFN-γ pathways. STAT1 sequence studies in the first patient showed a homozygous two-nucleotide deletion AG in exon 20 and the second infant carried a homozygous nucleotide substitution (T-C), resulting in the substitution of a proline for a leucine at amino-acid position 600 also in exon 20. Electrophoretic mobility shift assay (EMSA) studies showed impaired activation of ISGF3 in response to IFN-α in both infants. The EMSA data are consistent with our data which showed ISGF3 significantly accummulated (p-value < 0.01, Student's *t* test) in the EV clone 5 cells compared to the vIRF-2 expressing clone 3-9 cells in response to rIFN-α treatment (Mutocheluh, Hindle et al. 2011). This study by Dupuis et al demonstrated that the STAT1-containing complexes GAF and ISGF-3 were not activated in response to IFN-γ and IFN-α in the two infants homozygous at mutated *STAT1* alleles (Dupuis, Jouanguy et al. 2003).

However, when EBV infected B-cells from both infants were transiently transfected with wild-type *STAT1* allele, both GAS and ISRE-binding proteins were produced in the transfected cells in response to IFN-γ and IFN-α. This experiment provided additional evidence that defective STAT1 led to the patients death.

In a related study, Chapgier et al described the complex pathophysiology of complete STAT1 deficiency in a third unrelated Pakistani child (Chapgier, Wynn et al. 2006). The three month old child presented with severe disseminated BCG infection 8 weeks after BCG vaccination and subsequently died of viral illness. As the clinical features were consistent with a defect in the IFN-γ pathway additional investigations were organized. The results showed a complete inability of BCG to stimulate the patient's blood leukocytes to produce cytokines such as IL-12 or IFN-γ beyond background levels (Chapgier, Wynn et al. 2006). When *STAT1* was sequenced it revealed a homozygous mutation and western blot analysis of the patient's EBV-transformed B cells showed absence of STAT1 but presence of STAT3 expression (Chapgier, Wynn et al. 2006). These authors further stated IFN-α/β did not suppress HSV and VSV replication in fibroblasts from this child (ex vivo studies) although *in vivo* the patient was successful in clearing at least some viruses (Chapgier, Wynn et al. 2006).

These studies demonstrate formally that STAT1 deficiency prevents IFN-α/β and IFN-γ signaling in humans and advance our understanding of complete STAT-1 deficiency as a severe form of innate immune deficiency.

The OAS3/RNase L is an RNA decay pathway known to play an important role in the established endogenous antiviral pathway (Silverman 2007; Randall and Goodbourn 2008). The large isoform of the OAS family of antiviral proteins (OAS3, p100) was included in the study as a representative of the IFN-stimulated genes. OAS3 protein was also down-regulated by vIRF-2 most probably as a consequence of the down-regulation of the JAK-

STAT pathway (**Figure 4.4**). The OAS3 antiviral mechanism stems from the fact that when activated, its RNase L degrades ssRNA molecules including mRNA and viral RNA (Silverman 2007). It therefore makes biological sense for vIRF-2 to inhibit OAS3 in order to impair the antiviral innate defence system. Moreover, its downregulation in vIRF2- induced cells confirms the downstream effector functions of the type 1 IFN pathway are negatively affected by this KSHV protein. Others have reported the 1b isoform of mouse OAS gene (Oas1b) is a critical component of innate immunity to West Nile virus *in vivo* and *in vitro* (Perelygin, Scherbik et al. 2002; Kajaste-Rudnitski, Mashimo et al. 2006) and that Oas1b is capable of suppressing flavivirus infection in RNase L-deficient mouse cells. However, none of the OAS family members have been reported to affect KSHV. Because OAS3 is an IFN-stimulated gene its inhibition by vIRF-2 in this study could result from the inbition of the JAK-STAT pathway or vIRF-2 probably directly targeted it. The latter reason needs to be confirmed by other studies such as immunoprecipitation. Hence, the inhibition of OAS3 by vIRF-2 underscores OAS3's biological importance to the innate antiviral defence.

The IFN-α responsive gene sets whose biological processes include the positive regulation of transcription by RNA polymerase II (RNAPII) promoters were clustered together with the antiviral response and transcription regulation gene sets enriched by IFN-α treatment (**Table 4.3**). These data suggest transcription regulation of antiviral genes by RNAPII promoters has been down-regulated by vIRF-2.

The mechanism by which vIRF-2 downregulates the JAK-STAT pathway by specifically inhibiting STAT1 and IRF-9/p48 has been shown for the first time in this study (section 4.5.1). STAT1 anti-tumour activities gives credence to our prediction that vIRF-2 may play a carcinogenic role in KSHV biology. The inhibition of STAT1 by vIRF-2 does not only lead to defective antiviral pathway but tumorigenesis as well, since STAT1 is considered a tumour suppressor (Stephanou and Latchman 2003). Activation of STAT1

induces many pro-apoptotic and anti-proliferative genes. For example, IRF-1 is involved in IFN-γ/STAT1 dependent apoptosis of hematological malignancies (Sato, Selleri et al. 1997; Bernabei, Coccia et al. 2001), cervical carcinoma (Lee, Anderson et al. 1999) and Ewing tumour (Sanceau, Hiscott et al. 2000) cells. Furthermore, all-trans retinoic acid (ATRA) induces STAT1 phophorylation in myeloid cells, which in turn up-regulates the expression of the CDK inhibitor p27Kip1 and eventually triggers G0/G1 arrest (Dimberg, Karlberg et al. 2003). Taken together, this evidence may explain why the gene sets involved in cell cycle regulation were not enriched by vIRF-2 in the vIRF-2 induced clone 3-9 cells stimulated with IFN-α (**Table 4.4**) but rather in the non-vIRF-2 induced IFN-α stimulated clone 3-9 cells (**Table 4.3**). These data suggest vIRF-2 down-regulated the said gene sets as they were not enriched by vIRF-2 in the vIRF-2 induced cells treated with IFN-α (**Table 4.4**).

Besides cell cycle arrest, STAT1 promotes apoptosis in tumours by inducing the expression of cell death receptors and their ligands. IFN-γ-dependent STAT1 activation induces the expression of Fas and Fas ligand in haematopoeitic and colon carcinoma cells (Conti, Regis et al. 2007; Elahi, Zhang et al. 2008). Also, STAT1 promotes induction or activation of different members of the executor of cell death caspase family. For example, IFN-γ induces caspase-1 in a STAT1-dependent manner in breast cancer, epithelial carcinoma, T cell lymphoma, and together with caspase-3 and -7, in renal cell carcinoma (Kumar, Commane et al. 1997; Fulda and Debatin 2002; Egwuagu, Li et al. 2006). Our data suggest IFN-α stimulated gene sets involved in apoptosis were enriched by IFN-α in clone 3-9 cells (**Table 4.3**) but not vIRF-2 induced cells (**Table 4.4**). These data are consistent with the down-regulation of the apoptotic pathway by vIRF-2 at the transcription level (**Figure 4.6A**), probably through targeting STAT1.

STAT1 is required for optimal DNA damage-induced apoptosis by negatively regulating the p53-inhibitor mdm2 and acting as a p53 co-activator. It can also directly

interact with p53 and this association is enhanced following DNA damage (Thomas, Finnegan et al. 2004; Youlyouz-Marfak, Gachard et al. 2008). Therefore, the gene sets involved in DNA damage and repair were not enriched by vIRF-2 (**Table 4.4**) but rather by the non-vIRF-2 induced IFN-α stimulated cells (**Table 4.3**).

The enrichment of the gene sets involved in the angiogenic pathway by vIRF-2 (**Table 4.4**) could be attributed to the down-regulation of STAT1 by vIRF-2, because STATI is already known to play a key role in the inhibition of angiogenesis, acting on both endothelial and tumour cells. Moreover, angiogenesis is up-regulated in KS (Ye, Blackbourn et al. 2007) which could be attributed the inhibition of STAT1 by vIRF-2.

IFN-γ/STAT1 activation inhibits growth and tube formation in human umbilical vein endothelial cells (HUVEC) (Battle, Lynch et al. 2006) and suppresses the biological activity of VEGF through the inhibition of genes required for VEGF response, including angiopoietin-2, tissue inhibitor of matrix metalloproteinase (MMP)-1 and VEGF receptor 2 (Battle, Lynch et al. 2006). Consequently, the inhibition of STAT1 by vIRF-2 may also up-regulate growth factors active in angiogenesis, vasculogenesis and endothelial cell growth or KS cell proliferation and promote their migration in KSHV infected patients, consistent with the observation in our laboratory that KSHV infection increases HUVEC motility (Jeffrey and Blackbourn, unpublished observation).

STAT1 activation is pivotal for tumour immunosurveillance as it drives induction of MHC Class I, required for efficient display of antigens to effector T-lymphocytes and thus elicit anti-tumour immune response. For example, defective class I MHC inducibility was correlated with defective STAT1 phosphorylation in melanoma cells (Rodriguez, Mendez et al. 2007). Therefore in the context of KS or PEL the vIRF-2 deregulated JAK-STAT pathway could lead to reduced tumour immune serveillance. For example, the down-regulation of

IRF-1 and STAT1 (key players of the IFN-α/β pathway) by the oncogenic KSHV vIRF-1 protein has been reported as a contributory factor to PEL (Y Zhang 2009).

Taken together, the inhibition of STAT1 activity by vIRF-2 protein has revealed its mechanism controlling the antiviral response and has suggested its carcinogenic role in the biology of KSHV.

The RIG-I-like receptor pathway is one of the upstream events of the IFN-α receptor shown to be down-regulated by vIRF-2. The affected component is the RIG-I/DDX58 (**Figure 4.1B, Table 4.2**). RIG-I/DDX58 senses exogenous cytosolic viral RNA molecules and initiates a signaling cascade that involves binding of RIG-I-like receptor to MAVS. This interaction then activates TBK1, which phosphorylates IRF-3. MAVS also promotes activation of NF-κB. IRF-3 and NF-κB then translocate to the nucleus to induce the transcription of genes involved in antiviral defense (Moore and Ting 2008).

vIRF-2 activity was mapped to the RIG-I-like receptor pathway (**Figure 4.6A**) where *RIG-I/DDX58* and *MDA5/FIH1* have been shown to be down-regulated; the inhibition of RIG-I/DDX58 was confirmed by immunoblot assay in one experiment (**Figure 4.6B**). Viruses including human CMV have been shown to down-regulate RIG-I/DDX58 as a strategy to evade the RIG-I-mediated immune response (Scott 2009). Also, RIG-I-dependent sensing of poly(dA:dT) through the induction of an RNA polymerase III-transcribed RNA intermediate has been reported (Ablasser, Bauernfeind et al. 2009). These authors revealed a novel DNA-sensing pathway via RIG-I/DDX58. AT-rich dsDNA served as template and was transcribed by RNA polymerase III into dsRNA with a 5'-triphosphate moiety in a process that converted AT-rich DNA into RIG-I ligand (Ablasser, Bauernfeind et al. 2009). Therefore it makes biological sense for vIRF-2 to inhibit RIG-I/DDX58 in other to impair the innate antiviral pathway.

An antiviral gene essential for the function of RIG-I/DDX58 that was down-regulated by vIRF-2 is *ISG15* (TRIM25 or E3 ligase) (**Table 4.2, Figure 4.6A**). This protein is known to ubiquitinate RIG-I/DDX58 on lysine 172 in the second CARD domain, a residue necessary for RIG-I activation (Gack, Shin et al. 2007). ISG15 binds the RIG-I first CARD and subsequently ubiquitinates its second CARD. Mutation in both RIG-I CARDs abolished ISG15 interaction and eliminated polyubiquitination and antiviral activity (Gack, Kirchhofer et al. 2008). One reason vIRF-2 may down-regulate the ubiquitin ligase pathway is because unanchored ubiquitin chains (inherently present in the cell microenvironment) together with RIG-I form a potent viral RNA sensor that directly communicates with MAVS to promote IRF-3 and NF-κB activation (Zeng, Sun et al. 2010), leading to the antiviral response. The down-regulation of the RIG-I/DDX58 by vIRF-2 confirms our hypothesis that vIRF-2 may down-regulate events upstream of the IFN-α receptor.

The third antiviral pathway shown to be down-regulated by vIRF-2 is the ubiquitin ligase pathway (**Figure 4.7**, **Table 4.2**). The down-regulation of *UBE2L6* (one of about 40 enzymes in mammals) by vIRF-2 (**Figure 4.8**, **Table 4.2**) could significantly impair the E2 charging of ubiquitin molecules to E3 thereby blocking the activities of the K63-ubiquitin protein, which promotes RIG-I sensing, and signal transmission. For example, the N-terminal CARD domains of RIG-I can function without the requirement for viral RNA in the pathway activation. Zeng and colleagues made this finding when they incubated the N-terminal CARD domains of RIG-I with E2-conjugating enzymes and the ISG15/TRIM25 ubiquitin-like protein (Zeng, Sun et al. 2010). This incubation catalyzed the assembly of K63-ubiquitin chains on RIG-I resulting in MAVS-dependent activation of IRF-3. As described above, *ISG15/TRIM25* is down-regulated by vIRF-2. Moreover, the down-regulation of *UBE2L6* and the related ubiquitin ligase pathway by vIRF-2 may inherently impair the activity of the ubiquitin ligase pathway (**Figure 4.6A**), which is an integral part of the ubiquitin mediated-

proteasome pathway. The consequence is suppression of antiviral response, deregulation of cell cycle, promotion of tumourigenesis and suppression of the adaptive immune response pathway. These are classic mechanisms by which vIRF-2 subverts the innate and adaptive immune defence systems and perhaps promote cancer in humans.

Taken together, these data strongly suggest that the role of vIRF-2 protein in KSHV biology is the down-regulation of both type 1 and 2 IFN signaling pathways resulting in (i) increased resistance of many viruses especially the IFN-sensitive viruses to both IFN pathways and (ii) promote tumourigenesis in KSHV infected patients.

In the next chapter we will test the hypothesis that vIRF-2 rescues IFN-sensitive viruses from the type 1 IFN pathway.

Chapter 5 The biological significance of vIRF-2 anti-IFN property

Having established possible mechanisms by which vIRF-2 down-regulates the IFN-α/β pathway (chapter 4), in this chapter we aimed to test the hypothesis that vIRF-2 rescues IFN sensitive Chandipura and Encephalomyocarditis viruses from the antiviral pathway. Testing this hypothesis would help to determine *in vitro* the physiological significance of the role of vIRF-2 in KSHV biology.

The importance of IFNs is underscored by the observation that mice that lack the IFN-α/β receptor or proteins of the JAK-STAT signaling pathway have an increased sensitivity to many viral infections (Durbin, Hackenmiller et al. 1996; Meraz, White et al. 1996; Karst, Wobus et al. 2003). Furthermore, in humans inherited impairment of the STAT1-dependent response to human IFN-α/β results in susceptibility to viral diseases (Dupuis, Jouanguy et al. 2003; Chapgier, Wynn et al. 2006), see section 4.8.

5.1 Chandipura virus causes encephalitis in humans

The Chandipura virus was discovered in 1966 by Bhatt and Rodrigues, scientists of the Virus Research Centre (VRC) established by the Rockefeller Foundation in 1952 in Pune, India (Bhatt and Rodrigues 1967). They were investigating persons with fever in Chandipura in northern Maharashtra, near Nagpur in India, for dengue or chikungunya virus aetiology (Bhatt and Rodrigues 1967). Bhatt and Rodrigues named it Chandipura after the geographic location of its discovery (Bhatt and Rodrigues 1967). Scientists from the Centres for Disease Control (CDC) in the USA later classified it as a member of the *Rhabdoviridae* family, genus *Vesiculovirus*. Members of this genus include Lyssa (rabies) and vesicular stomatitis virus.

Chandipura virus came to the limelight in 2003, with the publication of a report by scientists in India on a large outbreak of an acute neurological illness of young children with high case-fatality rate, diagnosed as encephalitis and putatively associated with infection with Chandipura virus (Rao, Basu et al. 2004). In the same year another outbreak of Chandipura virus infection was reported in some districts of Gujarat, mostly among tribal children (Chadha, Arankalle et al. 2005).

5.2 Chandipura virus replication has been used to measure the activity of the type I IFN signaling pathway

The use of Chandipura virus replication as a measure of IFN antiviral activity has been reported by many groups including Easton and colleagues (Easton, Scott et al. 2011). These authors developed a novel approach to vaccine protection using defective interfering (DI) viruses. DI viruses are deletion mutants, deficient in replication, usually arise spontaneously from the genome of infectious viruses and can only multiply when co-infected with a genetically compatible infectious virus.

These authors previously successfully protected mice from lethal *in vivo* infection of many different subtypes of influenza A virus when they intranasally administered a protecting influenza A virus (Dimmock, Rainsford et al. 2008). Recently the authors reported that protecting influenza A virus also protected *in vivo* against genetically unrelated pneumovirus. The protection was achieved by stimulating the type I interferon pathway in the mice and lung samples from the mice were assayed for interferon type I activity by challenge with Chandipura virus. The readout was reduction in Chandipura virus-induced cytopathology in L929 cells (Easton, Scott et al. 2011). The authors work suggested quantifying Chandipura virus replication in the presence of IFN-α can be used to measure type I interferon activity *in vivo* or *in vitro* (Easton, Scott et al. 2011).

5.3 Investigating the impact of vIRF-2 on Chandipura virus replication

In chapter 4 we demonstrated that vIRF-2 expression down-regulates genes involved in the IFN-α/β pathway. Therefore, one way to assess the biological significance of this phenomenon is to determine *in vitro* if ectopic vIRF-2 expression rescues IFN-sensitive virus replication from the effects of IFN. This experiment was therefore performed with Chandipura virus.

Monolayers of EV clone 5 and vIRF-2 clone 3-9 cells were pre-treated with or without doxycycline and increasing amounts of rIFN-α (up to 300 IU/ml) for 30 hours before infection with Chandipura virus at a multiplicity of infection (MOI) of 0.1. The cell supernatants were harvested 24 hours later for quantification of the viral titre by plaque assay (**Figure 5.1**). In the non-IFN treated cells the viral yield recovered from the pair of cell clones indicated a marginal decrease in the vIRF-2 expressing clone 3-9 cells ($3.97x10^8$ PFU/ml) compared with EV clone 5 ($6.4x10^8$ PFU/ml). Moreover, increasing the amount of rIFN-α revealed vIRF-2 in clone 3-9 cells failed to rescue Chandipura virus replication from the rIFN-α as the recovered virus yield was persistently less than that recovered from the EV clone 5 cells (**Figure 5.1**). For example, in the pair of clones treated with 300 IU/ml rIFN-α, the virus yield recovered from the vIRF-2 clone 3-9 cells averaged $3.03x10^6$ PFU/ml compared with $1.01x10^7$ PFU/ml in the EV clone 5 cells (**Figure 5.1**). Although the Chandipura virus is IFN-sensitive, as demonstrated by the IFN dose dependent reduction of virus yield, the result suggests vIRF-2 decreased Chandipura virus replication in the vIRF-2 clone 3-9 cells, contrary to our expectation (**Figure 5.1**).

Given this unexpected result, we then investigated whether vIRF-2 expression could rescue replication of another interferon-sensitive virus, EMCV.

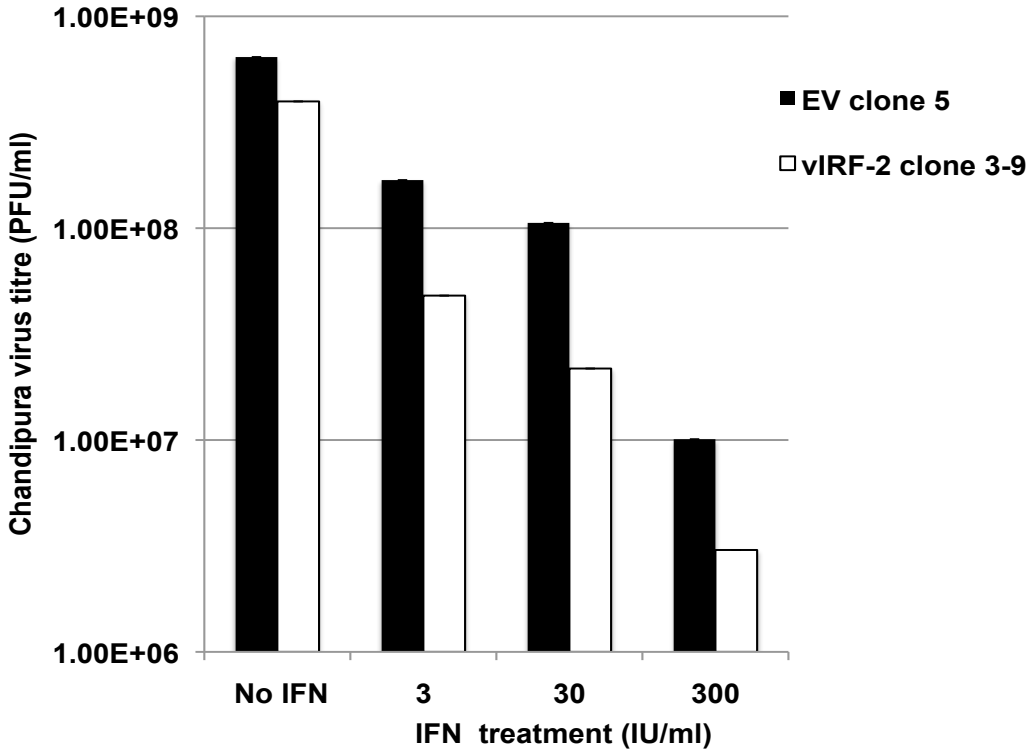

Figure 5.1 vIRF-2 expression does not rescue Chandipura virus replication from the IFN-α/β pathway. Monolayers of vIRF-2 clone 3-9 and EV clone 5 cells were pre-treated with doxycycline (1 μg/ml) and either none or increasing amounts of rIFN-α (3, 30, and 300 IU/ml) for 30 hours. The cells were then infected with Chandipura virus (MOI = 0.1) and incubated for 30 hours. The culture fluid was collected and virus titres determined by limiting dilution plaque assay on vero cells. After 24 hours of incubation, plaques were identified by crystal violet staining and counted. Data are presented as the mean Chandipura virus titre +/- standard deviation in clone 3-9 cells compared to the titre in EV clone 5 cells in two independent experiments, each performed in duplicate. Chandipura virus titre was statistically significant ($p < 0.01$, Student's *t*-test) between the pair of clones when treated with 300 IU/ml rIFN-α. The error bars are too small to be clearly visible.

5.4 EMCV causes myocarditis and encephalitis

The *Picornaviridae* family consists of a diverse group of viruses that cause a variety of human and animal diseases. The family consists of eight genera and the best studied is poliovirus (PV), the aetiologic agent of the paralytic disease poliomyelitis. The three PV serotypes are classified in the Enterovirus genus together with enterovirus type 70 (EV 70), which causes acute heamorrhagic conjunctivitis (see Pallansch M. 2007).

Cardioviruses are positive-strand RNA viruses in the *Picornaviridae* family that have been associated with myocarditis, encephalitis, and demyelinating disease in rodents (see Brahic, Bureau et al. 2005), (Liang, Kumar et al. 2008). The Cardiovirus genus consists of Theilovirus, the prototype of which is Theiler's murine encephalomyelitis virus (TMEV), and EMCV. Infection with EMCV is associated with sporadic cases and outbreaks of myocarditis and encephalitis in domestic pigs, in numerous species of nonhuman primates, and in other mammalian species (Grobler, Raath et al. 1995). The disease is often fatal with sudden death as the first indication of infection. Most outbreaks have been associated with captive animals, such as those found in piggeries, primate research centers and zoos.

5.5 EMCV replication has been used to measure the activity of the type I IFN signaling pathway

Type 1 IFN has been shown to regulate EMCV replication (Kato, Takeuchi et al. 2006). These authors challenged mice with EMCV as a model virus that is recognised by MDA5. Induction of cytokines such as IFN-β, IFN-α, and IL-6 was severely impaired in the sera of $MDA5^{-/-}$ mice challenged with EMCV (Kato, Takeuchi et al. 2006). $MDA5^{-/-}$ mice and mice null for the IFN-α/β receptor were highly susceptible to EMCV infection compared to littermate controls (Kato, Takeuchi et al. 2006). These experiments demonstrate the sensitivity of EMCV replication to type 1 IFN activity *in vivo*.

5.6 Investigating the impact of vIRF-2 on EMCV replication

Given the sensitivity of EMCV to type 1 IFN, we tested our hypothesis that vIRF-2 rescues IFN-sensitive viruses from the type 1 IFN antiviral pathway with this virus. Monolayers of EV clone 5 and vIRF-2 clone 3-9 cells were pre-treated with or without doxycycline and increasing amounts of rIFN-α (up to 300 IU/ml) for 30 hours before infection with encephalomyocarditis virus at a multiplicity of infection (MOI) of 0.1. The cell supernatant was harvested 24 hours later for quantification of the viral titre by plaque assay (**Figure 5.2**). In the non-IFN treated cells, the viral yield recovered from the pair of cell clones remained approximately the same. Thus, EMCV yield recovered from the vIRF-2-expressing clone 3-9 cells averaged $7.4x10^6$ PFU/ml, compared with an average of $6.6x10^6$ PFU/ml for EV clone 5 cells. However and as expected, increasing amounts of rIFN-α decreased significantly ($p< 0.01$, Student's *t* test) the yield of EMCV in the EV clone 5 cells by as much as two orders of magnitude (to $7.7x10^4$ PFU/ml for 300 IU rIFN-α/ml) (**Figure 5.2**). In contrast, the yield of EMCV recovered from the vIRF-2-expressing clone 3-9 cells was almost unchanged following IFN-α treatment ($2.9x10^6$ PFU/ml at 300 IU rIFN-α/ml) compared to untreated cells (**Figure 5.2**). These data provide evidence that vIRF-2 can mediate viral resistance to IFN and rescue IFN-sensitive EMCV replication.

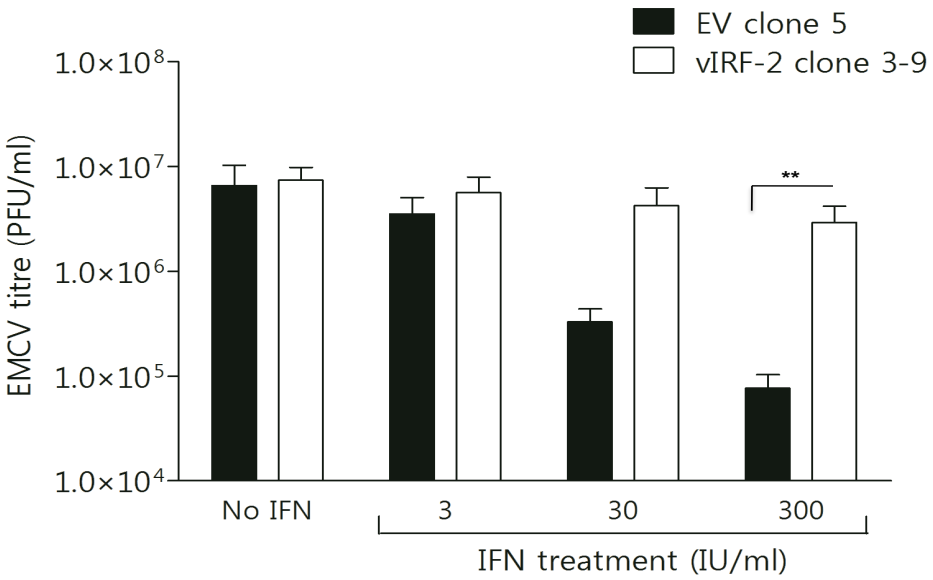

Figure 5.2 Effects of vIRF-2 on EMCV replication. Monolayers of vIRF-2 clone 3-9 and EV clone 5 cells were pre-treated with doxycycline (1 μg/ml) and either none or increasing amounts of rIFN-α (3, 30, and 300 IU/ml) for 30 hours. The cells were then infected with EMCV (MOI = 0.1) and incubated for 30 hours. The culture fluid was collected and EMCV titres determined by limiting dilution plaque assay on L929 cells. After 72 hours of incubation, plaques were identified by crystal violet staining and counted. Data are presented as the mean EMCV titre +/- standard deviation in clone 3-9 cells compared to the titre in EV clone 5 cells in three independent experiments, each performed in duplicate. In cells treated with 300 IU rIFNα/ml, the EMCV titre was statistically significant (**p <0.01, Student's *t*-test) when compared between the two clones.

5.7 Discussion

vIRF-1 and vIRF-3 can inhibit virus-mediated activation of IFN-α and IFN-β promoters by inhibiting the transactivating activities of cellular IRFs such as IRF-1 and IRF-3 (Burysek, Yeow et al. 1999; Lubyova and Pitha 2000). Also, vIRF-2 exon 1 or K11.1 has been shown to rescue VSV mRNA translation from IFN-induced block and we have shown in chapter 4 of this study that vIRF-2 down-regulates the IFN-α/β pathway. Hence, we investigated the biological significance of this phenomenon. We used a model system for these studies in which the extent of replication of Chandipura virus or EMCV was compared in the presence or absence of IFN-α treatment of vIRF-2 expressing clone 3-9 cells compared with EV clone 5 lacking vIRF-2.

Originally, we wanted to measure replication of wild type KSHV-BAC36 virus vs. KSHV-BAC36 deleted for vIRF-2 in the presence and absence of type 1 IFN, but that was aborted due to inherent problems with the KSHV-BAC36 (Yakushko, Hackmann et al. 2011). The bacterial artificial chromosome (BAC) for the KSHV genome was originally reported by Zhou and colleagues (Zhou, Zhang et al. 2002). BAC technology allows the mutagenesis of individual genes in complete herpesviral genomes and the functional analysis of the resulting phenotype (Borst, Hahn et al. 1999; Zhou, Zhang et al. 2002; Zhu, Li et al. 2006; Estep, Powers et al. 2007; Nagel, Dohner et al. 2008). Since the original publication (Zhou, Zhang et al. 2002) several mutagenesis investigations involving KSHV-BAC36 have been reported (Xu, AuCoin et al. 2005; Xu, Rodriguez-Huete et al. 2006; Zhu, Li et al. 2006; Ye, Zhou et al. 2008). Nevertheless, none has been able to achieve high titre virus of either KSHV-BAC36 or mutant derivatives for the de novo infection studies. Recently, Yakushko et al reported that the KSHV-BAC36 genome contains a duplication of a 9-kb LUR fragment in the terminal repeat area and proved that the BAC cassette is located within this duplication (Yakushko, Hackmann et al. 2011). These authors also demonstrated sequence coverage

across the KSHV genome when mapping all the 454 reads against the reference sequence (GenBank accession no. AF148805) with a Roche Mapper software package. This analysis showed up to 4 times the number of reads of positions at approximate nucleotides 25000 to 35000 which was consistent with an amplification of that part of the KSHV genome. This region (~ 25000 to ~35000) covered part of ORF19, as well as complete ORFs 18, 17, 16, K7, K6 and K5. This duplicated region was verified and confirmed by a Southern blot assay. These authors then hybridized KSHV-BAC36 DNA to a DNA microarray and found that probes mapping to a region comprising nt ~ 25000 to 35000 yielded hybridization signals that were about 2-fold higher than those observed for the remainder of the genome (Yakushko, Hackmann et al. 2011). The PCR analysis of the terminal repeat (TR) region yielded a band showing that the BAC cassette was located in the duplicated LUR fragment. These and other experiments performed by these authors provide evidence of a ~9-kb duplication of an LUR fragment inserted in the terminal repeat region that it contains the BAC cassette. These authors suggested that insertion of the BAC cassette within the duplication of an LUR fragment in the TR region could lead to homologous recombination in bacteria and the preferential loss of the intact KSHV LUR region, since the use of selection markers such as chloramphenicol to select the BAC cassette would favour the retention of the smaller LUR fragment containing the BAC cassette. Although the KSHV-BAC36 has been successfully used in many laboratories to analyse the functions of several KSHV genes in the context of the entire KSHV genome, the LUR duplication will complicate mutagenesis or knockout of viral genes especially those located within this duplication region. This limitation has hampered our vIRF-2 knockout studies.

We do not know why vIRF-2 expression failed to rescue the Chandipura virus from the antiviral effect of IFN-α. However, the expression of vIRF-2 in clone 3-9 cells did rescue EMCV replication from the antiviral effect of IFN-α pathway (**Figure 5.2**). The data

demonstrate a rIFN-α dose dependent reduction of EMCV titre in the EV clone 5 but not in the vIRF-2 expressing clone 3-9 cells. Also, the EMCV yield recovered from the vIRF-2 expressing clone 3-9 cells treated with rIFN-α at 300 IU/ml was approximately unchanged compared to that of untreated cells. In a similar experiment to study viral inhibition of IFN response, Morrison and Racaniello showed picornaviruses encoding the $2A^{pro}$ gene such as polio virus are able to replicate in cells that have been pre-treated with IFN-α, whereas others that do not encode the $2A^{pro}$ gene such as EMCV are exquisitely sensitivity to IFN and are unable to replicate in IFN-pre-treated cells (Morrison and Racaniello 2009). However, these authors showed EMCV chimeric viruses expressing the $2A^{pro}$ gene, replicated to higher titres in the IFN-pre-treated cells. The result of this study can be likened to the observation made in **Figure 5.2** indicating vIRF-2 antiviral property in KSHV is able to rescue the replication of other viruses such as EMCV. In another experiment, Morrison and Racaniello pre-treated HeLa cells with 1000 U/ml IFN-α for 24 hours and then infected the cells with EMCV, whose replication was inhibited by approximately 100-fold compared to mock treated cells (Morrison and Racaniello 2009). This result is consistent with ours (**Figure 5.2**) in which EV clone 5 cells were pre-treated with rIFN-α 300 IU/ml for 30 hours before being infected with EMCV. The replication of the virus was inhibited by ~100-fold.

The experiments performed in clone 3-9 and EV clone 5 were performed with both viruses at MOIs of 1 and 10 as well (data not shown) and a similar pattern of results were observed as with (**Figure 5.1, 5.2**) but the extent of IFN inhibition was not comparable. This result is consistent with that reported recently where HeLa cells were pre-treated with IFN-α 1000 IU/ml or left untreated and were infected with the Polio virus type 1 Mahoney (P1M) at MOI of 100, 10,1, or 0.1, and the viral titres were determined 24 hours postinfection. P1M was relatively resistant to IFN pretreatment at an MOI of 10 or 1, but IFN resistance declined substantially at MOI of 0.1 (Morrison and Racaniello 2009).

IFN antagonism of viruses can occur at two levels. Firstly, viral recognition leading to IFN production. In the present study we have shown vIRF-2 down-regulates the RIG-like receptor pathway by specifically inhibiting RIG-I and MDA5 PRRs that detect pathogen associated molecular patterns (**Figure 4.7**). Also, the JAK-STAT pathway is inhibited by vIRF-2 (chapter 4). Secondly, IFN signaling leading to ISG production. From the present study we have shown that ISG56 and OAS3 expression are inhibited by vIRF-2 (Chapters 3 and 4). Thus, expression of two (OAS3 and ISG56) of the over 300 known ISGs was confirmed in this study to be inhibited by vIRF-2. Taken together, the vIRF-2 mechanisms of evading the antiviral effect of IFN-α include avoidance of sensing by PRRs through the inhibition of their expression, the inhibition of antiviral signaling pathways and the inhibition of the expression of antiviral genes; giving credence to the impression that vIRF-2 is pleiotropic. These mechanisms presumably play a key role in the ability vIRF-2 to rescue EMCV replication from the antiviral effect of IFN-α. A typical type 1 IFN mechanistic action *in vitro* is: (i) OAS3 leads to the destruction of viral RNA (Dong, Xu et al. 1994; Silverman 2007), (ii) ISG56 suppresses both host and viral translation by binding to eukaryotic initiation factor 3 (Hui, Bhasker et al. 2003), (iii) induction of apoptosis and establishment of antiviral state in infected cells. Other viruses which have antagonized the IFN pathway at the IFN production step include hepatitis C virus inhibition of IRF-3 and NFκB activation through the NS3/4 protease (Foy, Li et al. 2005), VSV inhibition of IFN-β transcription by matrix protein (Ferran and Lucas-Lenard 1997) and binding of human papillomavirus 16 E6 oncoprotein to IRF-3 (Ronco, Karpova et al. 1998). Dengue virus also disrupts IFN signaling (Jones, Davidson et al. 2005). The identification of such viral immune evasion strategies provides strong evidence for the importance of the early innate immune system in the control of viral infections.

Taken together, in the context of KSHV infection, vIRF-2 together with other KSHV anti-IFN genes may enhance the replication of this virus in a fashion similar to that demonstrated for the model virus EMCV (**Figure 5.2**), through the continuous suppression of the innate antiviral pathway in particular and adaptive immune systems in general.

Chapter 6 General discussion

6.1 General discussion

The ultimate goal of this study was to investigate the impact of KSHV vIRF-2 on cell transcriptome profiles involved in the IFN-α/β pathway. Based on previous studies of vIRF-2 function, including our own laboratory, this study was designed to (i) reveal vIRF-2 down-regulated gene sets and associated biological pathways that regulate the IFN-α/β pathway, (ii) test the hypothesis that vIRF-2 inhibits pathways upstream and downstream of the IFN-α/β receptor, (iii) reveal the mechanisms by which vIRF-2 deregulates the IFN-α/β pathways leading to the circumvention of the innate immune antiviral response.

Immunological control of herpesviruses is achieved by both the adaptive and the innate immune systems. CD8+ T cells play crucial roles in the adaptive immune system (Liu, Khanna et al. 2000; Liu, Khanna et al. 2001; Braaten, Sparks-Thissen et al. 2005). IFN-α/β and natural killer cells play key roles in the innate immune response to herpesviral infections (see Areste and Blackbourn 2009).

The innate immune signaling pathway, being the first line of defence against microbial infection is critical for an effective antiviral immune response. It has therefore attracted much attention from many researchers in recent times (Krishnan, Selvarajoo et al. 2007; Loo and Gale 2007; Medzhitov 2007; Loo, Fornek et al. 2008). It is activated following sensing of infections by PRRs (Takeuchi and Akira 2010). TLRs were the first PRRs to be discovered. Recently, more intracellular PRRs have been identified that detect pathogen nucleic acids in the cytoplasm. The cytoplasmic RNA helicase-like receptors RIG-I and MDA5 act as sensors in coupling recognition of RNA virus infections to the type 1 IFN gene induction (Andrejeva, Childs et al. 2004; Takeuchi and Akira 2007; Yoneyama and Fujita 2007). Moreover, five intracellular DNA sensing proteins have been reported: (i)

DNA-dependent activator of IFN-regulatory factors (DAI). DAI was the first cytoplasmic DNA sensor to be identified and was shown to contribute to the type 1 IFN response to HSV-1 infection (Takaoka, Wang et al. 2007); (ii) absent in melanoma 2 (AIM2). Burckstummer and others were the first to report AIM2 as a cytoplasmic DNA sensor to activate the inflammasome when they (authors) screened proteins that associate with DNA and are transcriptionally regulated by IFN-β. This protein screen identified AIM2 as a new cytoplasmic DNA candidate sensor. These authors showed that AIM2 recognized dsDNA and activated the inflammasome via the adaptor protein ASC, leading to IL-1β maturation (Burckstummer, Baumann et al. 2009); (iii) RNA polymerase III. Two groups, Chiu and colleagues and Ablasser and colleagues identified a novel DNA-sensing pathway mediated by RNA polymerase III, which uses AT-rich dsDNA as a template to transcribe dsRNA containing 5'-triphosphate moiety, which is recognized by RIG-I leading to IFN production (Ablasser, Bauernfeind et al. 2009; Chiu, Macmillan et al. 2009); (iv) leucine-rich repeat flightless-interacting protein 1 (LRRFIP1). Yang and colleagues were the first group to show the cytosolic nucleic acid binding protein LRRFIP1 plays a role in the IFN production stimulated by VSV (Yang, An et al. 2010). These authors revealed LRRFIP1 bound exogenous nucleic acids and β-catenin resulting in increased IFN-β, which then leads to the production of type 1 IFN (Yang, An et al. 2010), and (v) IFN-γ-inducible protein 16 (IFI16), IFI16 was shown to be essential for IFN and cytokine response to HSV-1 infection (Unterholzner, Keating et al. 2010). Nothing is known about how vIRF-2 in particular and KSHV as a whole influence the above listed intracellular nucleic acid sensors in order to circumvent the innate antiviral immune response but the present study provides some clues (see below). Previous work in our laboratory showed that vIRF-2 inhibits the IFN-α/β pathway by inactivating IRF-1 and IRF-3. However, that alone may not be sufficient to impair the antiviral innate immune response pathway, since the IRF-3-independent

mechanism of inducing IFN-β and the innate antiviral response in cells such as those of myeloid lineage is reported to occur through an IPS-1-dependent signal that does not require IRF-3 and IRF-7 (Daffis, Suthar et al. 2009). Further more, Daffis and colleagues showed that the systemic type 1 IFN response in IRF-$3^{-/-}$ and IRF-$7^{-/-}$ double knockout (DKO) mice is blunted but not abolished (Daffis, Suthar et al. 2009), in line with their previous studies which also showed an absence of IRF-3 *in vivo* does not profoundly reduce the levels of type I IFN in serum after West Nile virus infection (Bourne, Scholle et al. 2007; Daffis, Samuel et al. 2007). These studies suggest the residual systemic type I IFN response is non-IRF-3-dependent. Furthermore, the activation of IRF-1 and IRF-3 is regulated by upstream PRRs and we reasoned vIRF-2 may target these PRRs to inhibit the IFN-α/β pathway

We first engineered a vIRF-2 stable inducible cell line in which the vIRF-2 expressing cassette is regulated by doxycycline and in parallel a negative control clone which does not express vIRF-2. This vIRF-2 clone 3-9 and negative control cell line EV clone 5 were then used for a series of studies prior to the DNA microarray investigation. The initial phase of these studies demonstrated 1 μg/ml doxycycline treatment of vIRF-2 clone 3-9 cells up to 36 hours provided maximal vIRF-2 expression (**Figures 3.1, 3.3**). The second experiment aimed to determine the concentration of rIFN-α capable of stimulating maximal activation of pISRE-luc activity in EV clone 5 cells. This concentration was established at 300 IU/ml rIFN-α for up to 36 hrs (**Figure 3.4**). These studies made it possible to conduct vIRF-2 functional assays which established vIRF-2 inhibited rIFN-α driven pISRE-luc activity by 52% in clone 3-9 cells (**Figure 3.5**). vIRF-2 was further characterized by IFA, which showed it is predominantly a nuclear resident protein (**Figure 3.8**).

vIRF-2 clones 20, 24 and their EV clone counterparts 1 and 4 lacking vIRF-2 were also engineered and vIRF-2 expression and functional studies were confirmed in these additional clones (**Figure 3.6**). As explained earlier, over 300 clones were screened and only

three clones were capable of suppressing rIFN-α stimulated pISRE-luc. The most likely explanation being that vIRF-2 expression is so leaky that rIFN-α treatment does not induce ISRE. Therefore greater suppression of ISRE and lack of induction due to leaky vIRF-2 expression was seen in the majority of clones.

Having established vIRF-2 is functional in clone 3-9 cells, RNA was prepared from cell sample sets M11A, M11B and M10 (**Figure 3.7 and Table 3.1**) and submitted for microarray profiling investigations. Due to the cost involved, the DNA microarray studies were performed for vIRF-2 clone 3-9 cells only.

Upon receipt of the microarray data we conducted exon array quality assessment analyses on all 12 GeneChips to ensure the data quality were consistent with guidelines suggested by Affymetrix (**Appendix II, Figures 1A-E**). The exon array raw data revealed 13542 genes were differentially expressed. We then compared the gene expression profile of -dox-IFN and -dox+IFN phenotypes (in triplicates) and identified 78 IFN up-regulated genes based on Limma p value less than 0.001; out of which 57 (73%) were significantly down-regulated by vIRF-2 (Limma $p< 0.05$) (**Figure 4.1**). To identify vIRF-2 regulated genes in the absence of IFN; the expression profile of untreated cells was compared with that of +dox-ifn treated cells, which identified 26 genes as differentially regulated by vIRF-2. 17/26 (65%) of these vIRF-2 regulated genes in the absence of IFN-α were significantly up-regulated by vIRF-2 based on Limma $p<0.05$. The remaining 9/26 (35%) genes were significantly down-regulated by vIRF-2 based on Limma $p<0.05$ (**Figure 4.1E**). The vIRF-2 regulated genes in the absence of IFN were not studied further due to time constraints.

Although 13/26 (50%) genes of the IFN-α down-regulated genes were up-regulated by vIRF-2, we elected not to pursue their study because they were not significantly enriched by the DAVID package. Instead, we focused on IFN-α-induced gene sets with common biological functions or biological pathways that were down-regulted by vIRF-2 expression.

The DAVID and GSEA packages were therefore employed to perform these analyses and summaries of these data analyses are presented (**Tables 4.2, 4.3, 4.4**). As expected, GO terms and gene sets involved in the 'Antiviral response' pathway are the most highly enriched and their annotation clustered at the top of the Tables.

Our initial hypothesis that vIRF-2 down-regulates IFN-α mediated events upstream and downstream of the IFN-α/β receptor was confirmed (**Tables 4.2** and **4.3**, respectively.) Although the data presented in each table were generated independently, i.e. with either the DAVID or the GSEA package, they both indicated that gene sets involved in antiviral responses, transcription regulation, cell cycle and apoptosis were down-regulated by vIRF-2. This study is the first to show vIRF-2 inhibits these pathways. Investigation of the JAK-STAT pathway revealed vIRF-2 down-regulated STAT1 & IRF-9 at the transcription level (**Figure 4.1**) and these findings were confirmed by immunoblot at the protein level (**Figure 4.4**). This result is consistent with the reduced ISGF-3 binding to cognate ISRE sequences (as determined by EMSA) by vIRF-2 expressing clone 3-9 compared to the EV clone 5 counterpart shown by Miss Laura Hindle in our laboratory (Mutocheluh, Hindle et al. 2011). These data also confirm our hypothesis that vIRF-2 is multifunctional and its targeted inhibition of IRF-1 and IRF-3 (Fuld, Cunningham et al. 2006; Areste, Mutocheluh et al. 2009) may not be sufficient to block the entire IFN-α/β pathway. The reduction of ISG56 (section 3.9) and OAS3 (section 4.5.1) by vIRF-2 measured the impact of vIRF-2 on the IFN-stimulated genes and was suggestive of being a consequence of the down-regulation of the IFN-α/β pathway.

To date, two distinct systems for RNA virus detection and IFN induction have been characterized. One is composed of the toll-like receptors and the other is the RIG-I-like receptor family. RIG-I and MDA5 of the RIG-I-like receptor family are known cytoplasmic sensors expressed in the majority of cell types and they detect intracellular RNA viruses. The

present study has shown the specific down-regulation of RIG-I/DDX58 and MDA5/IFIH1 by vIRF-2 at the transcription level (**Figure 4.1**). Interestingly, RIG-I/DDX58 was confirmed at the protein level to be substantially reduced by vIRF-2 accumulation in the vIRF-2 induced clone 20 cells treated with (+dox+ifn) compared with those of the non-vIRF-2 induced cells treated with (-dox+ifn) or EV clone 1 with the same treatment profile (**Figure 4.6B**). These results suggest the RIG-I-like receptor pathway may be inhibited by vIRF-2.

The inhibition of the RIG-I-like receptor pathway by vIRF-2 suggests the consequence is the reduced transduction of signaling cascades which converge upon activation and nuclear localization of three families of transcription factors: NF-κB, IRF-3 and ATF-2/cJun. Also, impaired RIG-I/DDX58 and or MDA5/IFIH1 responses would not be expected to recruit MAV adaptor protein under normal circumstance (Kawai, Takahashi et al. 2005; Meylan, Curran et al. 2005; Seth, Sun et al. 2005). MAV under normal circumstance relays the signal to TBK1 and IKK (Fitzgerald, McWhirter et al. 2003; Sharma, tenOever et al. 2003), which phosphorylates IRF-3 and IRF-7. Since the level of TBK1 is reduced by vIRF-2 in the vIRF-2 induced clone 20 compared with the EV clone 1 counterpart (**Figure 4.6B**), this result confirms the RIG-I-like receptor pathway is down-regulated by vIRF-2. These data are consistent with our prediction that IFN-α mediated events upstream of the IFN-α/β receptor are deregulated by vIRF-2. Another reason vIRF-2 may inhibit the RIG-I-like receptor pathway is that both RIG-I/DDX58 or MDA5/IFIH1 respond to viruses (Yoneyama, Kikuchi et al. 2005) and it makes biological sense to attenuate the viral PRR in order to evade innate immune response.

vIRF-2 inhibition of RIG-I/DDX58 or MDA5/IFIH1 has now opened a new avenue for work on how KSHV affects the intracellular PRRs including the above listed DNA sensors such as IFI16 (Unterholzner, Keating et al. 2010). IFI16 was down-regulated by vIRF-2 (**Figure 4.1 and Table 4.2**) and is known to be essential for the IFN and cytokine

response to HSV-1 infection (Unterholzner, Keating et al. 2010). Further, the inhibition of STAT1 by vIRF-2 in the JAK-STAT pathway (**Figure 4.5**) suggests vIRF-2 may contribute to KSHV oncogenesis.

The ISG56/IFIT1 family of genes (ISG54/IFIT2, ISG56/IFIT1, ISG58/IFIT5 and ISG60 /IFIT3) are down-regulated by vIRF-2 (**Table 4.2**) most probably as a consequence of the down-regulation of the IFN-α/β pathway since they are transcriptionally regulated by IFN-αβ and IFN-γ (Der, Zhou et al. 1998). As stated (section 3.9), a multitude of RNA- or DNA- viruses, viral and bacterial PAMPs can directly induce transcription of a subset of ISGs including ISG56 family genes suggesting the crucial role they play in the innate antiviral immune response. Interestingly, *ISG58/IFIT5* and *ISG60 /IFIT3* were originally discovered as ATRA-inducible genes (Niikura, Hirata et al. 1997). ATRA is used in the treatment of acute promyelocytic leukemia, as it induces differentiation of immature leukemic cells and prevents their further proliferation. However, induction of *ISG60 /IFIT3* is not directly by ATRA but partly by IFN-α, which is secreted after ATRA treatment and activates *ISG60 /IFIT3* transcription via the JAK-STAT pathway (Xiao, Li et al. 2006). This IFN-α activity provides further evidence that the ISG56 gene family members were down-regulated as a consequence of the down-regulation of the JAK-STAT pathway by vIRF-2. One of the best characterized cellular functions of the ISG56 is the inhibition of translation by binding to specific subunits of eIF3, thus presenting a mechanism of cell growth inhibition distinct from other ISGs like PKR and OAS. For example, Guo et al have shown that exogenous expression of human *ISG56/IFIT1* suppressed overall cellular translation by 40% in HT1080 cells, thus being as effective as IFN-β treatment (Guo and Sen 2000).

The general inhibition of cellular translation mediated by the *ISG56/IFIT1* family of proteins can be considered as part of a nonspecific antiviral program elicited by exposure of cells to IFNs or viral PAMPs, which induce the concerted expression of these and other ISGs.

But the repertoire of functions of the ISG56/IFIT1 gene family extends to virus-specific inhibitory functions. They are both translation-related and unrelated. For example, translation of the HCV positive-sense RNA genome is initiated by IRES-dependent ribosome recruitment, which, similar to cap-dependent translation, requires eIF3 (Lukavsky 2009). This process is known to be IFN-sensitive, since IFN induces the human ISG56/IFIT1 family of genes, which in turn inhibits HCV translation initiation both *in vitro* and within cells. Also, HCV-IRES translation is known to be more strongly compromised than cap-dependent translation in the presence of human ISG56/IFIT1. The inhibition depends on binding of human ISG56/IFIT1 to eIF3. The human ISG56/IFIT1 is found specifically in the ribosomal initiation complexes containing eIF3 and HCV RNA (Wang, Pflugheber et al. 2003). Therefore, IFN- or virus-induced human ISG56/IFIT1 contributes to the inhibition of HCV virus. Although KSHV vCyclin coding sequence contains an IRES element (Bieleski and Talbot 2001), the inhibitory effect of ISG56/IFIT1 on cellular protein translation regulation may not be biologically significant because vCyclin deregulates the cell cycle.

Taken together, we speculate that vIRF-2 down-regulates this human ISG56/IFIT1 gene family as a consequence of the down-regulation of the JAK-STAT pathway and the pleiotropic effects include: the rescue of virus replication as shown for EMCV (**section 5.6, Figure 5.2**), the inhibition of apoptosis (**Figure 4.6, Table 4.3**), the inhibition of cell migration and antiproliferation as a result of inhibition of IFITs (Lai, Chang et al. 2008).

Three genes encoding members of the Poly(ADP-ribosyl)polymerase superfamily (PARP 9, 12, 14) originally identified as enzymes that catalyze the attachment of ADP-ribose subunits to target proteins using NAD^+ as a substrate (Chambon, Weill et al. 1963; Fujimura, Hasegawa et al. 1967) were also down-regulated by vIRF-2 (**Table 4.2**). The ADP-ribose polymer is formed by sequential attachment of ADP-ribosyl moieties from NAD+. PARPs have been shown to be involved in DNA damage repair, cell death pathways, transcription

and chromatin modification/remodeling (see Kim, Zhang et al. 2005; Schreiber, Dantzer et al. 2006). PARPs are important targets for anti-cancer therapies (Fong, Boss et al. 2009). The first PARP purified and cloned, PARP 1 from human, remains the best studied, while PARPs 1 and 2 are the most abundant nuclear protein after histones (Virag and Szabo 2002) . The PARP-like family has been characterized in humans, where there are seventeen members that share the PARP catalytic domain (Ame, Spenlehauer et al. 2004; Hottiger, Hassa et al. 2010). In our previous studies, one of our experiments showed cleaved PARP levels were reduced in the presence of vIRF-2 compared with its absence regardless of the presence of caspase-3 siRNA, and we speculated that vIRF-2 might have anti-apoptotic activity (Areste, Mutocheluh et al. 2009). These data are consistent with Yu et al, who have provided evidence that PARP-1 activity triggers release of a mitochondrial pro-apoptotic protein called apoptosis-inducing factor (AIF) that promotes programmed cell death through a capase-independent pathway (Yu, Wang et al. 2002). Therefore, we speculate that vIRF-2 has evolved to down-regulate these PARPs in order to deregulate the cell cycle, gene transcription regulation and apoptotic pathways resulting in the deregulation of the antiviral pathways and promotion of tumourigenesis. Both the IFIT and the PARP GO terms (**Table 4.2**) were not confirmed by immunoblot due to time constrains.

The hypothesis that vIRF-2 anti-type 1 IFN effects could rescue EMCV from the IFN-α/β pathway was also confirmed (**Figure 5.2**). As stated (section 5.7), the best model system to determine the biological relevance of the deregulation of the type 1 IFN pathway by vIRF-2 is to compare titre of a KSHV-vIRF-2 mutant lacking vIRF-2 with that of WT when propagated in the presence or absence of IFN. Our original plan was to use KSHV-BAC36, which has been used for the purpose of mutagenesis studies by some groups since its establishment as an experimental model in 2002 (Zhou, Zhang et al. 2002; Gunther and Grundhoff 2010). Although, Dr. Simon Chanas in our laboratory created a KSHVBAC36-

vIRF-2 mutant, it could not be used due to our inability to reactivate it and produce virus. The reason is likely due to duplication of approximately 9-kb in the LUR fragment within the terminal repeat (Yakushko, Hackmann et al. 2011). This problem is discussed in section 5.1.

The replication kinetics of interferon sensitive Chandipura virus or EMCV in IFN-α pre-treated cells expressing vIRF-2 or not was studied. For unknown reason, vIRF-2 was not able to rescue Chandipura virus replication from the anti-viral effect of IFN-α (**Figure 5.1**). However, vIRF-2 was able rescue EMCV replication from this effect (**Figure 5.2**). It must be emphasized that the experiments involving each type of virus were performed in parallel; therefore the unexpected Chandipura virus result is unlikely to be experimental error. Nevertheless, the EMCV result confirms our hypothesis that the anti-type 1 IFN effects of vIRF-2 can rescue IFN-sensitive virus replication.

Taken together, the present study has established that vIRF-2 deregulates the entire type 1 IFN signaling pathway by specifically inhibiting key signaling proteins such as the RIG-I, MDA5, p38 and TBK1 of the early part of the IFN-α/β signaling pathway and STAT1 IRF-9 and OAS3 key signaling components of the JAK-STAT-ISRE pathway (**Figure 6.1**). The mechanisms by which vIRF-2 inhibits the IFN-α/β signaling pathway, the biological significance of these findings and the suggestive oncogenic property of vIRF-2 were shown in this study.

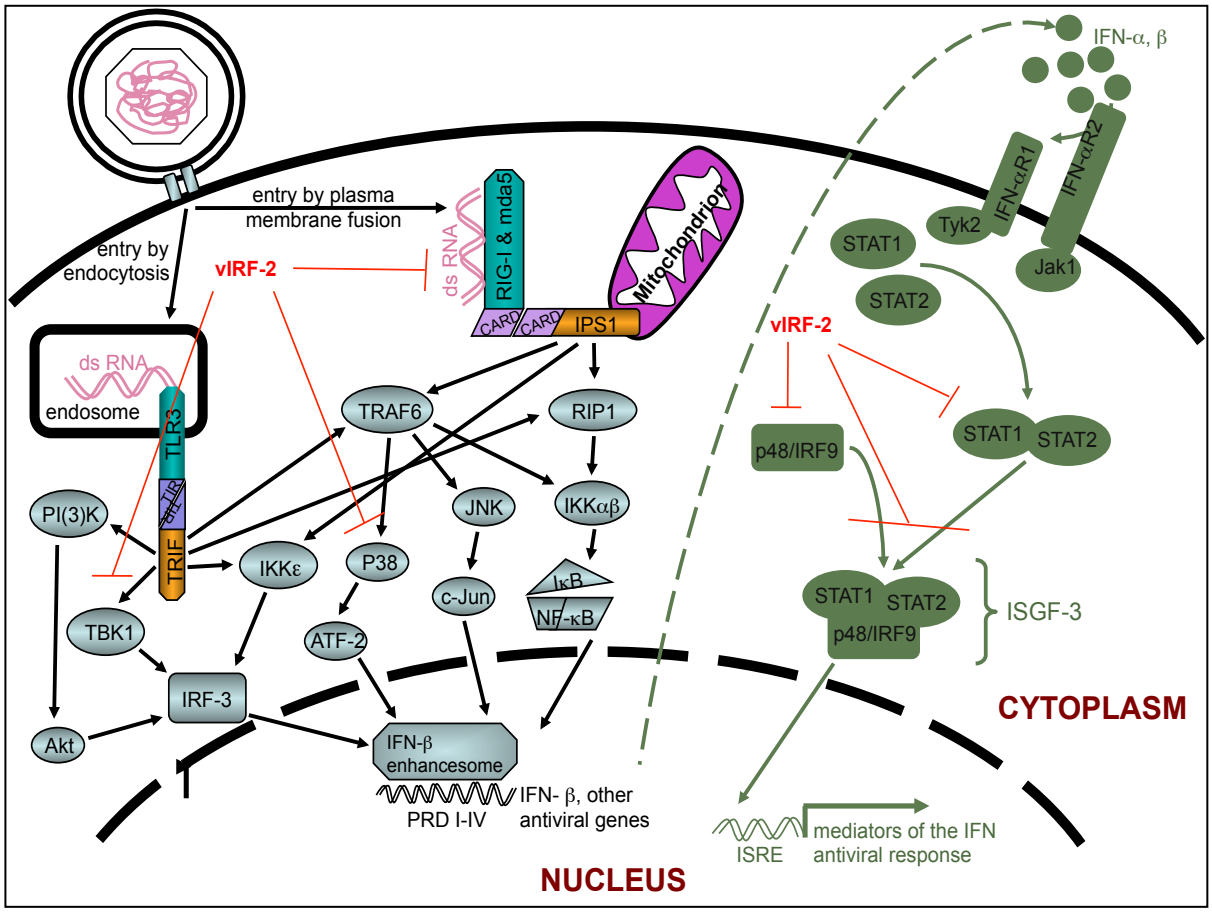

Figure 6.1. Proposed deregulation of the IFN-α/β signaling pathway by KSHV vIRF-2. The innate immune response to viral RNA has been well characterized in that the endosomal toll-like receptors (TLRs) and the cytoplasmic RIG-like receptors (RLRs) sense viral RNA, which leads to the induction of the IFN-α/β signaling pathway through activation of downstream signaling pathways (Pichlmair and Reis e Sousa 2007). Initiation of the early part of the IFN-α/β signaling pathway by TLR3 begins with TLR3 sensing dsRNA, which leads to recruitment of TLR adaptor protein TRIF; this then triggers activation of kinases including TBK1 and IKK-β, kinases that phosphorylate and activate the transcription factors IRF-3 and NF-κB respectively (Fitzgerald, McWhirter et al. 2003; Sharma, tenOever et al. 2003) Thereafter, IRF-3 and NF-κB translocate to the nucleus and mediate an antiviral gene induction program that includes the production of IFN-β. Cytosolic RNA is detected by the RLRs RIG-I and MDA5, which via the adaptor protein IPS-1 turn on a signaling pathway similar to that of TLR3 in the induction of IFN-β production via TBK1-mediated IRF-3 activation (Pichlmair and Reis e Sousa 2007). However, the present study shows the levels of RIG-I, MDA5, p38 and

TBK1 were reduced by vIRF-2 (indicated by red font and straight lines crossed at one end). Once the cell has responded to the infection through the production of IFN-α/β cytokines, they are secreted and can act in a paracrine and autocrine fashion to initiate the remainder of the IFN response (right side of illustration). This initiation occurs through the production of the IFN-stimulated gene factor (ISGF-3) followed by the activation and expression of IFN-stimulated response elements (ISRE)-containing promoters whose products establish the antiviral state in infected and uninfected bystander cells (Stark, Kerr et al. 1998). This process involves the recruitment and phosphorylation of signal transducer and activator of transcription factors (STAT1 and STAT2) by IFN-receptor-associated tyrosine kinases upon IFN binding. The heterodimerization of phosphorylated STAT1 and 2 recruits IRF-9 and form the ISGF-3 transcription factor complex. Because the ISRE is recognized by IRF-3 and ISGF-3 the genes active in the early kinetics in response to virus infection and those induced by the type 1 IFNs overlap. The present study has demonstrated that vIRF-2 inhibits STAT1 and IRF-9 (indicated by red font and straight lines crossed at one end) key proteins of the later part of IFN-α/β signaling pathway. Amended from (Rezaee, Cunningham et al. 2006; Areste and Blackbourn 2009).

6.2 Recommendations for future research

Future work in this area should aim to (i) verify the microarray data at the protein level as was done for the JAK-STAT-ISRE pathway in this study, for the IFITs, PARPs and the ubiquitin ligase conjugation pathways (**Table 4.2**); (ii) make a new KSHV-BAC knock out for vIRF-2 seperately and all four vIRFs together which would be used to assess the impact of all the KSHV vIRFs on the type 1 IFN pathway; (iii) construct a transgenic mouse for vIRF-2 and infect it with EMCV compared to WT mouse; (iv) verify how vIRF-2 down-regulates STAT1 and IRF-9. Other studies could investigate the impact of vIRF-2 on the intracellular PRRs, such as the recently discovered intracellular DNA sensing proteins like DAI, AIM2, RNA polymerase III and IFI16. Special attention could be paid to IFI16, which

was confirmed to be down-regulated in this study (**Figure 4.1 and Table 4.2**). It was recently reported to act as a sensor for exogenous DNA, but not RNA, directly detecting the presence of viral DNA, leading to activation factors and gene induction via a STING-dependent pathway (Unterholzner, Keating et al. 2010).

References

Abdollahi, A., K. A. Lord, et al. (1991). "Interferon regulatory factor 1 is a myeloid differentiation primary response gene induced by interleukin 6 and leukemia inhibitory factor: role in growth inhibition." Cell Growth Differ **2**(8): 401-407.

Ablashi, D. V., L. G. Chatlynne, et al. (2002). "Spectrum of Kaposi's sarcoma-associated herpesvirus, or human herpesvirus 8, diseases." Clin Microbiol Rev **15**(3): 439-464.

Ablasser, A., F. Bauernfeind, et al. (2009). "RIG-I-dependent sensing of poly(dA:dT) through the induction of an RNA polymerase III-transcribed RNA intermediate." Nat Immunol **10**(10): 1065-1072.

Agalioti, T., S. Lomvardas, et al. (2000). "Ordered recruitment of chromatin modifying and general transcription factors to the IFN-beta promoter." Cell **103**(4): 667-678.

Akira, S., S. Uematsu, et al. (2006). "Pathogen recognition and innate immunity." Cell **124**(4): 783-801.

Akula SM, F. P., Whitman AG, et al. (2004). "Raf promotes human herpesvirus-8 (HH8/KSHV) infection." Oncogene **23**(30).

Akula, S. M., N. P. Pramod, et al. (2001). "Human herpesvirus 8 envelope-associated glycoprotein B interacts with heparan sulfate-like moieties." Virology **284**(2): 235-249.

Akula, S. M., N. P. Pramod, et al. (2002). "Integrin alpha3beta1 (CD 49c/29) is a cellular receptor for Kaposi's sarcoma-associated herpesvirus (KSHV/HHV-8) entry into the target cells." Cell **108**(3): 407-419.

Al-khatib, K., B. R. Williams, et al. (2003). "The murine double-stranded RNA-dependent protein kinase PKR and the murine 2',5'-oligoadenylate synthetase-dependent RNase L are required for IFN-beta-mediated resistance against herpes simplex virus type 1 in primary trigeminal ganglion culture." Virology **313**(1): 126-135.

Alcami, A. (2003). "Viral mimicry of cytokines, chemokines and their receptors." Nat Rev Immunol **3**(1): 36-50.

Alexander, L., L. Denekamp, et al. (2000). "The primary sequence of rhesus monkey rhadinovirus isolate 26-95: sequence similarities to Kaposi's sarcoma-associated herpesvirus and rhesus monkey rhadinovirus isolate 17577." J Virol **74**(7): 3388-3398.

Allison, D. B., X. Cui, et al. (2006). "Microarray data analysis: from disarray to consolidation and consensus." Nat Rev Genet **7**(1): 55-65.

Ambroziak, J. A., D. J. Blackbourn, et al. (1995). "Herpes-like sequences in HIV-infected and uninfected Kaposi's sarcoma patients." Science **268**(5210): 582-583.

Ame, J. C., C. Spenlehauer, et al. (2004). "The PARP superfamily." Bioessays **26**(8): 882-893.

An, J., Y. Sun, et al. (2004). "Transcriptional coactivation of c-Jun by the KSHV-encoded LANA." Blood **103**(1): 222-228.

Andrejeva, J., K. S. Childs, et al. (2004). "The V proteins of paramyxoviruses bind the IFN-inducible RNA helicase, mda-5, and inhibit its activation of the IFN-beta promoter." Proc Natl Acad Sci U S A **101**(49): 17264-17269.

Andreoni, M., D. Goletti, et al. (2001). "Prevalence, incidence and correlates of HHV-8/KSHV infection and Kaposi's sarcoma in renal and liver transplant recipients." J Infect **43**(3): 195-199.

Ank, N., H. West, et al. (2006). "Lambda interferon (IFN-lambda), a type III IFN, is induced by viruses and IFNs and displays potent antiviral activity against select virus infections in vivo." J Virol **80**(9): 4501-4509.

Ank, N., H. West, et al. (2006). "IFN-lambda: novel antiviral cytokines." J Interferon Cytokine Res **26**(6): 373-379.

Antman, K. and Y. Chang (2000). "Kaposi's sarcoma." N Engl J Med **342**(14): 1027-1038.

Aoki, Y., E. S. Jaffe, et al. (1999). "Angiogenesis and hematopoiesis induced by Kaposi's sarcoma-associated herpesvirus-encoded interleukin-6." Blood **93**(12): 4034-4043.

Aoki, Y., K. D. Jones, et al. (2000). "Kaposi's sarcoma-associated herpesvirus-encoded interleukin-6." J Hematother Stem Cell Res **9**(2): 137-145.

Aoki, Y. and G. Tosato (1999). "Role of vascular endothelial growth factor/vascular permeability factor in the pathogenesis of Kaposi's sarcoma-associated herpesvirus-infected primary effusion lymphomas." Blood **94**(12): 4247-4254.

Aoki, Y., R. Yarchoan, et al. (2000). "Viral and cellular cytokines in AIDS-related malignant lymphomatous effusions." Blood **96**(4): 1599-1601.

Areste, C. and D. J. Blackbourn (2009). "Modulation of the immune system by Kaposi's sarcoma-associated herpesvirus." Trends Microbiol **17**(3): 119-129.

Areste, C., M. Mutocheluh, et al. (2009). "Identification of caspase-mediated decay of interferon regulatory factor-3, exploited by a Kaposi sarcoma-associated herpesvirus immunoregulatory protein." J Biol Chem **284**(35): 23272-23285.

Arnheiter, H., S. Skuntz, et al. (1990). "Transgenic mice with intracellular immunity to influenza virus." Cell **62**(1): 51-61.

Ascoli, V., F. Lo Coco, et al. (2002). "Human herpesvirus 8-associated primary effusion lymphoma in HIV--patients: a clinicopidemiologic variant resembling classic Kaposi's sarcoma." Haematologica **87**(4): 339-343.

Bach, E. A., M. Aguet, et al. (1997). "The IFN gamma receptor: a paradigm for cytokine receptor signaling." Annu Rev Immunol **15**: 563-591.

Bach, E. A., J. W. Tanner, et al. (1996). "Ligand-induced assembly and activation of the gamma interferon receptor in intact cells." Mol Cell Biol **16**(6): 3214-3221.

Ballestas, M. E., P. A. Chatis, et al. (1999). "Efficient persistence of extrachromosomal KSHV DNA mediated by latency-associated nuclear antigen." Science **284**(5414): 641-644.

Ballestas, M. E. and K. M. Kaye (2001). "Kaposi's sarcoma-associated herpesvirus latency-associated nuclear antigen 1 mediates episome persistence through cis-acting terminal repeat (TR) sequence and specifically binds TR DNA." J Virol **75**(7): 3250-3258.

Bandyopadhyay, S. K., G. T. Leonard, Jr., et al. (1995). "Transcriptional induction by double-stranded RNA is mediated by interferon-stimulated response elements without activation of interferon-stimulated gene factor 3." J Biol Chem **270**(33): 19624-19629.

Battle, T. E., R. A. Lynch, et al. (2006). "Signal transducer and activator of transcription 1 activation in endothelial cells is a negative regulator of angiogenesis." Cancer Res **66**(7): 3649-3657.

Bechtel, J., A. Grundhoff, et al. (2005). "RNAs in the virion of Kaposi's sarcoma-associated herpesvirus." J Virol **79**(16): 10138-10146.

Bechtel, J. T., R. C. Winant, et al. (2005). "Host and viral proteins in the virion of Kaposi's sarcoma-associated herpesvirus." J Virol **79**(8): 4952-4964.

Beissbarth, T., L. Hyde, et al. (2004). "Statistical modeling of sequencing errors in SAGE libraries." Bioinformatics **20 Suppl 1**: i31-39.

Beisser, P. S., C. Vink, et al. (1998). "The R33 G protein-coupled receptor gene of rat cytomegalovirus plays an essential role in the pathogenesis of viral infection." J Virol **72**(3): 2352-2363.

Benschop, R. J. and J. C. Cambier (1999). "B cell development: signal transduction by antigen receptors and their surrogates." Curr Opin Immunol **11**(2): 143-151.

Beral, V., T. A. Peterman, et al. (1990). "Kaposi's sarcoma among persons with AIDS: a sexually transmitted infection?" Lancet **335**(8682): 123-128.

Berkowitz, B., D. B. Huang, et al. (2002). "The x-ray crystal structure of the NF-kappa B p50.p65 heterodimer bound to the interferon beta -kappa B site." J Biol Chem **277**(27): 24694-24700.

Bernabei, P., E. M. Coccia, et al. (2001). "Interferon-gamma receptor 2 expression as the deciding factor in human T, B, and myeloid cell proliferation or death." J Leukoc Biol **70**(6): 950-960.

Bhatt, P. N. and F. M. Rodrigues (1967). "Chandipura: a new Arbovirus isolated in India from patients with febrile illness." Indian J Med Res **55**(12): 1295-1305.

Bieleski, L. and S. J. Talbot (2001). "Kaposi's sarcoma-associated herpesvirus vCyclin open reading frame contains an internal ribosome entry site." J Virol **75**(4): 1864-1869.

Blackbourn, D. J., E. Lennette, et al. (2000). "The restricted cellular host range of human herpesvirus 8." Aids **14**(9): 1123-1133.

Blackbourn, D. J. and J. A. Levy (1997). "Human herpesvirus 8 in semen and prostate." Aids **11**(2): 249-250.

Blackbourn, D. J., D. Osmond, et al. (1999). "Increased human herpesvirus 8 seroprevalence in young homosexual men who have multiple sex contacts with different partners." J Infect Dis **179**(1): 237-239.

Bluyssen, A. R., J. E. Durbin, et al. (1996). "ISGF3 gamma p48, a specificity switch for interferon activated transcription factors." Cytokine Growth Factor Rev **7**(1): 11-17.

Bluyssen, H. A., R. J. Vlietstra, et al. (1994). "Structure, chromosome localization, and regulation of expression of the interferon-regulated mouse Ifi54/Ifi56 gene family." Genomics **24**(1): 137-148.

Borst, E. M., G. Hahn, et al. (1999). "Cloning of the human cytomegalovirus (HCMV) genome as an infectious bacterial artificial chromosome in Escherichia coli: a new approach for construction of HCMV mutants." J Virol **73**(10): 8320-8329.

Boshoff, C., Y. Endo, et al. (1997). "Angiogenic and HIV-inhibitory functions of KSHV-encoded chemokines." Science **278**(5336): 290-294.

Boshoff, C., T. F. Schulz, et al. (1995). "Kaposi's sarcoma-associated herpesvirus infects endothelial and spindle cells." Nat Med **1**(12): 1274-1278.

Boshoff, C. and R. Weiss (2002). "AIDS-related malignancies." Nat Rev Cancer **2**(5): 373-382.

Boshoff, C. and R. A. Weiss (2001). "Epidemiology and pathogenesis of Kaposi's sarcoma-associated herpesvirus." Philos Trans R Soc Lond B Biol Sci **356**(1408): 517-534.

Bourne, N., F. Scholle, et al. (2007). "Early production of type I interferon during West Nile virus infection: role for lymphoid tissues in IRF3-independent interferon production." J Virol **81**(17): 9100-9108.

Bouvard, V., R. Baan, et al. (2009). "A review of human carcinogens--Part B: biological agents." Lancet Oncol **10**(4): 321-322.

Braaten, D. C., R. L. Sparks-Thissen, et al. (2005). "An optimized CD8+ T-cell response controls productive and latent gammaherpesvirus infection." J Virol **79**(4): 2573-2583.

Brahic, M., J. F. Bureau, et al. (2005). "The genetics of the persistent infection and demyelinating disease caused by Theiler's virus." Annu Rev Microbiol **59**: 279-298.

Brideau-Andersen, A. D., X. Huang, et al. (2007). "Directed evolution of gene-shuffled IFN-alpha molecules with activity profiles tailored for treatment of chronic viral diseases." Proc Natl Acad Sci U S A **104**(20): 8269-8274.

Brinkmann, M. M., M. Glenn, et al. (2003). "Activation of mitogen-activated protein kinase and NF-kappaB pathways by a Kaposi's sarcoma-associated herpesvirus K15 membrane protein." J Virol **77**(17): 9346-9358.

Briscoe, J., N. C. Rogers, et al. (1996). "Kinase-negative mutants of JAK1 can sustain interferon-gamma-inducible gene expression but not an antiviral state." Embo J **15**(4): 799-809.

Browning, P. J., J. M. Sechler, et al. (1994). "Identification and culture of Kaposi's sarcoma-like spindle cells from the peripheral blood of human immunodeficiency virus-1-infected individuals and normal controls." Blood **84**(8): 2711-2720.

Bruce J. Dezube, M. Z., David R. Sage, Jian-Feng Wang, Joyce D. Fingeroth (2002). "Characterization of Kaposi's sarcoma-associated herpesvirus/human herpesvirus-8 infection of human vascular endothelial cells: early events." Blood **100**.

Burckstummer, T., C. Baumann, et al. (2009). "An orthogonal proteomic-genomic screen identifies AIM2 as a cytoplasmic DNA sensor for the inflammasome." Nat Immunol **10**(3): 266-272.

Burger, R., F. Neipel, et al. (1998). "Human herpesvirus type 8 interleukin-6 homologue is functionally active on human myeloma cells." Blood **91**(6): 1858-1863.

Burysek, L. and P. M. Pitha (2001). "Latently expressed human herpesvirus 8-encoded interferon regulatory factor 2 inhibits double-stranded RNA-activated protein kinase." J Virol **75**(5): 2345-2352.

Burysek, L., W. S. Yeow, et al. (1999). "Functional analysis of human herpesvirus 8-encoded viral interferon regulatory factor 1 and its association with cellular interferon regulatory factors and p300." J Virol **73**(9): 7334-7342.

Burysek, L., W. S. Yeow, et al. (1999). "Unique properties of a second human herpesvirus 8-encoded interferon regulatory factor (vIRF-2)." J Hum Virol **2**(1): 19-32.

Cesarman, E., Y. Chang, et al. (1995). "Kaposi's sarcoma-associated herpesvirus-like DNA sequences in AIDS-related body-cavity-based lymphomas." N Engl J Med **332**(18): 1186-1191.

Chadha, M. S., V. A. Arankalle, et al. (2005). "An outbreak of Chandipura virus encephalitis in the eastern districts of Gujarat state, India." Am J Trop Med Hyg **73**(3): 566-570.

Chambon, P., J. D. Weill, et al. (1963). "Nicotinamide mononucleotide activation of new DNA-dependent polyadenylic acid synthesizing nuclear enzyme." Biochem Biophys Res Commun **11**: 39-43.

Chang, J., R. Renne, et al. (2000). "Inflammatory cytokines and the reactivation of Kaposi's sarcoma-associated herpesvirus lytic replication." Virology **266**(1): 17-25.

Chang, Y., E. Cesarman, et al. (1994). "Identification of herpesvirus-like DNA sequences in AIDS-associated Kaposi's sarcoma." Science **266**(5192): 1865-1869.

Chapgier, A., R. F. Wynn, et al. (2006). "Human complete Stat-1 deficiency is associated with defective type I and II IFN responses in vitro but immunity to some low virulence viruses in vivo." J Immunol **176**(8): 5078-5083.

Chatterjee, M., J. Osborne, et al. (2002). "Viral IL-6-induced cell proliferation and immune evasion of interferon activity." Science **298**(5597): 1432-1435.

Chattopadhyay, S., J. T. Marques, et al. (2010). "Viral apoptosis is induced by IRF-3-mediated activation of Bax." EMBO J **29**(10): 1762-1773.

Chee, M. S., A. T. Bankier, et al. (1990). "Analysis of the protein-coding content of the sequence of human cytomegalovirus strain AD169." Curr Top Microbiol Immunol **154**: 125-169.

Chen, C. W., Y. G. Tsay, et al. (2002). "The double-stranded RNA-activated kinase, PKR, can phosphorylate hepatitis D virus small delta antigen at functional serine and threonine residues." J Biol Chem **277**(36): 33058-33067.

Chen, S., K. B. Bacon, et al. (1998). "In vivo inhibition of CC and CX3C chemokine-induced leukocyte infiltration and attenuation of glomerulonephritis in Wistar-Kyoto (WKY) rats by vMIP-II." J Exp Med **188**(1): 193-198.

Chieux, V., W. Chehadeh, et al. (2001). "Inhibition of coxsackievirus B4 replication in stably transfected cells expressing human MxA protein." Virology **283**(1): 84-92.

Chiu, Y. H., J. B. Macmillan, et al. (2009). "RNA polymerase III detects cytosolic DNA and induces type I interferons through the RIG-I pathway." Cell **138**(3): 576-591.

Choi, J. K., B. S. Lee, et al. (2000). "Identification of the novel K15 gene at the rightmost end of the Kaposi's sarcoma-associated herpesvirus genome." J Virol **74**(1): 436-446.

Clemens, M. J. and A. Elia (1997). "The double-stranded RNA-dependent protein kinase PKR: structure and function." J Interferon Cytokine Res **17**(9): 503-524.

Clemens, M. J. and B. R. Williams (1978). "Inhibition of cell-free protein synthesis by pppA2'p5'A2'p5'A: a novel oligonucleotide synthesized by interferon-treated L cell extracts." Cell **13**(3): 565-572.

Colamonici, O., H. Yan, et al. (1994). "Direct binding to and tyrosine phosphorylation of the alpha subunit of the type I interferon receptor by p135tyk2 tyrosine kinase." Mol Cell Biol **14**(12): 8133-8142.

Colman, R. and D. J. Blackbourn (2008). "Risk factors in the development of Kaposi's sarcoma." AIDS **22**(13): 1629-1632.

Conti, L., G. Regis, et al. (2007). "In the absence of IGF-1 signaling, IFN-gamma suppresses human malignant T-cell growth." Blood **109**(6): 2496-2504.

Cotter, M. A., 2nd, C. Subramanian, et al. (2001). "The Kaposi's sarcoma-associated herpesvirus latency-associated nuclear antigen binds to specific sequences at the left end of the viral genome through its carboxy-terminus." Virology **291**(2): 241-259.

Cunha, A. M., A. Caterino-de-Araujo, et al. (2005). "Increasing seroprevalence of human herpesvirus 8 (HHV-8) with age confirms HHV-8 endemicity in Amazon Amerindians from Brazil." J Gen Virol **86**(Pt 9): 2433-2437.

Cunningham, C., S. Barnard, et al. (2003). "Transcription mapping of human herpesvirus 8 genes encoding viral interferon regulatory factors." J Gen Virol **84**(Pt 6): 1471-1483.

D'Andrea, L. D. and L. Regan (2003). "TPR proteins: the versatile helix." Trends Biochem Sci **28**(12): 655-662.

Daffis, S., M. A. Samuel, et al. (2007). "Cell-specific IRF-3 responses protect against West Nile virus infection by interferon-dependent and -independent mechanisms." PLoS Pathog **3**(7): e106.

Daffis, S., M. A. Samuel, et al. (2008). "Interferon regulatory factor IRF-7 induces the antiviral alpha interferon response and protects against lethal West Nile virus infection." J Virol **82**(17): 8465-8475.

Daffis, S., M. S. Suthar, et al. (2009). "Induction of IFN-beta and the innate antiviral response in myeloid cells occurs through an IPS-1-dependent signal that does not require IRF-3 and IRF-7." PLoS Pathog **5**(10): e1000607.

Dairaghi, D. J., R. A. Fan, et al. (1999). "HHV8-encoded vMIP-I selectively engages chemokine receptor CCR8. Agonist and antagonist profiles of viral chemokines." J Biol Chem **274**(31): 21569-21574.

Damania, B. (2004). "Oncogenic gamma-herpesviruses: comparison of viral proteins involved in tumorigenesis." Nat Rev Microbiol **2**(8): 656-668.

Davis-Poynter, N. J., D. M. Lynch, et al. (1997). "Identification and characterization of a G protein-coupled receptor homolog encoded by murine cytomegalovirus." J Virol **71**(2): 1521-1529.

Davison, A. J. (1992). "Channel catfish virus: a new type of herpesvirus." Virology **186**(1): 9-14.

Davison, A. J. (2002). "Evolution of the herpesviruses." Vet Microbiol **86**(1-2): 69-88.

Davison, A. J., R. Eberle, et al. (2009). "The order Herpesvirales." Arch Virol **154**(1): 171-177.

De Clercq, E. (2006). "Interferon and its inducers--a never-ending story: "old" and "new" data in a new perspective." J Infect Dis **194 Suppl 1**: S19-26.

de Souza, V. A., L. M. Sumita, et al. (2007). "Human herpesvirus-8 infection and oral shedding in Amerindian and non-Amerindian populations in the Brazilian Amazon region." J Infect Dis **196**(6): 844-852.

de Veer, M. J., H. Sim, et al. (1998). "IFI60/ISG60/IFIT4, a new member of the human IFI54/IFIT2 family of interferon-stimulated genes." Genomics **54**(2): 267-277.

Decker, L. L., P. Shankar, et al. (1996). "The Kaposi sarcoma-associated herpesvirus (KSHV) is present as an intact latent genome in KS tissue but replicates in the peripheral blood mononuclear cells of KS patients." J Exp Med **184**(1): 283-288.

Dedicoat, M., R. Newton, et al. (2004). "Mother-to-child transmission of human herpesvirus-8 in South Africa." J Infect Dis **190**(6): 1068-1075.

Der, S. D., A. Zhou, et al. (1998). "Identification of genes differentially regulated by interferon alpha, beta, or gamma using oligonucleotide arrays." Proc Natl Acad Sci U S A **95**(26): 15623-15628.

Devergne, O., E. Hatzivassiliou, et al. (1996). "Association of TRAF1, TRAF2, and TRAF3 with an Epstein-Barr virus LMP1 domain important for B-lymphocyte transformation: role in NF-kappaB activation." Mol Cell Biol **16**(12): 7098-7108.

Di Bartolo, D. L., M. Cannon, et al. (2008). "KSHV LANA inhibits TGF-beta signaling through epigenetic silencing of the TGF-beta type II receptor." Blood **111**(9): 4731-4740.

Diamond, M. S. (2009). "Mechanisms of evasion of the type I interferon antiviral response by flaviviruses." J Interferon Cytokine Res **29**(9): 521-530.

Dimberg, A., I. Karlberg, et al. (2003). "Ser727/Tyr701-phosphorylated Stat1 is required for the regulation of c-Myc, cyclins, and p27Kip1 associated with ATRA-induced G0/G1 arrest of U-937 cells." Blood **102**(1): 254-261.

Dimmock, N. J., E. W. Rainsford, et al. (2008). "Influenza virus protecting RNA: an effective prophylactic and therapeutic antiviral." J Virol **82**(17): 8570-8578.

Dittmer, D., M. Lagunoff, et al. (1998). "A cluster of latently expressed genes in Kaposi's sarcoma-associated herpesvirus." J Virol **72**(10): 8309-8315.

Dittmer, D. P. (2003). "Transcription profile of Kaposi's sarcoma-associated herpesvirus in primary Kaposi's sarcoma lesions as determined by real-time PCR arrays." Cancer Res **63**(9): 2010-2015.

Dong, B., L. Xu, et al. (1994). "Intrinsic molecular activities of the interferon-induced 2-5A-dependent RNase." J Biol Chem **269**(19): 14153-14158.

Douglas, J., B. Dutia, et al. (2004). "Expression in a recombinant murid herpesvirus 4 reveals the in vivo transforming potential of the K1 open reading frame of Kaposi's sarcoma-associated herpesvirus." J Virol **78**(16): 8878-8884.

Dourmishev, L. A., A. L. Dourmishev, et al. (2003). "Molecular genetics of Kaposi's sarcoma-associated herpesvirus (human herpesvirus-8) epidemiology and pathogenesis." Microbiol Mol Biol Rev **67**(2): 175-212, table of contents.

Dragan, A. I., V. V. Hargreaves, et al. (2007). "Mechanisms of activation of interferon regulator factor 3: the role of C-terminal domain phosphorylation in IRF-3 dimerization and DNA binding." Nucleic Acids Res **35**(11): 3525-3534.

Duboise, S. M., J. Guo, et al. (1998). "STP and Tip are essential for herpesvirus saimiri oncogenicity." J Virol **72**(2): 1308-1313.

Dupin, N., C. Fisher, et al. (1999). "Distribution of human herpesvirus-8 latently infected cells in Kaposi's sarcoma, multicentric Castleman's disease, and primary effusion lymphoma." Proc Natl Acad Sci U S A **96**(8): 4546-4551.

Duprez, R., V. Lacoste, et al. (2007). "Evidence for a multiclonal origin of multicentric advanced lesions of Kaposi sarcoma." J Natl Cancer Inst **99**(14): 1086-1094.

Dupuis, S., E. Jouanguy, et al. (2003). "Impaired response to interferon-alpha/beta and lethal viral disease in human STAT1 deficiency." Nat Genet **33**(3): 388-391.

Durbin, J. E., R. Hackenmiller, et al. (1996). "Targeted disruption of the mouse Stat1 gene results in compromised innate immunity to viral disease." Cell **84**(3): 443-450.

Easton, A. J., P. D. Scott, et al. (2011). "A novel broad-spectrum treatment for respiratory virus infections: influenza-based defective interfering virus provides protection against pneumovirus infection in vivo." Vaccine **29**(15): 2777-2784.

Egwuagu, C. E., W. Li, et al. (2006). "Interferon-gamma induces regression of epithelial cell carcinoma: critical roles of IRF-1 and ICSBP transcription factors." Oncogene **25**(26): 3670-3679.

Elahi, A., L. Zhang, et al. (2008). "HPP1-mediated tumor suppression requires activation of STAT1 pathways." Int J Cancer **122**(7): 1567-1572.

Elco, C. P., J. M. Guenther, et al. (2005). "Analysis of genes induced by Sendai virus infection of mutant cell lines reveals essential roles of interferon regulatory factor 3, NF-kappaB, and interferon but not toll-like receptor 3." J Virol **79**(7): 3920-3929.

Ellis, M., Y. P. Chew, et al. (1999). "Degradation of p27(Kip) cdk inhibitor triggered by Kaposi's sarcoma virus cyclin-cdk6 complex." Embo J **18**(3): 644-653.

Endres, M. J., C. G. Garlisi, et al. (1999). "The Kaposi's sarcoma-related herpesvirus (KSHV)-encoded chemokine vMIP-I is a specific agonist for the CC chemokine receptor (CCR)8." J Exp Med **189**(12): 1993-1998.

Ensoli, B. and M. Sturzl (1998). "Kaposi's sarcoma: a result of the interplay among inflammatory cytokines, angiogenic factors and viral agents." Cytokine Growth Factor Rev **9**(1): 63-83.

Escalante, C. R., J. Yie, et al. (1998). "Structure of IRF-1 with bound DNA reveals determinants of interferon regulation." Nature **391**(6662): 103-106.

Espert, L., P. Codogno, et al. (2007). "Involvement of autophagy in viral infections: antiviral function and subversion by viruses." J Mol Med **85**(8): 811-823.

Estep, R. D., M. F. Powers, et al. (2007). "Construction of an infectious rhesus rhadinovirus bacterial artificial chromosome for the analysis of Kaposi's sarcoma-associated herpesvirus-related disease development." J Virol **81**(6): 2957-2969.

Eychene, A., N. Rocques, et al. (2008). "A new MAFia in cancer." Nat Rev Cancer **8**(9): 683-693.

Fakhari, F. D. and D. P. Dittmer (2002). "Charting latency transcripts in Kaposi's sarcoma-associated herpesvirus by whole-genome real-time quantitative PCR." J Virol **76**(12): 6213-6223.

Fakhari, F. D., J. H. Jeong, et al. (2006). "The latency-associated nuclear antigen of Kaposi sarcoma-associated herpesvirus induces B cell hyperplasia and lymphoma." J Clin Invest **116**(3): 735-742.

Ferran, M. C. and J. M. Lucas-Lenard (1997). "The vesicular stomatitis virus matrix protein inhibits transcription from the human beta interferon promoter." J Virol **71**(1): 371-377.

Fiette, L., C. Aubert, et al. (1995). "Theiler's virus infection of 129Sv mice that lack the interferon alpha/beta or interferon gamma receptors." J Exp Med **181**(6): 2069-2076.

Fitzgerald, K. A., S. M. McWhirter, et al. (2003). "IKKepsilon and TBK1 are essential components of the IRF3 signaling pathway." Nat Immunol **4**(5): 491-496.

Fong, P. C., D. S. Boss, et al. (2009). "Inhibition of poly(ADP-ribose) polymerase in tumors from BRCA mutation carriers." N Engl J Med **361**(2): 123-134.

Ford, P. W., K. E. Hamden, et al. (2004). "Vascular endothelial growth factor augments human herpesvirus-8 (HHV-8/KSHV) infection." Cancer Biol Ther **3**(9): 876-881.

Foy, E., K. Li, et al. (2005). "Control of antiviral defenses through hepatitis C virus disruption of retinoic acid-inducible gene-I signaling." Proc Natl Acad Sci U S A **102**(8): 2986-2991.

Fujii, Y., T. Shimizu, et al. (1999). "Crystal structure of an IRF-DNA complex reveals novel DNA recognition and cooperative binding to a tandem repeat of core sequences." Embo J **18**(18): 5028-5041.

Fujimura, S., S. Hasegawa, et al. (1967). "Polymerization of the adenosine 5'-diphosphate-ribose moiety of nicotinamide-adenine dinucleotide by nuclear enzyme. I. Enzymatic reactions." Biochim Biophys Acta **145**(2): 247-259.

Fuld, S., C. Cunningham, et al. (2006). "Inhibition of interferon signaling by the Kaposi's sarcoma-associated herpesvirus full-length viral interferon regulatory factor 2 protein." J Virol **80**(6): 3092-3097.

Fulda, S. and K. M. Debatin (2002). "IFNgamma sensitizes for apoptosis by upregulating caspase-8 expression through the Stat1 pathway." Oncogene **21**(15): 2295-2308.

Gabriele, L., A. Fragale, et al. (2006). "IRF-1 deficiency skews the differentiation of dendritic cells toward plasmacytoid and tolerogenic features." J Leukoc Biol **80**(6): 1500-1511.

Gack, M. U., A. Kirchhofer, et al. (2008). "Roles of RIG-I N-terminal tandem CARD and splice variant in TRIM25-mediated antiviral signal transduction." Proc Natl Acad Sci U S A **105**(43): 16743-16748.

Gack, M. U., Y. C. Shin, et al. (2007). "TRIM25 RING-finger E3 ubiquitin ligase is essential for RIG-I-mediated antiviral activity." Nature **446**(7138): 916-920.

Gale, M., Jr. and G. C. Sen (2009). "Viral evasion of the interferon system." J Interferon Cytokine Res **29**(9): 475-476.

Gallo, R. C. (1998). "The enigmas of Kaposi's sarcoma." Science **282**(5395): 1837-1839.

Ganem, D. (2007). Kaposis sarcoma-associated herpesvirus. Fields Virology. H. P. Knipe D, Lippincott, Philadelphia, Pa**:** 2847-2888.

Gao, S. J., C. Boshoff, et al. (1997). "KSHV ORF K9 (vIRF) is an oncogene which inhibits the interferon signaling pathway." Oncogene **15**(16): 1979-1985.

Gao, S. J., L. Kingsley, et al. (1996). "KSHV antibodies among Americans, Italians and Ugandans with and without Kaposi's sarcoma." Nat Med **2**(8): 925-928.

Garber, A. C., J. Hu, et al. (2002). "Latency-associated nuclear antigen (LANA) cooperatively binds to two sites within the terminal repeat, and both sites contribute to the ability of LANA to suppress transcription and to facilitate DNA replication." J Biol Chem **277**(30): 27401-27411.

Garber, A. C., M. A. Shu, et al. (2001). "DNA binding and modulation of gene expression by the latency-associated nuclear antigen of Kaposi's sarcoma-associated herpesvirus." J Virol **75**(17): 7882-7892.

Garrigues, H. J., Y. E. Rubinchikova, et al. (2008). "Integrin alphaVbeta3 Binds to the RGD motif of glycoprotein B of Kaposi's sarcoma-associated herpesvirus and functions as an RGD-dependent entry receptor." J Virol **82**(3): 1570-1580.

Gires, O., F. Kohlhuber, et al. (1999). "Latent membrane protein 1 of Epstein-Barr virus interacts with JAK3 and activates STAT proteins." EMBO J **18**(11): 3064-3073.

Glenn, M., L. Rainbow, et al. (1999). "Identification of a spliced gene from Kaposi's sarcoma-associated herpesvirus encoding a protein with similarities to latent membrane proteins 1 and 2A of Epstein-Barr virus." J Virol **73**(8): 6953-6963.

Godden-Kent, D., S. J. Talbot, et al. (1997). "The cyclin encoded by Kaposi's sarcoma-associated herpesvirus stimulates cdk6 to phosphorylate the retinoblastoma protein and histone H1." J Virol **71**(6): 4193-4198.

Godfrey, A., J. Anderson, et al. (2005). "Inhibiting primary effusion lymphoma by lentiviral vectors encoding short hairpin RNA." Blood **105**(6): 2510-2518.

Goedert, J. J. (2000). "The epidemiology of acquired immunodeficiency syndrome malignancies." Semin Oncol **27**(4): 390-401.

Gordien, E., O. Rosmorduc, et al. (2001). "Inhibition of hepatitis B virus replication by the interferon-inducible MxA protein." J Virol **75**(6): 2684-2691.

Gossen, M. and H. Bujard (1992). "Tight control of gene expression in mammalian cells by tetracycline-responsive promoters." Proc Natl Acad Sci U S A **89**(12): 5547-5551.

Gossen, M., S. Freundlieb, et al. (1995). "Transcriptional activation by tetracyclines in mammalian cells." Science **268**(5218): 1766-1769.

Gradoville, L., J. Gerlach, et al. (2000). "Kaposi's sarcoma-associated herpesvirus open reading frame 50/Rta protein activates the entire viral lytic cycle in the HH-B2 primary effusion lymphoma cell line." J Virol **74**(13): 6207-6212.

Grandvaux, N., M. J. Servant, et al. (2002). "Transcriptional profiling of interferon regulatory factor 3 target genes: direct involvement in the regulation of interferon-stimulated genes." J Virol **76**(11): 5532-5539.

Greenlund, A. C., M. A. Farrar, et al. (1994). "Ligand-induced IFN gamma receptor tyrosine phosphorylation couples the receptor to its signal transduction system (p91)." Embo J **13**(7): 1591-1600.

Grisotto, M. G., A. Garin, et al. (2006). "The human herpesvirus 8 chemokine receptor vGPCR triggers autonomous proliferation of endothelial cells." J Clin Invest **116**(5): 1264-1273.

Grobler, D. G., J. P. Raath, et al. (1995). "An outbreak of encephalomyocarditis-virus infection in free-ranging African elephants in the Kruger National Park." Onderstepoort J Vet Res **62**(2): 97-108.

Grundhoff, A. and D. Ganem (2003). "The latency-associated nuclear antigen of Kaposi's sarcoma-associated herpesvirus permits replication of terminal repeat-containing plasmids." J Virol **77**(4): 2779-2783.

Guasparri, I., S. A. Keller, et al. (2004). "KSHV vFLIP is essential for the survival of infected lymphoma cells." J Exp Med **199**(7): 993-1003.

Gunther, T. and A. Grundhoff (2010). "The epigenetic landscape of latent Kaposi sarcoma-associated herpesvirus genomes." PLoS Pathog **6**(6): e1000935.

Guo, H. G., M. Sadowska, et al. (2003). "Kaposi's sarcoma-like tumors in a human herpesvirus 8 ORF74 transgenic mouse." J Virol **77**(4): 2631-2639.

Guo, J. and G. C. Sen (2000). "Characterization of the interaction between the interferon-induced protein P56 and the Int6 protein encoded by a locus of insertion of the mouse mammary tumor virus." J Virol **74**(4): 1892-1899.

Guo, J. T., J. Hayashi, et al. (2005). "West Nile virus inhibits the signal transduction pathway of alpha interferon." J Virol **79**(3): 1343-1350.

Haller, O., H. Arnheiter, et al. (1979). "Genetically determined, interferon-dependent resistance to influenza virus in mice." J Exp Med **149**(3): 601-612.

Hansen, A., S. Henderson, et al. (2010). "KSHV-encoded miRNAs target MAF to induce endothelial cell reprogramming." Genes Dev **24**(2): 195-205.

Haque, S. J. and B. R. Williams (1994). "Identification and characterization of an interferon (IFN)-stimulated response element-IFN-stimulated gene factor 3-independent signaling pathway for IFN-alpha." J Biol Chem **269**(30): 19523-19529.

Harada, H., M. Matsumoto, et al. (1996). "Regulation of IFN-alpha/beta genes: evidence for a dual function of the transcription factor complex ISGF3 in the production and action of IFN-alpha/beta." Genes Cells **1**(11): 995-1005.

Hayward, G. S. (1999). "KSHV strains: the origins and global spread of the virus." Cancer Biology **9**.

He, J., G. Bhat, et al. (1998). "Seroprevalence of human herpesvirus 8 among Zambian women of childbearing age without Kaposi's sarcoma (KS) and mother-child pairs with KS." J Infect Dis **178**(6): 1787-1790.

He, Z., B. Xin, et al. (2000). "Nuclear factor-kappaB activation is involved in LMP1-mediated transformation and tumorigenesis of rat-1 fibroblasts." Cancer Res **60**(7): 1845-1848.

Hengge, U. R., T. Ruzicka, et al. (2002). "Update on Kaposi's sarcoma and other HHV8 associated diseases. Part 1: epidemiology, environmental predispositions, clinical manifestations, and therapy." Lancet Infect Dis **2**(5): 281-292.

Herndier, B. and D. Ganem (2001). "The biology of Kaposi's sarcoma." Cancer Treat Res **104**: 89-126.

Hijikata, M., Y. Ohta, et al. (2000). "Identification of a single nucleotide polymorphism in the MxA gene promoter (G/T at nt -88) correlated with the response of hepatitis C patients to interferon." Intervirology **43**(2): 124-127.

Hinnebusch, A. G. (2006). "eIF3: a versatile scaffold for translation initiation complexes." Trends Biochem Sci **31**(10): 553-562.

Holash, J., P. C. Maisonpierre, et al. (1999). "Vessel cooption, regression, and growth in tumors mediated by angiopoietins and VEGF." Science **284**(5422): 1994-1998.

Holst, P. J., M. M. Rosenkilde, et al. (2001). "Tumorigenesis induced by the HHV8-encoded chemokine receptor requires ligand modulation of high constitutive activity." J Clin Invest **108**(12): 1789-1796.

Holzinger, D., C. Jorns, et al. (2007). "Induction of MxA gene expression by influenza A virus requires type I or type III interferon signaling." J Virol **81**(14): 7776-7785.

Honda, K., A. Takaoka, et al. (2006). "Type I interferon [corrected] gene induction by the interferon regulatory factor family of transcription factors." Immunity **25**(3): 349-360.

Honda, K., H. Yanai, et al. (2005). "IRF-7 is the master regulator of type-I interferon-dependent immune responses." Nature **434**(7034): 772-777.

Horisberger, M. A., M. Wathelet, et al. (1988). "cDNA cloning and assignment to chromosome 21 of IFI-78K gene, the human equivalent of murine Mx gene." Somat Cell Mol Genet **14**(2): 123-131.

Hottiger, M. O., P. O. Hassa, et al. (2010). "Toward a unified nomenclature for mammalian ADP-ribosyltransferases." Trends Biochem Sci **35**(4): 208-219.

Hovanessian, A. G. and J. Justesen (2007). "The human 2'-5'oligoadenylate synthetase family: unique interferon-inducible enzymes catalyzing 2'-5' instead of 3'-5' phosphodiester bond formation." Biochimie **89**(6-7): 779-788.

Howard, M. R., D. Whitby, et al. (1997). "Detection of human herpesvirus 8 DNA in semen from HIV-infected individuals but not healthy semen donors." Aids **11**(2): F15-19.

Hu, S., C. Vincenz, et al. (1997). "A novel family of viral death effector domain-containing molecules that inhibit both CD-95- and tumor necrosis factor receptor-1-induced apoptosis." J Biol Chem **272**(15): 9621-9624.

Huang da, W., B. T. Sherman, et al. (2009). "Systematic and integrative analysis of large gene lists using DAVID bioinformatics resources." Nat Protoc **4**(1): 44-57.

Hui, D. J., C. R. Bhasker, et al. (2003). "Viral stress-inducible protein p56 inhibits translation by blocking the interaction of eIF3 with the ternary complex eIF2.GTP.Met-tRNAi." J Biol Chem **278**(41): 39477-39482.

Igarashi, K., G. Garotta, et al. (1994). "Interferon-gamma induces tyrosine phosphorylation of interferon-gamma receptor and regulated association of protein tyrosine kinases, Jak1 and Jak2, with its receptor." J Biol Chem **269**(20): 14333-14336.

Isaacs, A. and J. Lindenmann (1957). "Virus interference. I. The interferon." Proc R Soc Lond B Biol Sci **147**(927): 258-267.

Iscovich, J., P. Boffetta, et al. (2000). "Classic kaposi sarcoma: epidemiology and risk factors." Cancer **88**(3): 500-517.

Ishak Mde, O., R. N. Martins, et al. (2007). "High diversity of HHV-8 molecular subtypes in the Amazon region of Brazil: evidence of an ancient human infection." J Med Virol **79**(10): 1537-1544.

Ishikawa, H. and G. N. Barber (2008). "STING is an endoplasmic reticulum adaptor that facilitates innate immune signalling." Nature **455**(7213): 674-678.

Ishikawa, H., Z. Ma, et al. (2009). "STING regulates intracellular DNA-mediated, type I interferon-dependent innate immunity." Nature **461**(7265): 788-792.

Janeway, C., A., Paul Travers, Mark Walport, Mark J. Shlomchik (2001). Signaling Through Immune System Receptors. Immunobiology**:** 203-240.

Janknecht, R. and T. Hunter (1996). "Transcription. A growing coactivator network." Nature **383**(6595): 22-23.

Janssen, R., J. Pennings, et al. (2007). "Host transcription profiles upon primary respiratory syncytial virus infection." J Virol **81**(11): 5958-5967.

Jean, S., K. M. LeVan, et al. (2001). "Herpes simplex virus 1 ICP27 is required for transcription of two viral late (gamma 2) genes in infected cells." Virology **283**(2): 273-284.

Jenner, R. G., M. M. Alba, et al. (2001). "Kaposi's sarcoma-associated herpesvirus latent and lytic gene expression as revealed by DNA arrays." J Virol **75**(2): 891-902.

Johnson, K. E. and D. M. Knipe (2010). "Herpes simplex virus-1 infection causes the secretion of a type I interferon-antagonizing protein and inhibits signaling at or before Jak-1 activation." Virology **396**(1): 21-29.

Jones, K. D., Y. Aoki, et al. (1999). "Involvement of interleukin-10 (IL-10) and viral IL-6 in the spontaneous growth of Kaposi's sarcoma herpesvirus-associated infected primary effusion lymphoma cells." Blood **94**(8): 2871-2879.

Jones, M., A. Davidson, et al. (2005). "Dengue virus inhibits alpha interferon signaling by reducing STAT2 expression." J Virol **79**(9): 5414-5420.

Joo, C. H., Y. C. Shin, et al. (2007). "Inhibition of interferon regulatory factor 7 (IRF7)-mediated interferon signal transduction by the Kaposi's sarcoma-associated herpesvirus viral IRF homolog vIRF3." J Virol **81**(15): 8282-8292.

Judde JG, L. V., Briere J et al. (2000). "Monoclonality or oligoclonality of human herpes 8 terminal repeat sequences in Kaposi's sarcoma and other diseases." J Natl Cancer Inst **92**.

Jung, J. U. and R. C. Desrosiers (1995). "Association of the viral oncoprotein STP-C488 with cellular ras." Mol Cell Biol **15**(12): 6506-6512.

Kajaste-Rudnitski, A., T. Mashimo, et al. (2006). "The 2',5'-oligoadenylate synthetase 1b is a potent inhibitor of West Nile virus replication inside infected cells." J Biol Chem **281**(8): 4624-4637.

Kaleeba, J. A. and E. A. Berger (2006). "Kaposi's sarcoma-associated herpesvirus fusion-entry receptor: cystine transporter xCT." Science **311**(5769): 1921-1924.

Kamijo, R., H. Harada, et al. (1994). "Requirement for transcription factor IRF-1 in NO synthase induction in macrophages." Science **263**(5153): 1612-1615.

Kanno, T., Y. Sato, et al. (2006). "Expression of Kaposi's sarcoma-associated herpesvirus-encoded K10/10.1 protein in tissues and its interaction with poly(A)-binding protein." Virology **352**(1): 100-109.

Karst, S. M., C. E. Wobus, et al. (2003). "STAT1-dependent innate immunity to a Norwalk-like virus." Science **299**(5612): 1575-1578.

Kasolo, F. C., M. Monze, et al. (1998). "Sequence analyses of human herpesvirus-8 strains from both African human immunodeficiency virus-negative and -positive childhood endemic Kaposi's sarcoma show a close relationship with strains identified in febrile children and high variation in the K1 glycoprotein." J Gen Virol **79 (Pt 12)**: 3055-3065.

Kasolo, F. C., E. Mpabalwani, et al. (1997). "Infection with AIDS-related herpesviruses in human immunodeficiency virus-negative infants and endemic childhood Kaposi's sarcoma in Africa." J Gen Virol **78 (Pt 4)**: 847-855.

Katano, H., Y. Sato, et al. (2000). "Expression and localization of human herpesvirus 8-encoded proteins in primary effusion lymphoma, Kaposi's sarcoma, and multicentric Castleman's disease." Virology **269**(2): 335-344.

Kato, H., O. Takeuchi, et al. (2006). "Differential roles of MDA5 and RIG-I helicases in the recognition of RNA viruses." Nature **441**(7089): 101-105.

Kawai, T., K. Takahashi, et al. (2005). "IPS-1, an adaptor triggering RIG-I- and Mda5-mediated type I interferon induction." Nat Immunol **6**(10): 981-988.

Kawakami, T., M. Matsumoto, et al. (1995). "Possible involvement of the transcription factor ISGF3 gamma in virus-induced expression of the IFN-beta gene." FEBS Lett **358**(3): 225-229.

Kaye, K. M., K. M. Izumi, et al. (1993). "Epstein-Barr virus latent membrane protein 1 is essential for B-lymphocyte growth transformation." Proc Natl Acad Sci U S A **90**(19): 9150-9154.

Kazanji, M., P. Dussart, et al. (2005). "Serological and molecular evidence that human herpesvirus 8 is endemic among Amerindians in French Guiana." J Infect Dis **192**(9): 1525-1529.

Kedes, D. H., M. Lagunoff, et al. (1997). "Identification of the gene encoding the major latency-associated nuclear antigen of the Kaposi's sarcoma-associated herpesvirus." J Clin Invest **100**(10): 2606-2610.

Kedes, D. H., E. Operskalski, et al. (1996). "The seroepidemiology of human herpesvirus 8 (Kaposi's sarcoma-associated herpesvirus): distribution of infection in KS risk groups and evidence for sexual transmission." Nat Med **2**(8): 918-924.

Kerr, I. M. and R. E. Brown (1978). "pppA2'p5'A2'p5'A: an inhibitor of protein synthesis synthesized with an enzyme fraction from interferon-treated cells." Proc Natl Acad Sci U S A **75**(1): 256-260.

Kerr, I. M., R. E. Brown, et al. (1977). "Nature of inhibitor of cell-free protein synthesis formed in response to interferon and double-stranded RNA." Nature **268**(5620): 540-542.

Kilger, E., A. Kieser, et al. (1998). "Epstein-Barr virus-mediated B-cell proliferation is dependent upon latent membrane protein 1, which simulates an activated CD40 receptor." Embo J **17**(6): 1700-1709.

Kim, M. Y., T. Zhang, et al. (2005). "Poly(ADP-ribosyl)ation by PARP-1: 'PAR-laying' NAD+ into a nuclear signal." Genes Dev **19**(17): 1951-1967.

Kim, T. K. and T. Maniatis (1997). "The mechanism of transcriptional synergy of an in vitro assembled interferon-beta enhanceosome." Mol Cell **1**(1): 119-129.

Kimball, S. R. (1999). "Eukaryotic initiation factor eIF2." Int J Biochem Cell Biol **31**(1): 25-29.

Kimura, T., K. Nakayama, et al. (1994). "Involvement of the IRF-1 transcription factor in antiviral responses to interferons." Science **264**(5167): 1921-1924.

Kliche, S., W. Nagel, et al. (2001). "Signaling by human herpesvirus 8 kaposin A through direct membrane recruitment of cytohesin-1." Mol Cell **7**(4): 833-843.

Klouche, M., N. Brockmeyer, et al. (2002). "Human herpesvirus 8-derived viral IL-6 induces PTX3 expression in Kaposi's sarcoma cells." Aids **16**(8): F9-18.

Knowles, D. M., G. Inghirami, et al. (1989). "Molecular genetic analysis of three AIDS-associated neoplasms of uncertain lineage demonstrates their B-cell derivation and the possible pathogenetic role of the Epstein-Barr virus." Blood **73**(3): 792-799.

Kochs, G. and O. Haller (1999). "Interferon-induced human MxA GTPase blocks nuclear import of Thogoto virus nucleocapsids." Proc Natl Acad Sci U S A **96**(5): 2082-2086.

Konstantinova, I. M., A. S. Tsimokha, et al. (2008). "Role of proteasomes in cellular regulation." Int Rev Cell Mol Biol **267**: 59-124.

Kotenko, S. V., L. S. Izotova, et al. (1995). "Interaction between the components of the interferon gamma receptor complex." J Biol Chem **270**(36): 20915-20921.

Kraus, T. A., J. F. Lau, et al. (2003). "A hybrid IRF9-STAT2 protein recapitulates interferon-stimulated gene expression and antiviral response." J Biol Chem **278**(15): 13033-13038.

Krishnan, H. H., Naranatt PP, Smith MS, et al (2004). "Concurrent expression of latent and a limited number of lytic genes with immune modulation and antiapoptotic function by Kaposi's sarcoma-associated herpesvirus early during infection of primary endothelial and fibroblast cells and subsequent decline of lytic gene expression." J Virol **78**(7).

Krishnan, H. H., N. Sharma-Walia, et al. (2005). "Envelope glycoprotein gB of Kaposi's sarcoma-associated herpesvirus is essential for egress from infected cells." J Virol **79**(17): 10952-10967.

Krishnan, J., K. Selvarajoo, et al. (2007). "Toll-like receptor signal transduction." Exp Mol Med **39**(4): 421-438.

Kumar, A., M. Commane, et al. (1997). "Defective TNF-alpha-induced apoptosis in STAT1-null cells due to low constitutive levels of caspases." Science **278**(5343): 1630-1632.

Kumar, K. P., K. M. McBride, et al. (2000). "Regulated nuclear-cytoplasmic localization of interferon regulatory factor 3, a subunit of double-stranded RNA-activated factor 1." Mol Cell Biol **20**(11): 4159-4168.

Lagos, D., M. W. Trotter, et al. (2007). "Kaposi sarcoma herpesvirus-encoded vFLIP and vIRF1 regulate antigen presentation in lymphatic endothelial cells." Blood **109**(4): 1550-1558.

Lagunoff, M., D. M. Lukac, et al. (2001). "Immunoreceptor tyrosine-based activation motif-dependent signaling by Kaposi's sarcoma-associated herpesvirus K1 protein: effects on lytic viral replication." J Virol **75**(13): 5891-5898.

Lagunoff, M., R. Majeti, et al. (1999). "Deregulated signal transduction by the K1 gene product of Kaposi's sarcoma-associated herpesvirus." Proc Natl Acad Sci U S A **96**(10): 5704-5709.

Lagunoff, M. G., D. (1997). "The structure and coding organization of the genomic termini of Kaposi's sarcoma-associated herpesvirus " Virology **236**: 147-154.

Lai, K. C., K. W. Chang, et al. (2008). "IFN-induced protein with tetratricopeptide repeats 2 inhibits migration activity and increases survival of oral squamous cell carcinoma." Mol Cancer Res **6**(9): 1431-1439.

Lan, K., D. A. Kuppers, et al. (2005). "Induction of Kaposi's sarcoma-associated herpesvirus latency-associated nuclear antigen by the lytic transactivator RTA: a novel mechanism for establishment of latency." J Virol **79**(12): 7453-7465.

Laurent-Rolle, M., E. F. Boer, et al. (2010). "The NS5 protein of the virulent West Nile virus NY99 strain is a potent antagonist of type I interferon-mediated JAK-STAT signaling." J Virol **84**(7): 3503-3515.

Lee, B. S., S. H. Lee, et al. (2005). "Characterization of the Kaposi's sarcoma-associated herpesvirus K1 signalosome." J Virol **79**(19): 12173-12184.

Lee, H., R. Veazey, et al. (1998). "Deregulation of cell growth by the K1 gene of Kaposi's sarcoma-associated herpesvirus." Nat Med **4**(4): 435-440.

Lee, H. R., Z. Toth, et al. (2009). "Kaposi's sarcoma-associated herpesvirus viral interferon regulatory factor 4 targets MDM2 to deregulate the p53 tumor suppressor pathway." J Virol **83**(13): 6739-6747.

Lee, K. Y., E. Anderson, et al. (1999). "Loss of STAT1 expression confers resistance to IFN-gamma-induced apoptosis in ME180 cells." FEBS Lett **459**(3): 323-326.

Lennette, E. T., D. J. Blackbourn, et al. (1996). "Antibodies to human herpesvirus type 8 in the general population and in Kaposi's sarcoma patients." Lancet **348**(9031): 858-861.

Leung, S., S. A. Qureshi, et al. (1995). "Role of STAT2 in the alpha interferon signaling pathway." Mol Cell Biol **15**(3): 1312-1317.

Li, H., T. Komatsu, et al. (2002). "The Kaposi's sarcoma-associated herpesvirus K12 transcript from a primary effusion lymphoma contains complex repeat elements, is spliced, and initiates from a novel promoter." J Virol **76**(23): 11880-11888.

Li, M., H. Lee, et al. (1998). "Kaposi's sarcoma-associated herpesvirus viral interferon regulatory factor." J Virol **72**(7): 5433-5440.

Li, M., H. Lee, et al. (1997). "Kaposi's sarcoma-associated herpesvirus encodes a functional cyclin." J Virol **71**(3): 1984-1991.

Liang, Z., A. S. Kumar, et al. (2008). "Phylogenetic analysis of the species Theilovirus: emerging murine and human pathogens." J Virol **82**(23): 11545-11554.

Lin, R., P. Genin, et al. (2001). "HHV-8 encoded vIRF-1 represses the interferon antiviral response by blocking IRF-3 recruitment of the CBP/p300 coactivators." Oncogene **20**(7): 800-811.

Lindenmann, J. (1962). "Resistance of mice to mouse-adapted influenza A virus." Virology **16**: 203-204.

Lindner, D. J. and E. C. Borden (1997). "Synergistic antitumor effects of a combination of interferon and tamoxifen on estrogen receptor-positive and receptor-negative human tumor cell lines in vivo and in vitro." J Interferon Cytokine Res **17**(11): 681-693.

Liu, C., Y. Okruzhnov, et al. (2001). "Human herpesvirus 8 (HHV-8)-encoded cytokines induce expression of and autocrine signaling by vascular endothelial growth factor (VEGF) in HHV-8-infected primary-effusion lymphoma cell lines and mediate VEGF-independent antiapoptotic effects." J Virol **75**(22): 10933-10940.

Liu, T., K. M. Khanna, et al. (2001). "Gamma interferon can prevent herpes simplex virus type 1 reactivation from latency in sensory neurons." J Virol **75**(22): 11178-11184.

Liu, T., K. M. Khanna, et al. (2000). "CD8(+) T cells can block herpes simplex virus type 1 (HSV-1) reactivation from latency in sensory neurons." J Exp Med **191**(9): 1459-1466.

Liu, W. and D. A. Saint (2002). "A new quantitative method of real time reverse transcription polymerase chain reaction assay based on simulation of polymerase chain reaction kinetics." Anal Biochem **302**(1): 52-59.

Livak, K. J. and T. D. Schmittgen (2001). "Analysis of relative gene expression data using real-time quantitative PCR and the 2(-Delta Delta C(T)) Method." Methods **25**(4): 402-408.

Loo, Y. M., J. Fornek, et al. (2008). "Distinct RIG-I and MDA5 signaling by RNA viruses in innate immunity." J Virol **82**(1): 335-345.

Loo, Y. M. and M. Gale, Jr. (2007). "Viral regulation and evasion of the host response." Curr Top Microbiol Immunol **316**: 295-313.

Lowther, W. J., P. A. Moore, et al. (1999). "Cloning and functional analysis of the human IRF-3 promoter." DNA Cell Biol **18**(9): 685-692.

Lubyova, B. and P. M. Pitha (2000). "Characterization of a novel human herpesvirus 8-encoded protein, vIRF-3, that shows homology to viral and cellular interferon regulatory factors." J Virol **74**(17): 8194-8201.

Lukavsky, P. J. (2009). "Structure and function of HCV IRES domains." Virus Res **139**(2): 166-171.

Luna, R. E., F. Zhou, et al. (2004). "Kaposi's sarcoma-associated herpesvirus glycoprotein K8.1 is dispensable for virus entry." J Virol **78**(12): 6389-6398.

Luttichau, H. R., I. C. Lewis, et al. (2001). "The herpesvirus 8-encoded chemokine vMIP-II, but not the poxvirus-encoded chemokine MC148, inhibits the CCR10 receptor." Eur J Immunol **31**(4): 1217-1220.

Ma, T., B. C. Jham, et al. (2010). "Viral G protein-coupled receptor up-regulates Angiopoietin-like 4 promoting angiogenesis and vascular permeability in Kaposi's sarcoma." Proc Natl Acad Sci U S A **107**(32): 14363-14368.

Mann, D. J., E. S. Child, et al. (1999). "Modulation of p27(Kip1) levels by the cyclin encoded by Kaposi's sarcoma-associated herpesvirus." Embo J **18**(3): 654-663.

Marie, I., J. E. Durbin, et al. (1998). "Differential viral induction of distinct interferon-alpha genes by positive feedback through interferon regulatory factor-7." Embo J **17**(22): 6660-6669.

Martin, J. N., D. E. Ganem, et al. (1998). "Sexual transmission and the natural history of human herpesvirus 8 infection." N Engl J Med **338**(14): 948-954.

Martro, E., A. Esteve, et al. (2007). "Risk factors for human Herpesvirus 8 infection and AIDS-associated Kaposi's sarcoma among men who have sex with men in a European multicentre study." Int J Cancer **120**(5): 1129-1135.

Matsuyama, T., T. Kimura, et al. (1993). "Targeted disruption of IRF-1 or IRF-2 results in abnormal type I IFN gene induction and aberrant lymphocyte development." Cell **75**(1): 83-97.

Mbulaiteye, S. M., R. J. Biggar, et al. (2002). "Pleural and peritoneal lymphoma among people with AIDS in the United States." J Acquir Immune Defic Syndr **29**(4): 418-421.

McCormick, C. and D. Ganem (2005). "The kaposin B protein of KSHV activates the p38/MK2 pathway and stabilizes cytokine mRNAs." Science **307**(5710): 739-741.

McGeoch DJ, D. A. (1999). "The descent of human herpesvirus 8." Semin Cancer Biol **9**.

Medzhitov, R. (2007). "Recognition of microorganisms and activation of the immune response." Nature **449**(7164): 819-826.

Mennechet, F. J. and G. Uze (2006). "Interferon-lambda-treated dendritic cells specifically induce proliferation of FOXP3-expressing suppressor T cells." Blood **107**(11): 4417-4423.

Meraz, M. A., J. M. White, et al. (1996). "Targeted disruption of the Stat1 gene in mice reveals unexpected physiologic specificity in the JAK-STAT signaling pathway." Cell **84**(3): 431-442.

Merika, M. and D. Thanos (2001). "Enhanceosomes." Curr Opin Genet Dev **11**(2): 205-208.

Meurs, E., K. Chong, et al. (1990). "Molecular cloning and characterization of the human double-stranded RNA-activated protein kinase induced by interferon." Cell **62**(2): 379-390.

Meylan, E., J. Curran, et al. (2005). "Cardif is an adaptor protein in the RIG-I antiviral pathway and is targeted by hepatitis C virus." Nature **437**(7062): 1167-1172.

Miller, G., L. Heston, et al. (1997). "Selective switch between latency and lytic replication of Kaposi's sarcoma herpesvirus and Epstein-Barr virus in dually infected body cavity lymphoma cells." J Virol **71**(1): 314-324.

Miyamoto, M., T. Fujita, et al. (1988). "Regulated expression of a gene encoding a nuclear factor, IRF-1, that specifically binds to IFN-beta gene regulatory elements." Cell **54**(6): 903-913.

Molden, J., Y. Chang, et al. (1997). "A Kaposi's sarcoma-associated herpesvirus-encoded cytokine homolog (vIL-6) activates signaling through the shared gp130 receptor subunit." J Biol Chem **272**(31): 19625-19631.

Montaner, S., A. Sodhi, et al. (2003). "Endothelial infection with KSHV genes in vivo reveals that vGPCR initiates Kaposi's sarcomagenesis and can promote the tumorigenic potential of viral latent genes." Cancer Cell **3**(1): 23-36.

Moore, C. B. and J. P. Ting (2008). "Regulation of mitochondrial antiviral signaling pathways." Immunity **28**(6): 735-739.

Moore, P. S., C. Boshoff, et al. (1996). "Molecular mimicry of human cytokine and cytokine response pathway genes by KSHV." Science **274**(5293): 1739-1744.

Moore PS, C. Y. (1998). "Antiviral activity of tumour-suppressor pathways: Clues from molecular piracy by KSHV." Trends Genet **14**.

Moore, P. S., S. J. Gao, et al. (1996). "Primary characterization of a herpesvirus agent associated with Kaposi's sarcomae." J Virol **70**(1): 549-558.

Moore PS, G. S., Dominguez G, et al. (1996). "Primary characterization of a herpesvirus agent associated with Kaposi's sarcoma." J Virol **70**.

Moore, P. S., L. A. Kingsley, et al. (1996). "Kaposi's sarcoma-associated herpesvirus infection prior to onset of Kaposi's sarcoma." Aids **10**(2): 175-180.

Moorthy, R. K. and D. A. Thorley-Lawson (1993). "Biochemical, genetic, and functional analyses of the phosphorylation sites on the Epstein-Barr virus-encoded oncogenic latent membrane protein LMP-1." J Virol **67**(5): 2637-2645.

Morrison, J. M. and V. R. Racaniello (2009). "Proteinase 2Apro is essential for enterovirus replication in type I interferon-treated cells." J Virol **83**(9): 4412-4422.

Muller, U., U. Steinhoff, et al. (1994). "Functional role of type I and type II interferons in antiviral defense." Science **264**(5167): 1918-1921.

Muralidhar, S., A. M. Pumfery, et al. (1998). "Identification of kaposin (open reading frame K12) as a human herpesvirus 8 (Kaposi's sarcoma-associated herpesvirus) transforming gene." J Virol **72**(6): 4980-4988.

Mutocheluh, M., L. Hindle, et al. (2011). "KSHV vIRF-2 inhibits type 1 interferon signalling by targeting ISGF-3." J Gen Virol.

Nador, R. G., E. Cesarman, et al. (1996). "Primary effusion lymphoma: a distinct clinicopathologic entity associated with the Kaposi's sarcoma-associated herpes virus." Blood **88**(2): 645-656.

Nagel, C. H., K. Dohner, et al. (2008). "Nuclear egress and envelopment of herpes simplex virus capsids analyzed with dual-color fluorescence HSV1(17+)." J Virol **82**(6): 3109-3124.

Nakamura, H., M. Lu, et al. (2003). "Global changes in Kaposi's sarcoma-associated virus gene expression patterns following expression of a tetracycline-inducible Rta transactivator." J Virol **77**(7): 4205-4220.

Naranatt, P. P., H. H. Krishnan, et al. (2004). "Host gene induction and transcriptional reprogramming in Kaposi's sarcoma-associated herpesvirus (KSHV/HHV-8)-infected endothelial, fibroblast, and B cells: insights into modulation events early during infection." Cancer Res **64**(1): 72-84.

Neipel F, A. J., Fleckkenstein B. (1997). "Cell-homologous genes in the Kaposi's sarcoma-associated rhadinovirus human herpesvirus 8: Determinants of its pathogenecity?" J Virol **71**.

Neipel, F., J. C. Albrecht, et al. (1997). "Human herpesvirus 8 encodes a homolog of interleukin-6." J Virol **71**(1): 839-842.

Neipel, F., J. C. Albrecht, et al. (1997). "Cell-homologous genes in the Kaposi's sarcoma-associated rhadinovirus human herpesvirus 8: determinants of its pathogenicity?" J Virol **71**(6): 4187-4192.

Neipel, F., J. C. Albrecht, et al. (1998). "Human herpesvirus 8--the first human Rhadinovirus." J Natl Cancer Inst Monogr(23): 73-77.

Nicholas, J. (2005). "Human gammaherpesvirus cytokines and chemokine receptors." J Interferon Cytokine Res **25**(7): 373-383.

Nicholas, J., V. Ruvolo, et al. (1997). "A single 13-kilobase divergent locus in the Kaposi sarcoma-associated herpesvirus (human herpesvirus 8) genome contains nine open reading frames that are homologous to or related to cellular proteins." J Virol **71**(3): 1963-1974.

Nicholas, J., V. R. Ruvolo, et al. (1997). "Kaposi's sarcoma-associated human herpesvirus-8 encodes homologues of macrophage inflammatory protein-1 and interleukin-6." Nat Med **3**(3): 287-292.

Nicholl, M. J., L. H. Robinson, et al. (2000). "Activation of cellular interferon-responsive genes after infection of human cells with herpes simplex virus type 1." J Gen Virol **81**(Pt 9): 2215-2218.

Nicola, A. V., J. Hou, et al. (2005). "Herpes simplex virus type 1 enters human epidermal keratinocytes, but not neurons, via a pH-dependent endocytic pathway." J Virol **79**(12): 7609-7616.

Niikura, T., R. Hirata, et al. (1997). "A novel interferon-inducible gene expressed during myeloid differentiation." Blood Cells Mol Dis **23**(3): 337-349.

Noguchi, T., S. Satoh, et al. (2001). "Effects of mutation in hepatitis C virus nonstructural protein 5A on interferon resistance mediated by inhibition of PKR kinase activity in mammalian cells." Microbiol Immunol **45**(12): 829-840.

Novick, D., B. Cohen, et al. (1994). "The human interferon alpha/beta receptor: characterization and molecular cloning." Cell **77**(3): 391-400.

Ogawa, S., J. Lozach, et al. (2005). "Molecular determinants of crosstalk between nuclear receptors and toll-like receptors." Cell **122**(5): 707-721.

Ojala, P. M., M. Tiainen, et al. (1999). "Kaposi's sarcoma-associated herpesvirus-encoded v-cyclin triggers apoptosis in cells with high levels of cyclin-dependent kinase 6." Cancer Res **59**(19): 4984-4989.

Ojala, P. M., K. Yamamoto, et al. (2000). "The apoptotic v-cyclin-CDK6 complex phosphorylates and inactivates Bcl-2." Nat Cell Biol **2**(11): 819-825.

Onoguchi, K., M. Yoneyama, et al. (2007). "Viral infections activate types I and III interferon genes through a common mechanism." J Biol Chem **282**(10): 7576-7581.

Osborne, J., P. S. Moore, et al. (1999). "KSHV-encoded viral IL-6 activates multiple human IL-6 signaling pathways." Hum Immunol **60**(10): 921-927.

Panne, D., T. Maniatis, et al. (2004). "Crystal structure of ATF-2/c-Jun and IRF-3 bound to the interferon-beta enhancer." Embo J **23**(22): 4384-4393.

Panne, D., T. Maniatis, et al. (2007). "An atomic model of the interferon-beta enhanceosome." Cell **129**(6): 1111-1123.

Panne, D., S. M. McWhirter, et al. (2007). "Interferon regulatory factor 3 is regulated by a dual phosphorylation-dependent switch." J Biol Chem **282**(31): 22816-22822.

Parravicini, C., B. Chandran, et al. (2000). "Differential viral protein expression in Kaposi's sarcoma-associated herpesvirus-infected diseases: Kaposi's sarcoma, primary effusion lymphoma, and multicentric Castleman's disease." Am J Pathol **156**(3): 743-749.

Parravicini, C., S. J. Olsen, et al. (1997). "Risk of Kaposi's sarcoma-associated herpes virus transmission from donor allografts among Italian posttransplant Kaposi's sarcoma patients." Blood **90**(7): 2826-2829.

Pati, S., M. Cavrois, et al. (2001). "Activation of NF-kappaB by the human herpesvirus 8 chemokine receptor ORF74: evidence for a paracrine model of Kaposi's sarcoma pathogenesis." J Virol **75**(18): 8660-8673.

Pauk, J., M. L. Huang, et al. (2000). "Mucosal shedding of human herpesvirus 8 in men." N Engl J Med **343**(19): 1369-1377.

Paun, A. and P. M. Pitha (2007). "The IRF family, revisited." Biochimie **89**(6-7): 744-753.

Pellet PE, R. B. (2006). "The Herpesviridae: a brief introduction. ." In: Knipe DM, Howley PM, Griffin DE, Lamb RA, Martin MA, Roizman B, Straus SE (eds) **Fields virology, 5th edn. Lippincott, Williams & Wilkins, Philadelphia**: 2479 - 2499.

Penn, I. (1997). "Kaposi's sarcoma in transplant recipients." Transplantation **64**(5): 669-673.

Perelygin, A. A., S. V. Scherbik, et al. (2002). "Positional cloning of the murine flavivirus resistance gene." Proc Natl Acad Sci U S A **99**(14): 9322-9327.

Pertel, P. E. (2002). "Human herpesvirus 8 glycoprotein B (gB), gH, and gL can mediate cell fusion." J Virol **76**(9): 4390-4400.

Pestka, S. (2000). "The human interferon alpha species and receptors." Biopolymers **55**(4): 254-287.

Pestka, S., C. D. Krause, et al. (2004). "Interferons, interferon-like cytokines, and their receptors." Immunol Rev **202**: 8-32.

Peters, K. L., H. L. Smith, et al. (2002). "IRF-3-dependent, NFkappa B- and JNK-independent activation of the 561 and IFN-beta genes in response to double-stranded RNA." Proc Natl Acad Sci U S A **99**(9): 6322-6327.

Pichlmair, A. and C. Reis e Sousa (2007). "Innate recognition of viruses." Immunity **27**(3): 370-383.

Pickart, C. M. (2004). "Back to the future with ubiquitin." Cell **116**(2): 181-190.

Plancoulaine, S., L. Abel, et al. (2000). "Human herpesvirus 8 transmission from mother to child and between siblings in an endemic population." Lancet **356**(9235): 1062-1065.

Platanias, L. C. (2005). "Mechanisms of type-I- and type-II-interferon-mediated signalling." Nat Rev Immunol **5**(5): 375-386.

Poole, E., B. He, et al. (2002). "The V proteins of simian virus 5 and other paramyxoviruses inhibit induction of interferon-beta." Virology **303**(1): 33-46.

Poole LJ, Z. J., Ciufo DM, et al. (1999). "Comparison of genetic variability at multiple loci across the genomes of the major subtypes of Kaposi's sarcoma-associated herpesvirus reveals evidence for recombination and for two distinct types of open reading frame K15 alleles at the right-hand end." J Virol **73**.

Prakash, O., Z. Y. Tang, et al. (2002). "Tumorigenesis and aberrant signaling in transgenic mice expressing the human herpesvirus-8 K1 gene." J Natl Cancer Inst **94**(12): 926-935.

Rady, P. L., A. Yen, et al. (1995). "Herpesvirus-like DNA sequences in non-Kaposi's sarcoma skin lesions of transplant patients." Lancet **345**(8961): 1339-1340.

Rainbow, L., G. M. Platt, et al. (1997). "The 222- to 234-kilodalton latent nuclear protein (LNA) of Kaposi's sarcoma-associated herpesvirus (human herpesvirus 8) is encoded by orf73 and is a component of the latency-associated nuclear antigen." J Virol **71**(8): 5915-5921.

Ramachandran, A., J. P. Parisien, et al. (2008). "STAT2 is a primary target for measles virus V protein-mediated alpha/beta interferon signaling inhibition." J Virol **82**(17): 8330-8338.

Randall, R. E. and S. Goodbourn (2008). "Interferons and viruses: an interplay between induction, signalling, antiviral responses and virus countermeasures." J Gen Virol **89**(Pt 1): 1-47.

Rao, B. L., A. Basu, et al. (2004). "A large outbreak of acute encephalitis with high fatality rate in children in Andhra Pradesh, India, in 2003, associated with Chandipura virus." Lancet **364**(9437): 869-874.

Rappocciolo, G., H. R. Hensler, et al. (2008). "Human herpesvirus 8 infects and replicates in primary cultures of activated B lymphocytes through DC-SIGN." J Virol **82**(10): 4793-4806.

Rezaee, S. A., C. Cunningham, et al. (2006). "Kaposi's sarcoma-associated herpesvirus immune modulation: an overview." J Gen Virol **87**(Pt 7): 1781-1804.

Rivas, C., A. E. Thlick, et al. (2001). "Kaposi's sarcoma-associated herpesvirus LANA2 is a B-cell-specific latent viral protein that inhibits p53." J Virol **75**(1): 429-438.

Roberts, W. K., A. Hovanessian, et al. (1976). "Interferon-mediated protein kinase and low-molecular-weight inhibitor of protein synthesis." Nature **264**(5585): 477-480.

Rock, K. L., C. Gramm, et al. (1994). "Inhibitors of the proteasome block the degradation of most cell proteins and the generation of peptides presented on MHC class I molecules." Cell **78**(5): 761-771.

Rodriguez, T., R. Mendez, et al. (2007). "Distinct mechanisms of loss of IFN-gamma mediated HLA class I inducibility in two melanoma cell lines." BMC Cancer **7**: 34.

Roizman, B., and A.E. Sears (2001). Herpes Simplex Viruses and Their Replication Fields Virology. D. M. K. B.N. Fields, and P.M. Howley (ed),, Lippincott - Raven Publishers, Philadelphia, Pa. **2:** 2231 - 2295.

Roizman, B., Knipe, D.M., Whitley, R.J. (2007). "Herpes Simplex Virus." Fields virology, 5th edition. Lippincott, Williams and Wilkins, Philadelphia: 2501 - 2072.

Ronco, L. V., A. Y. Karpova, et al. (1998). "Human papillomavirus 16 E6 oncoprotein binds to interferon regulatory factor-3 and inhibits its transcriptional activity." Genes Dev **12**(13): 2061-2072.

Rose, T. M. (2005). "CODEHOP-mediated PCR - a powerful technique for the identification and characterization of viral genomes." Virol J **2**: 20.

Russo, J. J., R. A. Bohenzky, et al. (1996). "Nucleotide sequence of the Kaposi sarcoma-associated herpesvirus (HHV8)." Proc Natl Acad Sci U S A **93**(25): 14862-14867.

Saha, S. K., E. M. Pietras, et al. (2006). "Regulation of antiviral responses by a direct and specific interaction between TRAF3 and Cardif." EMBO J **25**(14): 3257-3263.

Saito, T., D. M. Owen, et al. (2008). "Innate immunity induced by composition-dependent RIG-I recognition of hepatitis C virus RNA." Nature **454**(7203): 523-527.

Sakatsume, M., K. Igarashi, et al. (1995). "The Jak kinases differentially associate with the alpha and beta (accessory factor) chains of the interferon gamma receptor to form a functional receptor unit capable of activating STAT transcription factors." J Biol Chem **270**(29): 17528-17534.

Samaniego, F., S. Pati, et al. (2001). "Human herpesvirus 8 K1-associated nuclear factor-kappa B-dependent promoter activity: role in Kaposi's sarcoma inflammation?" J Natl Cancer Inst Monogr(28): 15-23.

Samuel, M. A., K. Whitby, et al. (2006). "PKR and RNase L contribute to protection against lethal West Nile Virus infection by controlling early viral spread in the periphery and replication in neurons." J Virol **80**(14): 7009-7019.

Sanceau, J., J. Hiscott, et al. (2000). "IFN-beta induces serine phosphorylation of Stat-1 in Ewing's sarcoma cells and mediates apoptosis via induction of IRF-1 and activation of caspase-7." Oncogene **19**(30): 3372-3383.

Sarkar, S. N., K. L. Peters, et al. (2004). "Novel roles of TLR3 tyrosine phosphorylation and PI3 kinase in double-stranded RNA signaling." Nat Struct Mol Biol **11**(11): 1060-1067.

Sarkar, S. N. and G. C. Sen (2004). "Novel functions of proteins encoded by viral stress-inducible genes." Pharmacol Ther **103**(3): 245-259.

Sato, M., N. Hata, et al. (1998). "Positive feedback regulation of type I IFN genes by the IFN-inducible transcription factor IRF-7." FEBS Lett **441**(1): 106-110.

Sato, M., H. Suemori, et al. (2000). "Distinct and essential roles of transcription factors IRF-3 and IRF-7 in response to viruses for IFN-alpha/beta gene induction." Immunity **13**(4): 539-548.

Sato, M., N. Tanaka, et al. (1998). "Involvement of the IRF family transcription factor IRF-3 in virus-induced activation of the IFN-beta gene." FEBS Lett **425**(1): 112-116.

Sato, T., C. Selleri, et al. (1997). "Inhibition of interferon regulatory factor-1 expression results in predominance of cell growth stimulatory effects of interferon-gamma due to phosphorylation of Stat1 and Stat3." Blood **90**(12): 4749-4758.

Schena, M., D. Shalon, et al. (1996). "Parallel human genome analysis: microarray-based expression monitoring of 1000 genes." Proc Natl Acad Sci U S A **93**(20): 10614-10619.

Schlee, M., E. Hartmann, et al. (2009). "Approaching the RNA ligand for RIG-I?" Immunol Rev **227**(1): 66-74.

Schlee, M., A. Roth, et al. (2009). "Recognition of 5' triphosphate by RIG-I helicase requires short blunt double-stranded RNA as contained in panhandle of negative-strand virus." Immunity **31**(1): 25-34.

Schmidt, A., T. Schwerd, et al. (2009). "5'-triphosphate RNA requires base-paired structures to activate antiviral signaling via RIG-I." Proc Natl Acad Sci U S A **106**(29): 12067-12072.

Schreiber, V., F. Dantzer, et al. (2006). "Poly(ADP-ribose): novel functions for an old molecule." Nat Rev Mol Cell Biol **7**(7): 517-528.

Schwartz, R. A. (1996). "Kaposi's sarcoma: advances and perspectives." J Am Acad Dermatol **34**(5 Pt 1): 804-814.

Schwarz, M. and P. M. Murphy (2001). "Kaposi's sarcoma-associated herpesvirus G protein-coupled receptor constitutively activates NF-kappa B and induces proinflammatory cytokine and chemokine production via a C-terminal signaling determinant." J Immunol **167**(1): 505-513.

Scott, I. (2009). "Degradation of RIG-I following cytomegalovirus infection is independent of apoptosis." Microbes Infect **11**(12): 973-979.

Searles RP, B. E., Axthelm MK, Wong S.W. (1999). "Sequence and genomic analysis of a Rhesus macaque rhadinovirus with similarity to Kaposi's sarcoma-associated herpesvirus/human herpesvirus 8." J Virol **73**.

Sekimoto, T., K. Nakajima, et al. (1996). "Interferon-gamma-dependent nuclear import of Stat1 is mediated by the GTPase activity of Ran/TC4." J Biol Chem **271**(49): 31017-31020.

Senger, K., M. Merika, et al. (2000). "Gene repression by coactivator repulsion." Mol Cell **6**(4): 931-937.

Seo, T., D. Lee, et al. (2002). "Viral interferon regulatory factor 1 of Kaposi's sarcoma-associated herpesvirus interacts with a cell death regulator, GRIM19, and inhibits interferon/retinoic acid-induced cell death." J Virol **76**(17): 8797-8807.

Seo, T., J. Park, et al. (2001). "Viral interferon regulatory factor 1 of Kaposi's sarcoma-associated herpesvirus binds to p53 and represses p53-dependent transcription and apoptosis." J Virol **75**(13): 6193-6198.

Servant, M. J., B. Tenoever, et al. (2002). "Overlapping and distinct mechanisms regulating IRF-3 and IRF-7 function." J Interferon Cytokine Res **22**(1): 49-58.

Seth, R. B., L. Sun, et al. (2005). "Identification and characterization of MAVS, a mitochondrial antiviral signaling protein that activates NF-kappaB and IRF 3." Cell **122**(5): 669-682.

Sharma, S., B. R. tenOever, et al. (2003). "Triggering the interferon antiviral response through an IKK-related pathway." Science **300**(5622): 1148-1151.

Sharma-Walia N, N. P., Krishnan HH, et al. (2004). "Kaposi's sarcoma herpevirus envelope glycoprotein gB induces the integrin-dependent focal adhesion kinase-Src-phosphatidylinositol 3-kinase-rho GTPase signal pathways and cytoskeletal rearrangements.
." J Virol **78**(8).

Sharma-Walia N, N. P., Krishnan HH, et al. (2005). "ERK1/2 and MEK1/2 induced by Kaposi's sarcoma-associated herpesvirus early duing infection of target cells are essential for expression of viral genes and for establishemt of infection." J Virol **79**(16).

Sharp, T. V., H. W. Wang, et al. (2002). "K15 protein of Kaposi's sarcoma-associated herpesvirus is latently expressed and binds to HAX-1, a protein with antiapoptotic function." J Virol **76**(2): 802-816.

Sherr, C. J. (1996). "Cancer cell cycles." Science **274**(5293): 1672-1677.

Shin, Y. C., H. Nakamura, et al. (2006). "Inhibition of the ATM/p53 signal transduction pathway by Kaposi's sarcoma-associated herpesvirus interferon regulatory factor 1." J Virol **80**(5): 2257-2266.

Shuai, K., G. R. Stark, et al. (1993). "A single phosphotyrosine residue of Stat91 required for gene activation by interferon-gamma." Science **261**(5129): 1744-1746.

Si, H. and E. S. Robertson (2006). "Kaposi's sarcoma-associated herpesvirus-encoded latency-associated nuclear antigen induces chromosomal instability through inhibition of p53 function." J Virol **80**(2): 697-709.

Silverman, R. H. (2007). "Viral encounters with 2',5'-oligoadenylate synthetase and RNase L during the interferon antiviral response." J Virol **81**(23): 12720-12729.

Smith, J. A., S. C. Schmechel, et al. (2006). "Reovirus induces and benefits from an integrated cellular stress response." J Virol **80**(4): 2019-2033.

Smyth, G. K. (2004). "Linear models and empirical bayes methods for assessing differential expression in microarray experiments." Stat Appl Genet Mol Biol **3**: Article3.

Sodhi, A., S. Montaner, et al. (2000). "The Kaposi's sarcoma-associated herpes virus G protein-coupled receptor up-regulates vascular endothelial growth factor expression and secretion through mitogen-activated protein kinase and p38 pathways acting on hypoxia-inducible factor 1alpha." Cancer Res **60**(17): 4873-4880.

Soulier, J., L. Grollet, et al. (1995). "Kaposi's sarcoma-associated herpesvirus-like DNA sequences in multicentric Castleman's disease." Blood **86**(4): 1276-1280.

Spear, P. G. and R. Longnecker (2003). "Herpesvirus entry: an update." J Virol **77**(19): 10179-10185.

Spiller, O. B., L. Mark, et al. (2006). "Dissecting the regions of virion-associated Kaposi's sarcoma-associated herpesvirus complement control protein required for complement regulation and cell binding." J Virol **80**(8): 4068-4078.

Stark, G. R., I. M. Kerr, et al. (1998). "How cells respond to interferons." Annu Rev Biochem **67**: 227-264.

Staskus, K. A., W. Zhong, et al. (1997). "Kaposi's sarcoma-associated herpesvirus gene expression in endothelial (spindle) tumor cells." J Virol **71**(1): 715-719.

Stephanou, A. and D. S. Latchman (2003). "STAT-1: a novel regulator of apoptosis." Int J Exp Pathol **84**(6): 239-244.

Stine, J. T., C. Wood, et al. (2000). "KSHV-encoded CC chemokine vMIP-III is a CCR4 agonist, stimulates angiogenesis, and selectively chemoattracts TH2 cells." Blood **95**(4): 1151-1157.

Su, I. J., Y. S. Hsu, et al. (1995). "Herpesvirus-like DNA sequence in Kaposi's sarcoma from AIDS and non-AIDS patients in Taiwan." Lancet **345**(8951): 722-723.

Subramanian, A., P. Tamayo, et al. (2005). "Gene set enrichment analysis: a knowledge-based approach for interpreting genome-wide expression profiles." Proc Natl Acad Sci U S A **102**(43): 15545-15550.

Swanton, C., D. J. Mann, et al. (1997). "Herpes viral cyclin/Cdk6 complexes evade inhibition by CDK inhibitor proteins." Nature **390**(6656): 184-187.

Takaoka, A., S. Hayakawa, et al. (2003). "Integration of interferon-alpha/beta signalling to p53 responses in tumour suppression and antiviral defence." Nature **424**(6948): 516-523.

Takaoka, A., Z. Wang, et al. (2007). "DAI (DLM-1/ZBP1) is a cytosolic DNA sensor and an activator of innate immune response." Nature **448**(7152): 501-505.

Takeuchi, O. and S. Akira (2007). "Recognition of viruses by innate immunity." Immunol Rev **220**: 214-224.

Takeuchi, O. and S. Akira (2010). "Pattern recognition receptors and inflammation." Cell **140**(6): 805-820.

Taki, S., S. Nakajima, et al. (2005). "IFN regulatory factor-2 deficiency revealed a novel checkpoint critical for the generation of peripheral NK cells." J Immunol **174**(10): 6005-6012.

Talbot, S. J., R. A. Weiss, et al. (1999). "Transcriptional analysis of human herpesvirus-8 open reading frames 71, 72, 73, K14, and 74 in a primary effusion lymphoma cell line." Virology **257**(1): 84-94.

Talon, J., C. M. Horvath, et al. (2000). "Activation of interferon regulatory factor 3 is inhibited by the influenza A virus NS1 protein." J Virol **74**(17): 7989-7996.

Tamura, T., H. Yanai, et al. (2008). "The IRF family transcription factors in immunity and oncogenesis." Annu Rev Immunol **26**: 535-584.

Tang, X., J. S. Gao, et al. (2007). "Acetylation-dependent signal transduction for type I interferon receptor." Cell **131**(1): 93-105.

Taniguchi, T. and A. Takaoka (2001). "A weak signal for strong responses: interferon-alpha/beta revisited." Nat Rev Mol Cell Biol **2**(5): 378-386.

Taniguchi, T. and A. Takaoka (2002). "The interferon-alpha/beta system in antiviral responses: a multimodal machinery of gene regulation by the IRF family of transcription factors." Curr Opin Immunol **14**(1): 111-116.

Terenzi, F., D. J. Hui, et al. (2006). "Distinct induction patterns and functions of two closely related interferon-inducible human genes, ISG54 and ISG56." J Biol Chem **281**(45): 34064-34071.

Terenzi, F., S. Pal, et al. (2005). "Induction and mode of action of the viral stress-inducible murine proteins, P56 and P54." Virology **340**(1): 116-124.

Terenzi, F., C. White, et al. (2007). "Tissue-specific and inducer-specific differential induction of ISG56 and ISG54 in mice." J Virol **81**(16): 8656-8665.

Thanos, D. and T. Maniatis (1995). "Virus induction of human IFN beta gene expression requires the assembly of an enhanceosome." Cell **83**(7): 1091-1100.

Thomas, M., C. E. Finnegan, et al. (2004). "STAT1: a modulator of chemotherapy-induced apoptosis." Cancer Res **64**(22): 8357-8364.

Tomkowicz, B., S. P. Singh, et al. (2005). "Mutational analysis reveals an essential role for the LXXLL motif in the transformation function of the human herpesvirus-8 oncoprotein, kaposin." DNA Cell Biol **24**(1): 10-20.

Tomlinson, C. C. and B. Damania (2004). "The K1 protein of Kaposi's sarcoma-associated herpesvirus activates the Akt signaling pathway." J Virol **78**(4): 1918-1927.

Tomlinson, C. C. and B. Damania (2008). "Critical role for endocytosis in the regulation of signaling by the Kaposi's sarcoma-associated herpesvirus K1 protein." J Virol **82**(13): 6514-6523.

Torisu, H., K. Kusuhara, et al. (2004). "Functional MxA promoter polymorphism associated with subacute sclerosing panencephalitis." Neurology **62**(3): 457-460.

Uematsu, S. and S. Akira (2007). "Toll-like receptors and Type I interferons." J Biol Chem **282**(21): 15319-15323.

Unterholzner, L., S. E. Keating, et al. (2010). "IFI16 is an innate immune sensor for intracellular DNA." Nat Immunol **11**(11): 997-1004.

Uze, G. and D. Monneron (2007). "IL-28 and IL-29: newcomers to the interferon family." Biochimie **89**(6-7): 729-734.

Vart, R. J., L. L. Nikitenko, et al. (2007). "Kaposi's sarcoma-associated herpesvirus-encoded interleukin-6 and G-protein-coupled receptor regulate angiopoietin-2 expression in lymphatic endothelial cells." Cancer Res **67**(9): 4042-4051.

Vectors:, N. T. (2000). "pTRE2pur & pTRE2hyg " Clontechniques **XV (4):20**.

Verschuren, E. W., J. Klefstrom, et al. (2002). "The oncogenic potential of Kaposi's sarcoma-associated herpesvirus cyclin is exposed by p53 loss in vitro and in vivo." Cancer Cell **2**(3): 229-241.

Virag, L. and C. Szabo (2002). "The therapeutic potential of poly(ADP-ribose) polymerase inhibitors." Pharmacol Rev **54**(3): 375-429.

Wabinga, H. R., D. M. Parkin, et al. (1993). "Cancer in Kampala, Uganda, in 1989-91: changes in incidence in the era of AIDS." Int J Cancer **54**(1): 26-36.

Wacher, C., M. Muller, et al. (2007). "Coordinated regulation and widespread cellular expression of interferon-stimulated genes (ISG) ISG-49, ISG-54, and ISG-56 in the central nervous system after infection with distinct viruses." J Virol **81**(2): 860-871.

Wang, C., J. Pflugheber, et al. (2003). "Alpha interferon induces distinct translational control programs to suppress hepatitis C virus RNA replication." J Virol **77**(7): 3898-3912.

Wang, H. W., M. W. Trotter, et al. (2004). "Kaposi sarcoma herpesvirus-induced cellular reprogramming contributes to the lymphatic endothelial gene expression in Kaposi sarcoma." Nat Genet **36**(7): 687-693.

Wang, S., S. Liu, et al. (2001). "Kaposi's sarcoma-associated herpesvirus/human herpesvirus-8 ORF50 gene product contains a potent C-terminal activation domain which activates gene expression via a specific target sequence." Arch Virol **146**(7): 1415-1426.

Wathelet, M., S. Moutschen, et al. (1986). "Molecular cloning, full-length sequence and preliminary characterization of a 56-kDa protein induced by human interferons." Eur J Biochem **155**(1): 11-17.

Wathelet, M. G., C. H. Lin, et al. (1998). "Virus infection induces the assembly of coordinately activated transcription factors on the IFN-beta enhancer in vivo." Mol Cell **1**(4): 507-518.

Wawer, M. J., S. M. Eng, et al. (2001). "Prevalence of Kaposi sarcoma-associated herpesvirus compared with selected sexually transmitted diseases in adolescents and young adults in rural Rakai District, Uganda." Sex Transm Dis **28**(2): 77-81.

Weber, K. S., H. J. Grone, et al. (2001). "Selective recruitment of Th2-type cells and evasion from a cytotoxic immune response mediated by viral macrophage inhibitory protein-II." Eur J Immunol **31**(8): 2458-2466.

Whitby, D., M. Luppi, et al. (1998). "Human herpesvirus 8 seroprevalence in blood donors and lymphoma patients from different regions of Italy." J Natl Cancer Inst **90**(5): 395-397.

Whitby, D., V. A. Marshall, et al. (2004). "Genotypic characterization of Kaposi's sarcoma-associated herpesvirus in asymptomatic infected subjects from isolated populations." J Gen Virol **85**(Pt 1): 155-163.

Wies, E., A. S. Hahn, et al. (2009). "The Kaposi's Sarcoma-associated Herpesvirus-encoded vIRF-3 Inhibits Cellular IRF-5." J Biol Chem **284**(13): 8525-8538.

Wullaert, A., K. Heyninck, et al. (2006). "Ubiquitin: tool and target for intracellular NF-kappaB inhibitors." Trends Immunol **27**(11): 533-540.

Xiao, S., D. Li, et al. (2006). "RIG-G as a key mediator of the antiproliferative activity of interferon-related pathways through enhancing p21 and p27 proteins." Proc Natl Acad Sci U S A **103**(44): 16448-16453.

Xu, L. G., Y. Y. Wang, et al. (2005). "VISA is an adapter protein required for virus-triggered IFN-beta signaling." Mol Cell **19**(6): 727-740.

Xu, Y., D. P. AuCoin, et al. (2005). "A Kaposi's sarcoma-associated herpesvirus/human herpesvirus 8 ORF50 deletion mutant is defective for reactivation of latent virus and DNA replication." J Virol **79**(6): 3479-3487.

Xu, Y., A. Rodriguez-Huete, et al. (2006). "Evaluation of the lytic origins of replication of Kaposi's sarcoma-associated virus/human herpesvirus 8 in the context of the viral genome." J Virol **80**(19): 9905-9909.

Y Zhang, D. P. a. S. F. (2009). "Activation of interferon signaling pathway in primary effusion lymphoma cells by inhibition of viral interferon regulatory factor 1 of Kaposi's sarcoma-associated herpesvirus." Infectious Agents and Cancer **4**(Suppl 2).

Yakushko, Y., C. Hackmann, et al. (2011). "Kaposi's sarcoma-associated herpesvirus bacterial artificial chromosome contains a duplication of a long unique-region fragment within the terminal repeat region." J Virol **85**(9): 4612-4617.

Yan, H., K. Krishnan, et al. (1996). "Phosphorylated interferon-alpha receptor 1 subunit (IFNaR1) acts as a docking site for the latent form of the 113 kDa STAT2 protein." Embo J **15**(5): 1064-1074.

Yang, H., G. Ma, et al. (2004). "Mechanism for transcriptional synergy between interferon regulatory factor (IRF)-3 and IRF-7 in activation of the interferon-beta gene promoter." Eur J Biochem **271**(18): 3693-3703.

Yang, P., H. An, et al. (2010). "The cytosolic nucleic acid sensor LRRFIP1 mediates the production of type I interferon via a beta-catenin-dependent pathway." Nat Immunol **11**(6): 487-494.

Yang, T. Y., S. C. Chen, et al. (2000). "Transgenic expression of the chemokine receptor encoded by human herpesvirus 8 induces an angioproliferative disease resembling Kaposi's sarcoma." J Exp Med **191**(3): 445-454.

Ye, F. C., D. J. Blackbourn, et al. (2007). "Kaposi's sarcoma-associated herpesvirus promotes angiogenesis by inducing angiopoietin-2 expression via AP-1 and Ets1." J Virol **81**(8): 3980-3991.

Ye, F. C., F. C. Zhou, et al. (2008). "Kaposi's sarcoma-associated herpesvirus latent gene vFLIP inhibits viral lytic replication through NF-kappaB-mediated suppression of the AP-1 pathway: a novel mechanism of virus control of latency." J Virol **82**(9): 4235-4249.

Ye, F. C., F. C. Zhou, et al. (2004). "Disruption of Kaposi's sarcoma-associated herpesvirus latent nuclear antigen leads to abortive episome persistence." J Virol **78**(20): 11121-11129.

Yoneyama, M. and T. Fujita (2007). "RIG-I family RNA helicases: cytoplasmic sensor for antiviral innate immunity." Cytokine Growth Factor Rev **18**(5-6): 545-551.

Yoneyama, M. and T. Fujita (2009). "RNA recognition and signal transduction by RIG-I-like receptors." Immunol Rev **227**(1): 54-65.

Yoneyama, M., M. Kikuchi, et al. (2005). "Shared and unique functions of the DExD/H-box helicases RIG-I, MDA5, and LGP2 in antiviral innate immunity." J Immunol **175**(5): 2851-2858.

Yoneyama, M., M. Kikuchi, et al. (2004). "The RNA helicase RIG-I has an essential function in double-stranded RNA-induced innate antiviral responses." Nat Immunol **5**(7): 730-737.

Youlyouz-Marfak, I., N. Gachard, et al. (2008). "Identification of a novel p53-dependent activation pathway of STAT1 by antitumour genotoxic agents." Cell Death Differ **15**(2): 376-385.

Yu, S. W., H. Wang, et al. (2002). "Mediation of poly(ADP-ribose) polymerase-1-dependent cell death by apoptosis-inducing factor." Science **297**(5579): 259-263.

Zeng, W., L. Sun, et al. (2010). "Reconstitution of the RIG-I pathway reveals a signaling role of unanchored polyubiquitin chains in innate immunity." Cell **141**(2): 315-330.

Zhang, J. J., U. Vinkemeier, et al. (1996). "Two contact regions between Stat1 and CBP/p300 in interferon gamma signaling." Proc Natl Acad Sci U S A **93**(26): 15092-15096.

Zhao, T., L. Yang, et al. (2007). "The NEMO adaptor bridges the nuclear factor-kappaB and interferon regulatory factor signaling pathways." Nat Immunol **8**(6): 592-600.

Zhong, W., H. Wang, et al. (1996). "Restricted expression of Kaposi sarcoma-associated herpesvirus (human herpesvirus 8) genes in Kaposi sarcoma." Proc Natl Acad Sci U S A **93**(13): 6641-6646.

Zhou, A., J. Paranjape, et al. (1997). "Interferon action and apoptosis are defective in mice devoid of 2',5'-oligoadenylate-dependent RNase L." EMBO J **16**(21): 6355-6363.

Zhou, F. C., Y. J. Zhang, et al. (2002). "Efficient infection by a recombinant Kaposi's sarcoma-associated herpesvirus cloned in a bacterial artificial chromosome: application for genetic analysis." J Virol **76**(12): 6185-6196.

Zhou, Z., O. J. Hamming, et al. (2007). "Type III interferon (IFN) induces a type I IFN-like response in a restricted subset of cells through signaling pathways involving both the Jak-STAT pathway and the mitogen-activated protein kinases." J Virol **81**(14): 7749-7758.

Zhu, F. X., X. Li, et al. (2006). "Functional characterization of Kaposi's sarcoma-associated herpesvirus ORF45 by bacterial artificial chromosome-based mutagenesis." J Virol **80**(24): 12187-12196.

Zhu, H., J. P. Cong, et al. (1997). "Use of differential display analysis to assess the effect of human cytomegalovirus infection on the accumulation of cellular RNAs: induction of interferon-responsive RNAs." Proc Natl Acad Sci U S A **94**(25): 13985-13990.

Zong, J., D. M. Ciufo, et al. (2002). "Genotypic analysis at multiple loci across Kaposi's sarcoma herpesvirus (KSHV) DNA molecules: clustering patterns, novel variants and chimerism." J Clin Virol **23**(3): 119-148.

Zong, J. C., D. M. Ciufo, et al. (1999). "High-level variability in the ORF-K1 membrane protein gene at the left end of the Kaposi's sarcoma-associated herpesvirus genome defines four major virus subtypes and multiple variants or clades in different human populations." J Virol **73**(5): 4156-4170.

Appendices:

Appendix I Commonly used reagents and solutions, antibodies, and plasmids

Appendix A

Table 1. Reagents and chemicals

Reagents / Chemical	Supplier
Sodium orthovanadate	Santa cruz biotechnology
Phosphatase inhibitor cocktail B	Santa cruz biotechnology
Protease inhibitor cocktail set III	Calbiochem
Nonidet-P40 (NP40)	BDH
Acrylamide / bis-acrylmide (30% Solution)	Sigma
Phenylmethylsulfonyl fluoride (PMSF)	Santa cruz biotechnology
Puromycin dihydrochloride	Sigma
G418 disulfate salt	Sigma
p-Coumaric Acid	Sigma
Methanol Ethanol	Fisher Scientific
Double distilled water,	Sigma
2X reaction mixture (PCR)	EUROGENTEC S.A
Coomassie blue	Bio-Rad Laboratories
Bradford Reagent	Bio-Rad Laboratories
Tris base	Fisher Scientific
Sodium chloride	Fisher Scientific
Glycine	Fisher Scientific
Sodium dodecyl sulphate (SDS)	Fisher Scientific
Glycerol	Fisher Scientific
Ammonium persulphate	BioRad
Bradford reagent	BioRad
Trypan Blue solution	Sigma

Tetramethylethylenediamine (TEMED)	Sigma
Moloney Murine Leukemia Virus Reverse Transcriptase (MMLV RT) Random primers DNAse Taq polymerase RNAse Inhibitor (Rnasin, 40 U/µl)	Applied Biosystems
X-ray film	Amersham Hyperfilm, GE Health Care Limited
Lipofectamine 2000	Invitrogen
Luciferase Reporter Assay Kit	Promega
Polyinosinic Polycytidylic acid potassium salt (poly I:C)	Sigma
Fungizone Amphotericin B	GIBCO
Doxycycline hyclate	Sigma
Penicillin	Sigma
Triton X-100	Sigma
Bovine serum albumin	Sigma
Tween 20 molecular grade	Sigma
Immobilon-P membrane filter type: Polivinylidene difluoride, pore size: 0.45µm, cut size: 7 cm X 8.4 cm)	Millipore
Protein markers	Lonza
Nail varnish	Rimmel
EndoFree Plasmid Maxi – cat. No. 12362	QIAGEN
Rneasy Mini Kit – cat. No. 74104	QIAGEN
4', 6-diamidino-2-phenylindole, dihydrochloride	DAPI
Recombinant Human Interferon Alpha B2 (rIFN-α)	PBL Interferon Source
DMEM	Invitrogen
Enhanced chemiluminence (ECL)	Gene Flow
Fibronectin, 0.1% solution from bovine	SIGMA

plasma	
ProLong Gold antifade reagent	Invitrogen
Human GAPDH 20X (4310884E)	Applied Biosystems

Appendix B. Antibodies

Table 1 Primary antibodies

Antibodies	Host species	Suppl-ier	Dilution	Lysis buffer	% SDS PAGE	Electro-phoresis run voltage	Incuba-tion time	Catalo-gue Number
IFNAR1	Rabbit	Abcam	1:500	Non-ionic	8	40 MA	48 hrs	ab45172
p-TYK2 Tyr1054/1055	Rabbit	CST	1:200	Non ionic	8	40 MA	48 hrs	#9321
TYK2	Rabbit	CST	1:200	Non-ionic	8	40 MA	16 hrs	SC-169
JAK1	Rabbit	CST	1:200	Non-ionic	8	40 MA	16 hrs	SC-277
p-STAT1 Tyr701	Rabbit	SCB	1:500	Non-ionic	8	40 MA	16 hrs	#9167
STAT1	Rabbit	SCB	1:1000	Non-ionic	8	40 MA	16 hrs	SC-346
p-STAT2 Tyr689	Rabbit	Milipore	1:200	Non-ionic	8	40 MA	16 hrs	#07-224
STAT2	Rabbit	SCB	1:200	Non-ionic	8	40 MA	16 hrs	SC-476
p48/IRF-9	Rabbit	SCB	1:300	Buffer E	10	150 V	16 hrs	SC-10793
OAS3	Rabbit	Abcam	1:300	Buffer E	10	150 V	16 hrs	ab71780

GAPDH	Mouse	Sigma Aldrich	1:2000	Buffer E	10	150 V	16 hrs	G8795
Cmyc-vIRF-2	Mouse	DJB Lab	1:2000	Buffer E	10	150 V	16 hrs	N/A
RIG-I	Rabbit	Abcam	1:1000	Buffer E	10	150 V	16 hrs	Ab65588
TBK-1	Rabbit	Gene Tex	1:1000	Buffer E	10	150 V	16 hrs	GTX 108338S

- The blotted membranes were incubated with diluted primary antibodies in 5% w/v bovine serum albumin, 1X tris-buffered saline, 0.05% Tween-20 at 4^{o}C with gentle shaking for the indicated times.
- 10 µl of phosphatase inhibitor cocktail B (table 2.1) was added per 1 ml of the primary antibody buffer solution for phosphor-specific antibodies.
- Transfer: 300 MA
- NI: Non-ionic detergent lysis buffer.
- S C: Santa Cruz Biotechnology.
- CST: Cell Signaling Technology.
- DJB Lab: Professor David Blackbourn's laboratory
- MA: Milli Ampere
- V: Volts

Table 2. Secondary antibodies

Antibodies	**Host species**	**Supplier**	**Dilution**	**Incubation time**	**Catalogue number**
Anti Mouse-FITC	Sheep	DAKO	1:100	1 hr	
Anti Mouse HRP conjugate	Goat	DAKO	1:2000	1 hr	P0447
Anti Rabbit HRP conjugate	Goat	DAKO	1:2000	1 hr	P0448

The blotted membranes were incubated with diluted secondary antibodies in 0.05% w/v bovine serum albumin, 1X tris-buffered saline, 0.05% Tween-20 at 4^{o}C with gentle shaking for the indicated times.

Appendix C. Plasmids

Table 1.

Plasmid name	Final Concentration	Profile
pISRE-luc	**250 ng/well (6-well plate)**	A luciferase reporter plasmid containing tandem repeats of the *ISG56* ISRE driving the expression of a firefly luciferase reporter gene.
pRLSV-40	**1 ng/well (6-well plate)**	Contains a constitutively active CMV promoter driving the expression of a *Renilla* luciferase reporter gene.
pTRE2-pur-myc-*vIRF-2*	**1000 ng/well (6-well plate)**	pTRE2-pur-myc (the tetracycline responsive vector) carrying the vIRF-2 expression cassette
pTRE2-pur-myc	**1000 ng/well (6-well plate)**	The tetracycline responsive vector (does not expresss vIRF-2) referred to as 'empty vector'.

Appendix D. Commonly used buffer and other solutions

Table 1.

Solution	Composition
Lysis buffer E	100 mM Tris-HCl pH 8, 100Mm NaCl, 2 mM EDTA, 2 mM EGTA, 1% NP-40, 0.5% Na Deoxycholate, 0.5 mM PMSF.
Non-ionic detergent Lysis buffer	50 mM Tris HCI pH 8.0, 50 mM NaCI, 5 mM EDTA, 1% Triton X-100, 50 mM sodium fluoride, 1 mM sodium orthorvanadate, 0.05% SDS, 10 mM Sodium pyrophosphate, 1 mM PMSF, Protease Inhibitor cocktail set III cat no. 535140 (used at 1:100 dilution)
4X Tris-SDS-HCI, pH 6.8	0.5 M Tris-Cl, 0.4% SDS
4X Tris-SDS-HCI, pH 8.8	1.5 M Tris-Cl, 0.4% SDS
Trypsin	0.5% w/v Trypsin – EDTA
Enhanced Chemiluminescence solutions	(A) 0.22 g Luminol, 5 ml DMSO. (B) 0.07 g Coumaric Acid, 5 ml DMSO.
10X Electrophoresis / Running buffer	Tris base 30.24 g, Glycine 142.5 g, 1L dH_2O, adjust pH 8.4
1X Electrophoresis / Running buffer 1 L	100 ml 10X electrophoresis buffer, 0.1% of 20% SDS, 1L dH_2O
5% BSA	5% w/v Bovine Serum Albumin, 1X TBS, 0.05% Tween-20
10X Transfer buffer 1 L	Tris 30.3 g, Glycine 142.5 g & 1 L dH_2O, pH to 8.4
1X Transfer buffer 1 L	100 ml 10X transfer buffer, 20% methanol, 700 ml dH_2O
10X Phosphate buffered saline 1 L	10.9 g Na_2HPO_4 (anhydrous), 3.29 g NaH2PO_4 (anhydrous), 1 L distilled water, pH to 7.2

Tris Buffered Saline-Tween Solution (TBS-T) 1 L	100 ml TBS, 0.05% Tween-20, 900 ml dH_2O.
2X Loading sample buffer 10 ml	1 M Tris-HCl, pH 6.8, 4 ml 10% SDS, 2 ml glycerol, 2.5 ml β-mecaptoethanol, 500 µl bromophenol blue (1%)
Luria Bertani (LB) Broth	10 g NaCl, 10 g bactopeptone, 5 g yeast extract in 1L distilled water, pH 7.5
Coomasie blue stain	0.02% w/v Coomasie Brilliant Blue, 50% v/v methanol, 43% v/v water, 7% acetic acid
Destaining solution	5% v/v methanol, 88% v/v water, 7% v/v acetic acid
Stripping buffer	100 mM β-mercaptoethanol, 2% SDS, 62.5 mM Tris-HCl, pH 6.7
Permeabilisaton solution 20 ml	19 ml PBS, 1 ml 10% NP40, 2 g sucrose

Appendix II Quality assessment metrics of exon arrays

Table 1. List of quality assessment metrics used to identify potential outlier arrays within the expression data set.

Metrics	Definition
Probe level metrics	
pm_mean	Is the mean of the raw intensity for all of the perfect matched (PM) probes on the array prior to any intensity transformation (e.g. background correction). It can also be used to ascertain whether certain chips are unusually dim or bright.
bgrd_mean	Is the mean of raw intensity of probes used to measure background prior to any intensity transformation such as RMA algorithm background normalisation.
Probeset summarisation based metrics	
rle_mean	Is the mean absolute relative log expression (rle) for all probesets analysed. For example, the signal estimate of a given probeset of a particular chip was taken and the difference in log base 2 of the median signal value of that probset was calculated over all the chips
mad_residual_mean	Is the mean of the absolute deviation of the residuals from the median. To account for the different signal intensities returned when different probes hybridize to a common target, the RMA or PLIER algorithms have models to identify problematic chips. The difference between actual signal values and that predicted by the model is called residual.
all_probesets	Stands for all probesets analysed and will be the most representative of the quality of the data being used downstream.
pos_vs_neg_auc	Area under the curve (AUC) discriminates probesets signal intensities between positive and negative controls. An AUC of 1 reflects perfect separation whereas an AUC value of 0.5 reflects no separation.

Internal quality control metrics	
bac_spike	Probe sets hybridize to pre-labeled bacteria spike control. Used mainly to identify problems with hybridization and or GeneChip.
Polya_spike	Is the set of polyadenylated RNA spike used to identify problems with target RNA.
Neg_control	Is a set of putative intron based probes sets from putative housekeeping genes.
pos_control	Is the set of putative exon based probesets from the putative housekeeping genes

The quality assessment metrics and associated definitions presented (Table 4.2) were sourced from the Affymetrix GeneChip and Exon Array Whitepaper Collection (see Affymetrix) which guides users to perform quality assessment of exon and gene arrays.

(A)

Figure 1A. pm_mean. The CEL files were uploaded in EC and a multichip analysis was performed according to standard instructions and a plot of the pm_mean was generated. GeneChip names and profiles are displayed on the x-axis and their corresponding signal intensity levels displayed on the y-axis. GeneChip names are explained in Table 4.1.

(B)

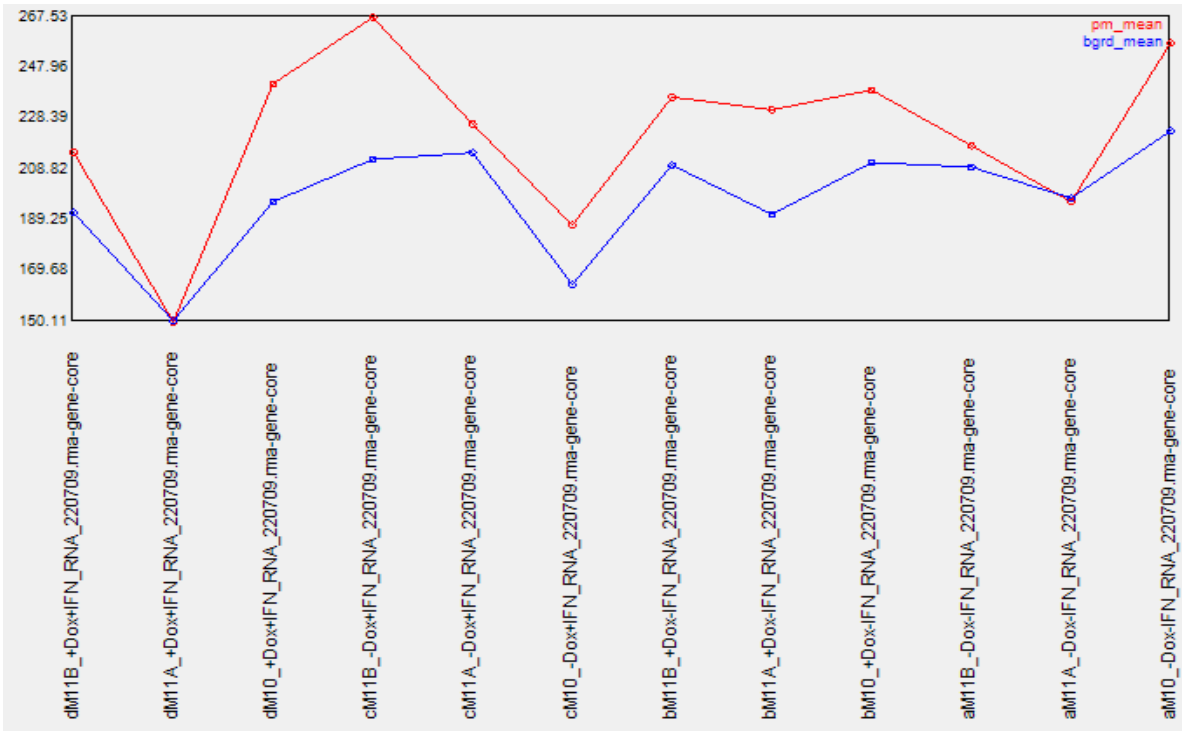

Figure 1B. pm_mean vs bgrd_mean. This figure was generated as described for (A). A plot of pm_mean vs bgrd_mean was generated to facilitate their comparisons. pm_mean (Red) and bgrd_mean (Blue). GeneChip names and profiles are displayed on the x-axis and their corresponding signal intensity levels displayed on the y-axis. GeneChip names are explained in Table 4.1.

(C)

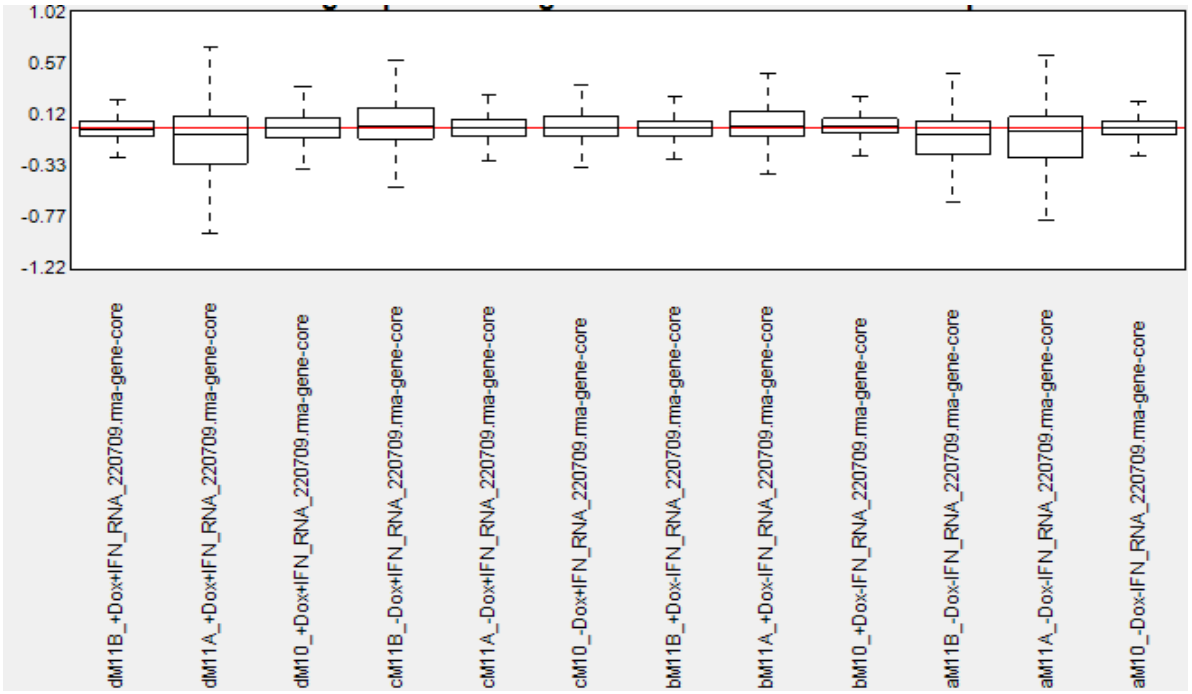

Figure 1C. Median relative log expression. Box plots for the relative log expression values of all probesets were generated in EC. The middle bar in each box is the median rle. These should be zero in most applications and deviations from zero typically indicate a skewness of signal intensities towards outlier. GeneChip names and profiles are displayed on the x-axis and their corresponding signal intensity levels are displayed on the y-axis. GeneChip names are explained in Table 4.1.

(D)

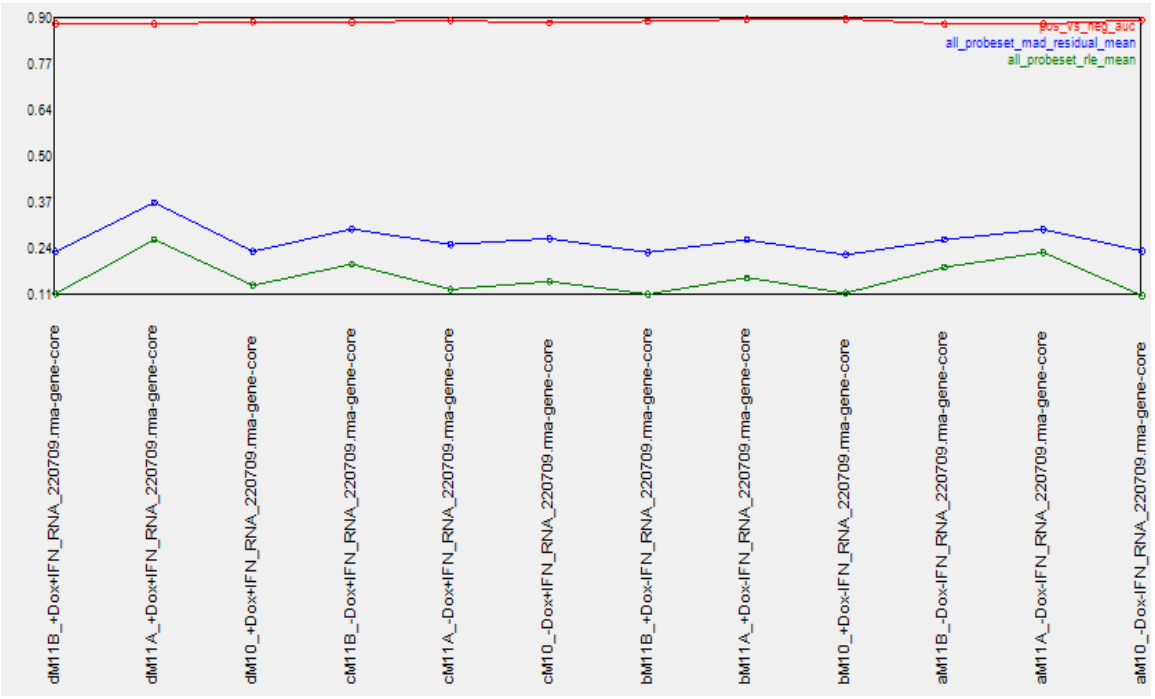

Figure 1D. Three summarisation probesets metrics. All three metrics: pos_vs _ neg _ auc (red), all_probesets_mad_residual_mean (blue) and all_probesets_rle_mean (green) were generated in EC. GeneChip names and profiles are displayed on the x-axis whereas their corresponding signal intensity levels are displayed on the y-axis. GeneChip names are explained in Table 4.1.

(E)

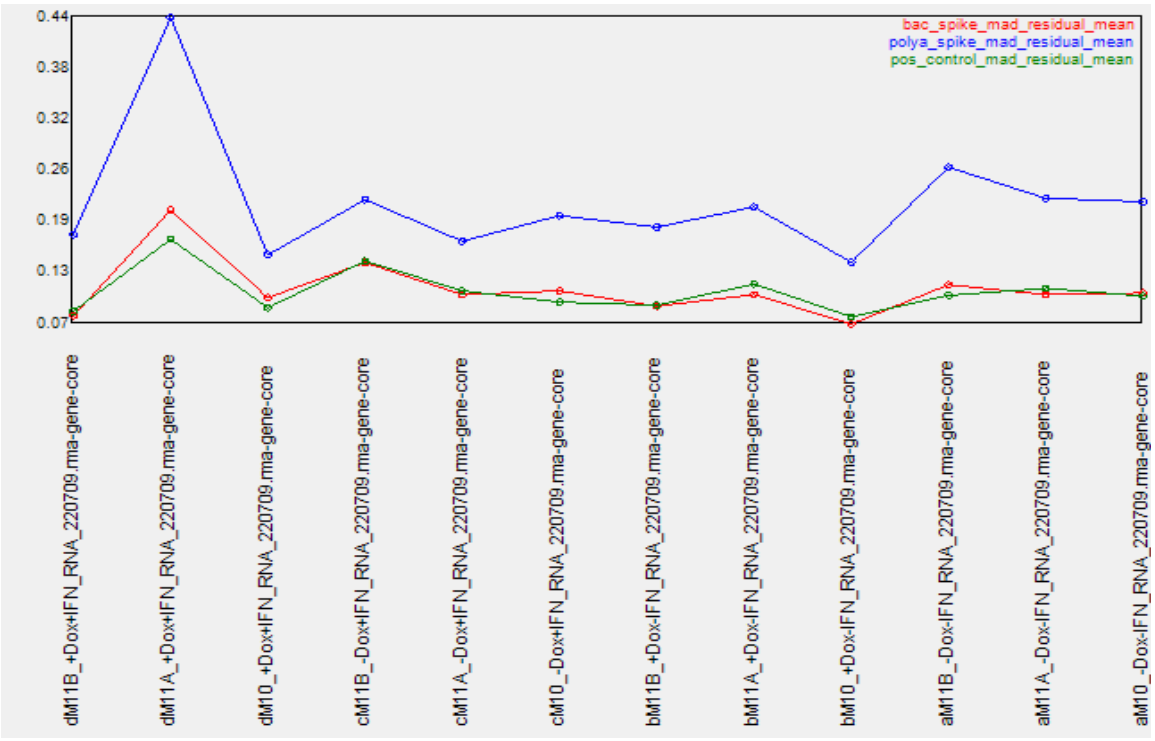

Figure 1E. All three internal quality control metrics: bac_spike_ mad_ residual_mean (red), polya_spike_mad_residual_mean (blue), pos_control_mad_ residual_ mean (green) were also generated in EC. GeneChip names and profiles are displayed on the x axis whereas their corresponding signal intensity levels are displayed on the y-axis. GeneChip names are explained in Table 4.1.

Appendix III Publications arising from this work

1. Kaposi's sarcoma-associated herpesvirus viral interferon regulatory factor-2 inhibits type 1 interferon signalling by targeting interferon-stimulated gene factor-3. **J Gen Virol. 2011 Oct;92(Pt 10):2394-8. Epub 2011 Jun 22.**

2. Identification of caspase-mediated decay of interferon regulatory factor-3, exploited by a Kaposi sarcoma-associated herpesvirus immunoregulatory protein. **J Biol Chem. 2009 Aug 28;284(35):23272-85. Epub 2009 Jun 24.**